ProQuest LLC.
789 East Eisenhower Parkway
P.O. Box 1346
Ann Arbor, MI 48106 – 1346

Thermal Curing of Concrete with Conductive Polymer Technology

David Gerald Catley

A thesis submitted in partial fulfilment of the requirements of
Sheffield Hallam University
for the degree of Doctor of Philosophy

March 2009

Confidentiality Agreement

The University wishes to make clear that the attached academic submission is passed for your attention under a strict obligation of confidentiality. The contents, subject matter and the other such details concerning this work should not be discussed with any person not acting on behalf of the university nor should it be made public.

Abstract

"Concrete is used on the majority of all construction projects. It is manufactured using the core constituents of a cement binder, typically Portland Cement, proportions of coarse and fine aggregates and water. The strength development of concrete is achieved by the addition of water that reacts with the binder in the form of a hydration reaction. This hydration reaction or strength development is dependant on two primary curing factors, time and temperature. Increasing the rate of strength development of concrete by elevating the curing temperature at early ages has advantages of maximising concrete production and reducing manufacturing time. Increasing the temperature of early age concrete up to 70 deg C is used in precast plants where it is critical for a minimum strength to be achieved within a certain time period to allow the removal of the concrete sections from moulds and forms. Various practices are adopted by precast concrete manufacturers to achieve the early strengths required to maximise production, both thermal and non-thermal. These include heating the various mix constituents of the concrete, using unnecessarily high cement contents within the mix, using large quantities of chemical admixtures or by increasing the ambient temperature of plants within which the elements are manufactured. In precast concrete plants the use of steam to elevate the curing temperature of the concrete is the most commonly adopted technique. However, it is inefficient and rarely provides controlled temperatures to the concrete as recommended in approved codes of practices and standards.

This research programme has investigated the use of an alternative heating technology for concrete curing, optimising a unique Conductive Polymer Technology (CPT). The application and optimisation of the CPT material to provide heat curing to concrete within the laboratory, in-situ and within precast concrete plants has been investigated. The electrical properties of the CPT were investigated to determine their relationship with the size of the concrete elements. This was done for various CPT materials with different Characteristic Resistances. Having gained an in depth understanding of the electrical properties of the CPT, various heating Jackets were designed and manufactured to thermally cure concrete elements at early ages. The Jackets were designed with various outer protective materials. The effect of CPT curing on the strength and shrinkage, both at early ages and long-term, was determined. The thermal performance of the heating jackets was determined for each application including the uniformity of the heating provided into the concrete element. The interaction of the heat generated by hydration and CPT heating for larger elements was also investigated.

The results showed that the CPT materials varied depending upon their manufacture and required target resistance. The thermal blankets had the capability to uniformly heat concrete elements at various ambient temperatures, to temperatures required by standards and approved codes of practice for accelerated curing of concrete. This uniform heating resulted in greater compressive strength of laboratory scale concrete elements with reduced shrinkage. The research identified the important parameters for CPT jacket design and

materials selection e.g. the importance of the contact between CPT heating elements and the concrete element and the selection of appropriate insulation materials

The test programme also investigated the durability of CPT under different exposure conditions. The results from testing the CPT material under conditions such as freeze thaw, heating & cooling and wetting & drying showed that wetting and drying had the most significant affect on the CPTs resistance, altering by 10%. Other tests of durability included punching holes of various sizes into the CPT samples to determine their effect on the CPT's resistance. This was found to be directly linked to the area of CPT material removed.

The manufacture, performance and operation of the CPT materials has also been investigated to provide an understanding of its mode of heating and its effect on concrete curing. The concept of maturity has been used to determine relationships between strength development and thermal curing and energy requirement for thermal curing when using CPT."

Keywords

Temperature; Temperature profile; Conductive Polymer Technology; Heat of Hydration; Thermal Blankets; Thermal Liners; Thermal curing; Accelerated curing; Maturity Factor. Temperature; Temperature profile; Carbon Polymer Technology; Heat of Hydration;

Acknowledgements

The author would like to particularly acknowledge the following five people without whom the following research work could not have been conducted:-

- **Professor Pritpal Mangat (Sheffield Hallam University):** For his advice and support; and for sharing his knowledge and experience both on a personal and professional level.

- **Patrick O'Grady (PJO Industrial / Inditherm plc):** For his drive and enthusiasm towards the research programme and its objectives.

- **Iordanis Chidiroglou (Sheffield Hallam University):** For his assistance during the latter period of the research programme.

- **Bob Skelton and Geoff Harwood (Sheffield Hallam University):** For their support and assistance within the construction materials & structures laboratories at Sheffield Hallam University.

In addition the author would like to acknowledge the contribution made by the following people and organisations:-

- **Dr Finbar O'Flaherty** and the staff of the **Centre for Infrastructure Management** at **Sheffield Hallam University.**

- **Colin Tarry** and **Alan Duffty** of **Inditherm plc.**

- **The DTi's Knowledge Transfer Partnership (KTP) programme.**

- **The European Union's** FP6 Instrument, Specific Research Funding for SMEs programme and the partners of the LOVACS project.

Candidates Declaration

I herby declare that no portion of the work referred to in this thesis has been submitted in support of an application for another degree or qualification of this or any other institution of learning. All sources of information have been acknowledged.

Candidate

David Gerald Catley – March 2009

Director of studies

Professor Pritpal Mangat –March 2009

For Mum and Dad.

Contents

List of Figures

Chapter 2

Chapter 3

Chapter 4

Chapter 5

Chapter 6

Chapter 7

Chapter 8

Chapter 9

Chapter 10

List of Tables

Chapter 2

Chapter 4

Chapter 5

Chapter 6

Chapter 7

Chapter 8

Chapter 9

Chapter 10

Chapter 1. Introduction

1.1. Background to Research

Concrete is used in most construction projects. Its constituents are a cement binder, typically Ordinary Portland Cement (OPC), proportions of coarse and fine aggregates and water. The strength development of concrete is achieved by adding water which reacts with the binder in a resulting hydration reaction. The rate of hydration and the properties of concrete can be altered by varying the proportions of the mix constituents. The hydration reaction and strength development of concrete depend on two primary factors, time and temperature. Hydration is a reaction which continues at a steadily declining rate over a long time in the presence of free water and unhydrated cement within the concrete matrix. This continued hydration and thus development of strength, is very much an advantage of the material in terms of its long-term durability. However, the rate of strength development within the first few hours and days after casting can be of greater importance particularly if construction times are to be reduced, construction costs minimised and manufacturing volumes increased. Therefore a key consideration in the manufacture of concrete is the rate of strength development at early age.

Increasing the rate of strength development of concrete at early ages has advantages of maximising the production of concrete elements and reducing the time before external forces (e.g. prestress) can be applied. The strength development of concrete depends on the rate of hydration of the cement binder and the availability of water. This reaction can be accelerated by increasing the temperature of the concrete mix at early ages. The strength of a concrete mix depends on the water cement ratio (W/C); the lower this value the greater the strength.

Increasing the temperature of early age concrete up to 70 deg C is used in the manufacture of precast and prestressed concrete. In precast plants it is critical to achieve a minimum target strength of the concrete within a certain time period to allow the removal of the concrete elements from moulds and forms. It is also critical that a target compressive strength of concrete is achieved so that prestressing forces can be applied. The sooner concrete elements can support their dead and imposed loads (e.g. prestressing), the sooner moulds and forms can be freed and reused, speeding up the production of the elements.

Various practices, both thermal and non-thermal, are adopted by precast concrete manufacturers to achieve the early strengths required to maximise production. These include heating the various mix constituents, using excessively high cement contents, using large quantities of chemical admixtures (accelerators) or by heating the ambient environment within which the elements are manufactured. Often all these are used which can significantly increase the cost of precast concrete production. The use of steam is the most commonly

adopted curing technique in precast plants. It is used to heat the concrete either by using steam 'captured' in networks of pipes running adjacent to the concrete moulds; or by 'live' steam either injected into the concrete mix or in make shift tents erected around the moulds in which concrete is cast.

Heat curing concrete with steam is an inefficient practice and rarely provides controlled curing temperatures to the concrete as recommended in approved codes of practice and standards (ACI306, BS8110). The traditional steam curing systems consume large quantities of fossil fuels and produce large volumes of CO_2. For example, a typical precast concrete plant manufacturing 50,000 m^3 of concrete per annum consumes 4,000 – 5,000 litres of diesel per day (Tarmac Precast Concrete plant, Tallington). This equates to CO_2 production of 2,412 tonnes per annum (assuming 2.68 kg of CO_2 emitted per litre of diesel consumed). This equates to approximately 0.5 tonnes of CO_2 emitted per m^3 of concrete produced. A typical precast element is cured for 5 – 18 hours.

A heating medium that conducts heat directly to the concrete rather than heating the concrete moulds via the ambient would provide a more controllable and energy efficient solution for accelerating early age hydration of concrete. This concept is the basis of the following research programme.

1.2. Scope of Research

This research programme will provide direct heat transfer to early age concrete by optimising a unique Conductive Polymer Technology (CPT), developed by the South Yorkshire company, Inditherm plc. The CPT material comprises of a polymer coating loaded with fine carbon particles, to form a conductive compound. The compound is applied to a textile fabric to form a flexible conductive heating membrane.

The CPT material is used to form heating elements of various sizes. The elements are operated by low voltages up to 50 Volts and can achieve temperatures up to 120 deg C. The material can provide a temperature control of +/-1 deg C. CPT elements can be manufactured for small applications such as heated pizza bags or large scale applications such as under pitch heating for sports fields. The heat output of the CPT elements can be changed by altering the width between the conductive rails applied to the material. Electronic control systems can be used with the CPT material to profile the temperature with time.

The proposed research will optimise the CPT material to provide heat to concrete in moulds and also to insitu concrete cast in cold weather. The research will determine relationships between the size of the concrete element, the type of concrete, the external ambient temperature and the CPT curing temperatures. The heat generated by hydration of cement

and its interaction with the CPT temperature will also be considered. The programme will develop CPT curing systems for trials at precast concrete plants and develop guidelines for the design of such curing systems. It is expected that the development of the systems and the greater understanding of the technology will result in commercial opportunity both for the developer of the material and the end users adopting such systems.

1.3. Project Objectives

The project has the following objectives:

I) To gain a full understanding of the hydration of cement within a concrete matrix, reviewing existing curing techniques and literature on concrete curing at elevated temperatures.

II) To evaluate the electrical and thermal properties of the CPT materials including design limitations, design parameters and thermal performance of various CPT materials. Establish some simple, practical design parameters for the use of the CPT for accelerated curing and frost protection of early age concrete.

III) To determine the suitability of CPT for concreting application and to determine the effect of CPT thermal energy input on early age strength and durability, including strength development and shrinkage

IV) To determine the interaction between heat of hydration and CPT thermal input for 'mass' concrete samples

V) To determine the performance of CPT curing under cold ambient conditions including cold joints.

VI) To conduct field trials of CPT in a manufacturing environment for accelerated curing of precast concrete.

VII) To investigate the durability of CPT membrane and curing jackets under extreme conditions simulating the concrete construction environment.

1.4. Thesis Structure

The thesis structure is as follows:

Chapter 2 presents a review of relevant literature. It reviews various concrete curing techniques and strength development of concrete in environments such as precast concrete manufacturing plants and during cold weather. The chapter evaluates comparable curing technologies to CPT and their suitability for thermal curing.

Chapter 3 presents CPT design fundamentals and electrical configurations including application of electrical theory. It also discusses the primary materials used to manufacture CPT and the potential affects these have on its performance.

Chapter 4 describes the various materials and monitoring equipment used throughout the testing programme, including the design and manufacture of various CPT Jackets and blankets for curing concrete, control units and operating systems and concrete mixes used throughout testing.

Chapter 5 describes the test procedure and presents results on the relationship between resistance, current and operating voltage in order to determine if basic electrical theory can be applied and used for the design of CPT elements. The chapter determines if there is a linear proportionality between the applied voltage to CPT elements and the current passing in order to determine if CPT is an ohmic or non ohmic material.

Chapter 6 describes the test procedure for investigating the heat transfer characteristics of the CPT material into early age concrete for accelerated curing. It determines if CPT Jackets are capable of heating small scale laboratory samples to temperatures comparable to existing curing techniques, such as steam curing at 50 – 70 deg C. The chapter considers what affect CPT curing has on properties such as strength and shrinkage.

Chapter 7 describes the test procedure to determine the suitability of CPT for curing large concrete elements comparable in dimension to those cured in precast plants. The chapter considers the interaction between the heat applied through CPT and the internal heat of hydration developed within a concrete element. The chapter considers different heat curing profiles. It also considers how evenly CPT heats concrete and what affect this has on strength development through concrete elements.

Chapter 8 investigates the suitability of CPT for concrete curing applications both on site and within precast curing plants. The chapter presents results determining the suitability of CPT

jackets for curing concrete during low ambient winter conditions for the construction of foundation elements and also for use on precast concrete moulds.

Chapter 9 describes the test procedures used to investigate the durability of CPT and cover materials used to manufacture heating jackets for curing concrete. Results reported in this chapter include the impact of freeze thaw cycles, wetting and drying cycles and direct contact of CPT with concrete. The chapter investigates the effect of holes within CPT elements and the exposure conditions on the long term performance of CPT.

Chapter 10 discusses and analyses the results of the various tests undertaken in Chapters 5-9. It considers the relationships between surface / volume ratio, area heated by the CPT and thermal properties of the concrete elements and strength. The chapter introduces the concept of maturity.

Chapter 12 presents conclusions form the research project and provides recommendations for further work.

Chapter 2. Literature Review

2.1. Introduction

Concrete is a complex material with many variables affecting its characteristics. Achieving the required properties often requires the use of additives or specified curing techniques. Altering the curing conditions can have a dramatic affect on the strength development and durability of the concrete which can be advantageous in some applications. Good curing provides hydration of cement and, therefore, high strength.

Accelerating the hydration processes of cement has many advantages within the concrete industry and in particular the pre-stressed and precast concrete sectors. Increasing the early strength gain of concrete provides economic benefits by increasing production and reducing production area required (e.g. pre-stressing beds). The early strength development of concrete is critical in the manufacture of precast concrete to enable the elements to be removed from the moulds allowing the moulds to be cleaned and prepared for subsequent elements. Early age strength is particularly important within the prestressed concrete sector (precast or in-situ) of the industry, as an adequately high strength is required before the pre-stressing tendons are released to transfer the pre-stress to the concrete. Often this release of prestress is conducted in two stages, the first after 10-15 hours and the second after a period of 3 – 5 days after casting. This process helps to eliminate cracking and improve the ultimate performance of the element. Examples of such elements are car park slabs. These slabs are typically very slender with a low volume / surface ratio, hence, typically do not increase in temperature as a result of hydration and, are therefore, susceptible to low ambient conditions where frost damage may occur. For the purpose of this research thesis the periods early, medium and long term for concrete elements have been defined in Table 2.1 below.

	Early age	Medium age	Long – term
On-site (insitu)	1-5 days	5 – 28 days	>28
Precast	5 – 24 hours	3-10 days	>10

Table 2.1. Definition of early, medium and long-term in terms of concrete strength development

This chapter will review the current methods of accelerated curing, the principles of each method and the potential of adopting CPT technology to provide efficient accelerated curing. The fundamentals of cement and concrete technology which affect the strength development and curing are also reviewed within this chapter.

2.2. Fundamentals of Concrete

Concrete comprises of aggregate (course and fine), cement and water, mixed in suitable proportions to give the required characteristics. When cement (traditionally Ordinary Portland Cement, OPC) comes into contact with water, a chemical reaction of hydration takes place. Over a period of hours the cement will undergo initial set. The process of hydration continues after initial set, leading to strength gain of the concrete. The strength of concrete carries on increasing for many months, however, the strength at 28 days is usually specified in practice, as by this time a high proportion of the final strength (for most concretes) is achieved. If the process of hydration is accelerated, the 28 day strength developed under standard curing conditions (20 deg C 60% RH) can be achieved more rapidly. This can provide major economic gains in terms of production and project duration. If the specified 28-day strength can be achieved at 12 – 24 hours, productivity of standard elements such as railway sleepers can be increased dramatically.

The main strength and durability controlling parameter of concrete is the water / cement ratio, the lower this ratio the greater the strength, assuming the concrete can be fully compacted. However, at very low water cement ratios the mix is so dry it cannot be fully compacted, and therefore optimum strength cannot be gained. Typically water / cement ratios of 0.4 to 0.5 result in mixes of good workability without admixtures. For acceptable mix design, cement content has to be sufficiently high to provide strength and durability, but not too high to cause problems such as excessive shrinkage or cracking. The range of cement contents used in practice are shown in Table 2.2 (Neville 1995 and Cement and Concrete Association).

	Typical Water / Cement ratio's	Typical cement contents
On-site (insitu) Structural	0.4 – 0.5	350 – 500 kg/m^3
Insitu Non structural	0.45 – 0.6	200 – 350 kg/m^3
Precast	0.2 – 0.5	450 – 500 kg/m^3

Table 2.2. Range of cement contents and w/c ratios used for practical mixes (Neville 1995 and Cement and Concrete Association)

Shrinkage is another important property of concrete. Shrinkage occurs due to the gradual removal of water from the cement paste (Neville 1995). Shrinkage is of particular in prestressed concrete as greater shrinkage reduces the tension within prestressed tendons, thereby reducing load carrying capacity of an element. Shrinkage may be of increased concern with high temperature curing of concrete at early ages due to the potential of evaporating free water within the concrete that may otherwise be available for continuous hydration. The formation of micro-cracks within concrete is also a very significant factor when considering the affects of temperature and low humidity curing (SP Shah and G Winter 1968).

Partial replacement of primary concrete constituents such as aggregate or cement with pozzolanic materials such as fly-ash, silica-fume and GGBS is quite common. Although these materials can be extremely advantageous in improving the durability and workability of concrete, their inclusion often retards the early age strength development. This is due to the pozzolanic reaction of these materials, their reaction with $CaOH_2$ being secondary to the hydration reaction of OPC. However, similar to the hydration reaction of cement, this pozzolanic reaction can be accelerated at elevated temperatures. The use of such materials is becoming increasingly common within precast concrete manufacture due to improved performance, economic and ecological pressures. For these reasons their inclusion has been considered throughout this research programme.

2.3. Strength Development of Concrete

Ordinary Portland Cement (OPC) is made from basic materials of lime and clay containing alumina and silicates, which are combined at high temperatures (about 1500 deg C) to produce OPC with the following four major constituent compounds.

Tricalcium silicate	**$3CaO.SiO_2$**	**C_3S**
Dicalcium silicate	**$2CaO.SiO_2$**	**C_2S**
Tricalcium aluminate	**$3CaO.Al_2O_3$**	**C_3A**
Tetracalcium aluminoferrite	**$4CaO.Al_2O_3Fe_2O_3$**	**C_4AF**

These four compounds create calcium silicate hydrate gel (C-S-H) after hydration, forming a solid matrix. The hydration reactions of these compounds are temperature dependant to a greater or lesser extent.

The performance of cement depends on the proportion of glass-like material within the cement clinker. This is controlled by the rate of cooling of the above compounds from high temperatures during manufacture. This affects the degree of crystallisation, and the amount of amorphous (glass like) material present in the cooled clinker prior to it being ground into fine particles (standard OPC or rapid-hardening OPC depending upon its fineness). The rate of cooling of the clinker particularly affects the characteristics of the Dicalcium Silicate compound C_2S, which can have up to four forms.

The proportions of the these compounds can be calculated by using the Bogue composition technique (R H Bogue et al (1955)) given by the following expressions:-

$\% C_3S = 4.07(CaO) - 7.60 (SiO_2) - 6.72(Al_2O_3) - 1.43(Fe_2O_3) -2.85(SO_3)$

$\% C_2S = 2.87(SiO_2) - 0.75(3CaO.SiO_2)$

$\% C_3A = 2.65(Al_2O_3)$

The Bogue composition method underestimates the amount of Tricalcium Silicate C_3S and over estimates Dicalcium Silicate C_2S, because other oxides replace some of the Calcium oxide CaO in the C_3S. This is because chemically pure C_3S and C_2S do not occur in Portland cement clinker.

In addition to these four major compounds, there are other minor compounds such as MgO, TiO_2, MnO_3, K_2O and Na_2O. The minor compounds of Na_2O and K_2O (typically 0.3-1.2% of cement mass), known as alkalis, are of particular interest as they can cause alkali aggregate reaction, leading to disintegration of concrete (Neville A M 1995). These minor compounds are controlled by careful selection of raw materials used to manufacture cements. Typical proportions of the major compounds rapid hardening OPC are given in Table 2.3.

Compound	% by weight
C_3S	65
C_2S	8
C_3A	14
C_4AF	9

Table 2.3. Typical compound compositions within rapid hardening Portland cement (Czernin 1962)

The very rapid hydration reaction of C_3S is retarded by the addition of gypsum, whereas the reaction of C_2S is naturally more gradual. It is therefore the hydration reaction of C_2S which needs to be accelerated for rapid strength development.

2.4. Hydration of Portland Cement

When the compounds C_2S, C_3S, C_3A and C_4AF are combined with water, the aluminates and silicates form products of hydration which in time produce a firm hard mass (Neville A M 1995). All compounds of Portland Cement are anhydrous (contain no water), so when brought into contact with water they are attacked and decomposed forming hydrated compounds. Temporarily supersaturated and unstable solutions are formed. This reaction is exothermic. However, over time, these solutions deposit their excess solids and tend to come into equilibrium with the hydrated compounds produced. These deposited compounds form layers of hydrated silicate on other cement particles slowing down the rate of hydration. When tricalcium silicate C_3S or dicalcium silicate C_2S compounds react with water, calcium hydroxide solution is split off and nucleates and grows in the available capillary pore spaces. The calcium hydroxide splits away and a calcium silicate gel (C-S-H) of lower basicity is formed during the hydration reaction. The composition of the C-S-H gel is not one of constant ratios between the Ca, Si and water as these ratios vary over time. This ratio is often

described as the $CaO:SiO_2$ ratio of the gel. The composition of the C-S-H gels produced during the hydration of the anhydrous silicates changes during the period of the reaction and also varies with the water : cement ratio and the temperature during the hydration reaction. This variation of the development of C-S-H gel with temperature is of particular interest to this research programme.

When finely ground C_3S is mixed with water, the reaction for complete hydration can be given as:-

$2C_3S + 6H = 3C\text{-}S\text{-}H + 3CH$

$2(3CaO.SiO_2) + 6H_2O = 3Ca.2SiO_2.3H_20 + 3Ca(OH)_2$

Complete hydration of C_3S can take over 1 year. However, the hydration process can be accelerated by increasing the fineness of the compound (Lea Frederick M 1970). An OPC with an increased fineness is referred to as rapid hardening OPC (RHPC) which is frequently used in precast concrete plants to increase early age strength development of concrete elements, particularly if thermal curing options are not available.

The process of hydration of C_2S is similar to C_3S. C_2S, however, produces a C-S-H gel with a lower CaO : SiO_2 ratio. As with the C_3S compounds, hydrated layers are formed on the particles, but the coating of C_2S is thicker and increases over time. For complete hydration the reaction can be given as:-

$2C_2S + 4H = 3C\text{-}H\text{-}S + CH$

$2(2CaO.SiO_2) + 4H_2O = 3CaO.2SiO_2.3H_2O + Ca(OH)_2$

The hydraulic reactions for both C_2S and C_3S are exothermic, therefore, the initial rate of hydration is related to the rate of heat produced. The rate of heat produced is not uniform but peaks at different stages. In summary,

- **Tricalcium silicate (C_3S)**. Hydrates and hardens rapidly and is largely responsible for initial set and early strength. Portland cements with higher percentages of C_3S will exhibit higher early strength.

- **Dicalcium silicate (C_2S)**. Hydrates and hardens slowly and is largely responsible for strength increases beyond one week.

- **Tricalcium aluminate (C_3A)**. Hydrates and hardens the quickest. Liberates a large amount of heat almost immediately and contributes somewhat to early strength.

Gypsum is added to Portland cement to retard C_3A hydration. Without gypsum, C_3A hydration would cause a flash set.

- **Tetracalcium aluminoferrite (C_4AF)**. Hydrates rapidly but contributes very little to strength. Its presence allows lower kiln temperatures in Portland cement manufacturing. Gives colour to Portland cement.

2.5. Thermal Properties of Concrete

The two main characteristics that affect heat transfer through concrete are, i) Thermal Conductivity and ii) Specific Heat Capacity. These can be very different depending upon the age of concrete. At early ages the thermal properties are similar to that of a liquid; whereas as its age and strength increases, the concrete will have thermal properties more comparable to a solid with a crystalline structure.

2.5.1. *Thermal Conductivity*

The thermal conductivity of concrete, λ_c, is the rate of heat transport through it. Two main factors influence the thermal conductivity of concrete, the aggregate type and moisture content. Published values of thermal conductivity vary considerably but are typically within the range 1.0 to 2.5 W/m.K. This range is due in part to the different moisture conditions under which tests have been conducted and in part to the variation of aggregate properties (Clauser and Huenges, 1995) (Ciria 660)

With regard to the prediction of temperature rise in hydrating concrete it is only the moisture content within the first day or so that is important. During this period the volume of free water will be reducing as the cement hydrates and the thermal conductivity will reduce accordingly. It has been reported that the thermal conductivity of maturing concrete is about 33 per cent higher than that of hardened concrete (Ruiz *et al*, 2003). Based on this observation the CIRIA 660 report proposed the following relationship between thermal conductivity at time, *t*, λ_{ct}, and the initial thermal conductivity λ_{ci}.

$$\lambda_{ct} = \frac{\lambda_{ci}}{(1.33 - 0.33[a_t / a_{ult}])} \qquad \text{[Eq 2.1]}$$

Where;

λ_{ci}	=	the initial thermal conductivity (W/m.K) at time t=0
λ_{ct}	=	thermal conductivity at time (t) (W/m.K)
α_t	=	the degree of hydration at time *t*
α_{ult}	=	The ultimate degree of hydration
t	=	Time (s)

The initial thermal conductivity can be calculated using a multiphase model from the CIRIA 660 report if the properties of the individual constituents are known. Various models have been used to predict concrete properties, the most common being the series model and the parallel model. The series model is of the form given in equation 2.2:-

$$\frac{1}{\lambda_c} = \frac{v_a}{\lambda_a} + \frac{v_s}{\lambda_s} + \frac{v_{ce}}{\lambda_{ce}} + \frac{v_w}{\lambda_w} \qquad \text{[Eq 2.2]}$$

The parallel model is given in equation 2.3:-

$$\lambda_c = v_a.\lambda_a + v_s.\lambda_s + v_{ce}.\lambda_{ce} + v_w.\lambda_w \qquad \text{[Eq 2.3]}$$

Where;

λ_c	=	Thermal conductivity (concrete)
$\lambda_{a,s,ce,w}$	=	Thermal conductivity of each component (aggregate, sand, cement and water)
$v_{a,s,ce,w}$	=	Volume fraction of each component (aggregate, sand, cement and water) (m^3)

It is generally assumed that the series and parallel models represent the lower and upper bound values respectively. Concrete comprises discrete aggregate and sand particles within a continuous matrix and the true model will lie somewhere between the two estimates. As the aggregate represents about 70 per cent of the volume and the cement paste about 30 per cent, the value of λ_{ci} is estimated by taking a weighted average of the results from the series and parallel models in the ratio 70:30. The results are given in Table 2.4.

Rocktype		Examples	Thermal conductivity, W/m.K						
			Aggregate			Concrete			
						Aggregate and sand		Aggregate with silicious sand	
			Mean	SD	Lower 95 %	Mean	Lower 95 %	Mean	Lower 95 %
Metamorphic	High quartz content	Quartzite	5.8	0.4	5.14	3.2	2.91	3.2	2.91
	Low quartz content	Gneisses, hornfels, schist, slate	2.9	0.6	1.92	1.86	1.37	2.34	2.01
Plutonic	Low in feldspar	Granite, diorite, gabbro	3	0.6	2.02	1.91	1.42	2.37	2.05
	High in feldspar	Syenite, grano-syenite, syentite, syenite porphyry	2.8	0.4	2.14	1.81	1.48	2.31	2.09
Volcanic	Low porosity	Basalt, rhyolite	2.9	0.7	1.75	1.86	1.28	2.34	1.95
Sedimentary	Chemical sediments	Limeston, dolomite, cherty	2.6	0.7	1.45	1.71	1.12	2.24	1.84
	Physical sediments	Sandstone	2.4	0.6	1.42	1.61	1.05	2.18	1.83

Table 2.4. Estimated values of thermal conductivity ay early age (5 days) for concretes using different aggregate types. Aggregate data were obtained from Clauser and Huenges (1995)

It can be seen from Table 2.4 that for many rock types a similar value of thermal conductivity is obtained. Table 2.4 also highlights that the most notable exception is quartzite. Based on the above data from the CIRIA 660 report, proposed values for use in modelling of early age temperature rise in concrete are given in Table 2.5.

Aggregate type	Thermal conductivity of concrete (W/m.K)	
	Sand and aggregate from same rock type	Aggregate from defined rock type with siliceous sand
Quartzite and siliceous gravels with high quartz content	2.9	2.9
Granite, gabbros, hornfels	1.4	2.0
Dolerite, basalt	1.3	1.9
Limestone, sandstone, chert	1.0	1.8

Table 2.5. Proposed values of thermal conductivity of concrete for use in early age thermal modelling (CIRIA 660 Appendix 2)

2.5.2. *Specific Heat Capacity*

The specific heat of concrete is determined by the specific heat of the individual components and their relative proportions. It has been reported that the range for mass concrete may vary from 0.75 to 1.17 kJ/kg deg C (USACE, 1997). This is a very significant variation, indicating that the temperature rise associated with a particular amount of heat input may vary by as much as ± 20 per cent from a mean value of about 0.96 kJ/kg deg C. It is important that a representative value is used in any model for temperature prediction.

Two factors in particular influence the specific heat of concrete, the aggregate type and the water content, the former because it constitutes the largest proportion of the mass and the latter because it is the component with the highest specific heat (greater than 4 times that of the other mix constituents). Reported values of specific heat for rocks range from 0.8 to 1.0 kJ/kg deg C and for a typical structural concrete this variation alone may result in values from 1.0 to 1.15 kJ/kg deg C. Dealing with the water content is more complicated as the specific heat differs for free water (4.18 kJ/kg deg C) and bound water (2.22 kJ/kg deg C) in concrete. To calculate the specific heat for concrete it is necessary to know the relative amounts of free and bound water and this is determined by the degree of hydration.

Calculated early age values for typical structural concretes using aggregate with an assumed specific heat of 0.8 kJ/kg.C are estimated to be in the range from 0.97 to 1.07 kJ/kg deg C with ultimate values generally being 5 to 10 per cent lower, the difference being greatest for concretes with high levels of fly ash or GGBS. Figure 2.1 allows a rapid estimate of specific heat to be made based on the cement content and w/c ratio of the concrete (CIRIA report 660). Where the specific heat of the aggregate is known to be greater than 0.8 kJ/kg deg C, the values for concrete in Figure 2.1 should be increased by 0.8 times the change in the value for the aggregate. So for aggregate with a specific heat of 0.9 kJ/kg deg C, concrete with a value of 1.01 would increase by 0.8.(0.9-0.8) = 0.08 to 1.09 kJ/kg deg C.

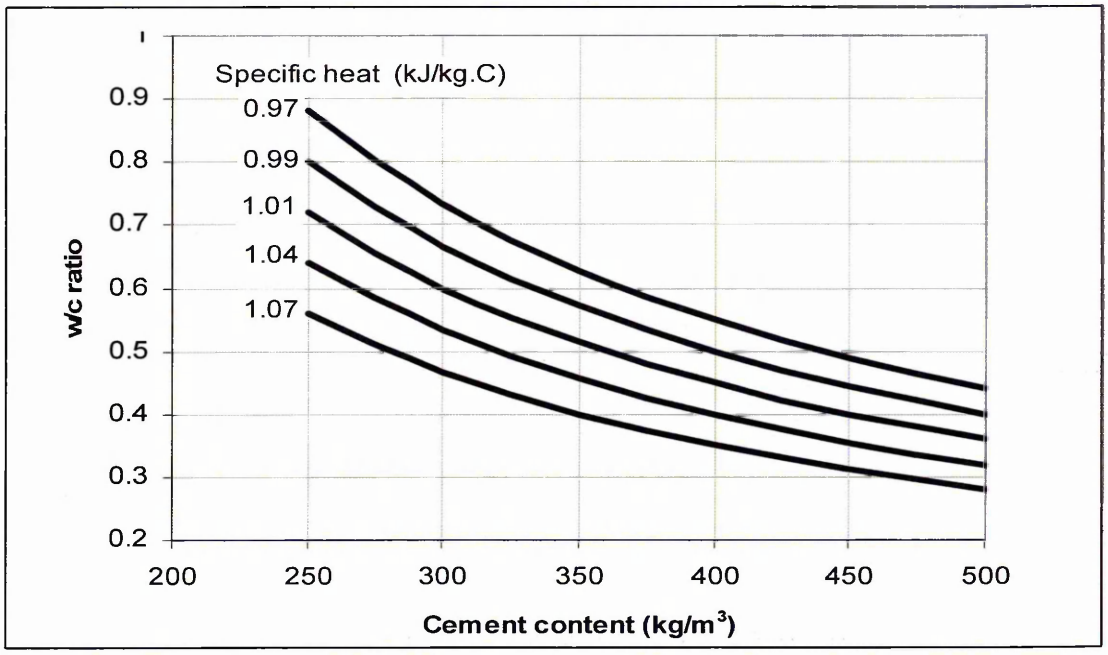

Figure 2.1. The relationship between cement content, w/c ratio and early-age specific heat (assuming the specific heat of the aggregate is 0.8 kJ/kg°C) (CIRIA 660)

2.6. Heat of Hydration

Of the four major strength developing compounds identified in sections 2.3 and 2.4, the reaction of Tricalcium aluminate C_3A is the fastest. The speed of the reaction of C_3A is often slowed down by the addition of gypsum ($CaSO_4.2H_2O$). Gypsum is added to the cement clinker to stop flash setting of the cement paste. However, the purity of the gypsum and free alkalis within the gypsum can cause alkali silica reaction and also influence the false set. When gypsum is not present within the system, C_3A reacts with water to form a variety of crystalline hydration products, C_3AH_6 being the ultimately stable hydration product.

The resulting heat of hydration of the four major compounds for typical CEM I (OPC) is given in Table 2.6.

Compound	Heats of hydration at the given age [J/g]					
	3 days	7 days	28 days	90 days	180 days	360 days
C_3S	410	461	477	511	507	569
C_2S	80	75	184	230	222	260
C_3A	712	787	846	787	913	837
C_4AF	121	180	201	197	306	126

Table 2.6. Heat of hydration of the four major compounds of cement clinker LOVACS Mid term reports - 2 UMM (Warszawa 1991)

C_3A releases the highest amount of heat at early ages (3-7 days). However, due to its higher content in OPC (Table 2.3, section 2.3), C_3S will contribute the greatest towards heat

generated by hydrating cement. Figure 2.2 shows the typical profile of heat generated with time.

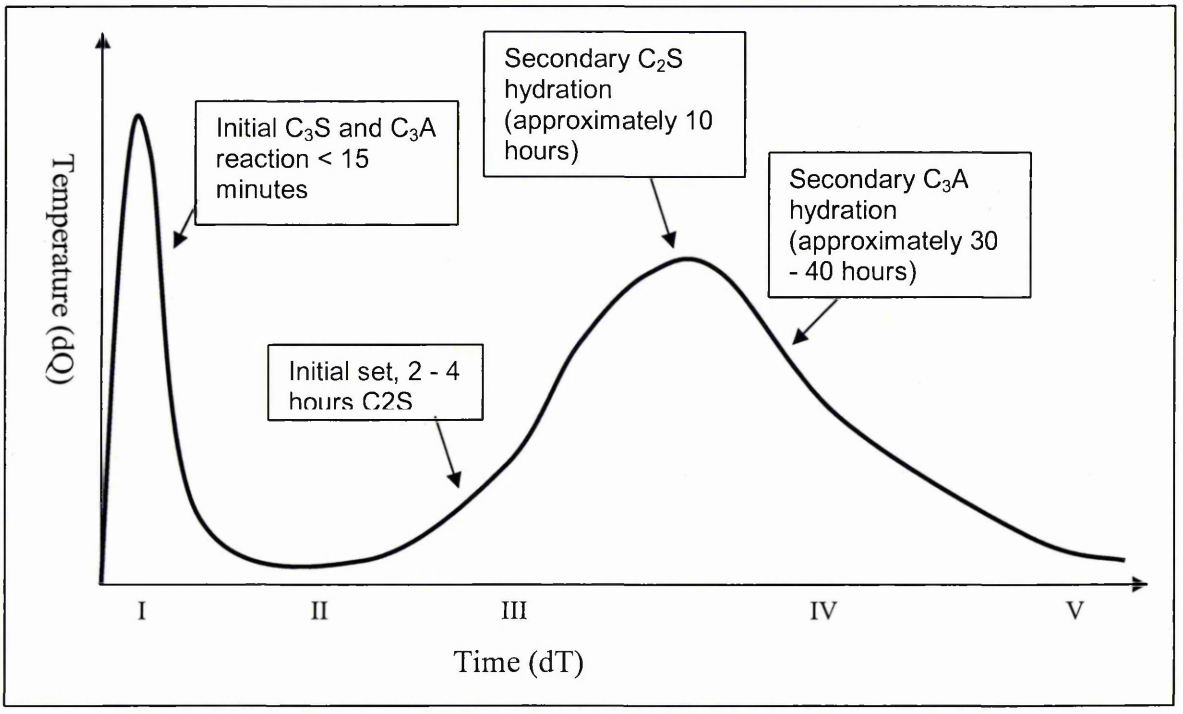

Figure 2.2. Heat generated due to cement hydration within a typical concrete mix

The heat of hydration curve is split into five sections, these are:-

I. The initial reaction (typically 15 – 30 minutes)
II. Induction (typically 1 – 4 hours)
III. Acceleratory period (typically 4 – 10 hours)
IV. Deceleratory period (typically beyond 10 hours)

2.7. Acceleration of the Hydration Reaction with Temperature

The hydration reactions of the four major compounds within cement clinker are temperature dependant. The external temperature during hydration can greatly affect the degree of hydration of cement within a concrete mix as shown in Table 2.7, (Lerch W and C L Ford).

Cement Type	Heat of Hydration developed at:-			
	4 deg C	24 deg C	32 deg C	41 deg C

	J/g	cal/g	J/g	cal/g	J/g	cal/g	J/g	cal/g
I	154	36.9	285	68.0	309	73.9	335	80.0
III	221	52.9	348	83.2	357	85.3	390	93.2
IV	108	25.7	195	46.6	192	45.8	214	51.2

Table 2.7. Heat of Hydration developed after 72 hours (3 days) at different temperatures (Lerch W and Ford C L)

Table 2.7 shows that for a typical Type-I cement the heat generated by hydration can be more than doubled by increasing the curing temperature from 4 deg C to 41 deg C.

The results of Table 2.7 are of particular importance to this study as they show that by efficiently providing uniform heat to concrete at early ages (less than three days), the degree of hydration of cement can be accelerated and thus the rate of strength gain accelerated. It also indicates that once the hydration reaction is triggered by external heat, the internal heat generated by cement hydration within a concrete element will further accelerate hydration resulting in rapid strength gain, particularly if the concrete element is well insulated.

Because the heat given out during hydration progresses over time, and the rate of this progression is dependent on temperature, it is possible to estimate the extent of hydration by tracking time and temperature. This is the concept of maturity and will be considered in greater detail in section 2.17 following the review of existing curing techniques, and the introduction to CPT technology.

2.8. Temperature Effects on Concrete

Typically, increasing the temperature of concrete during early ages increases the early strength by speeding up the hydration reaction. However, increasing the early strength of concrete through high temperature curing is thought to have an adverse affect on the quality of the concrete, resulting in a more porous concrete. (Neville A M 1995).

Increasing the curing temperature of a cement paste produces a greater number of pores due to a lack of diffusion of the hydrated cement products between the particles of the cement paste. The gel / space rule states that increasing the number of pores within a mixture decreases the strength of the cement paste (Neville A M 1995). Increasing the curing temperature for three days to a maximum of 38°C has reduced the 28 day strength by up to 22% (Richardson D N). Other detrimental effect of heating concrete at early ages is the formation of ettringite (Calcium Sulphoaluminate hydrate). This needle like crystal structure, if formed within concrete, can exert internal mechanical pressures having detrimental affects on concrete strength (delayed ettringite formation) (B Mather 1984)(P K Mehta 1993).

Figure 2.3 shows one day and 28 day strengths of concrete samples cured at temperatures ranging from 12 – 50 deg C.

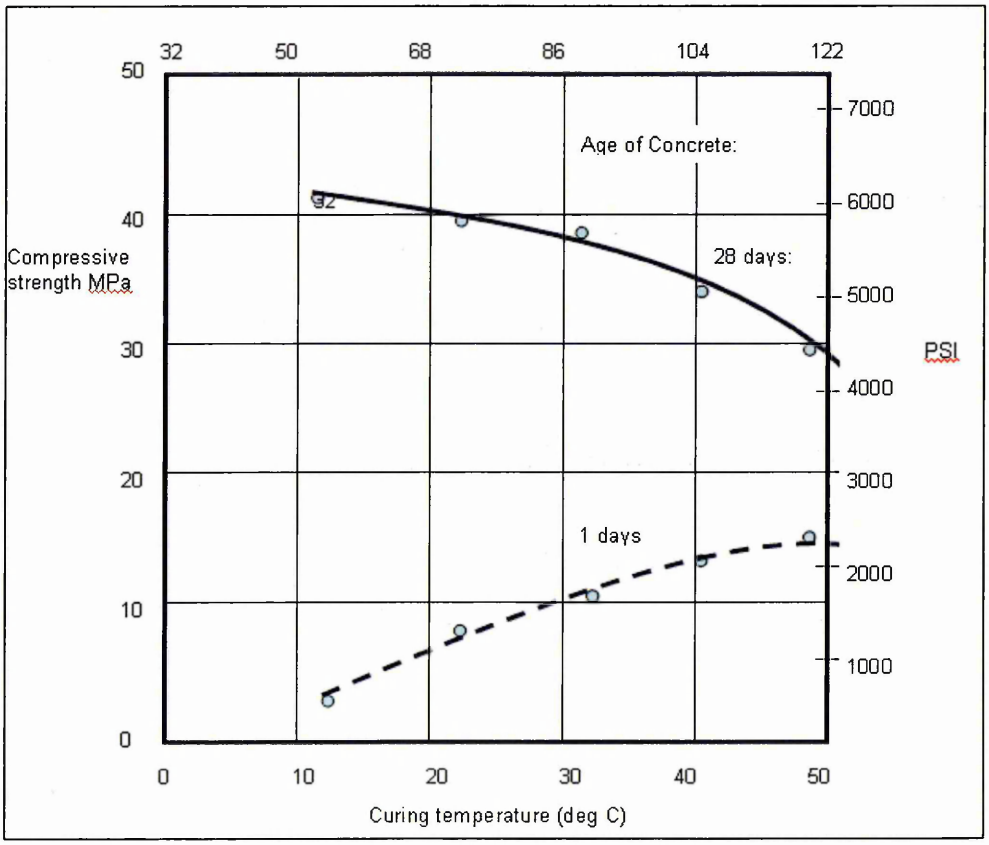

Figure 2.3. Influence of curing temperature on compressive strength at 1 and 28 days (specimens tested after cooling to 23 deg over a period of two hours) GJ Verbeck and RA Helmuth 1968)

Figure 2.3 shows that when using high temperature curing, leads to lower long-term (28 day) strength of concrete, while increasing the rate of early age (1 day) strength gain. Therefore, there is a requirement for a compromise between the loss of longer term strength and the gains in the efficiency of the manufacturing process provided by rapid strength development.

The use of high temperature curing is beneficial for concretes containing pozzolanic materials as partial replacement of OPC. The secondary hydration of such materials is slower than OPC but has the advantage of reducing costs and improving the workability and durability of the mix. Using high temperature curing increases the rate of hydration of such materials.

Sakir Erdogdu and Sirin Kurbetci (1998) have shown that the primary factors determining the behaviour of cements under heat curing are fineness and composition of Portland cements, type and amount of additives used in blended cements, and temperature cycle parameters.

Steam curing is the primary method of heating concrete at early ages to accelerate the rate of strength development.

2.8.1. *Delayed Ettringite Formation*

Ettringite otherwise known as calcium sulphoaluminate, is found in all portland cement concretes. Calcium sulphate sources, such as gypsum, are added to Portland cement to prevent rapid setting and improve strength development they are also present in supplementary cementitious materials and admixtures such as gypsum and other sulphate compounds react with calcium aluminate in the cement to form ettringite within the first few hours after mixing with water. Essentially all of the sulphur in the cement is normally consumed to form ettringite within 24 hours. The formation of ettringite results in a volume increase in the fresh, plastic concrete. Due to the concrete's plastic condition, this expansion is harmless and unnoticed. However, the early age formation of ettringite can become an issue if the strength development of concrete is accelerated and the concrete makes the transition from plastic to chrystaline structure before the formation of ettringite (Portland Cement association 2001)

Delayed ettringite formation refers to a condition usually associated with temperature cured concrete exposed to temperatures over approximately 70°C. Following exposure to such temperatures at early ages, the concrete can undergo expansion and cracking caused by later ettringite formation. This occurs due to high temperature decomposition of any initial ettringite formed and holds the sulphate and alumina tightly in the calcium silicate hydrate (C-S-H) gel of the cement paste. The normal formation of ettringite is thus impeded.

Over time and in the presence of moisture the sulphate and alumina (ettringite) can dissolve from the confines of the C-S-H to form ettringite in cooled and hardened concrete. After months or years the ettringite can form in confined locations within the paste. Since the concrete is rigid and if there are insufficient voids to accommodate the ettringite volume increase, expansion and cracks can occur. In addition, some of the initial ettringite formed before heating may be converted to monosuphoaluminate at high temperatures and upon cooling, revert back to ettringite. Because ettringite takes up more space than monosulphoaluminate from which it forms, the transformation is an expansive reaction resulting in deleterious cracking (RL Day 1992). When considering the application of CPT for accelerated thermal curing of concrete, the presence and consequence of ettringite formation has to be kept in mind.

2.9. Steam Curing of Concrete at Atmospheric Pressure

Steam curing under atmospheric pressure is currently the preferred method of elevated temperature curing within the precast and prestressed sectors of the industry, as it is suited to high volume productions for a variety of concrete units (Patel H H 1996). Steam curing at atmospheric pressure is restricted to temperatures below 100 deg C. The two most commonly used methods are 'free' steam in conjunction with large curing chambers and 'captive steam'. Free steam is applied directly to the exposed and mould surfaces of the concrete. Typically this is conducted in low pressure steam curing chambers or tunnels often transporting the concrete members to be cured on conveyor belts (Neville A M 1995). Figure 2.4 shows the use of live steam to cure a concrete pipe in a typical precast concrete plant.

Figure 2.4. Free steam curing of prestressed pipes (Picture courtesy of Prefabet Precast Concrete Ltd)

The captive steam method usually comprises of portable boxes or plastic covers placed over precast members with steam being introduced through flexible pipes running beneath the forms or the moulds. The aim is to reduce the loss of heat away from the mould and concrete. This is of particular significance in the United Kingdom where the majority of precast concrete plants are located in open sided factories allowing breeze with a cooling effect to pass the moulds, particularly in winter. This is comparable to cold weather concreting on site. Figure 2.5 shows captive steam pipes fixed adjacent to a concrete mould.

There are many disadvantages of applying steam through a captured system relating to the upkeep, maintenance and fuel costs for the system. In terms of performance, although the steam leaving the plant boiler is at temperatures of 80 - 90 deg C, if the pipe network is

particularly extensive, steam at the end of the network can be at temperatures below 30 deg C, or even condense back to water within the pipe. The primary disadvantage is that elements positioned close to the boiler outlet gain strength at a greater rate compared to elements at the end of the pipe network. If all the elements are removed from moulds or prestressing forces are released at the same time, there is a significant risk of failure of the elements towards the end of the pipe network.

Figure 2.5. Captured steam pipe network running adjacent to steel 'Double-T' mould (picture courtesy of Tarmac Precast Concrete Ltd)

However, depending upon its application, steam can have many advantages over other high temperature curing methods because the temperature is applied in conjunction with water (for live steam application). This results in optimum moisture conditions during curing, resulting in greater cement hydration and, therefore, a better quality of concrete on the surface of the member. In addition to the application of steam at atmospheric pressure, steam can be applied at increased pressures and hence higher temperature. High pressure steam curing or Autoclaving is carried out in pressurised steam vessels, with steam pressures above atmospheric resulting in temperatures above 100°C. Compared to steam curing at atmospheric pressure the superheated steam must not be allowed to be in contact with the concrete, as this would cause drying of the concrete (Neville A M 1995). Autoclaving is generally used for the manufacture of aerated concrete blocks where proportions of lime and aluminium powder are used to 'foam' the mix in addition to the standard concrete constituents discussed. The process of Autoclaving is not comparable with steam curing at atmospheric pressure as it increases the strength of cement in conjunction with other mix constituents

such as aluminium powder and lime. For the purpose of this research study, pressurised steam curing will not be considered further.

2.10. Hot Mix Curing

Hot mix curing relies on raising the temperature of the fresh concrete to at least 32°C (Neville 1995). This can be done by either heating the aggregates or mix water prior to mixing. When heating the constituents, consideration has to be given to the order in which the concrete constituents are mixed - hot water at 70 deg C may be used to elevate the mix temperature by 20 deg C, but direct contact with the cement has to be avoided to prevent flash set, unwanted hydration and chemical reactions detrimental to the long term performance of the concrete (National Ready Mix Concrete Association 1960) (BS 8110).

Hot mix curing is achieved either by preheating the constituents or injecting steam into the mix, directly or through metal coils. The process allows the removal of formwork at very early ages (after several hours). However, hot mix curing can reduce the long term strength of the concrete by 10 to 20% (Neville 1995). To achieve maximum results the use of well insulated formwork is required as this reduces temperature gradients within the concrete element.

Hot mix curing is used in cold climates, at temperatures below 0°C. ACI 306R-88 defines cold weather as the average of the maximum and minimum temperatures recorded at three consecutive days being less than 5°C as well as when the air temperature during at least 12hrs in any 24hr period is less than 10°C. Care has to be taken when preheating constituents to avoid concrete with undesired characteristics. Neville advises that heating the water above 60°C to 80°C can result in a flash set of the concrete mix. The National cold Weather Ready Mix Association (USA) advises that aggregate should not be heated above 52°C and not to use frozen aggregates.

As with all temperature curing methods, care has to be taken to avoid large temperature gradients within a concrete member. In cold weather such temperature gradients can be caused by placing concrete against frozen ground, using frozen formwork, or removing formwork too quickly.

2.11. Direct Electric Curing

Early strength of concrete within the precast industry is often gained by using direct electric curing. Direct electric current was first used in the railway sleeper industry with single cell moulds (Heritage I et al 2000), however, developments of the technology can be applied to multiple mould situations. There are restrictions to adopting such techniques using high current and voltages to power heating elements over lengths exceeding 150m (not un-common for extruded prestressed beams). The basic concept of direct electrical curing is to

use the prestressed tendons within the concrete to conduct electricity and act as heating elements. However, consideration has to be given to the safety and isolation of such systems. Such systems have been trialled with varied success. Further consideration has to be given to the mode of powering the curing system; AC supply (instead of DC) risks the potential of electrolysis. Neville 1995, also states that when passing current through concrete alternating current is used to avoid hydrolysis of the cement paste (Neville 1995).

2.12. Other Temperature Curing Techniques

Other thermal curing techniques used include passing current through insulated resistance wires embedded in the concrete member, heating reinforcement within the concrete and using electrical blankets. Passing current through insulated electric wires embedded within the concrete is similar to the direct electric current technique discussed above, and also the steam curing method through embedded pipes within the concrete. The insulated electric curing uses 'trace' heating cables. These cables typically operate at 240 Volts a.c. In all these systems, the spacing between adjacent heating elements is critical to ensure a fairly uniform heating profile.

The use of heating blankets has been investigated on a much smaller scale than the other curing techniques. This is primarily due to durability and performance. Traditionally the blankets use either electrical heating trace elements as described above or flexible pipe networks through which steam (or hot water) is passed. Again, as mentioned above, the uniformity of heating is dependant upon the spacing of the heating circuit. A consequence of this is that if the spacing is doubled, either the electrical power required or the volume of steam required is doubled. The performance of such blankets is highly dependant upon the insulation used as trace heating elements and flexible pipes convect heat through the whole circumference and not just the surface area in contact with the concrete or mould.

Figure 2.6 shows the extent to which contractors will position flexible hoses adjacent to concrete moulds prior to casting and covering with insulation blankets. This technique is particularly adopted for cold weather concreting. The thermal blankets or external heating is applied to a) heat the ambient around a cast concrete member, or b) preheat the mould or form prior to casting.

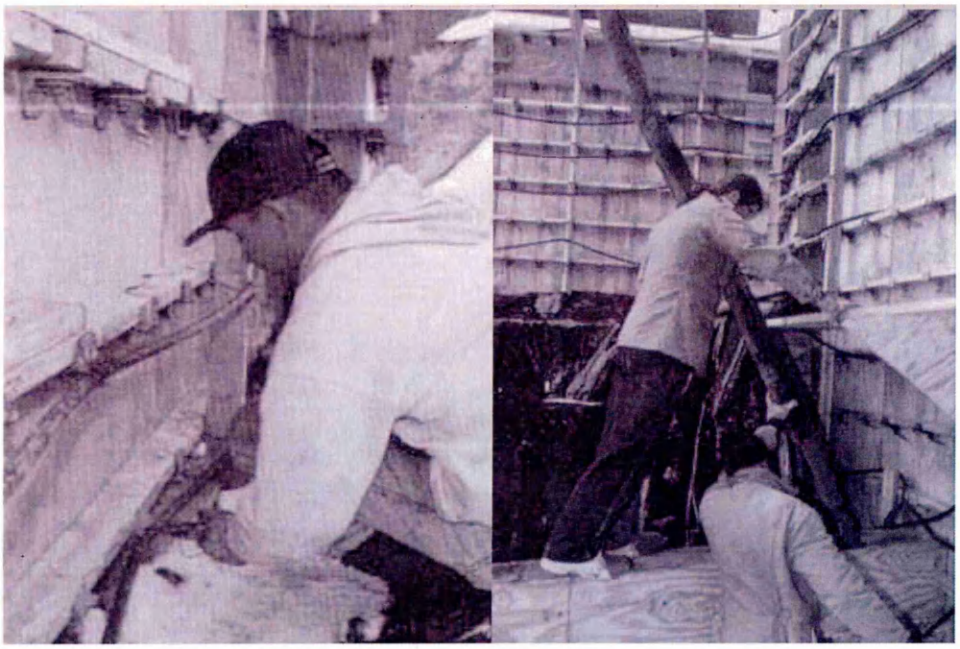

Figure 2.6. Positioning of hoses prior to casting and insulating with blankets

There are other curing techniques employed within laboratory conditions, such as heated water baths, but these are not practicable for general use in fabrication plants or on site.

2.13. Conductive Polymer Technology

Conductive Polymer Technology (CPT) is a thermal heating material. It is a low resistance flexible fabric that provides uniform heat distribution without localised hot or cold spots. The material is manufactured by loading a conductive polymer with conductive particles (the manufacture and design of the CPT material is considered in Chapter 3.0). The material can be configured to various dimensions to fit individual applications, providing surface heat densities of up to 300 W/m^2. Typically the elements operate between 24 - 50 Volts to provide highly controlled temperature profiles up to 120 deg C using very low power input compared with traditional systems which operate at 240 V or 110 V or steam systems.

The material provides heat over a large surface area compared to the 10 – 15mm of electrical trace heating or water pipes and thus it consumes significantly less energy per m^3 production of concrete. A part of the review prior to undertaking this research was to compare the typical energy consumptions of CPT systems and steam curing. Results of this analysis are given in Appendix 1 (Tarmac Precast Concrete case study: CPT vs. Steam curing). In summary, based on typical CPT and steam curing systems adopted within a concrete plant, the total energy used to produce one m^3 of concrete is given in Table 2.8.

	Energy Consumption per m^3 of concrete	Energy Consumption per m^3 of concrete (Joules)
CPT Materials	64kWh @ £0.06/kWh/m^3	230 x 10^6 Joules / m^3
Steam	26.21lit/m^3	1040 x 10^6 Joules / m^3

Table 2.8. Energy comparisons of CPT heating and steam curing

(Assuming; 1 KWh = 3.6 x 10^6 Joules, 1 Litre of diesel = 40 x 10^6 Joules)

Unlike captured steam lines, the performance of the CPT technology can be tailored from mould-to-mould and its performance is not affected by its position along the line from say, the boiler plant.

Heating systems using the CPT optimise insulation layers, minimising the heat loss from the rear of the heating material, the mould and the concrete within it. Unlike traditional heat curing systems, the application of CPT can be controlled to within 1 deg C depending on the electronic control selected. It is thought that this advantage over the other antiquated systems provide optimum curing regimes to maximise performance for early age strength and cold weather concreting.

2.14. Optimum High Temperature Curing Profiles

Optimum cycles of high temperature curing are required to achieve maximum early age compressive strength. Typically, all the methods listed above have been applied using a common curing profile (with the exception of hot mix curing) shown Figure 2.8 (Saul). It consists of a pre curing period, a heating period, a sustained temperature period and a cooling period.

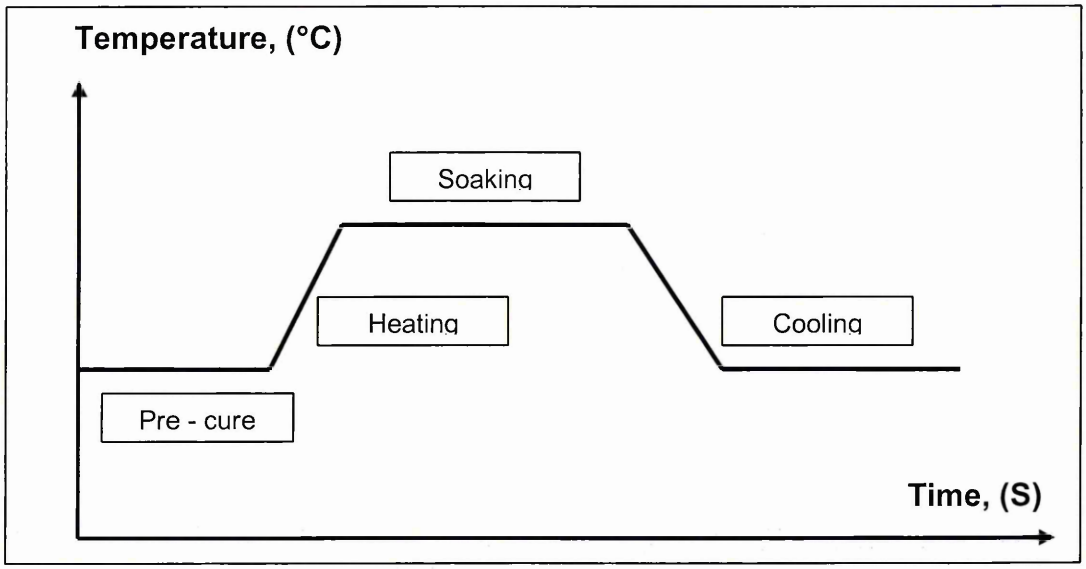

Figure 2.8. General temperature profile for accelerated curing of concrete

Literature has highlighted that the typical duration of a temperature cycle is 18 – 24 hours, to achieve maximum strength at 1 day and also to fit in with working shifts. Increasing the duration of high temperature curing further is restricted due to economic constraints: If large concrete members are required to be cured for up to three days, expense would become a major factor. Sakir Erdogdu and Sirin Kurbetci (1998) applied heat treatment cycles with a total duration of 22 hours to minimise the degree of structural disintegration of mortar specimens. This is similar to the curing cycle given by ACI 517.2R-87 which suggests a delay period of 2 to 5 hours (from the time of mixing), heating at a rate of 22-44°C per hour up to a maximum temperature of 50 - 82°C, storage at a maximum temperature and a cooling period within 18 hours. In comparison Patel et al (1996) used a cycle of a 7 hour delay period, a 3 hour heating period, a 9 hour dwell and a 3 hour cooling period (total 22 hour curing period). This was based upon a precast concrete manufactures' method for curing OPC mixes with PFA replacement.

The delay (pre-cure) period before heating is applied is of particular importance to the curing of concrete and the strength achieved at early and later ages. Neville A M (1995) reports that temperature curing used to accelerate early strength leads to a partial reduction in the long-term strength of concrete. This reduction for steam cured concrete is due to the presence of very fine cracks (micro-cracks) caused by the expansion of air bubbles in the cement paste. This trapped air expanding during temperature application results in tensile forces within the cement paste. To reduce cracking caused by air bubble expansion, Neville suggests a delay period following the casting of the concrete to allow an initial set of the concrete which provides enough resistance to the tensile forces caused by the expanding air. The delay required before applying steam curing depends on the temperature of the steam. Shideler

and Chamberlin (1949) provided data relating to the curing temperature and initial delay period, which were plotted in graphical form by Saul (1954). Figure 2.9 shows the optimum delay periods for steam curing taken from the graph plotted by Saul (1954). Figure 2.9 shows that lower curing temperature requires lower delay period. For each steam curing temperature, there is an optimum delay period. Using a shorter or longer delay period adversely affects the long-term strength of the material. Sakir Erdogdu and Sirin Kurbetci (1998) varied all periods of the curing cycle and found that generally a four hour delay period provided the greatest compressive strengths at 24 hours. A four hour delay period was also used in investigations of the microstructure of concrete cured at elevated temperatures (H H Patel et al 1994).

Temperature deg C	Optimum delay, hours
38	2
54	2
74	6
85	6

Table 2.9. Optimum delay periods, Saul (1994)

The desired delay period also depends on the size and shape of the concrete elements, the water content and the type of cement used within the mix.

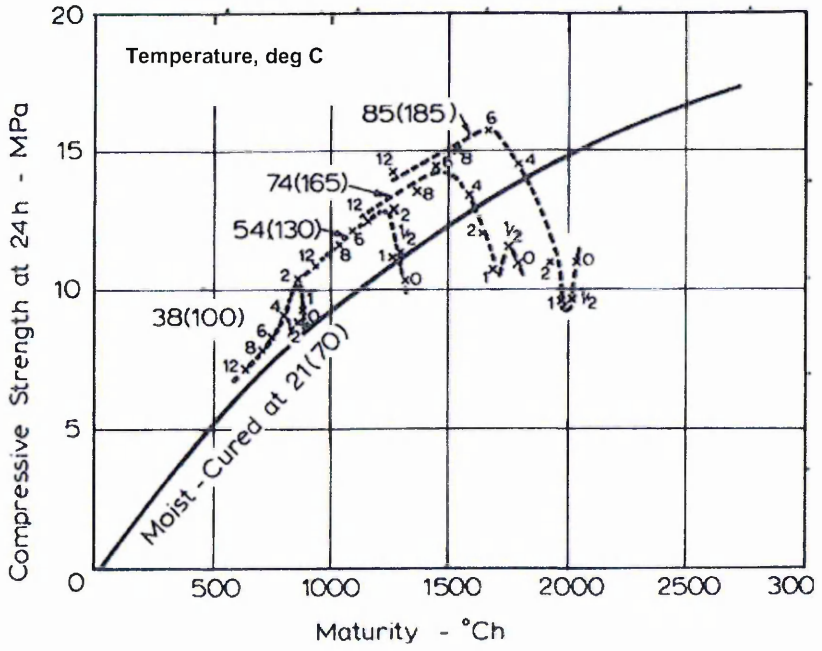

Figure 2.9. Effect of delay in steam curing on early age strength with maturity (Small figures indicate the delay in hours before curing at the temperature indicated (Neville 1995)

Figure 2.9 shows that the optimum delay period ranges from 2-6 hours. It shows for all temperatures that if heat is applied within the first hour after casting there is a more dramatic difference in the compressive strength of the concrete at 24 hours compared with heat being applied at 2-6 hours (the optimum delay period). The graph also clearly shows that the lower the curing temperature, the shorter the delay period required before high temperature curing can be applied. It also shows that for each curing temperature there is an optimum delay period, increasing with temperature; 2 hours for 38 deg C, 6 hours for 85 deg C it is 6 hours.

The optimum curing temperature depends on the type of concrete; the constituents and the mix proportions. Figure 2.9 shows that the optimum temperature for achieving maximum strength at 24 hours was 85°C. This agrees with the results of Sakir Erdogdu and Sirin Kurbetci (1998), who obtained a corresponding temperature of 80°C. They also concluded that curing temperatures above 80°C have a detrimental affect on the strength of the concrete. H H Patel 1994 also concluded that specimens cured at 85°C showed micro-cracks forming a prominent network. In practice such a high temperature may not be achievable by traditional temperature curing methods, and is more likely to be in the region of 70°C.

The rate at of heating and cooling is of particular importance in minimising the risk of micro cracking and reducing evaporation of water from concrete. The size of the member is also important as steep temperature gradients throughout the member during curing are to be avoided. Neville (1995) states that a trial and error approach is necessary, however ACI 517.2R-87 recommends rates ranging between 33°C per hour for small units and 11°C per hour for larger units. Sakir Erdogdu and Sirin Kurbetci (1998) used a rate of 15°C per hour, H H Patel (1994) used a rate of 13°C per hour for laboratory samples cured at 85°C for 6 hours.

Unlike traditional curing techniques, CPT can be controlled to a specific heating rate as recommended in ACI 517.2R-87 and Erdogdu and Kurbetci. Also, unlike other curing techniques, CPT 'gently' heats a concrete. The temperature of the CPT rises along with the concrete being cured. As well as controlling the rate of heating, the cooling rate of a concrete element can also be controlled by the CPT. It is predicted the mode of heating provided by CPT at controlled rates of heating will reduce the impact on ettringite formation as discussed in section 2.8.1 and the impact on long-term strength of concrete. In addition, because of the flexible nature of CPT, it can be 'wrapped' and formed in the form of a jacket around an element being cured, thus reducing evaporation and reducing the risk of microcraking again providing a more durable concrete.

2.15. Standards for Thermal Curing of Concrete at Early Ages

The review of literature provides no set standards that govern the use of steam curing. Steam curing methods also appear to be based on experience, possibly as a result of a lack of control over such methods.

2.16. Cold Weather Concreting

ACI 306R – 6 recommends the best practice for cold weather concreting. The standard defines cold weather conditions as:-

> *"A period when, for more than 3 consecutive days, the following conditions exist.: 1) the average daily air temperature is less than 5 deg C (40 deg F) and 2) the air temperature is not greater than 10 deg C (50 deg F) for more than one-half of any 24 hour period."*

The average daily air temperature is the mean of the highest and lowest air temperatures occurring during 24 hours from midnight to midnight. The standard recommends procedures for the protection of concrete at early ages to prevent frost damage.

The standard also recommends additional protection required for concrete to gain adequate strength in cold weather. It recommends curing temperatures of concrete, temperature records during winter conditions, the temperature of mix constituents prior to mixing, the preparation of areas prior to placing the concrete, the duration of protection, methods to determine the insitu strength and types of protective insulation covers. Cold weather conditions affect the rate of hydration of cement; for ordinary Portland cement the rate of hydration is halved by every drop of 10 deg C.

Winter curing protection is required to maintain the temperature of the concrete above the critical saturation level. Above this point, the concrete will develop a compressive strength above 3.5 N/mm^2. A typical concrete mix will achieve a minimum strength of 3.5 N/mm^2 after two days when cured at temperatures above 5 deg C, (ACI 306 1997). At this strength the concrete can resist a single freeze thaw cycle. After achieving strength of 3.5 N/mm^2 concrete will achieve its ultimate potential strength with time despite exposure to cold conditions. Curing concrete in cold weather should follow the recommendations in CSA Standard A23.1, and ACI 306 (1997), Cold-Weather Concreting

United Kingdom standards relating to the curing of concrete at low temperature include The British Rail Specification, EHQ/SP/0/105. It states that during 'Concreting in cold weather' the contractor shall keep accurate records of the maximum and minimum air temperatures to gauge if weather precautions should be taken. It also states that the minimum air temperature

at the time of placing should not be less than 10 deg C, and that all surfaces with which the fresh concrete will come into contact, including those of formwork, reinforcement and hardened concrete, should be free from snow, ice and frost preferably at a temperature close to that of fresh concrete. For curing purposes, the British Rail Specification states that curing and protection of the concrete is required against premature drying-out from solar radiation and wind, and from low temperatures and frost. With regard to the striking of formwork, the specification refers to BS 8110-1:1997 Structural use of Concrete, detailing the minimum period prior to striking.

2.16.1. *BS 8110-1:1997 Structural use of Concrete. Code of Practice for Design and Construction*

Tables 2.10 and 2.11 have been extracted from BS 8110-1:1997 Structural use of Concrete.

Type of concrete	**Ambient Conditions after casting**	**Minimum periods of curing and protection**	
		Average surface temperature of concrete	
		5 deg C to 10 deg C	t deg C (any temperature between 10 deg C and 25 deg C)
		Days	Days
PC 42.5 or PC 52.5 to BS12	**Average**	**4**	$\frac{60}{t+10}$
SRPC 42.5 to BS 4027	**Poor**	**6**	$\frac{80}{t+10}$
All cements indicated in Table 1 of BS 5328-1:1997 except for PC 52.5 to BS 12, SRPC 42.5 to BS 4027 and supersulfated cement	**Average**	**6**	$\frac{80}{t+10}$
	Poor	**10**	$\frac{140}{t+10}$
All	**Good**	**No special requirements**	

Table 2.10. Minimum periods of curing and protection

Table 2.10 shows that the number of days recommended for cast concrete to be protected is a function of the average surface temperature of the concrete. The minimum recommended time of curing and protection is 4 days for surface temperatures above 5 deg C. When the surface temperature of the concrete is at 25 deg C the minimum curing and protection time is 2-3 days.

Table 2.11 recommends the minimum period before striking of formwork after casting. The minimum recommended time for striking formwork is 12 hours, for vertical formwork on concrete with a surface temperature of 16 deg C and above.

Type of Formwork	**Minimum Period before striking**	
	Surface temperature of concrete	
	16 deg C and above	t deg C (any temperature between 0 deg and 16 deg C)
Vertical formwork to columns, walls and large beams	**12h**	$\frac{300}{t+10}$ h
Soffit formwork to slabs	**4 days**	$\frac{100}{t+10}$ days
Soffit formwork to beams and props and slabs	**10 days**	$\frac{250}{t+10}$ days
Props to beams	**14 days**	$\frac{360}{t+10}$ days
NOTE This table can be applied to PC and SRPC of higher cement strength classes		

Table 2.11. Minimum period before striking formwork

Table 2.10 and 2.11 can be used to estimate the minimum period for striking formwork which can be achieved when using a thermal curing method, such as CPT. It is assumed that the most vulnerable zone for frost attack will be the surface zone which records the lowest temperature. Assuming a concrete element cured at 2 deg C (Element B) and an identical element cured and maintained at 35 deg C surface temperature (Element A), the following formwork striking times can be calculated.

$$T = \frac{300}{t+10}h$$

Minimum time before the striking of formwork:

$$\text{Element A} = \frac{300}{35+10} = 12 \text{ hours}$$

$$\text{Element B} = \frac{300}{2+10} = 25 \text{ hours}$$

The example shows that by increasing the average surface temperature of an element, the period prior to the striking of the formwork can be reduced dramatically, in this case by 18 hours.

2.17. Maturity Method

The maturity method is a technique which combines the effects of time and temperature on the strength development of concrete (Carino, N.J. and Lew H.S. 2001). It relies on the temperature history of the concrete to estimate strength development during the curing period when moisture is available for cement hydration. The temperature history, monitored at strategic locations, is used to calculate the *Maturity Index*. The *maturity index, also* known as the temperature-time factor (Carino, N.J. and Lew H.S. 2001), is based on the maturity rule that states "*Concrete of the same mix at the same maturity (reckoned in temperature-time) has approximately the same strength whatever combination of temperature and time go to make up that maturity".* The maturity method can be adopted to determine the in-situ strength of concrete if specimens are cured at multiple, constant temperatures and the compressive strength is determined at multiple intervals. The maturity index can be recorded or calculated from temperature history of a concrete element and then compared to the pre-determined data in graphical form to obtain the approximate strength of the in-situ concrete. The maturity equation is expressed as the product of curing time and temperature. For example, the *Nurse-Saul expression* is:

$$M = \sum_{0}^{t} (T - T_0)\Delta t \qquad \text{[Eq 2.4]}$$

M	=	maturity (usually in deg C-hours or deg C-days)
Δt	=	time interval
T	=	average temperature of the PCC during the time interval, Δt, being considered
T_0		datum temperature - the temperature below which PCC shows no strength gain with time (-10 deg C is most commonly used)

2.18. Controlled Permeability Formwork

Controlled Permeability Formwork (CPF) is not a means of temperature curing, but a newly developed type of formwork that gives greater durability and resistance to chemical attack of concrete members. CPF is designed to improve the surface zone of a member by creating a better quality of concrete on the surface. It is envisaged that CPT could potentially be incorporated into CPF systems. CPF uses a textile liner on the formwork allowing air bubbles and surface water to drain out, but retaining cement particles (J S Coutinho 2001). The use of a textile liner layer allows the water / cement ratio on the surface of the member to be reduced, resulting in the quality of the concrete at the surface of the member being superior. This provides a very dense surface skin as the textile liner makes enough water available for curing at the right time to achieve increased hydration. J S Coutinho (2001) performed investigations comparing traditional formwork with Controlled Permeability Formwork and found that the surfaces cast against the CPF had no blowholes. The CPF (Zemdrain) also gave significant increases in the surface hardness of the concrete with an increase of 68%. An improved quality of the concrete on the surface of a member can have many advantages such as greater resistance to chemical attack by hazardous substances such as chlorides, and a reduction in damage caused by freeze thaw cycles. Combining the effects of CPT with CPF has the potential of providing both optimum temperature and moisture conditions to concrete resulting in high strength durable concrete to be produced at early ages. This could be of particular application in maritime conditions where construction times may be minimised and exposure conditions are severe.

2.19. Temperature Gradient Control

Cracking is usually caused by temperature gradients within elements such as mass concrete where internal heat generated by hydration can be in excess of 80 deg C. a. If the extremities of such a mass element are exposed to cold ambient conditions the difference in temperature throughout the element can induce internal stresses resulting in cracking particularly in early age concrete.

This is also relevant to slender structures with high surface / volume ratios. Such elements do not have sufficient thickness / mass of concrete to allow for heat generated through hydration to compensate for cold ambient conditions, thus making them more susceptible to cold ambient conditions as heat is lost through the increased exposed surfaces.

It is envisaged that CPT systems can be used to match internal concrete temperatures to the surface zone temperatures of concrete elements reducing large temperature gradients in mass concrete elements and heating / insulating more slender elements. This can be done by casting thermocouples within the core of a concrete element and feeding the internal

temperature to an electronic control which can control and match the CPT curing temperature at the surfaces of the concrete element to the same temperature.

2.20. Optimisation of Cement Content and Pozzolans

By adopting a thermal curing technique such as CPT, there is the potential to increase the efficiency of a concrete mix by using less cement, or by partially replacing cement with a pozzolan such as Pulverised Fuel Ash, or GGBS (latent hydraulic cement). The use of these materials is more economical than cement and they typically produce concrete with higher long term strengths, greater durability and retard the formation of ettringite which can be detrimental to long term performance. In addition if greater strengths at early ages can be achieved by using pozzolans and a suitable method of heat curing, stronger concrete elements can be produced more economically.

2.21. Discussion

The literature review provides no set standards that govern the use of steam curing or other high temperature curing procedures. The methods used in practice appear to be based on experience and are often applied for periods of time to fit into typical work shifts. There is also an emphasis on minimising water loss from the concrete, either by covering members during curing, or applying temperature in conjunction with steam.

CPT as a curing technique could be used in similar applications to steam curing, giving a greater control of temperature cycling than is available with steam curing. CPT, however, would not have the advantage of supplying water/steam for curing. However, CPT blankets seal the concrete being cured and retain moisture for concrete curing. Other advantages such as a reduced shrinkage would arise compared to high temperature curing accompanied by drying of concrete. The optimum temperatures for accelerated curing are in the region of 30°C –80 °C, however accurate control of temperature is difficult in the steam curing methods. A high degree of control, however, is achievable by CPT, which can include cycles of different temperature curing.

In general a curing temperature of 80°C provides optimum results, a delay period before applying heat was 2 – 6 hrs.

2.22. Concluding Remarks

- The use of high temperature curing to increase early age strength is widespread within the concrete industry
- The most commonly used method is atmospheric steam curing
- Reducing moisture loss during curing is essential

- Current curing methods do not provide good temperature control
- Delay periods of 2 – 6 hours are required to optimise curing
- Heat curing cycles are typically between 10 – 24 hours

Chapter 3. Theory of Conductive Polymer Technology

3.1. Introduction

Conductive Polymer Technology (CPT) material comprises fine carbon particles uniformly dispersed in an elastomeric carrier at weights of 20 % to 75% to carrier polymer levels. Preferably, the carrier is an elastomeric polymer. The carbon particles and the elastomeric polymer are formed together into a compound. After checking its properties, the compound is manufactured into a web or flexible sheets and then applied to a flexible cotton backing. The electrical resistance of the material per unit area can also be decreased by applying additional layers. The CPT can be configured into electrical elements by applying conductive silver tape (conductive rails), allowing a potential to be applied through the element.

CPT material is manufactured in runs of up to 100 metres. Individual elements are then cut to the desired size. Figure 3.1 shows the CPT after manufacture. The CPT is manufactured to various resistances to enable appropriate heating to be provided from individual elements. When a charge is passed between two points on the material, its resistance per unit area generates a uniform temperature across the surface between the two points, due to the electrical agitation and bonding of the sharp edged carbon particles. It is assumed that the heat (energy) on the surface of the CPT is caused by friction and interaction of the carbon particles during agitation. The generation of a uniform temperature over the surface results in the technology being suitable for a variety of applications.

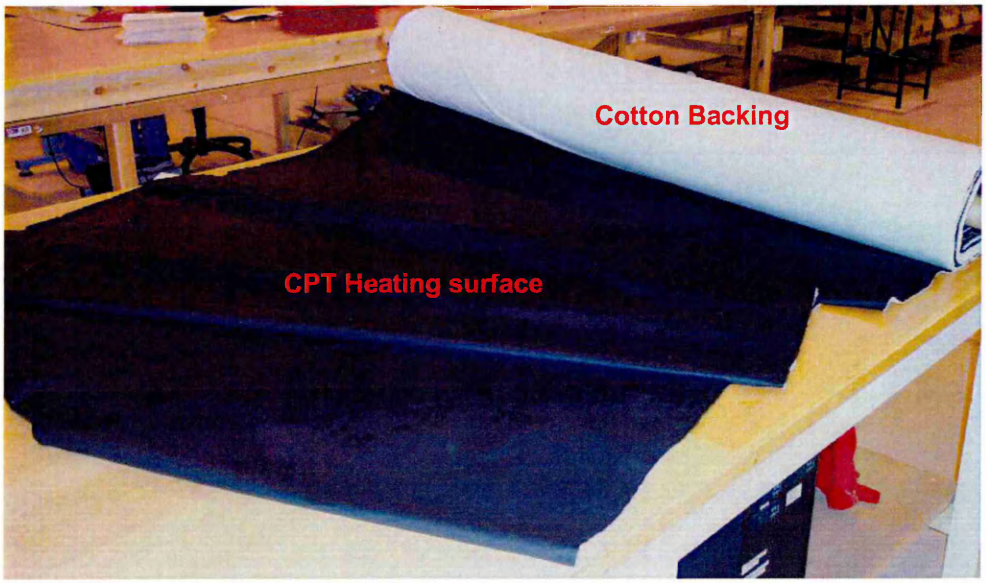

Figure 3.1. CPT prior to configuration into heating elements

The heat output or heat density (W/m^2) on the surface of CPT heating elements is configured by varying three design variables; the resistance (R) of the material, the spacing between

conducting rails (see Figure 3.5) and the Voltage (potential difference) applied to the material. These three variables are discussed briefly in the next section.

3.1.1. *Ohms Law*

The electrical resistance of any material is measured as the potential difference required per unit current in that material, hence the resistance (R) is quantified as:-

$$R = \frac{V}{I} \qquad \text{[Eq 3.1]}$$

V = Voltage (Volts)
I = Current (Amps)
R = Resistance (Ohms)

Equation 3.1 shows that a potential difference (V) is required to maintain an electrical current (I) through a material, therefore all materials have a resistance (R). It is also known that some materials become more heated than others despite the rate of flow (electrical current) being the same.

Ohms law applies to Ohmic conductors such as metals, such that;

$$V \propto I \qquad \text{[Eq 3.2]}$$

Or

$$V = IR \qquad \text{[Eq 3.3]}$$

Where R is a material constant. The relationship is shown in Figure 3.2

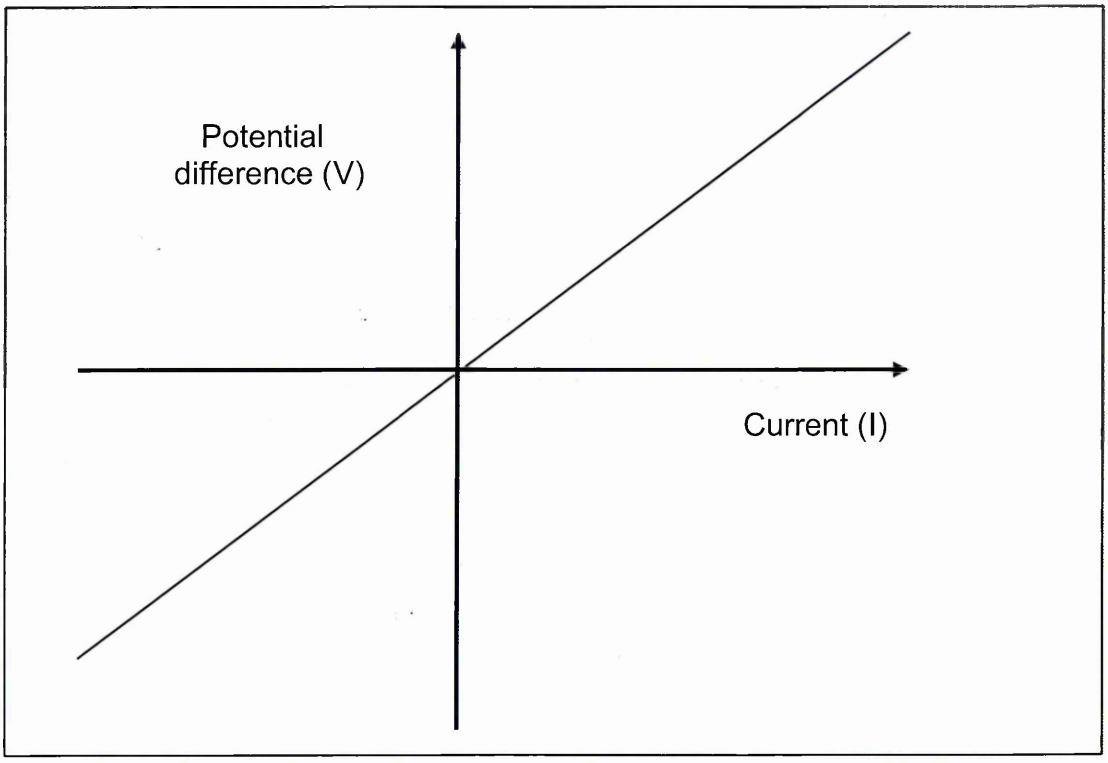

Figure 3.2. Linear relationship between voltage V and Current I for an Ohmic metal

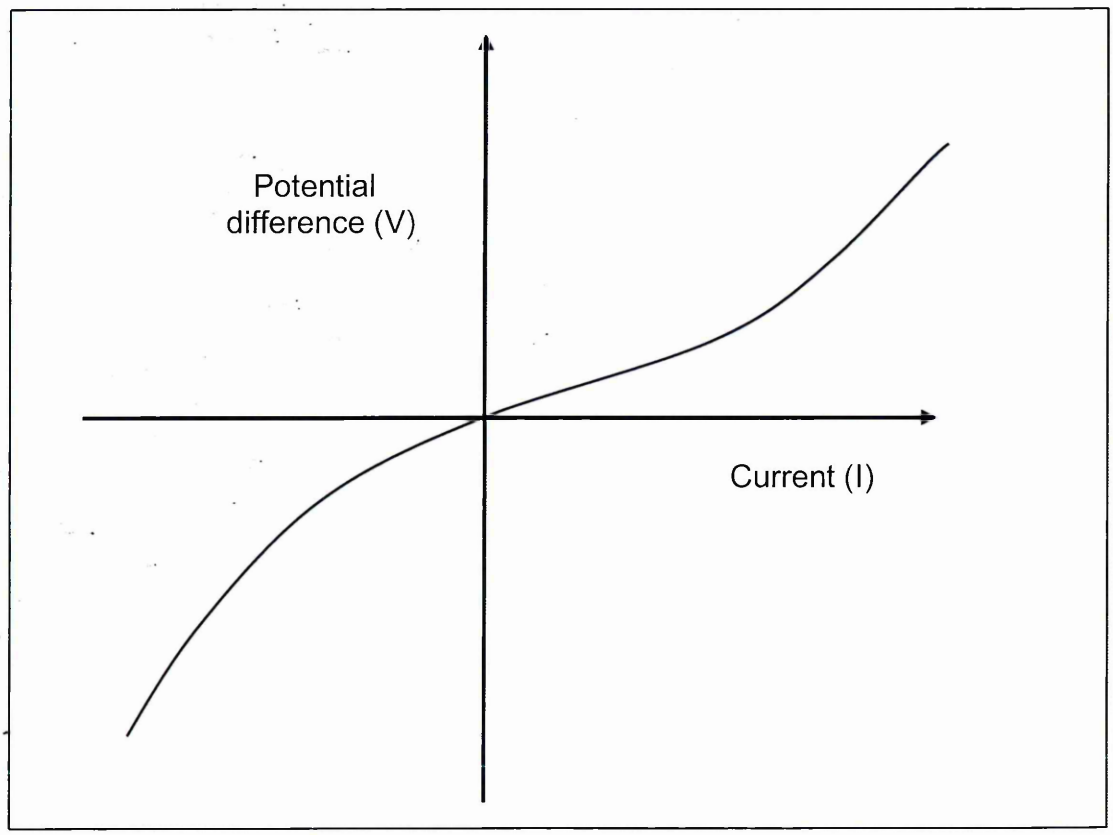

Figure 3.3. Non-Linear relationship between voltage V and Current I for non-Ohmic semi conductors

Figure 3.3 shows that for non metallic materials, i.e. non Ohmic conductors such as semi conducting materials, the relationship between V and I is not linear as shown in Figure 3.3. Ohms law states that in metals (ohmic conductors) the resistance does not change if the applied potential difference is altered, whereas Figure 3.3 shows that this is not the case for non-ohmic materials.

3.1.2. *Resistivity*

All materials have an electrical resistivity, also known as specific electrical resistance, which represents how strongly a material opposes the flow of electric current (I). The resistivity of an element primarily depends on temperature, length and cross sectional area. Equation 3.4 gives an expression for the resistance for a typical element shown in Figure 3.4.

$$R = \frac{\rho L}{A} \qquad \text{[Eq 3.4]}$$

ρ	=	Electrical resistivity (Ωm)
R	=	Electrical resistance of the material (ohms) (Ω)
L	=	Length of the element (m)
A	=	Cross-sectional area of the element (m^2)

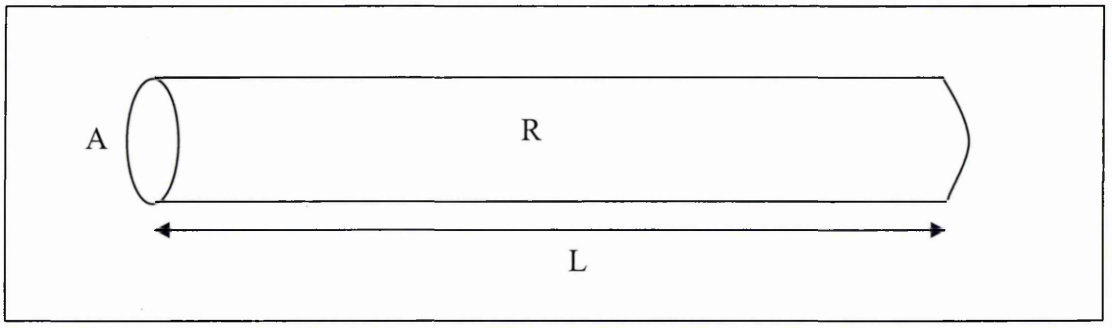

Figure 3.4. Relationship between R, *ρ*, *L* and A for a wire element

In general, electrical resistivity of metals increases with temperature, while the resistivity of semiconductors decreases with temperature.

The higher the temperature of a conductor the greater the molecular vibrations and the number of collisions leading to an increased conversion of energy to heat. The change in resistance of a conductor, $(R_t - R_0)$, is experimentally found to be proportional to the rise in temperature and to the original resistance R_0.

$$(R_t - R_o) \text{ is proportional to } (R_0 \times t) \qquad \text{[Eq 3.5]}$$

Therefore;

$$(R_t - R_o) = \alpha R_0 t \qquad \text{[Eq 3.6]}$$

Where

R_t	=	*Resistance (Ohms)*
R_o	=	*Resistance (Ohms) at datum temperature*
t	=	*Temperature (Kelvin)*
α	=	*Temperature Coefficient of Resistance (K^{-1})*

The temperature coefficient of resistance is defined as the fractional change in resistance per unit change in temperature.

$$\alpha = \frac{R_t - R_0}{R_0 t} \qquad \text{[Eq 3.7]}$$

Therefore;

$$R_t = R_0(1+\alpha t) \qquad \text{[Eq 3.8]}$$

Units of temperature coefficient of resistance α are per degree Celsius (/ deg C) or K-1. The change of sample dimensions, such as length and cross sectional area have a small effect on resistivity compared to the effect of temperature.

This not the case for a semi-conductor. The Carbon based CPT is a semi-conductor. The temperature dependence of the resistivity of a semi-conductor is given by the Steinhart-Hart equation:

$$1/t = A + B\ln(R) + C(\ln(R))^3 \qquad \text{[Eq 3.9]}$$

t	=	Temperature (Kelvin)
R	=	Resistance (Ohms)
A, B, C	=	Empirical constants

The typical characteristics of conductors, insulators and semi conductors are that conductors, normally metals, have very low electrical resistivity of the order of 1×10^{-6} ohm-meters; insulators have very high electrical resistivity of the order of 1×10^{13} ohm-meters and Semi conductors are neither good conductors nor good insulators and have resistivity values

between the two. A material commonly used as a semi-conductor is carbon. It is the carbon within it that enables the CPT material to conduct and generate a relatively uniform heat source over its surface.

3.1.3. *Conductive Properties of Carbon*

Carbon can be an alternative to metals providing similar electrical properties with the benefit of lower density. Advantages of carbon are that it is typically inert and compatible with a variety of polymer systems, as within the CPT material. Carbon particles provide electrical conductance through bonding systems that exist between adjacent particles which can be part of a larger polymer molecular bonding system. Within a polymer, this conductive continuity can be improved by reducing the carbon particle size or 'filling' between the larger particles to improve conductive pathways. However, unlike ohmic conductors, the relationship between current and potential difference is non-linear, hence the resistance of the material is dependant on the potential difference applied. Unlike most semi-conductors, the resistance of carbon increases with temperature. i.e. it has a negative coefficient of thermal resistance.

3.2. Manufacture of CPT

The CPT material can be manufactured to a variety of resistances per unit surface area within certain limits. For concreting applications, the resistances selected are 20 ohm (Red), 50 ohm (Grey) and 150 ohm (Green). The use of the three different resistances gives flexibility in design, for example, in some applications there may only be the space for relatively narrow elements of CPT heating material, whereas for larger surface area applications such as in-situ concrete slabs, there may be no restriction to the width of the CPT, even though the heating flux required may be the same in both cases.

Unlike other heating solutions which are prone to hot and cold spots, the CPT requires a potential of between 24 to 50 Volts to maintain an electrical flow resulting in a uniform heat output on its surface. Figure 3.5 shows a typical CPT heating element with conductive rails (silver tapes) through which voltage is applied. The spacing between the conductive rails is l_t (Figure 3.5) and the width, W.

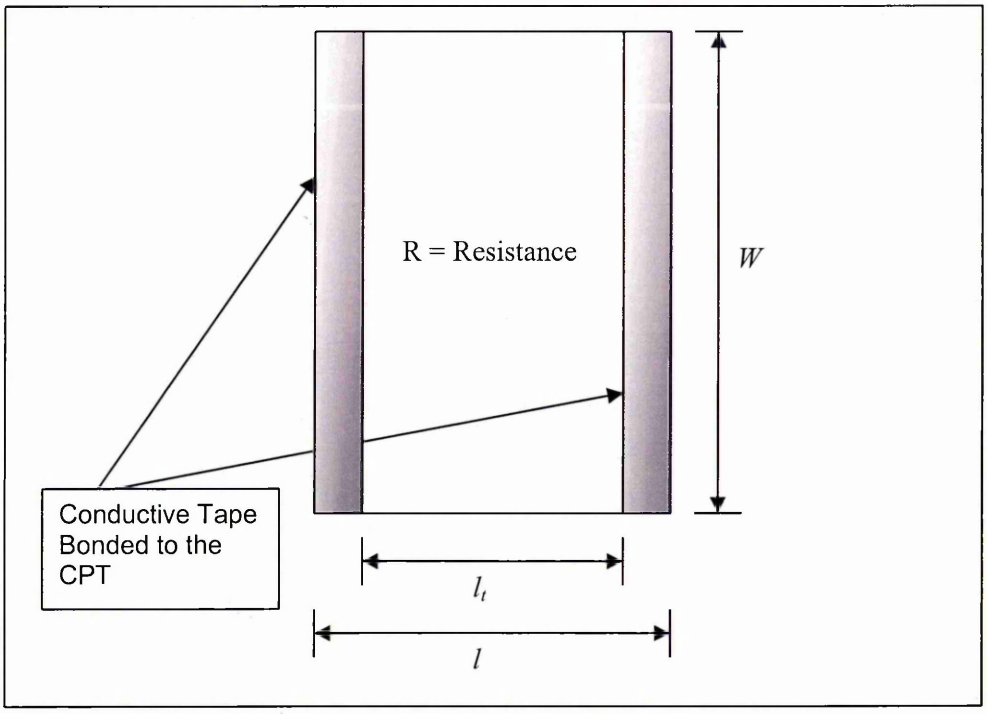

l = Element length (mm)

W = Width of test sample (mm)

l_t = Distance between conductive rails (mm)

Figure 3.5. A typical CPT element

The length of the CPT element across which voltage is applied is l_t and the cross sectional area A = WT where T is the thickness of the element.

3.2.1. *Control of Resistance*

During the manufacture of CPT the resistance per unit area is achieved by varying the proportion of carbon particles to the elastomeric polymer. In addition, the resistance can be altered by varying the number of uniform layers applied to the backing material, thus increasing the cross sectional area and therby reducing the resistance per m^2 of the CPT. This standard resistance of the material determined during manufacture is called the Characteristic Resistance R_{ID}.

The Characteristic resistance R_{ID} is measured during manufacture of the CPT rolls. Two strips of Chomerics Cho-Foil (rail), 25mm wide are bonded in parallel as shown in Figures 3.6 and 3.7, such that they are exactly 162mm apart (inside edges of the tape). Using a calibrated multi-meter the resistance of each sample is measured between the rails (across point 1-1, 2-2 and 3-3, Figure 3.7) at room temperature. This value is then averaged for a minimum of 3 samples per 10 metres of roll length to give the Characteristic Resistance R_{ID}.

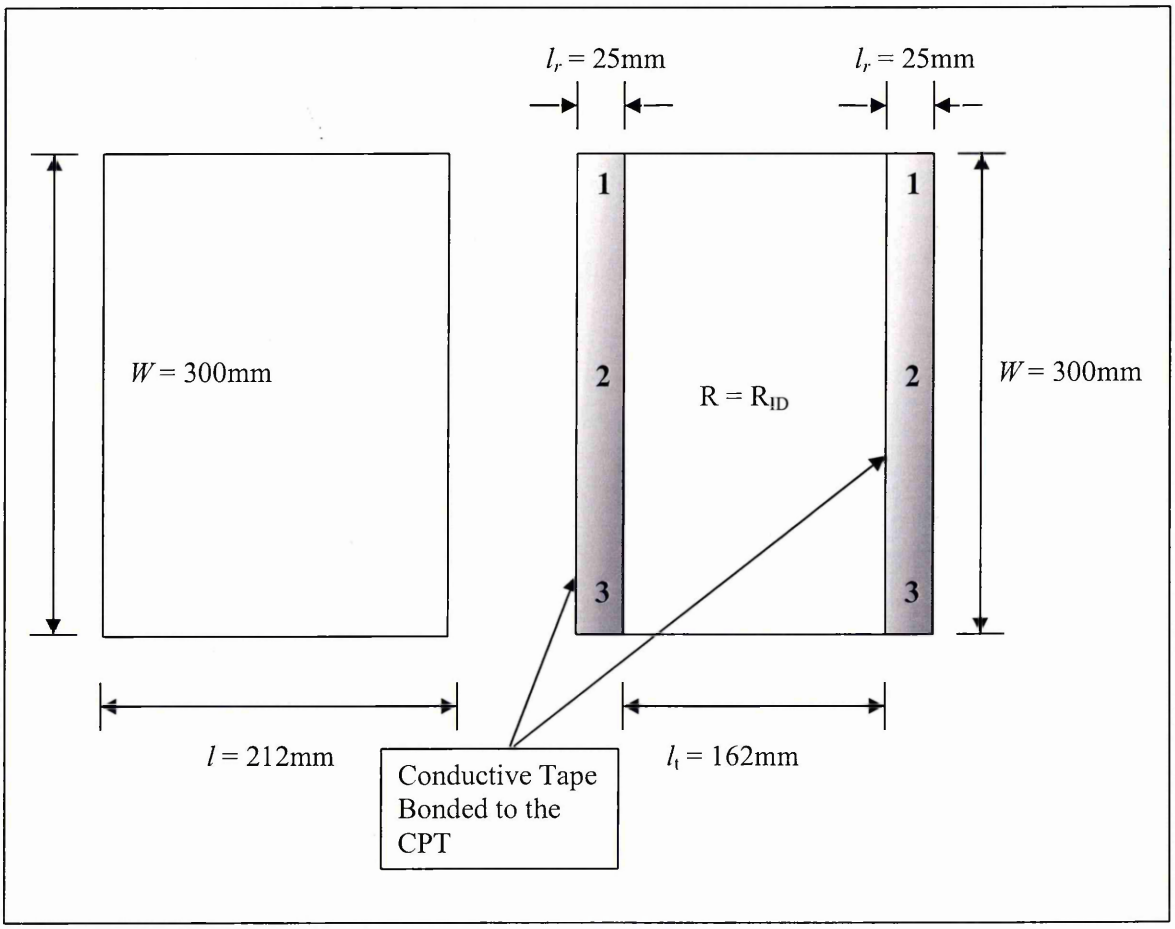

Figure 3.6. Sample dimensions of CPT used to determine R_{ID}

Figure 3.7. Sample of CPT with conductive rails to determine R_{ID}

l	=	Element length (mm)
W	=	Width of test sample (mm)
l_t	=	Distance between conductive rails (mm)
l_r	=	Width of conductive rail (mm)

R_{ID} is rarely the same as the Target Resistance R_T, specified prior to manufacture. The CPT materials are usually referred to by their target resistance R_T specified before manufacture.

3.3. Manufacture of CPT Elements

Conductive rails are applied to the CPT in order to allow current to pass through distance l. These rails are normally bonded in parallel, otherwise the resistance between the rails would vary along the length (Figure 3.8) since there is a relationship between the distance between rails and the resistance. The application of non-parallel rails will produce non-uniform heat across the CPT element due to the varying resistance.

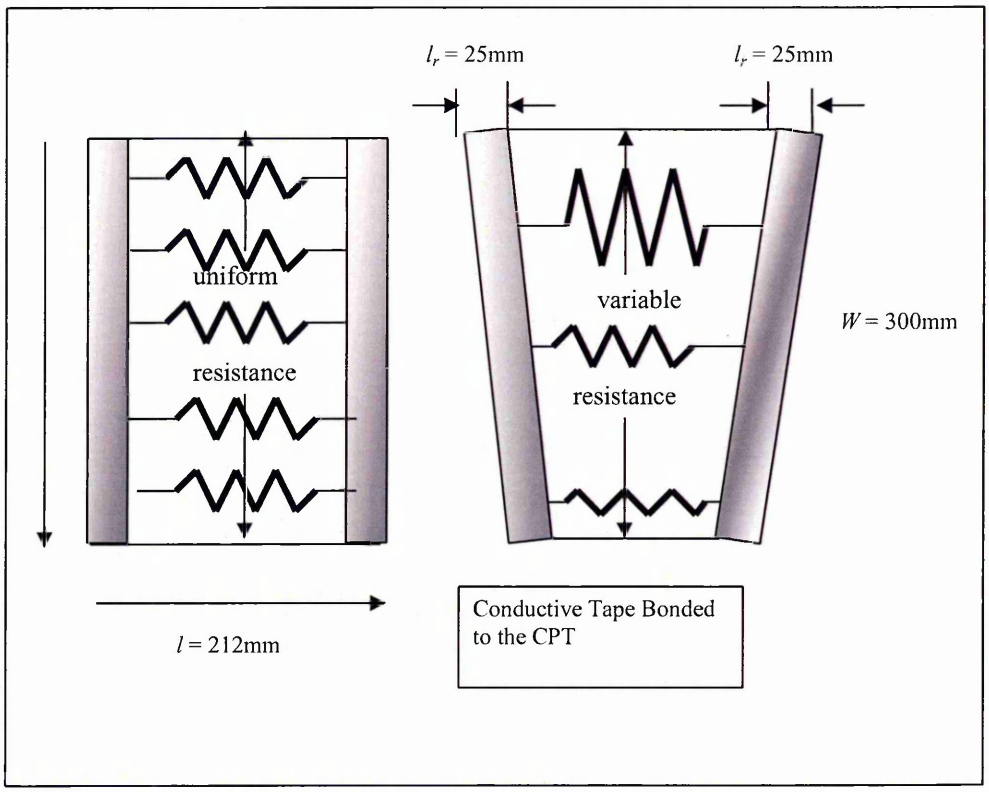

Figure 3.8. Parallel and non-parallel conductive rails resulting in uniform and non-uniform heat distribution respectively

3.3.1. *Bonding of the Conductive Rails*

Good bonding of the conductive rail to the CPT is critical to the performance of the heating element. The efficiency of current flow between the conductors (the silver tape) depends on the contact between the tape and the CPT material. To maximise the current flow, a conductive glue is used to make the bond between the CPT material and the silver / Chromerics tape. The conductance between the silver tape and the CPT material is not fully understood, however, it has been recognised that the critical point of contact between the CPT material and the tape, with respect to current flow, is the inside edge (point A) as shown in Figure 3.9.

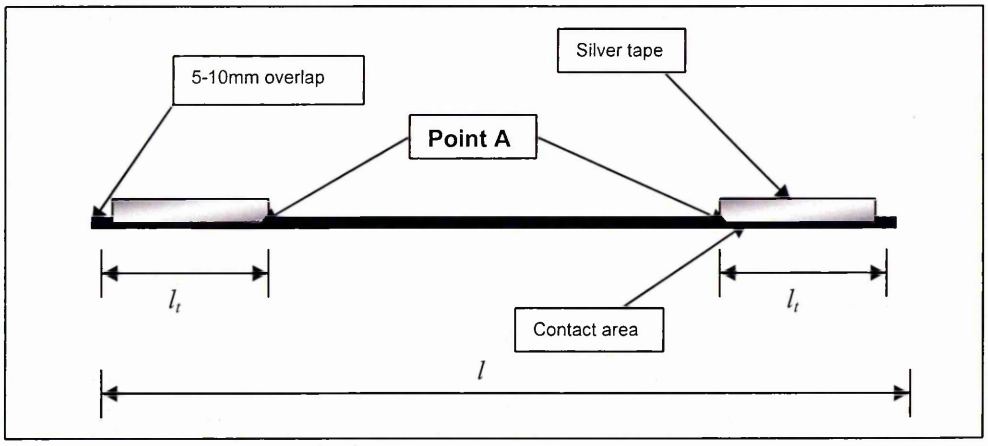

Figure 3.9. Positioning of conductive tape onto the CPT material (end view)

3.3.2. *Operating Voltage*

The design parameters which control heat output are the resistance of the CPT, the size of the element, and its operating voltage. The use of potential differences has been restricted to below 48 Volts. An electrical system using 50 Volts or below is described as SELV system (Safe Extra Low Voltage) requiring a reduction in the insulation and protection, provided it is not earthed. A full definition of a SELV system given by the British Standard 16th Edition IEE Regulations is: -

"An electrical system in which the voltage cannot exceed ELV (Extra Low Voltage) under normal conditions, and under single-fault conditions, including earth faults in other circuits". A SELV circuit must have:-

- protective-separation (i.e., double insulation, reinforced insulation, or protective screening) from all circuits other than SELV and PELV (Protective Extra Low Voltage) (i.e, all circuits that might carry higher voltages)
- simple separation from other SELV systems, PELV systems and from earth (ground).

The safety of a SELV circuit is provided by

- the extra-low voltage
- the low risk of accidental contact with a higher voltage;
- the lack of a return path through earth (ground) that electrical current could take in case of contact with a human body.

The design of a SELV circuit typically involves an isolating transformer, guaranteed minimum distances between conductors, and electrical insulation barriers. The electrical connectors of SELV circuits should be designed such that they do not mate with connectors commonly used for non-SELV circuits.

For this reason the operating voltage of the CPT is usually between 12 – 50 Volts. For the purpose of some testing within this research programme this operating voltage may be exceeded, however, for applications where there is the potential of third party use, the operating voltage will be within this range. The CPT also has the capability of being operated by either DC or AC.

3.3.3. *Attaching the Power Cables*

A connection is required on each of the parallel rails to power the element. A connection is made at the same position on each end of the rail (Figure 3.10). The conductive tape is folded over at each end as shown in Figure 3.10. There are two options for making the connection, a soldered connection or a press stud and crimp connection.

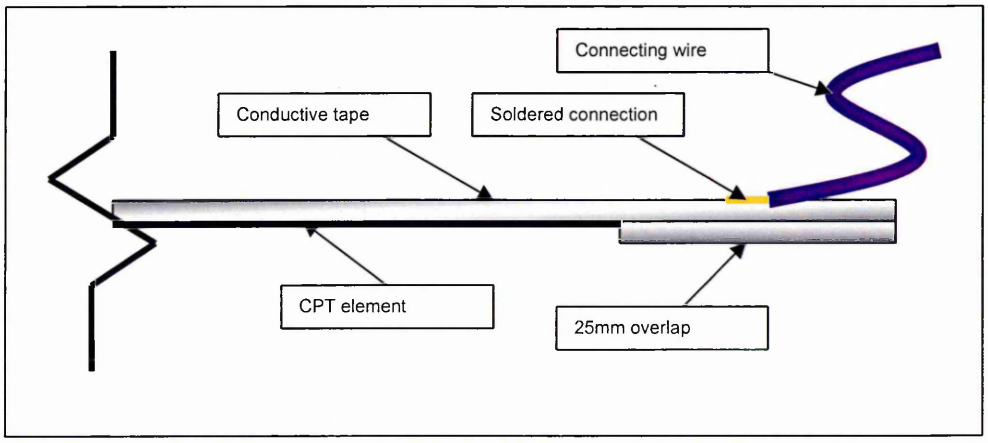

Figure 3.10. Simple solder connection (side view)

The advantage of using a solder connection is its speed. However, using the press stud and crimp fixing enables a more mechanical and durable fixing. The press stud presses the CPT, and the two sides of the Chromerics tape together providing additional support from the underside of the CPT element. By using a crimp, a connection of greater mechanical strength is also provided compared to the simple solder connection. Figure 3.10 shows the detail of the simple solder connection compared to the crimp connection shown in Figure 3.11.

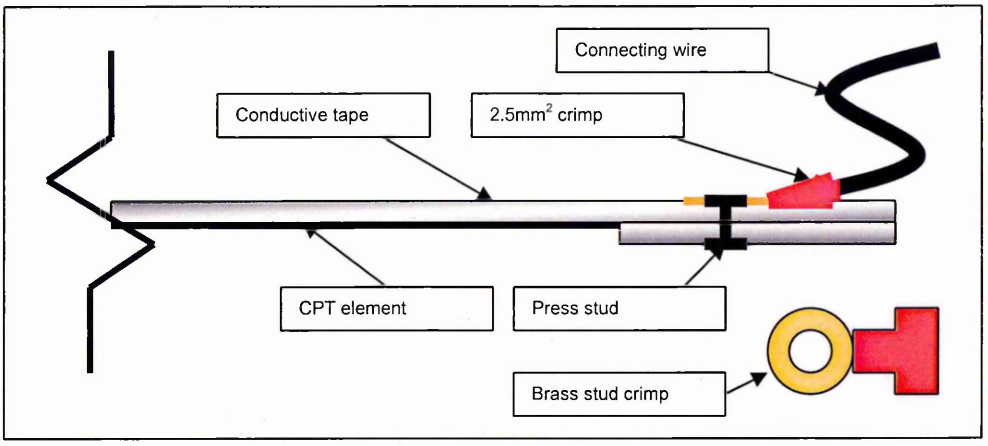

Figure 3.11. Crimp and press stud electrical connection (side view)

The cross sectional areas of the power cables used to connect the CPT elements have also to be based on the estimated current in each element. Typically this area is $2.5mm^2$ for elements with a current rating of below 16 Amps.

3.3.4. *Connecting Numerous Elements*

Assuming that each CPT element is a resistance, numerous CPT elements can be inter connected either in series or parallel. There are advantages and disadvantages of each method. Figure 3.12 shows two similar CPT elements connected in series. The total resistance is given by the expression:-

$$R_T = R_1 + R_2 + R_3 \ldots\ldots\ldots + R_n \qquad \text{[Eq 3.10]}$$

Where,

R_T = Total resistance

R_n = Resistance of individual elements

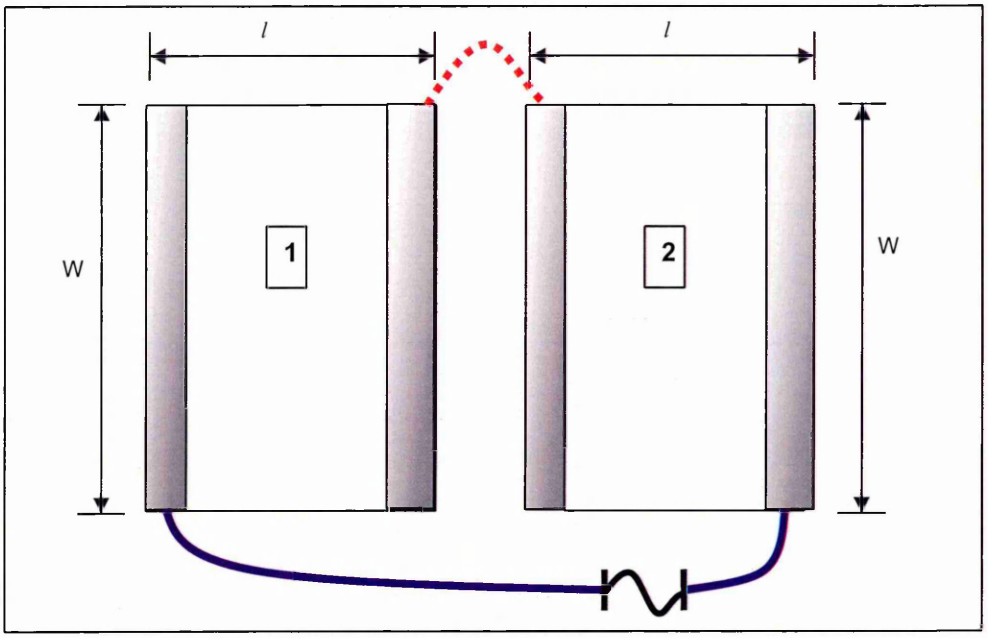

Figure 3.12. Similar CPT elements connected in series

Figure 3.13 shows two similar CPT elements connected in parallel. The major advantage of connecting in parallel is that if the CPT material in elements 1 fails, element 2 will continue to function regardless, providing there is not break in either of the conductive rails on element 1. The following expression applies to elements connected in parallel:-

$$1/R_T = 1/R_1 + 1/R_2 + 1/R_3 \ldots\ldots + 1/R_n \qquad \text{[Eq 3.11]}$$

Where,

R_T = Total resistance

R_n = Resistance of individual elements

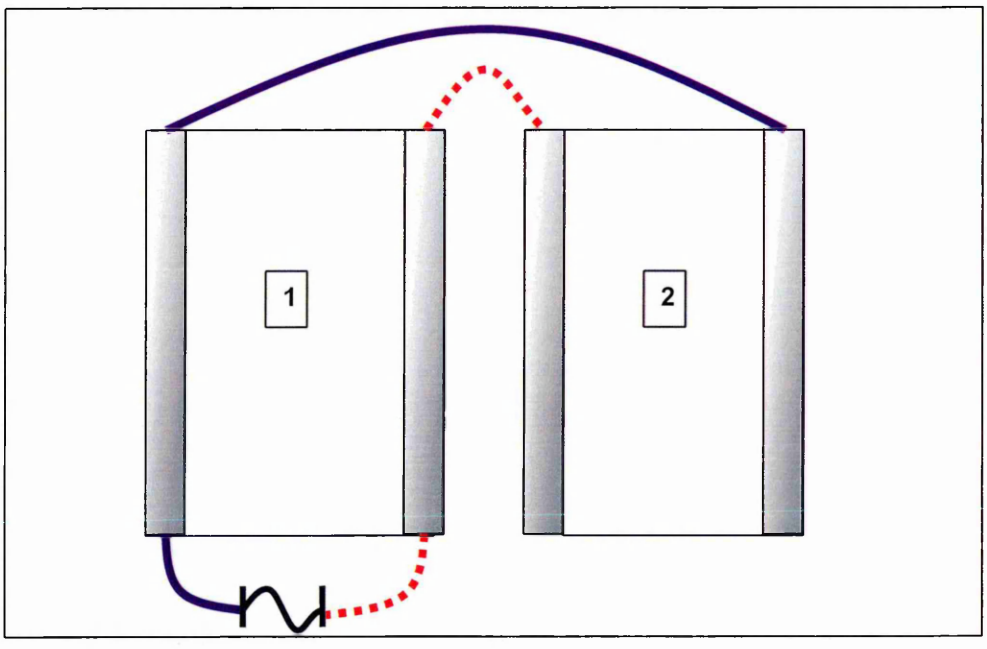

Figure 3.13. CPT elements connected in parallel

The failure of either of the conductive rails on element 1 having a detrimental effect on the operation of element 2, can be prevented by wiring two CPT elements as shown in Figure 3.13.

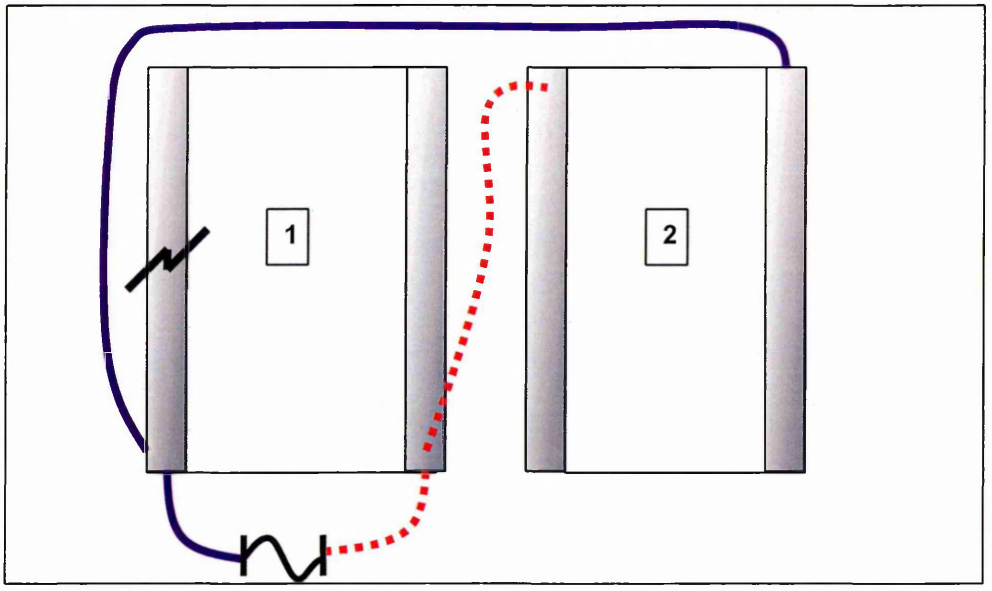

Figure 3.14. Similar CPT elements wired in parallel to maintain function in case either is damaged

Figure 3.14 shows that if there is a 'break' in either conductive rail of element 1, element 2 would continue to operate. Wiring in this way allows both elements to operate independently, i.e the elements do not have to be the same size, hence the same resistance.

3.3.5. *Common Rail (Series)*

Another option in configuring the CPT elements is to use a common central rail. This can be done by either using a common central rail in series or in parallel. The configuration of a CPT element connected in series is shown in Figure 3.15.

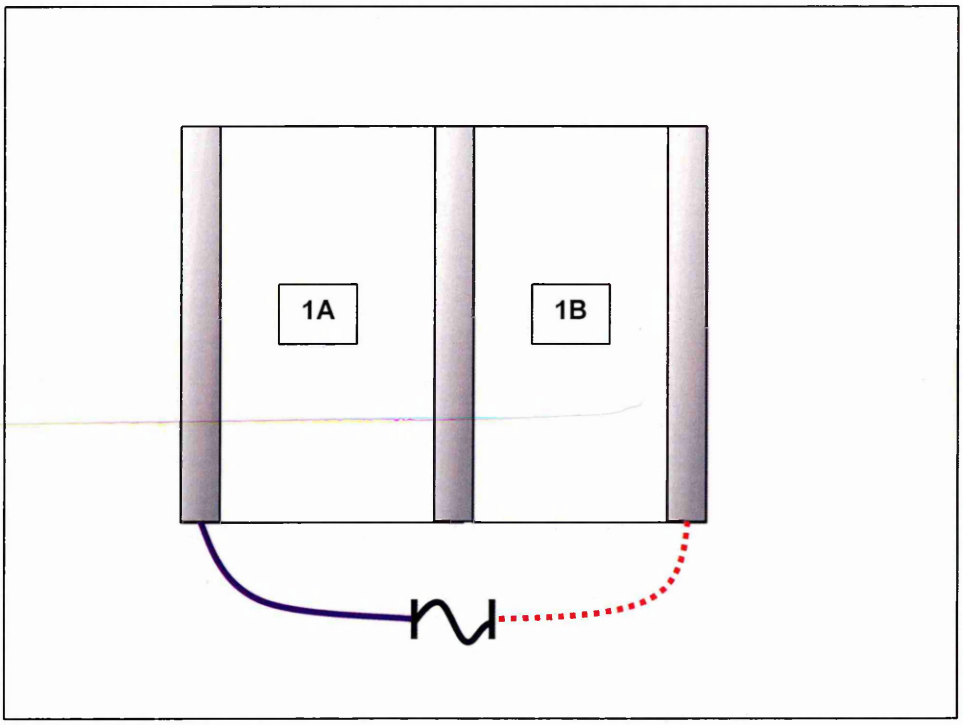

Figure 3.15. CPT element with common middle rail (series)

Again similar to connecting two separate elements, the proportions and size of the CPT area each side of the common rail need to be the same. If this is not the case, the common rail acts as a potential divider and the voltage across each side of the element is divided by the ratios of the element width each side of the rail. Again, similar to connecting two separate elements in series, the failure of the CPT either side of the common rail results in the total element not functioning. This is also demonstrated by equation 3.12 below.

$$R_T = R_{1A} + R_{1B} \qquad \text{[Eq 3.12]}$$

If 1B failed it would have an infinite resistance and hence no current flow, as the resistance of the whole system would be infinite.

3.3.6. *Common Rail (Parallel)*

Figure 3.16 shows a common rail element configured in parallel. The advantage of configuring in this way is that if either side of the CPT fails, the other will still function. It also allows different proportions of CPT on either side, both to be supplied by voltage at the same potential difference. Unlike connecting in series where the applied voltage is proportioned between the two elements, when applied in parallel, the supply voltage is the same as the voltage across each element (CPT area between parallel rails).

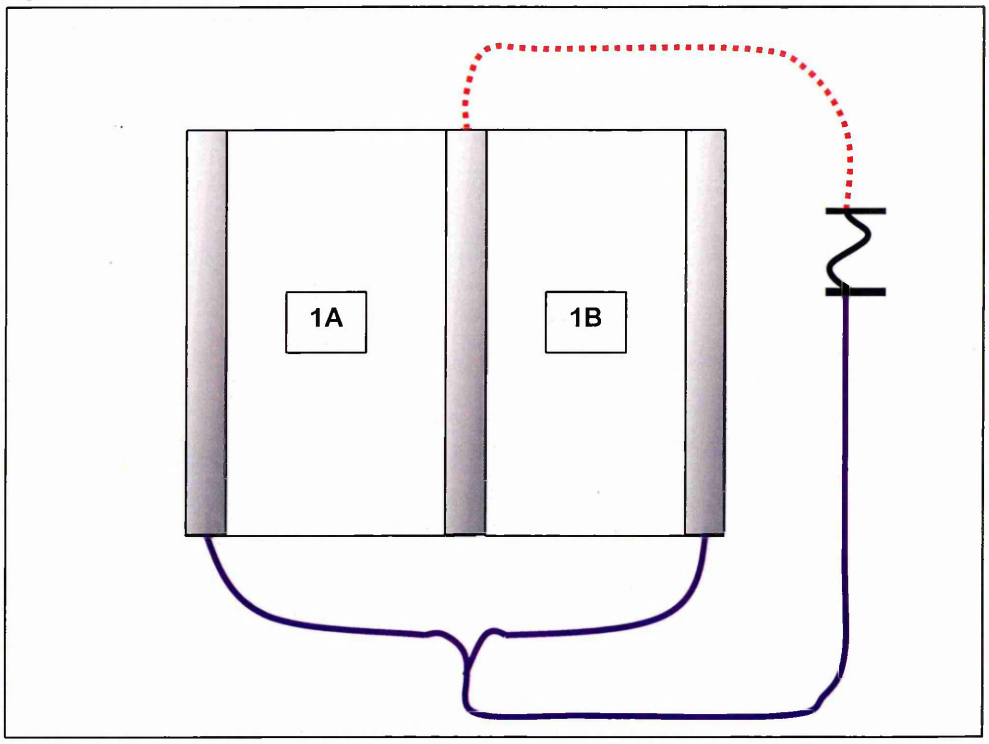

Figure 3.16. CPT element with common middle rail (parallel)

In summary, when connecting elements in series, the sum of the potential difference across each element equals the total Voltage applied to the circuit; whereas in parallel, the sum of the currents over each element equals the current required by the entire circuit, and the potential difference across each element is the same as that applied to the total circuit. This can be proved from first principles using Ohm's law equation as given below;

$$1/R_T = 1/R_{1A} + 1/R_{1B} \qquad \text{[Eq 3.13]}$$

If 1B failed it would have an infinite resistance and the resistance of the whole system would operate with the resistance halving and hence the current consumption and power input and output halving.

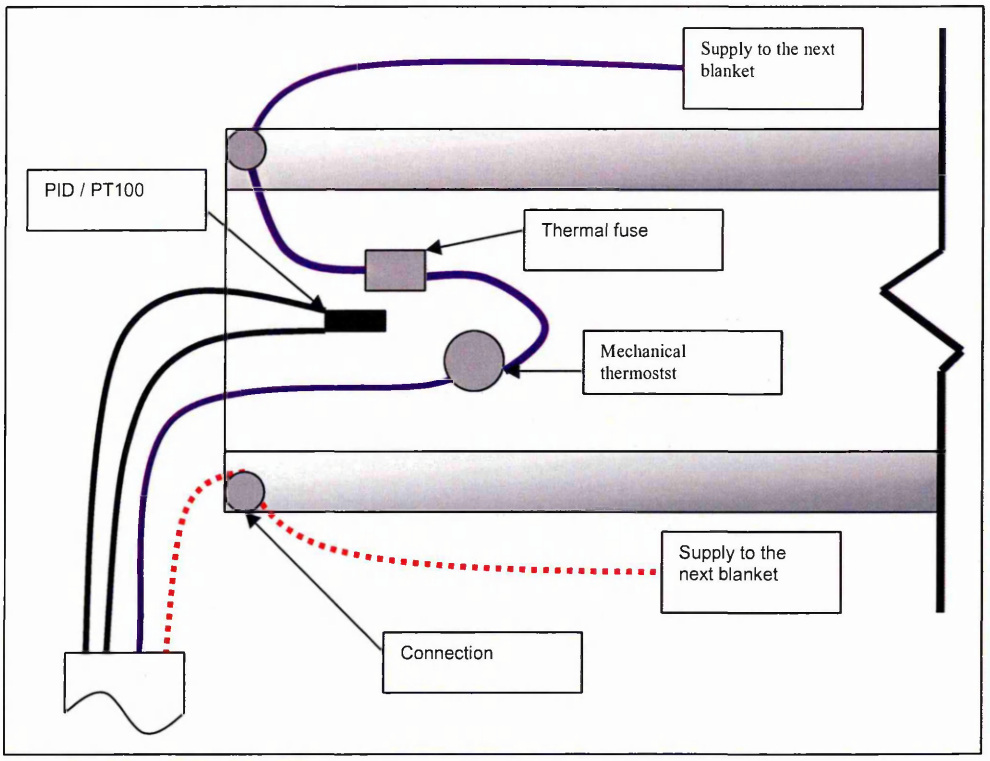

Figure 3.17. Wiring of CPT element

Figure 3.17 shows the typical wiring configuration of a CPT element. A number of elements wired like this could be linked in parallel to heat a large area. The Figure shows a thermal fuse and mechanical (bi-metallic) thermostat connected in series along one of the power supplying cables. It also shows an additional electronic probe used in conjunction with an electronic PID (proportional–integral–derivative) temperature monitor to control the surface temperature. The thermal fuse is a non re-settable device used as a fail safe device, and the mechanical (bi-metallic) and electronic temperature control systems are used as primary temperature control. The mechanical temperature thermostat and electronic device are selected to operate at temperatures below the maximum operating temperature of the CPT.

Chapter 4. Materials Specification, Thermal Jacket Design and Instrumentation

4.1. Introduction

Various concreting applications were selected to conduct tests and trials as part of the research programme. The various designs of blankets and jackets manufactured for each application will be discussed in this chapter. Also other materials and equipment used throughout the testing programme will be introduced, such as electrical transformers and power generators used to power the jackets / blankets, concrete mix designs and the material used to manufacture the jackets. Data monitoring equipment used to record variables such as temperature, shrinkage and electrical properties such as resistance, voltage and current is also described.

4.2. Blanket / Jacket Design

Table 4.1 lists the jackets and blankets designed and manufactured for this research programme. These are separated into three main areas, initial laboratory testing (Chapter 6) using small laboratory scale elements, further laboratory testing (Chapter 7) using larger representative elements, In-situ concreting and precast concrete application (Chapter 8). The dimensions of the test samples produced and the mould description for each are given in Table 4.1.

Jacket ID	Test samples of concrete, dimensions	Brief description of jacket application
Lab 100	100mm x 100mm x 100mm	Standard cast iron steel mould
Lab 300	300mm x 75mm x 75mm	Mild steel prismatic mould
Inter 400	400mm x 400mm x 400mm	Bespoke mild steel mould
Insitu 1500	800mm x 800m x 1500mm	Excavated Foundation
Preacst 6500	120mm x 6500mm x 150mm	Precast concrete mould

Table 4.1. Jacket ID's and applications

Figure 4.1 shows a typical cross section through a thermal blanket / Jacket incorporating the CPT element. The general arrangement is a composite 'sandwich' comprising of the three major functional elements, the outer protective element, the CPT heating element and the insulative layer within the blanket.

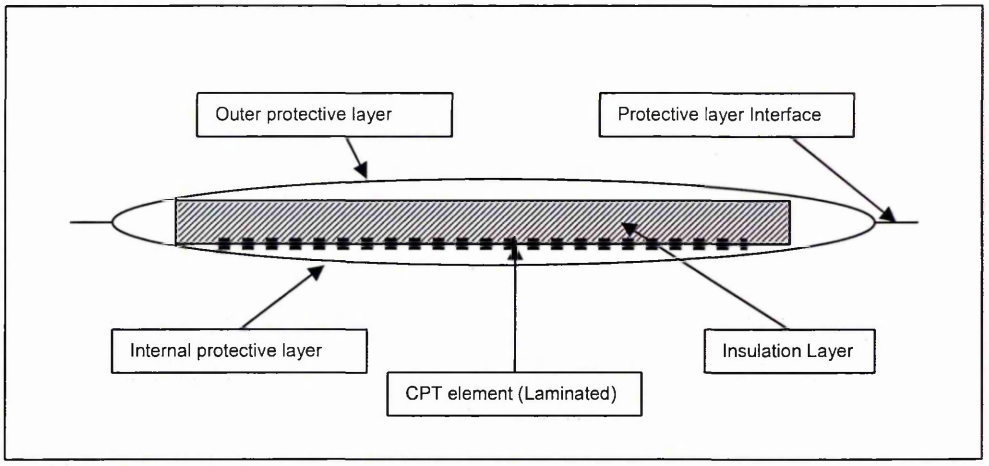

Figure 4.1. Cross section through a typical CPT heating blanket

4.2.1. *Outer Protective Materials*

The primary function of the outer material of the Blanket / Jacket is to protect the CPT elements within. The selection of the outer material is dependant upon the application of the blanket. A number of factors need to be taken into account when manufacturing a blanket for concreting applications. These include the chemical properties, conductivity, the thickness and unit weight and the materials' ability to wrap around moulds - primarily related to the flexibility, the tensile strength and satisfactory bond of the material to similar and dissimilar materials.

The chemical reactions of concrete can be a deciding factor for the selection of the outer material. Where the blanket is to have direct contact with concrete being cured, materials such as silicon and glass cloth are avoided due to their incompatibility with concrete and alkali environments. However, for other applications where the blankets are to heat concrete through a mould (as described in Chapters 6 and 7) the use of such materials may be advantageous. A summary of the various outer protection materials used throughout this research programme are given in Table 4.2.

Material ID	Colour	Description
LGPVC	Grey / Green	Light-weight PVC coated polyester weave
PVC	Blue	PVC coated polyester weave
SCGC	Grey	Silcon coated glass cloth
PTFE	Grey	PTFE coated glass cloth

Table 4.2. Details of outer materials

Glass weave and polyester were the primary materials selected as they provided both the thermal characteristics and mechanical properties required. Table 4.3 provides the physical properties of the materials.

Materials	Unit Weight (g/m^2)	Thickness (mm)
LGPVC	410	0.37
PVC	620	0.42
SCGC	400	0.4
PTFE	390	0.35

Table 4.3. Outer material details

4.2.2. *Protective layer interface*

Figure 4.1 shows the interface(s) where the internal and external outer protective layers meet. At these points the two materials are required to be bonded. The three ways of bonding the internal and external protective layers are as follows:

a) The two layers are sewn together with a 'nomex' thread with suitable mechanical and thermal properties.

b) The protective layers are welded together using a hot-bar high frequency heat welding machine, with a weld width of 10mm – RF Weld.

c) The use of a double sided bonding material layer that bonds the internal and external layers.

4.2.3. *Insulation Layers*

The insulation layer within the CPT blanket / Jacket is used to direct heat from the CPT to the concrete, and minimise heat losses away from the concrete. The various insulation materials used are given in Table 4.4.

Material ID	Description
Rockwool 25	Flexible mineral wool material, 25mm thick
Rockwool 50	Flexible mineral wool material, 50mm thick
Slab 25	Rigid mineral wool, 25mm thick
Thinsulate	Flexible insulation material
Foam	Closed cell polyurethane foam

Table 4.4. Description of insulation materials

The physical and thermal properties of the various insulation layers are provided in Table 4.5.

Materials	Thickness (mm)	Conductivity (W/mK)	Thermal resistance (m^2K/W)
Rock 25	25	0.033	1.5
Rock 50	50	0.033	0.7
Slab 25	25	0.037	0.7
Foam	15mm	-	-

Table 4.5. Properties of insulation layers

4.2.4. *CPT Heating layer*

As shown in Figure 4.1 the CPT layer is located between the internal protective layer and the insulation layer within the blanket. The Polymer surface of the CPT element is positioned to face the rear side of the internal protection layer to maximise heat transfer. The cotton surface of the CPT element is positioned and secured against the insulation layer. During manufacture, the CPT insert is bonded face down on a layer of glass cloth weave to increase its strength, particularly in applications where the blanket is to be applied and removed frequently. The mounted CPT element is then secured to the insulation layer using a spray adhesive that is capable of withstanding the maximum operating temperature of the CPT element, and maintaining the bond. The composite of the CPT layer and the insulation are then inserted into a 'pouch' formed by the protective layers, these are then secured to complete the manufacture process of the composite blanket.

In addition, a number of the blankets manufactured used a CPT insert that was laminated. The CPT material, following the application of the parallel conductive rails and the application of the laquer, is passed through a plastic laminations machine as shown in Figure 4.2 which further protects the CPT element from mechanical damage, damage from water, chemical attack and also improves the overall durability of the blanket. All inserts manufactured in this manner were laminated with a 0.3μm polyvinyl chloride sheet.

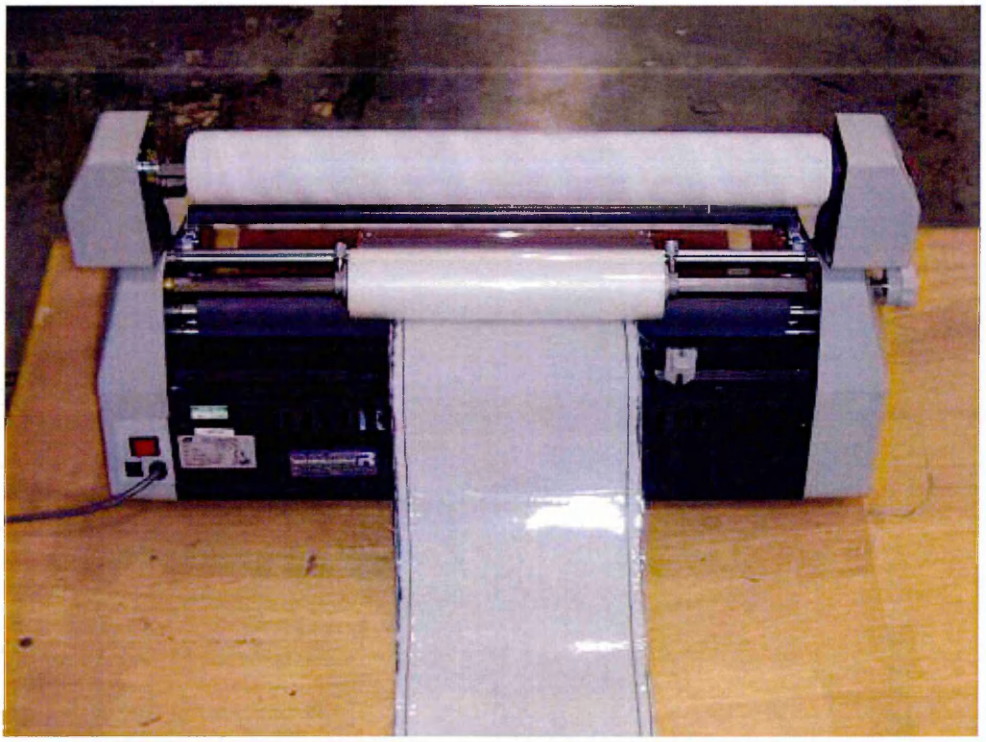

Figure 4.2. Lamination machine through which the CPT element is passed

Following lamination the CPT is connected to a cable to supply power to the insert and this is passed through an IP (ingress protection) 65 rated gland. This rating of gland ensures the interface between the gland and the blanket is water tight and resistant to dust and particle ingress, both very important when considering a typical concrete environment.

4.2.5. *Cable*

The cable used in the research programme was Y-Y PVc coated. This enabled flexibility and protection to the blanket user. Typically 4-core or 7-core cable was used. For the 4-core cable the cores were assigned as follows:-

Core 1	Supply voltage (+ve)
Core 2	Supply voltage (-ve)
Core 3	Electronic control – out
Core 4	Electronic control – return

Table 4.6. Core assignment for 4 – core cable

The blankets were powered in 'lines'. A line is determined by the supply to the blanket and restricted by the available current. As discussed in Chapter 3 a 'line' has the capacity to supply a number of CPT elements simultaneously, usually arranged in parallel, up to 16

Amps. Where a second line was required a seven core cable was used with the cores assigned as follows

Core 1	Supply voltage (+ve) (line 1)
Core 2	Supply voltage (-ve) (line 1)
Core 3	Supply voltage (+ve) (line 2)
Core 4	Supply voltage (-ve) (line 2)
Core 5	Electronic control – out
Core 6	Electronic control – return
Core 7	Earth – Not used

Table 4.7. Core assignment for 7 – core cable

All cables had core diameters of 2.5mm with a 20 amp rating at 50 volts. Each 'line' within the blankets was designed to draw 16 Amps to allow for inaccuracies relating to the electrical design of the CPT elements, to compensate for heat losses due to resistance in the cable particularly at low voltages and for excessive lengths of cable, greater than 10m.

For applications in aggressive environments the jackets were designed or re-fitted with S-Y cable. This cable had double PVC insulation with braid sheath between the two insulation layers to provide the cable with additional mechanical protection. This cable was used for blankets using both 4-core and 7-core connecting cable as required.

4.2.6. *Connectors*

Various electrical connectors were used to connect the blankets to power supply / transformer units. The type of connector used depended upon the following factors:-

- The number of CPT elements within a particular blanket, i.e the size of the required heating area
- The power of the CPT elements within the blankets
- Expected duration of operation of each blanket.

For blankets supplied by 4-core cable an **Amphenol ™** 4-way connector was used. Similar to the interface glands between the blankets and the connecting cables, these were IP65 rated with copper terminals and secured in place with a screw mechanism. A number of variations of the connector were used. 'Panel mounted' connectors were used to mount on the side of the power supply units. 'In-line' connectors were used to link between blankets and these consisted of a male and female type connection. Figure 4.3 shows a male – female in-line connection.

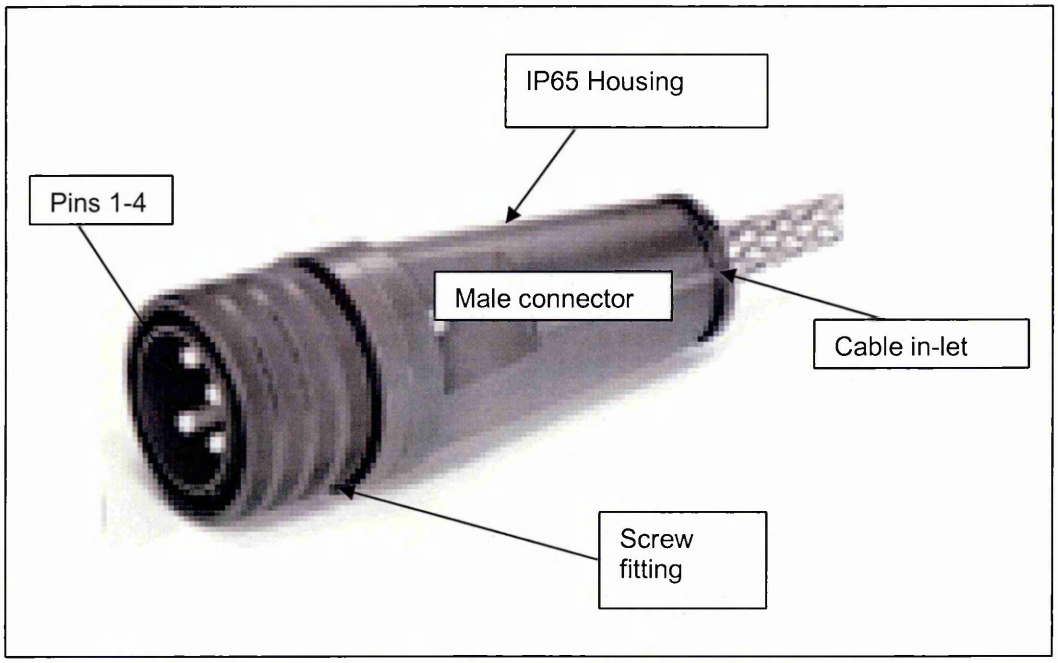

Figure 4.3. Amphenol type connector, Male – Female in-line connector with S-Y braided cable

For connection to blankets requiring a 7-core input, **Buccaneer Bulgin** connectors were used. Unlike the 4-core connectors these were IP 68 rated to provide resistance to the ingress of water under pressure. Considering the requirements of the connectors such as durability and the number and thickness of cores to be accommodated, the Buccaneer Bulgin connector was most commonly used (Figure 4.4).

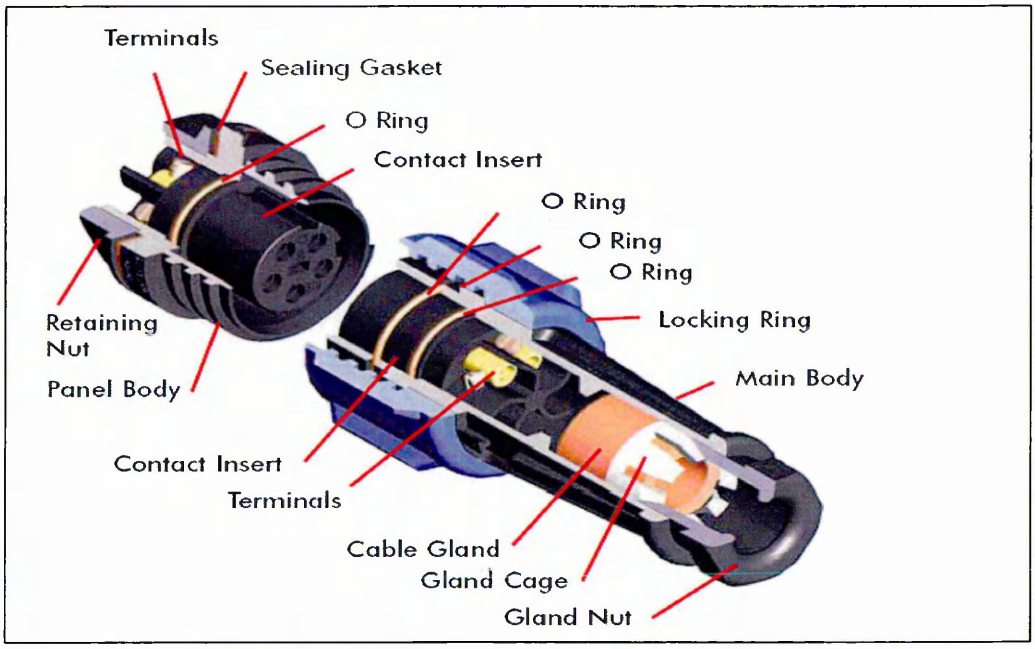

Figure 4.4. Typical Bulgin 900 series In-line connector (image courtesy of (http://www.bulgin.co.uk)

4.2.7. *Blanket Securing Mechanisms*

Various methods were used to fasten the blanket in position in different applications, as follows:-

a) Velcro, to allow a secure flexible fixing which is adjustable, durable and maintains the flexibility of the jacket. The strength of the fastening is dependant upon the location and the area of Velcro, on both the 'soft' eyelet side and the hard 'hook' side. To maintain a suitable fastening the Velcro has to be kept clean of debris such as concrete. However moisture has little impact on its performance. Velcro can be used on small and large applications.

b) Straps and D-clips allow a blanket to be positioned, re-adjusted and tightened easily. They are not affected by moisture. The strength of the fastening depends upon the tensile strength of the strap and the D-clip. The suitability of the fixing is also dependant upon the number of straps and D-clips and the spacing between additional fastenings.

c) Eyelets are suitable when a blanket is required to be secured to a soft strata. Examples are the blanket lining of concrete foundations cast in cold weather. The Blankets can be secured and maintained in place prior to concreting.

4.3. CPT Blankets used in the Tests

The blankets used in this test programme are described in this section.

4.3.1. *LAB 100 Jacket*

Figure 4.5 shows the general arrangement for the heating blanket LAB 100, designed and manufactured to fit a 100mm x 100mm x 100mm cube mould as discussed in Chapter 6.

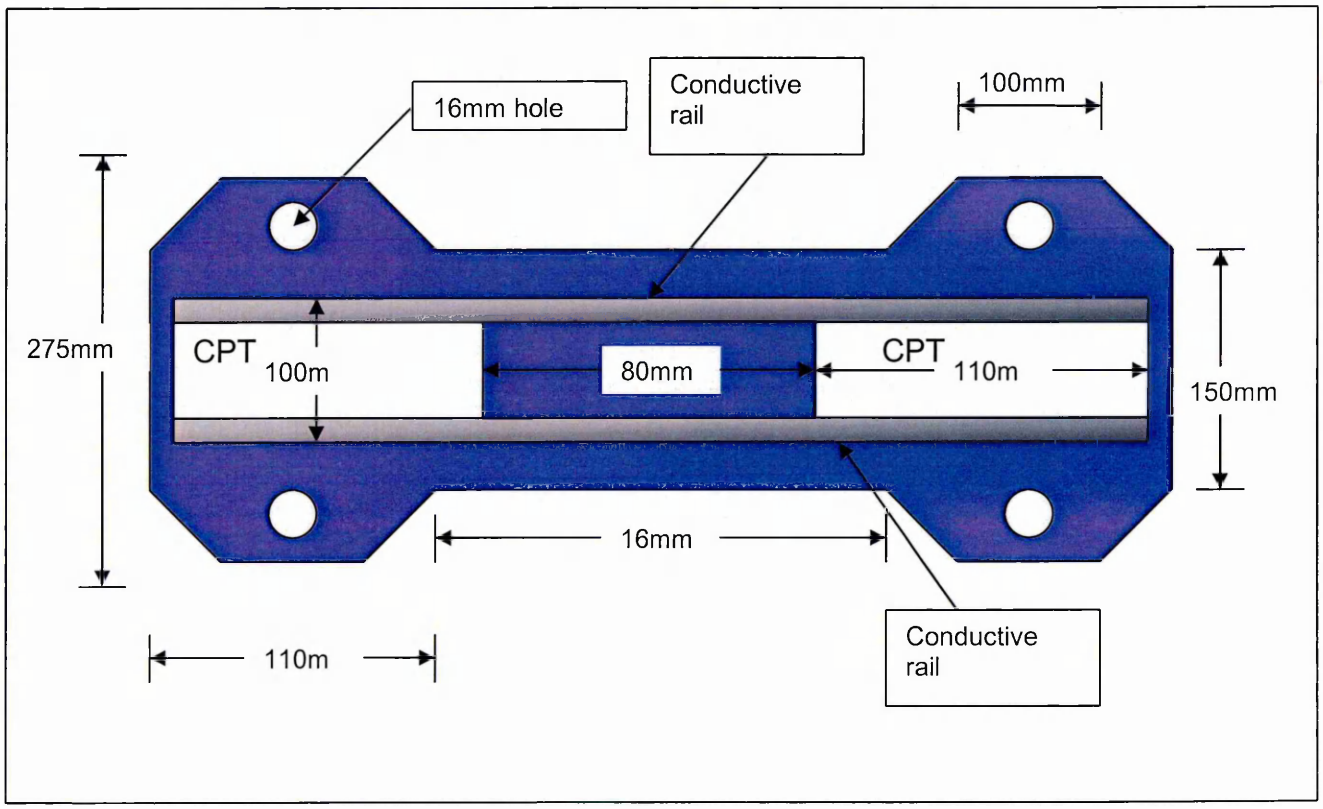

Figure 4.5. General Lay-out of Blanket CPT LAB-100 (not to scale)

The holes within the blanket allow it to be secured to the mould as an integral heating element. For this reason no insulation layer was used on these moulds. To reduce losses from the mould a separate insulation jacket was used. Figure 4.5 shows a section within the blanket where the CPT was removed, but the parallel conductive rails remain. This was done to minimise the power rating of the blanket whilst still allowing a slim-line jacket to be made utilising the conductive rails.

Blanket Properties (General)	
Blanket ID	LAB 100
Overall blanket dimensions	275mm x 510mm Approximately
Number of blankets per application	1
CPT inserts per blanket	1
Colour	Various
Securing mechanism	Integrated within the mould
CPT Insert Properties	
CPT type	CPT 20 ohm heating material (Red)
CPT width (*l*)	110 mm
Rail length (W)	335 mm
Rail width	25 mm
Rail configuration	Double parallel
Insulation Properties	
Insulation	None
Insulation thickness	N/A
K – value	N/A
Protective material properties	
Internal protective layers	PVC / PTFE / Silicon glass
External protective layers	PVC / PTFE / Silicon glass
Protective layer interface	Bonded (Double sided tape) / Sewn
Maximum operating temperature	75 deg C – 120 deg C
Electrical Specification	
Operating Voltage	24 Volts (ac)
Current (@ 24 Volts)	1.45 Amps
Power rating	35 Watts
Resistance	ohms
Temperature Control	
Primary Temperature Control	Bi-metallic thermal cut -outs
Operating limits	50 / 60 / 70 deg C +/- 10 deg C
Temperature probe	N/A
Secondary temperature Control	N/A
Operating limits	N/A
Over temperature Protection	
Integrated thermal fuse	156 deg C
Estimated CPT surface temp	120 deg C
Power Source	
Power supply ID	Carrell Electronic Control
Connector type	Amphenol 4-pole plug and socket
Cable type	4 – core 2.5 mm diameter Y-Y
Cable length	3m

Table 4.8. LAB 100 Jacket specification

4.3.2. *LAB 300 Jacket*

Figure 4.6 shows the general arrangement for the heating jacket LAB 300 designed and manufactured to fit 300mm x 75mm x 75mm prism moulds as discussed in Chapter 6.

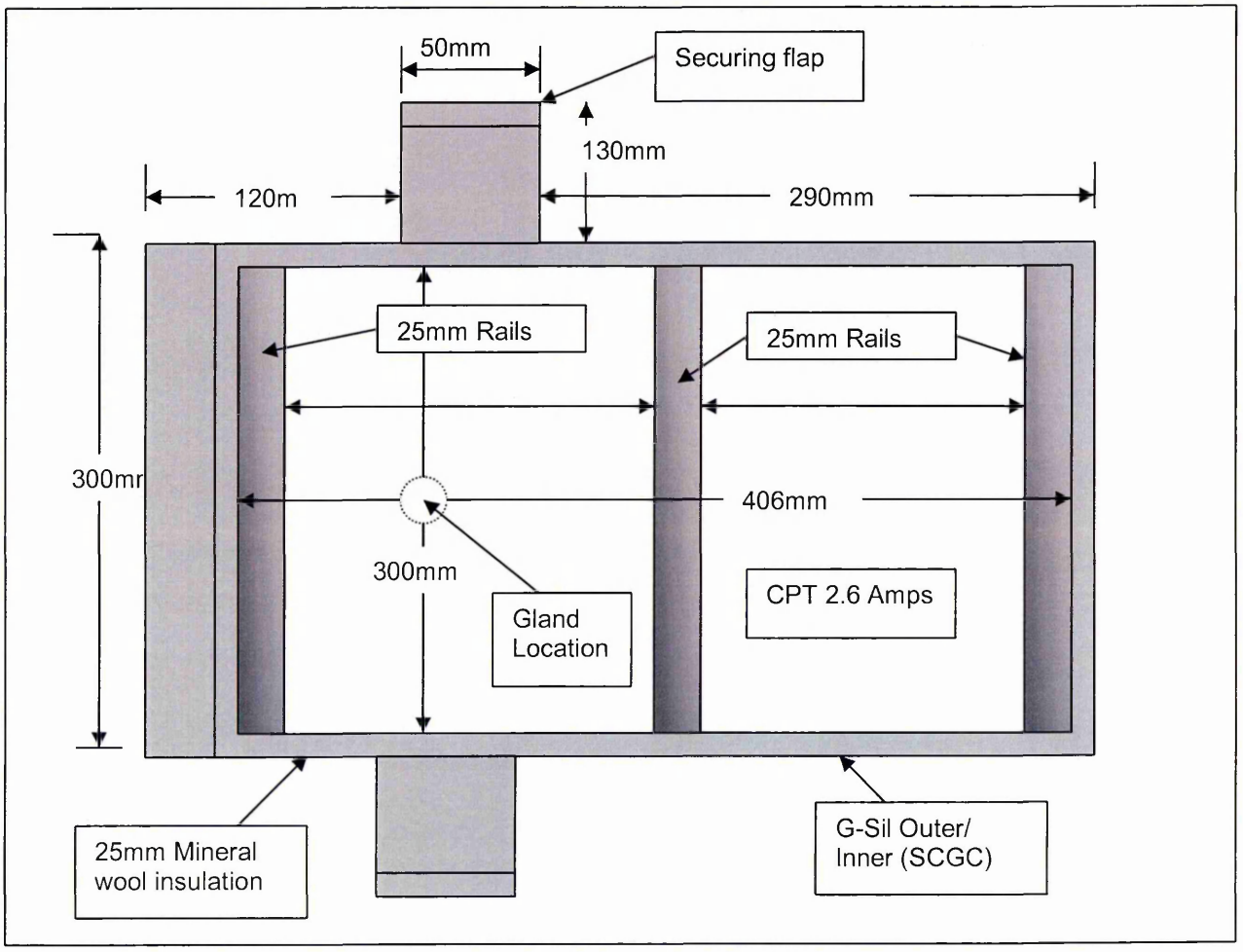

Figure 4.6. General Lay-out of Blanket CPT LAB-300 (Not to scale)

Figure 4.6 shows that the LAB - 300 jacket used a central common rail when configuring the CPT. The element was wired is parallel as discussed in Section 3.3. Unlike the LAB 100 jacket, the LAB 300 had 25mm mineral wool (Rock 25) insulation within the jacket.

Blanket Properties (General)	
Blanket ID	LAB 300
Overall blanket dimensions	330mm x 460mm Approximately
Number of blankets per application	1
CPT inserts per blanket	1
Colour	Grey
Securing mechanism	Velcro
CPT Insert Properties	
CPT type	CPT 20 ohm heating material (Red)
CPT width (*l*)	406 mm
Rail length (W)	300 mm
Rail width	25 mm
Rail configuration	Common rail parallel
Insulation Properties	
Insulation	Rockwool / mineral insulation
Insulation thickness	25mm
K – value	0.001
Protective material properties	
Internal protective layers	Silicon coated glass cloth
External protective layers	Silicon coated glass cloth
Protective layer interface	Sewn – Nomex thread
Maximum operating temperature	< 150 deg C
Electrical Specification	
Operating Voltage	24 Voltage
Current (@ 24 Volts)	2.6 Amps
Power rating	63 Watts
Resistance	-
Temperature Control	
Primary Temperature Control	Programmable electronic control
Operating limits	> 120 deg C
Temperature probe	NTC probe
Secondary temperature Control	Bi-metallic thermal cut –outs
Operating limits	>120 deg C
Over temperature Protection	
Integrated thermal fuse	156 deg C
Estimated CPT surface temp	120 deg C
Power Source	
Power supply ID	Programmable electronic control
Connector type	Amphenol 4-pole plug and socket
Cable type	4 – core 2.5 mm diameter Y-Y
Cable length	3m

Table 4.9. LAB 300 Jacket specification

4.3.3. *LAB 400 Jacket*

Figure 4.7 shows the general arrangement for the heating jacket LAB 400 designed and manufactured to fit a mould 400mm x 400mm x 400mm cube as discussed in Chapter 7.

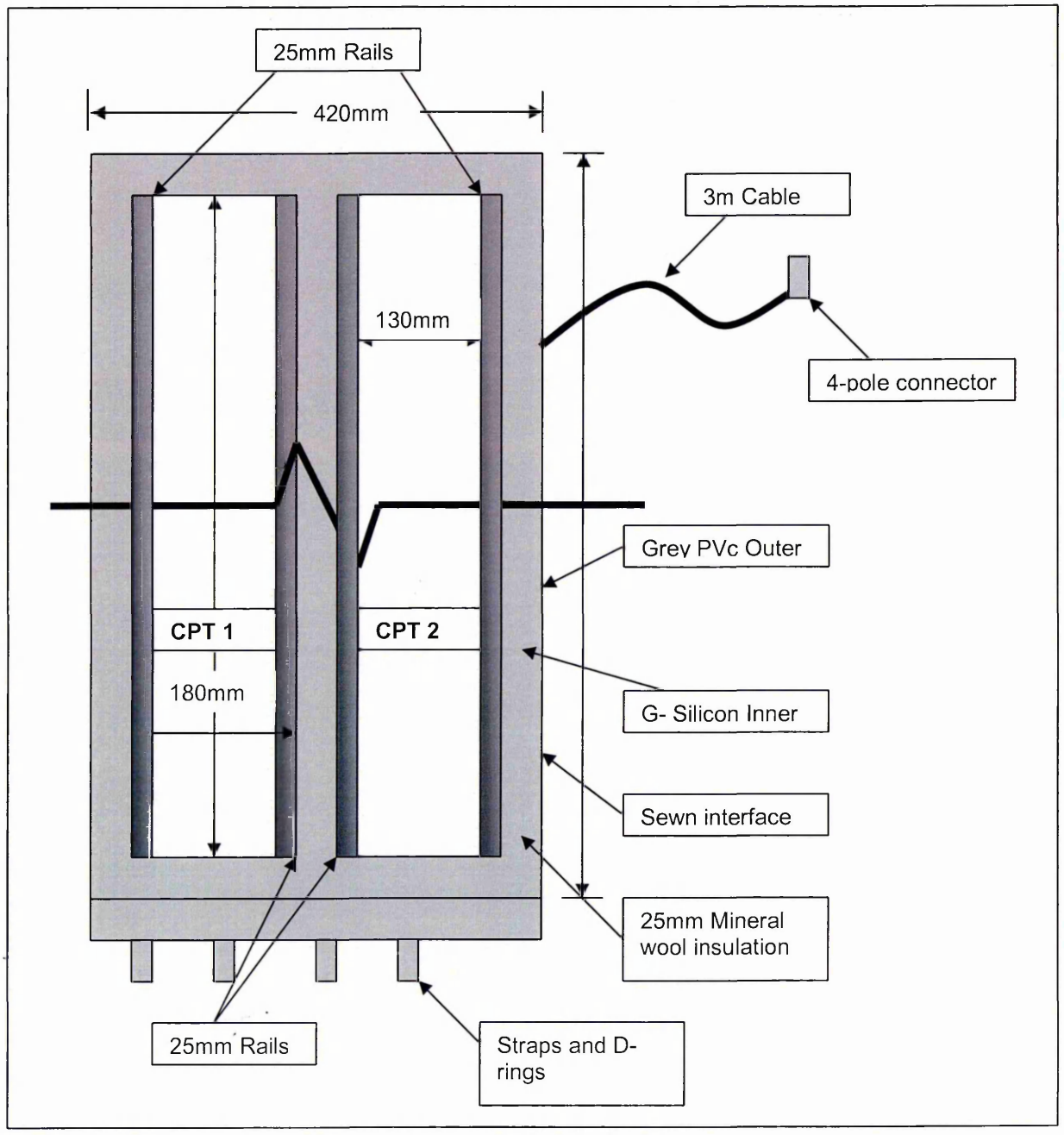

Figure 4.7. LAB 400 Jacket

The LAB 400 Jacket was designed to wrap around a cube mould 400mm x 400mm x 400mm as discussed in Chapter 7. The configuration of the jacket was two CPT elements wired in parallel.

Blanket Properties (General)	
Blanket ID	LAB 400
Overall blanket dimensions	1800mm x 450mm Approximately
Number of blankets per application	4
CPT inserts per blanket	2
Colour	Grey
Securing mechanism	D rings, straps and Velcro hook & eye
CPT Insert Properties	
CPT type	Inditherm I40
CPT width (*l*)	180mm
Rail length (W)	1600
Rail width	25mm
Rail configuration	Single element - parallel
Insulation Properties	
Insulation	Rockwool / mineral insulation
Insulation thickness	25mm
K – value	0.001
Protective material properties	
Internal protective layers	Silicon coated glass cloth
External protective layers	Grey PVC
Protective layer interface	Sewn – Nomex thread
Maximum operating temperature	< 150 deg C
Electrical Specification	
Operating Voltage	24 Voltage
Current (@ 24 Volts)	18.3 Amps
Power rating	440 Watts
Resistance	
Temperature Control	
Primary Temperature Control	Programmable electronic control
Operating limits	> 120 deg C
Temperature probe	NTC probe
Secondary temperature Control	Bi-metallic thermal cut -outs
Operating limits	>110 deg C
Over temperature Protection	
Integrated thermal fuse	156 deg C
Estimated CPT surface temp	120 deg C
Power Source	
Power supply ID	Programmable electronic control
Connector type	Amphenol 4-pole plug and socket
Cable type	4 – core 2.5 mm diameter Y-Y
Cable length	3m

Table 4.10. LAB 400 Jacket specification

4.3.4. *INSITU 1500 Jacket (Side)*

Figure 4.8 shows the general arrangement for the heating jacket INSITU-1500 designed and manufactured to cure a rail stanchion foundation 900mm x 900mm x 1500mm as discussed in Chapter 8.

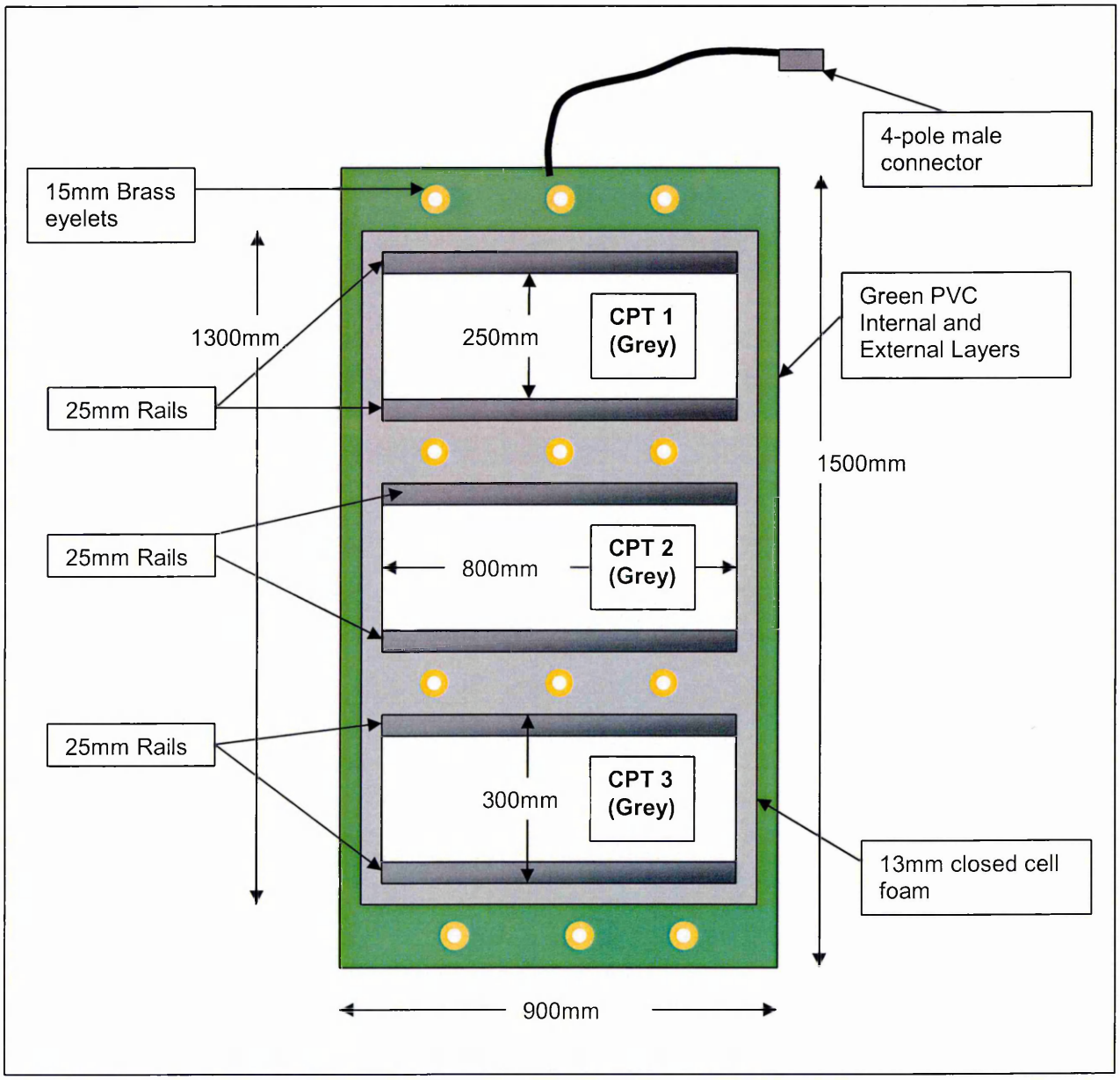

Figure 4.8. INSITU 1500 Jacket (Side)

The foundation was lined with 4 of the above jackets positioned on each internal face of the foundation, secured using pegs. The upper (ground level) surface of the concrete foundation was also heated using a heating jacket (Figure 4.9).

Blanket Properties (General)	
Blanket ID	Insitu 1500
Overall blanket dimensions	1500mm x 900 mm
Number of blankets per application	4
CPT inserts per blanket	3
Colour	Green
Securing mechanism	Eyelets and pegs
CPT Insert Properties	
CPT type	Inditherm Grey
CPT width (*l*)	400mm
Rail length (W)	600mm
Rail width	25mm
Rail configuration	Single elements in parallel
Insulation Properties	
Insulation	Closed cell foam
Insulation thickness	15mm
K – value	0.002
Protective material properties	
Internal protective layers	Green PVC – LGPVC
External protective layers	Green PVC – LGPVC
Protective layer interface	Laminated
Maximum operating temperature	50 deg C
Electrical Specification	
Operating Voltage	> 50 Volts
Current (@ 50 Volts)	1.8 Amps per m
Power rating (per blanket)	90 Watts per m
Resistance	25 – 30 ohms per m
Temperature Control	
Primary Temperature Control	N/A – Free running
Operating limits	> 90 deg C
Temperature probe	N/A
Secondary temperature Control	N/A
Operating limits	> 90 deg C
Over temperature Protection	
Integrated thermal fuse	121 deg C
Estimated CPT surface temp	50 deg C
Power Source	
Power supply ID	Portable tool transformer
Connector type	Amphenol 4 pole
Cable type	Y-Y 4 core 2.5 mm
Cable length	Various

Table 4.11. INSITU 1500 Jacket specification (side)

4.3.5. *INSITU 1500 Jacket (Upper)*

Figure 4.9 shows the general arrangement for the jacket used to heat the external surface of the rail stanchion foundation as described in Chapter 8 and used in conjunction with the heating Jackets shown in Figure 4.8.

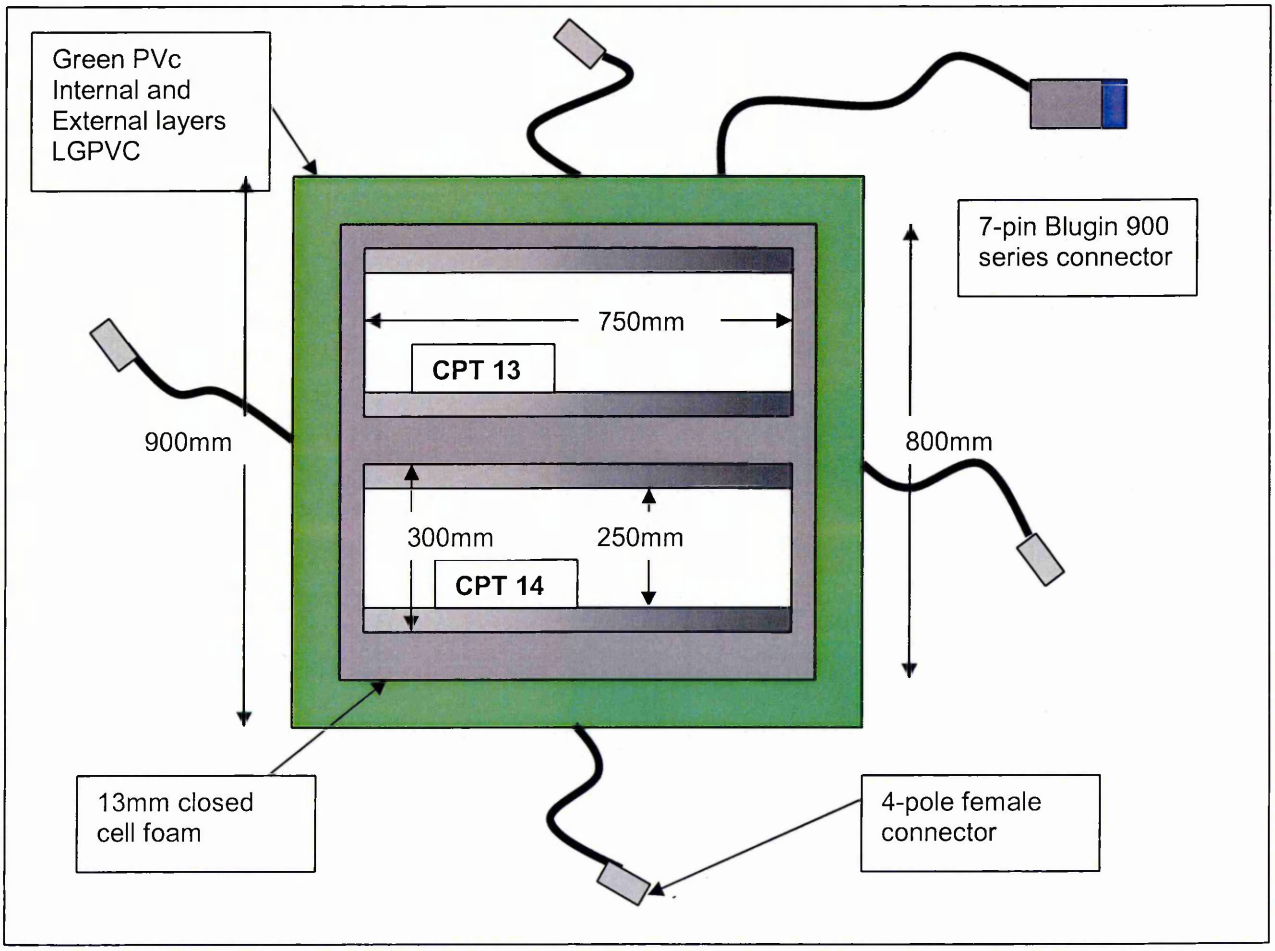

Figure 4.9. INSITU 1500 Jacket (Upper)

Blanket Properties (General)	
Blanket ID	Insitu 1500 – Lid
Overall blanket dimensions	900 mm x 900 mm
Number of blankets per application	1
CPT inserts per blanket	2
Colour	Green
Securing mechanism	Eyelets and pegs
CPT Insert Properties	
CPT type	Inditherm Grey
CPT width	400mm
Rail length	750mm
Rail width	25mm
Rail configuration	Single elements in parallel
Insulation Properties	
Insulation	Closed cell foam
Insulation thickness	15mm
K – value	0.002
Protective material properties	
Internal protective layers	Green PVC – LGPVC
External protective layers	Green PVC – LGPVC
Protective layer interface	Laminated
Maximum operating temperature	50 deg C
Electrical Specification	
Operating Voltage	> 50 Volts
Current (@ 24 Volts)	1.8 Amps per m
Power rating	90 Watts per m
Resistance	25 – 30 ohms per m
Temperature Control	
Primary Temperature Control	N/A – Free running
Operating limits	> 90 deg C
Temperature probe	N/A
Secondary temperature Control	N/A
Operating limits	> 90 deg C
Over temperature Protection	
Integrated thermal fuse	121 deg C
Estimated CPT surface temp	50 deg C
Power Source	
Power supply ID	Portable tool transformer
Connector type	Amphenol 4 pole
Cable type	Y-Y 7 core 2.5 mm
Cable length	Various

Table 4.12. INSITU 1500 Jacket specification (upper)

4.3.6. *PRECAST 6500 Jacket*

Figure 4.10 shows the general arrangement for the heating jacket PRECAST – 6500 designed and manufactured to cure a full-scale precast concrete terrace section as described in Chapter 9.

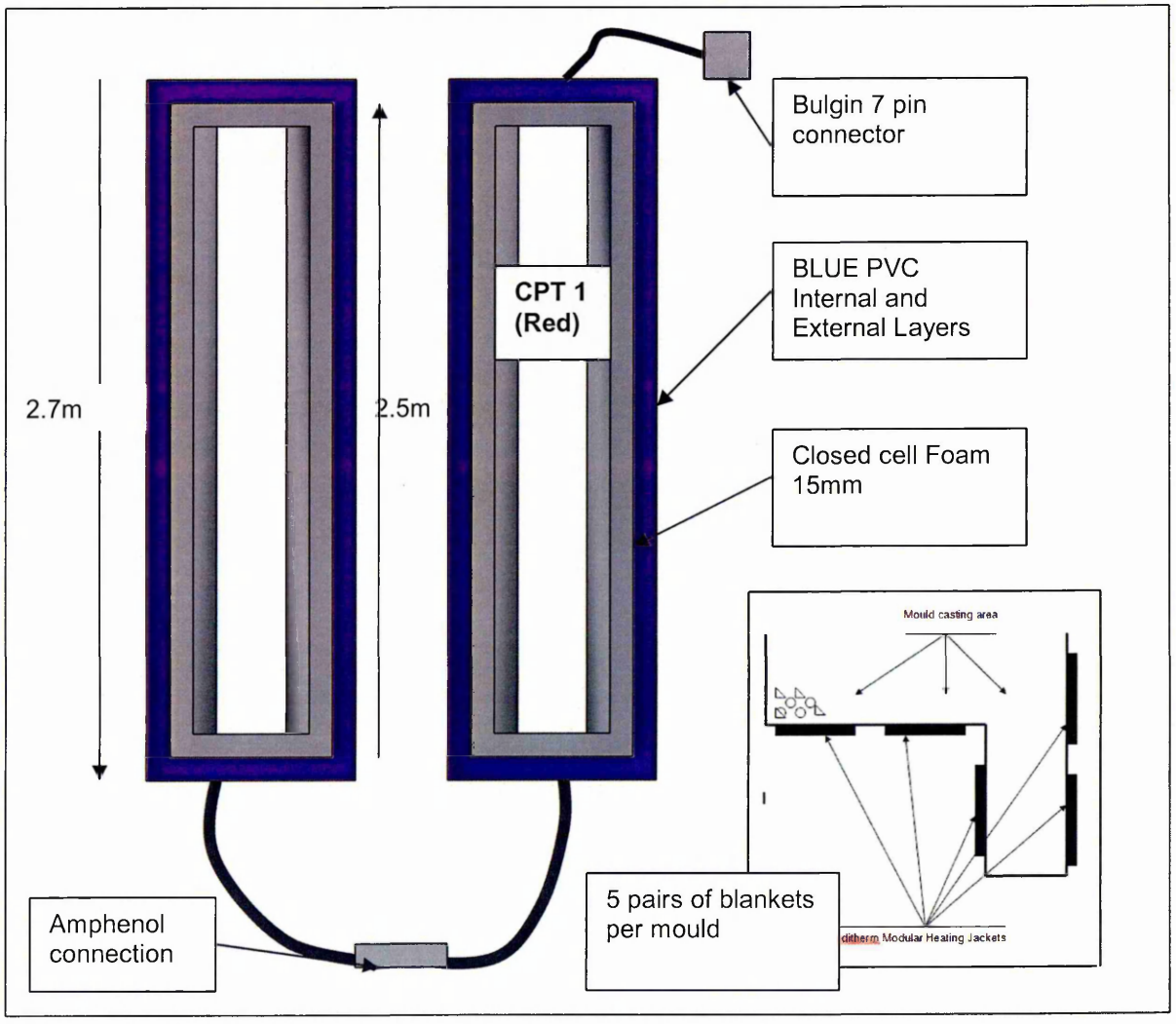

Figure 4.10. Precast 6500 Jacket

The heating system for the precast concrete mould consisted of 10 heating jackets, each measuring 2,700mm x 280mm for insertion into a precast concrete terrace mould. The jackets were designed to 'wedge' between the external strengthening ribs of the mould. Two sets of the jackets were positioned at the underside of the mould, and three sets to the side of the mould. Further details of the application of the Jackets is described in Chapter 9.

Blanket Properties (General)	
Blanket ID	PRECAST 6500
Overall blanket dimensions	2700 x 280 mm
Number of blankets per application	10
CPT inserts per blanket	1
Colour	Blue
Securing mechanism	Wedge
CPT Insert Properties	
CPT type	Inditherm Red
CPT width (*l*)	2500 mm
Rail length (W)	2500 mm
Rail width	250mm
Rail configuration	Single elements in parallel
Insulation Properties	
Insulation	Closed cell Foam
Insulation thickness	15mm
K – value	N/A
Protective material properties	
Internal protective layers	PVC
External protective layers	PVC
Protective layer interface	Lamination
Maximum operating temperature	70 deg C
Electrical Specification	
Operating Voltage	24 – 36 Volts
Current (@ 24 Volts)	Unknown
Power rating	Unknown
Resistance	Unknown
Temperature Control	
Primary Temperature Control	PID control
Operating limits	120 deg C
Temperature probe	PT 100
Secondary temperature Control	Mechanical thermostat
Operating limits	90 deg C
Over temperature Protection	
Integrated thermal fuse	121 deg C
Estimated CPT surface temp	70 deg C
Power Source	
Power supply ID	Precast control unit
Connector type	7 pin bulging
Cable type	Y – Y 7 core 2.5 m
Cable length	Various

Table 4.13. PRECAST 6500 Jacket specification

4.4. Transformer Control Units

Custom control and transformer units were used to operate the blankets at up to 50 Volts using alternating current. A general overview of the testing equipment details and wiring diagrams of the transformers and power equipment are given in Appendix 3. Two electronic control systems were used throughout the testing:-

a) The Carrel PT100 controller was used to control the surface temperature of the CPT within the various Jackets. The Carrell controller used a PT100 probe attached to the surface of the CPT element within the Jacket. The probe fed back the operating temperature and regulated the power to the CPT depending on the temperature set by the user.

b) The West 4000 temperature controller operated in the same manner as the Carrell controller, except it also has the capability to regulate the rate of temperature rise and fall of the CPT elements. This was controlled using a K-type thermocouple probe.

4.5. Concrete Mix Designs

Various concrete mix designs and material constituents were used in laboratory and field testing.

4.5.1. *Laboratory Concrete*

A concrete mix was designed to achieve a characteristic compressive strength of 50N/mm^2 at 28 days with a slump of between 50 – 75mm. The mix was designed using the code of practice: 'Design of Normal concrete mixes by the Building Research Establishment Ltd 1997. The mix was designed using a nominal coarse aggregate size of 10mm. This was a washed rounded gravel aggregate. The fine aggregate grading was Zone M. Results of the sieve analysis are given in Table 4.14.

Sieve size	material retained on the sieve	Percentage retained
(Um)	(gm)	%
2.36	347.90	17.40
1.18	186.60	9.33
850	75.50	3.78
600	114.60	5.73
425	201.70	17.92
300	463.20	23.16
212	258.70	12.94
150	100.40	5.02
0	89.00	4.45
Sum	**2000.00**	**100**

Table 4.14. Sieve analysis of fine aggregate showing zone M grading

Table 4.15 gives the concrete mix proportions used throughout the laboratory testing programme.

Constituent	Quantities kg/m^3
OPC	400
Fine Aggregate	628
Coarse Aggregate	1167
Water	180

Table 4.15. Mix design for concrete Mix A

All concrete batches were mixed using oven dried aggregates and standard OPC CEM I 42.5N conforming to EN 197-1 :1992. No admixtures were used.

Concrete was mixed in a 50 litre capacity horizontal pan type concrete mixer. Workability of the fresh concrete was measured by a slump test (BS 1881: Part 102/BS EN 12350-2). Control samples were cast and tested in compression at various ages throughout the programme.

4.5.2. *Concrete mixes used on site and in trials*

Major full scale site trials were conducted. The first was on a rail track site provided by the contractor Jarvis Rail and the second was within a precast concrete plant of Tarmac Precast Concrete Ltd.

The concrete at the rail track site was used to cast two stanchion foundations. Ready mix concrete was used which was delivered to site by truck from the supplier Tarmac Readymix in Selby, North Yorkshire. It was a standard Ordinary Portland Cement Structural concrete mix, C35 (35 N/mm^2 @ 28 days) as specified in British Rail OHL specification reference 084/021/001. The mix was designed for 'severe exposure conditions' in accordance with BS 5328 - part 1. The mix specification is given in Table 4.16.

Constituent	Quantities kg/m^3
Minimum cement content	325 kg/m^3
Maximum free w/c ratio	0.55
Nominal maximum aggregate size	20mm
Workability (slump)	75mm

Table 4.16. Specification for Mix B used in rail track stanchion foundations

The third concrete mix (Mix C) which was used in trials at the Tarmac Precast Concrete Ltd Plant at Tallington is given in Table 4.17.

Constituent	Quantities kg/m^3
Cement CEM I 52.5	312 kg/m^3
GGBS	133 kg/m^3
0-4mm limestone dust	776 kg/m^3
4-10mm granite	1018 kg/m^3
Admixture (workability)	3.2 kg/m^3
Water	180 kg/m^3

Table 4.17. Specification for Mix C used in precast concrete units

The concrete was used to cast L-shaped terrace sections at the Tarmac Precast Concrete Ltd plant at Tallington.

4.6. Temperature recording and thermocouples

Thermocouples of various Types were used to record temperature. Predominantly, however, K-Type thermocouples were used within the laboratory for their higher degree of accuracy. However, the K-Type thermocouples were more susceptible to interference from external sources. In field tests, T-Type thermocouples were used. These were significantly more

robust and less susceptible to external interference. Details of each thermocouple and operating limits are given in Table 4.18.

Type	Materials used	Temp. range	Insulation
K	Chromel / Alumel	-200 to 1200 deg C	PVC
T	Copper / Constatan	-200 to 350 deg C	PVC

Table 4.18. K and T – Type thermocouples used throughout the experimental programme

Thermocouples are susceptible to electrical interference since they measure temperature by small changes in potential difference between the two constituent materials used to manufacture the thermocouple. A method of 'sealing' the thermocouples from moisture had to be developed to protect them during tests and allowing results of a required accuracy to be obtained. This was done by sealing the thermocouples with an electrical 'Butt' crimp, traditionally used to connect two pieces of electrical cable. The thermocouple end was then sealed and secured within the crimp using an epoxy resin. A diagram showing the sealing of the thermocouple is given in Figure 4.11. This is a typical K-Type arrangement. For the T-Type arrangement, both individual wires are insulated, then a secondary insulation with a thin wire braid covers and insulates both wires to protects the thermocouple from external electro-magnetic interference.

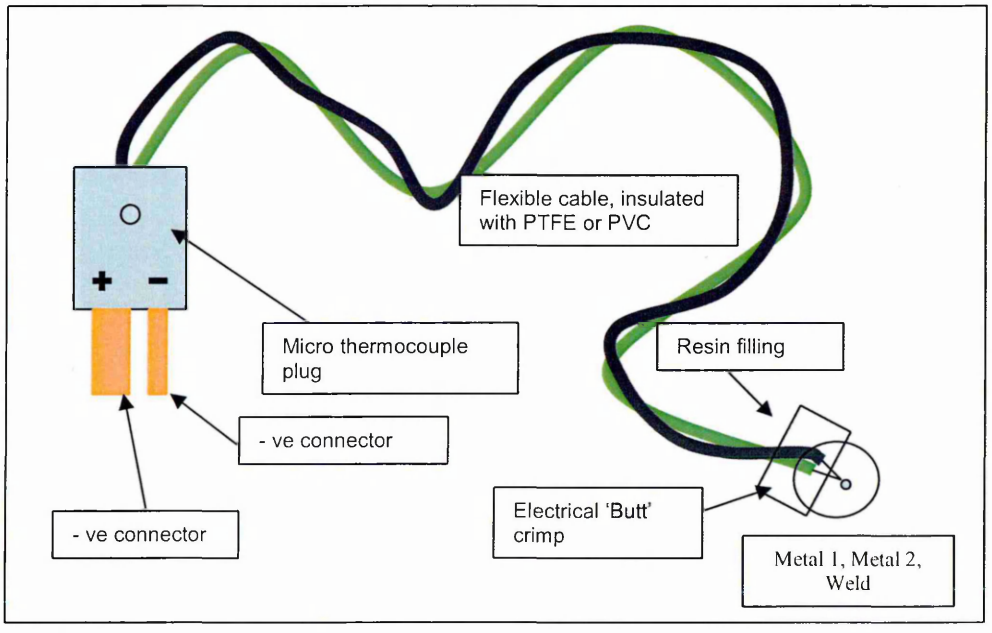

Figure 4.11. Thermocouple configuration and 'butt' crimp resin protection method.

All thermocouples were calibrated in order to avoid inserting faulty thermocouples in concrete and ensuring accurate results. Firstly, the thermocouples were placed together in a glass of ice and water for three minutes and then in a glass of water at 70 deg C. The performance of the thermocouples was assessed by comparison and any faulty ones rejected. Thermocouples placed directly adjacent to the CPT material were insulated electrically using insulation tape.

A thermocouple was threaded through a thin plastic tube to the point where it was crimped, allowing the thermocouple to be located within the concrete at the required location, then the tube pulled out of the concrete leaving the thermocouple exposed in position. When elements containing steel reinforcement were used, the thermocouples were attached to the reinforcement.

Temperature data was recorded on two types of data acquisition The first was the Pico TC-08 multi-function data acquisition unit with 8 input channels. Data was processed on Picolog for windows and imported into Excel. The second was a *Datataker*. This was a 10 channel unit with the capability to add an additional 10 channels. This had the advantage of remote logging powered by a battery.

4.7. Shrinkage Strain Measurement

A 300mm axial Demec strain gauge was used to measure the shrinkage strain of 300mm x 75mm x 75mm samples. The gauge used was reference Gauge No. (34/29), 1 division represents a strain of 1.077×10^{-5}.

4.8. Controlled Environments

Various controlled environments were use throughout the test programme to cure and store concrete elements prior to and during testing.

4.8.1. *Environmental Control Room*

All concrete samples were stored in the environment controlled room at Sheffield Hallam University prior to testing. Within this room the temperature and Relative Humidity are maintained at 20 deg C and 60 % respectively.

4.8.2. *Temperature – Humidity Chamber*

A Sanyo Atmos Chamber Type MTH – 4400/4400 PR within the materials testing laboratory at Sheffield Hallam University (calibrated by the Lowe group) was used to replicate steam curing environments during tests described in Chapter 6.It was also used for tests to

determine the durability of CPT materials as described in Chapter 10. Figure 4.12 shows a picture of the chamber.

Figure 4.12. Environment and temperature controlled chamber

4.9. Other Data Acquisition

Other data recorded during the test programme included the power consumption of the blankets during operation. This was done using a KWh meter appropriate to the size of the sample being tested. All the electrical characteristics of the CPT samples were measured with a Fluke True-rms Clamp meter (type 600A AC/DC). Details of measurement accuracy for the instrument can be seen in Table 4.19 and is given in full in Appendix 4.

Alternating Current	~ A	Range	0 – 999.9 A
		Accuracy	2% +/- 5 counts (10 – 100 Hz)
		AC Response	True RMS
DC Current	⎓ A	Range	0 -999.9 Amps
		Accuracy	2% + 3 counts
Alternating Voltage	~ V	Range	0 – 600.0 Volts
		AC Accuracy	True RMS
DC Voltage	⎓ V	Range	0 – 600.0 Volts
		Accuracy	1% + 5 counts
Resistance	Ω	Range	0 – 600.0 Ohms
		Accuracy	1.5% +/- counts

Table 4.19. Electrical meter specification

The meter used calculated the true RMS value which is the actual square-root of the average of the square of the curve, and not to the average of the absolute value of the curve or rather a mathematical conversion. A digital meter was used as it is potable and could be used when trialing CPT on site and in precast plants. The meter was calibrated by the manufacturer and was supplied with a certification of calibration. The range of measurements required to be taken meant that analogue laboratory equipment did not have sufficiently large measurement ranges and were too bulky.

Chapter 5. Basic Relationships of CPT

5.1. Introduction

This chapter will investigate the relationship between operating voltage of CPT elements, current and resistance, to determine if basic electrical theory can be applied to CPT elements. Understanding this relationship is critical for CPT element design so that the power requirement of sets of CPT elements and corresponding heat out-put can be predicted allowing suitable control equipment and transformers to be designed and manufactured. This chapter will also determine if there is a linear proportionality between the applied voltage to CPT elements and the current passing and, therefore, determining if the material is an ohmic or non-ohmic conductor.

5.2. Experimental Procedure

Three CPT materials of different Target Resistances R_T were used. The target resistances R_T were 20 ohm, 50 ohm and 150 ohm, as used throughout the research programme. These were the desired nominal resistances aimed for during manufacture of the CPT material, as described in Section 3.2. Each of the three CPT's are represented by the colours RED (R_T = 20 ohms), GREY (R_T = 50 ohms) and GREEN (R_T = 150 ohms).

To gain a greater understanding of the electrical properties of the CPT material and to establish a generic relationship between the power input and the heat output, the three CPTs (defined by their R_T of 20, 50 and 150 ohm) were tested to determine the resistance of different elements of various lengths l, and widths W. The true root mean squared Fluke meter measurement device, as described in section 4.9, was used for all electrical requirements (Voltage, Current and Resistance).

5.2.1. *Characteristic Resistance*

For each batch of CPT material, reference test elements of dimensions, 300mm x 212mm were configured from various rolls of a CPT batch, as shown in Figure 5.1. Samples were taken from up to 23 rolls of each batch of CPT, at the ends and from the middle of each roll. Each roll was approximately 25m long, 1m wide. The resistance of each test sample was measured using a calibrated multi-meter. The resistance was taken at the three opposite points as shown in Figure 5.1.

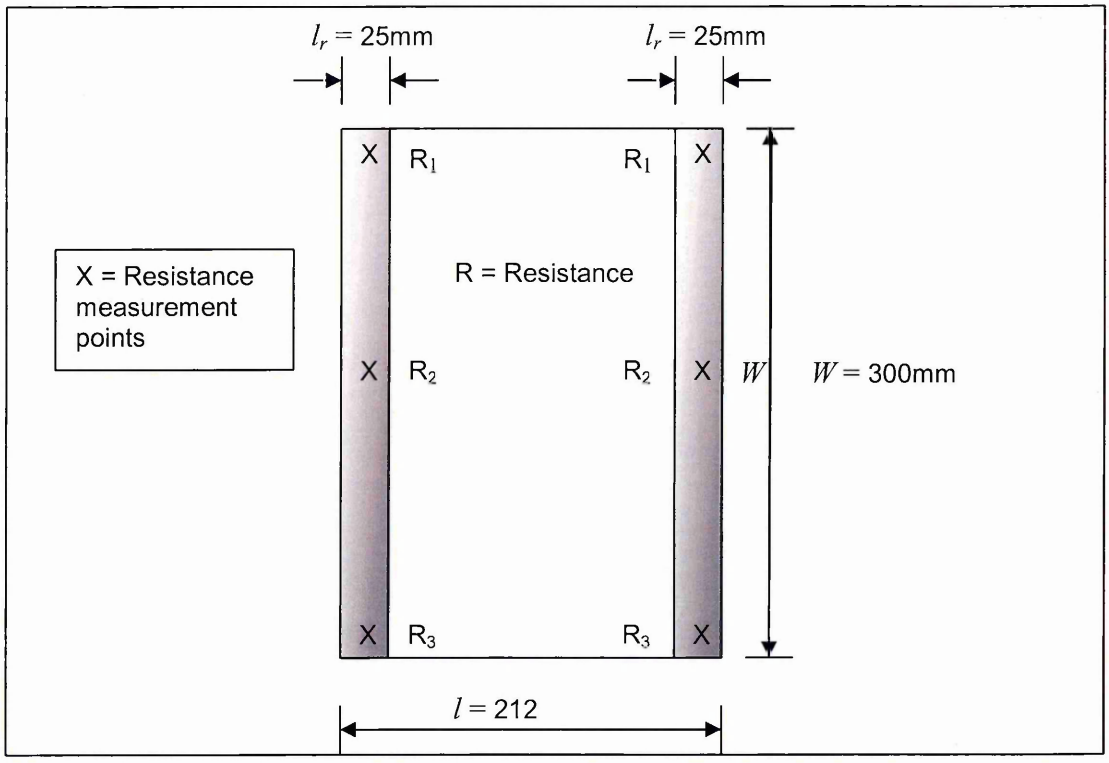

Figure 5.1. Determination of Characteristic Resistance R_{ID}

l	=	Element length (mm)
l_r	=	Width of conductive rails (mm)
W	=	Width of element (length of rail) (mm)

The average of the three resistance measurements was taken. This average value is defined as the Characteristic Resistance of each material, R_{ID}.

5.2.2. *Relationship between Element Length and Resistance*

For each of the three CPTs, six elements were manufactured at width, W, of 1m and various lengths (l): 120mm, 200mm, 280mm, 360mm, 420mm and 550mm. Figure 5.2 shows the CPT configurations tested.

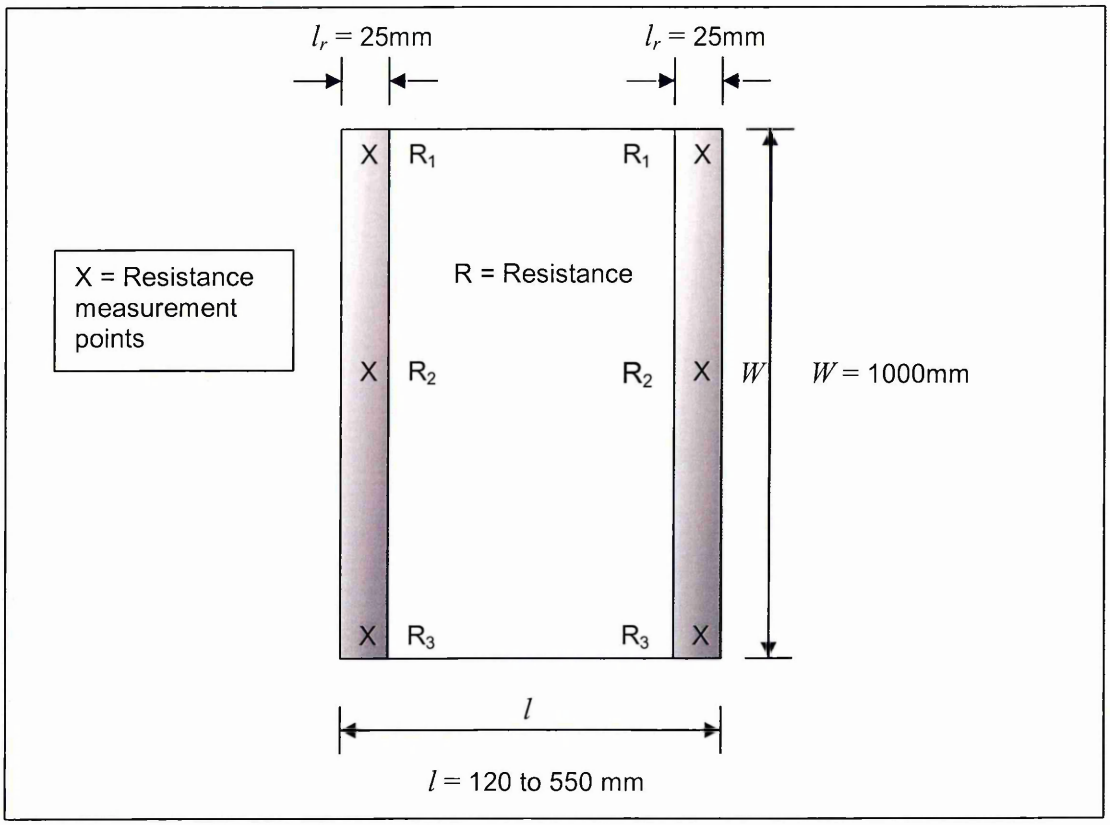

Figure 5.2. CPT element configuration and resistance measurement locations

l	=	Element length (mm)
l_r	=	Width of conductive rails (mm)
W	=	Width of element (length of rail) (mm)

The resistance was measured using a calibrated multi-meter between the two conductive rails across points marked X in Figure 5.2, as described in Chapter 3. All tests were conducted at a constant ambient temperature of 22 deg C.

5.2.3. *Relationship between Element Width and Resistance*

Another set of CPT elements was configured to determine the relationship between resistance R and the width, W, of the conductive element (i.e. the length of the parallel conductive rails). For each of the three CPTs of R_T 20 ohm, 50 ohm and 150 ohm, four elements each of length l, 120mm, 200mm, 280mm and 400mm (distance between the outer most points of the conductive rails) were configured at various widths W of 150mm, 200mm 500mm, 800mm 1500mm and 2000mm as shown in Figure 5.3.

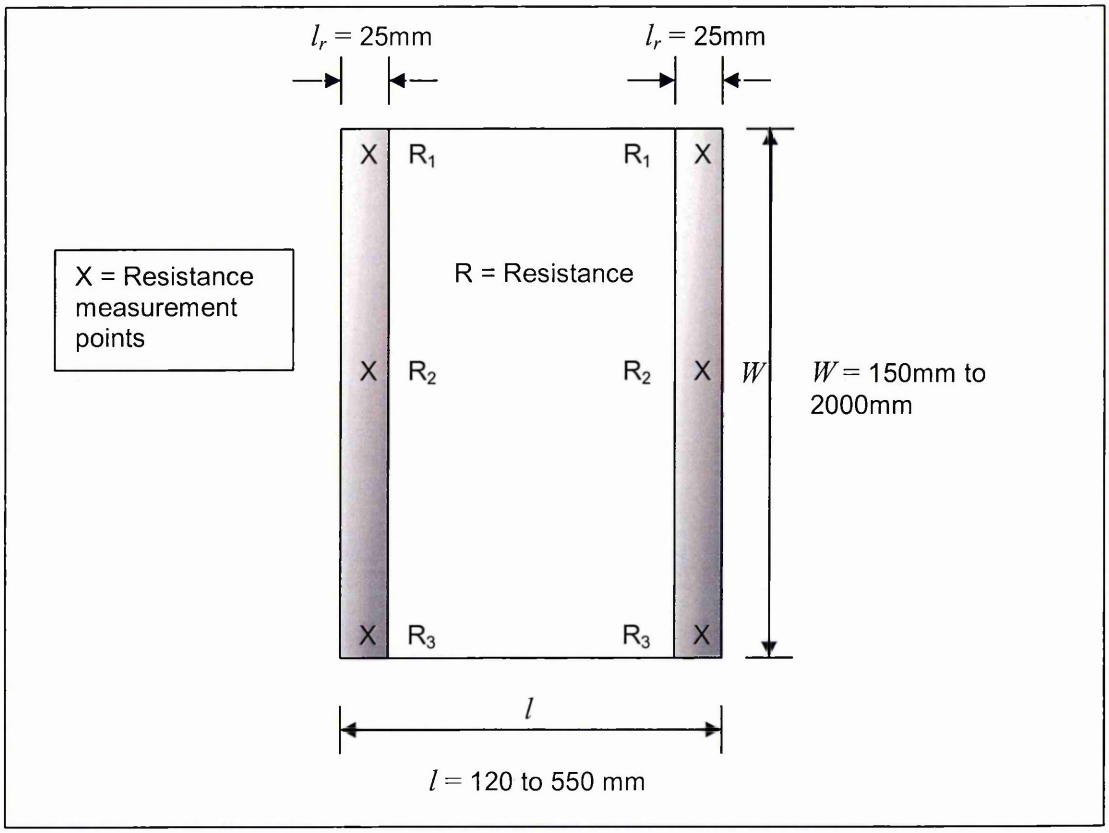

Figure 5.3. CPT configuration and resistance measurement points

l	=	Length of test sample, (element) (distance between outside edges of the rails) (mm)
l_r	=	Width of conductive rails (mm)
W	=	Width of test sample (element) (length of conductive rail) (mm)

Again, the resistance was measured using a calibrated multi-meter as described in the previous section. By undertaking this test it was envisaged that a relationship between the CPTs width W, and resistance R can be determined, and also linked with the results from the previous section.

5.2.4. *Relationship between Current and Applied Voltage for Elements of Various Lengths*

Following the measurement of the resistance of the three types of CPT elements of various lengths l at 1m widths, a potential difference was applied between the two conductive rails for each element. This was undertaken using 5 different potential differences for each element, (12 Volts, 18 Volts, 24 Volts, 30 Volts and 36 Volts) and the corresponding current flowing through the CPT material between the two conductive rails was measured using the calibrated multi-meter connected in series to the elements. By conducting this test a

relationship between current and length for each element could be determined. For each of the three CPT materials, the relationship between element length and current at various applied voltages was plotted. The Voltage was applied from an alternating supply using a variable transformer. The setup is shown in Figure 5.4.

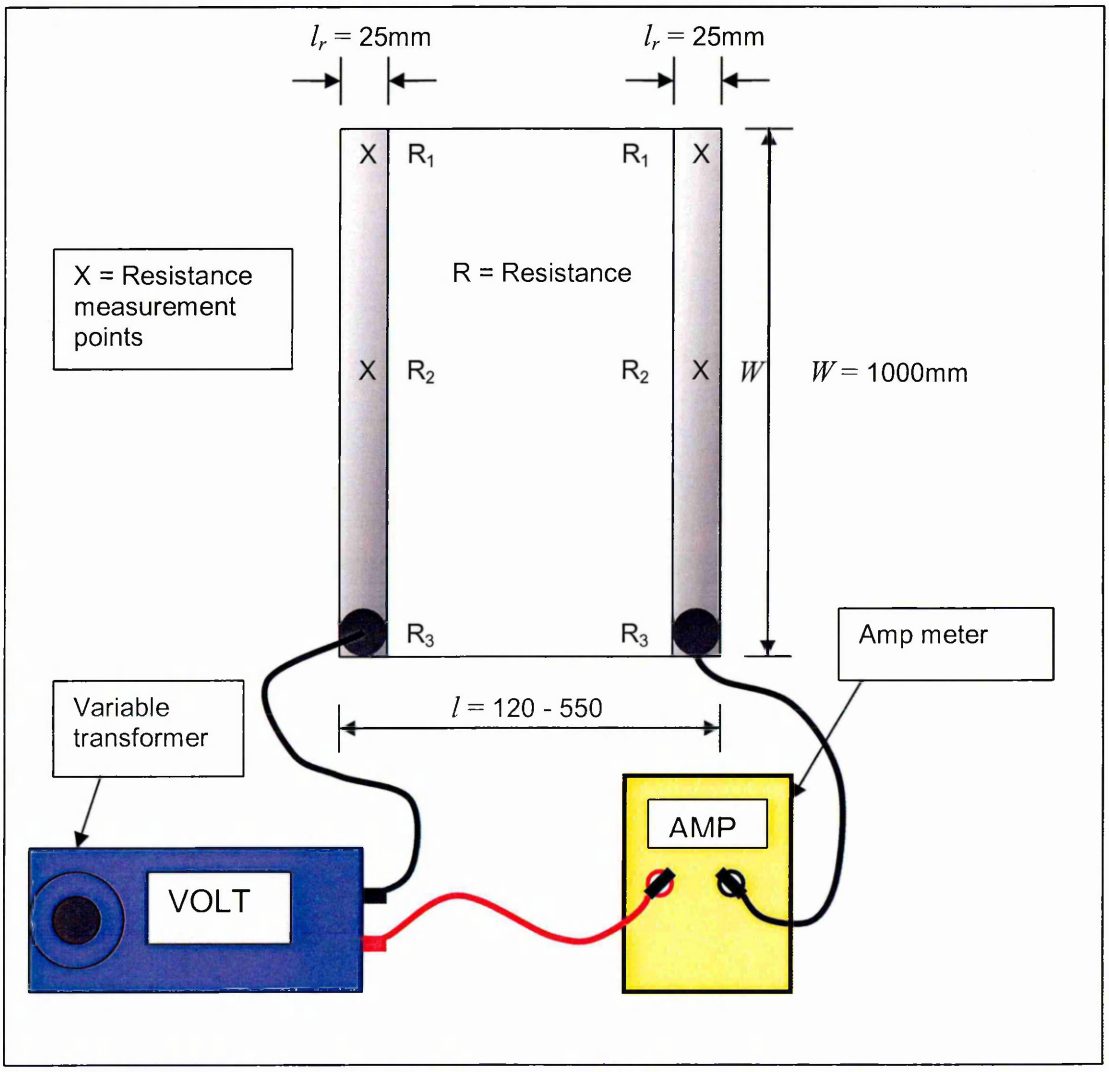

Figure 5.4. CPT configuration and current measurement points

5.3. Results

5.3.1. *Characteristic Resistance*

The Characteristic resistance R_{ID} (average resistance of each batch of CPT) is always slightly different from the Target Resistance R_T since the application of CPT layers on the cotton fabric cannot be controlled to greater precision. Figure 5.5 shows the values of the measured characteristic resistance, $R_{ID,}$ and the corresponding desired Target Resistance R_T for the three CPTs.

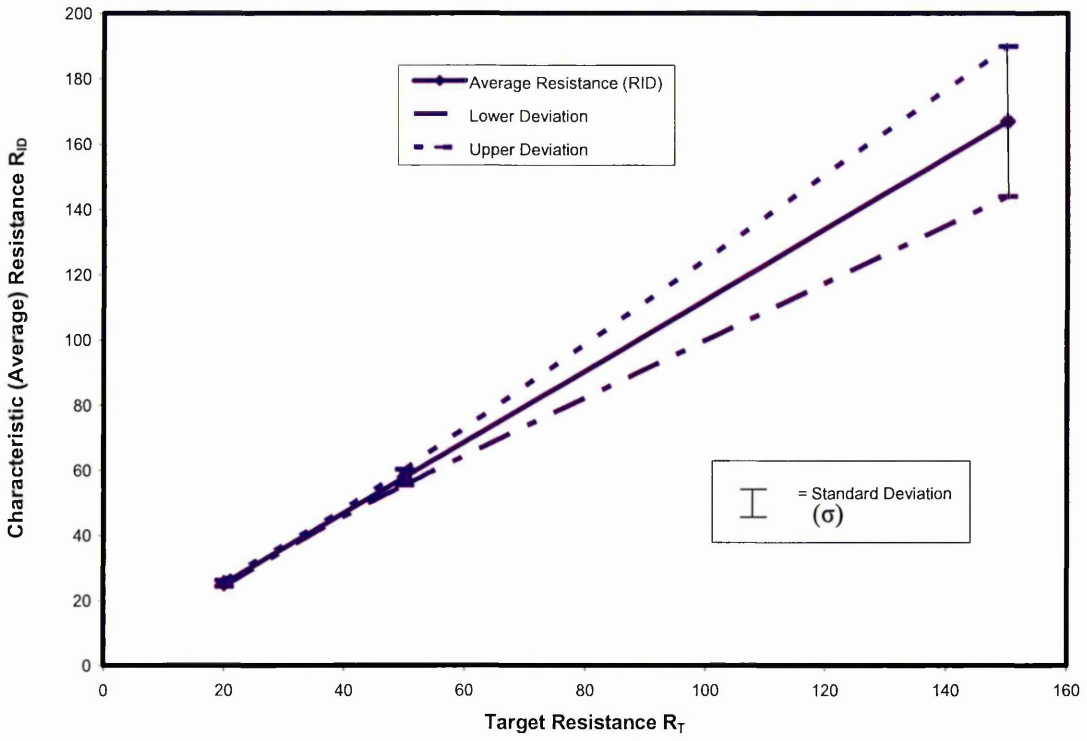

Figure 5.5. Batch resistances (Characteristic and Target) for the three CPT's

The range of test data, given and Table 5.1, shows that closer tolerances can be achieved for CPT materials of a lower target resistance as shown by the standard deviation (σ). Table 5.1, shows that as the Characteristic Resistance of a batch increases so does the spread of resistance, shown by the standard deviation. For the R_T = 20 ohm material, the maximum variation in resistance over all samples tested was 4.3 ohms (approximately +/- 0.92% compared to the mean) whereas for the R_T = 150 ohm material, the spread between the upper and lower values was 75 ohms (approximately +/- 22.92%) of the Characteristic Resistance.

Target Resistance (R_T)	Characteristic Resistance (R_{ID})	Maximum Resistance (R_{MAX})	Minimum Resistance (R_{MIN})	Stan Dev (σ)	R_{MAX} - R_{MIN}
20 ohm	25.4 ohms	28.3 ohms	24.0 ohms	0.92	4.3 ohms
50 ohm	57.9 ohms	66.3 ohms	50.0 ohms	2.45	16.3 ohms
150ohm	167.04 ohms	203 ohms	128 ohms	22.94	75 ohms

Table 5.1. Summary of batch resistances

The average resistance of a batch gives the Characteristic Resistance, R_{ID}, for each CPT. The standard deviation gives an indication of the resistance spread within the batch.

Throughout this Chapter the three CPTs will be referred to by their Target Resistance, R_T, of 20ohm, 50ohm and 150ohm and their corresponding colours Red, Grey and Green. Corresponding R_{ID} (Characteristic Resistance) values, however, will be used in the analysis of experimental data.

5.3.2. *Relationship between Element Length and Resistance*

Figure 5.6 shows the relationship of the measured resistance and the element length, l (distance between the outer most edges of the conductive rail) for each CPT, for elements of width W = 1m.

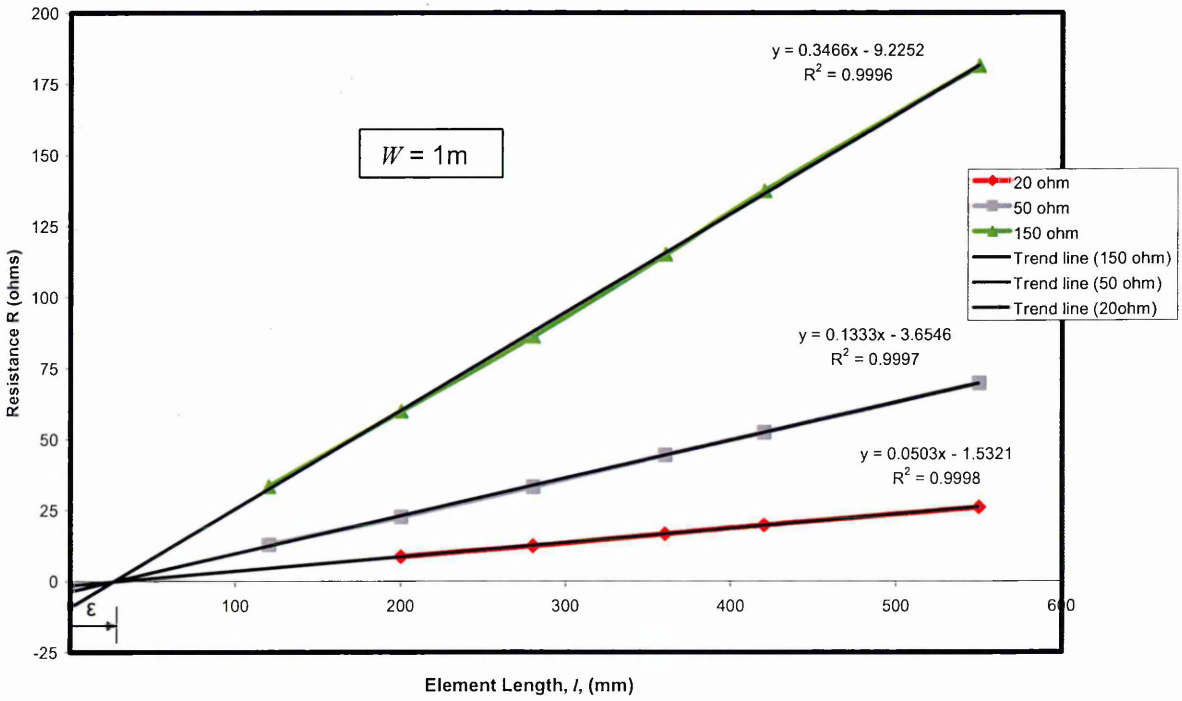

Figure 5.6. Graph of measured resistance versus element length

Figure 5.6 shows that for each CPT there is a linear relationship between the length, l, and the resistance of each element. It can be seen from Figure 5.6 that for each CPT the line of best fit intercepts the x-axis at approximately 25 - 35mm. This value will be defined as ε, 'the effective length factor', where $(l - \varepsilon)$ equals the effective length, l_{eff}. This indicates that the actual length of the conductive path extends from somewhere between the inner and outer most edges of the parallel conductive rails. The exact values of ε can be found by calculating the x-intercept for each CPT material in Figure 5.6 using the best-fit equations for each CPT. This can be done with confidence as the coefficient of correlation, R^2, for each straight line is greater than 0.99. When the resistance is zero the corresponding value for length, ε, can be expressed as;

$$\text{At } R = 0, \quad X = \varepsilon = c / m \qquad \text{[Eq 5.1]}$$

Where;

R	=	Resistance (ohms)
ε	=	Effective length factor (mm) – intercept on x-axis
c	=	Y- axis intercept of the linear equations
m	=	Gradient of the linear equations

The calculated value of ε for each CPT tested is given in Table 5.2.

CPT Type	m	c	ε
RED (R_T = 20 ohms)	0.0503	1.5321	30.4 mm
GREY (R_T = 50 ohms)	0.1333	3.6546	27.41 mm
GREEN (R_T = 150 ohms)	0.3466	9.2252	26.61 mm

Table 5.2. Summary of batch resistances

The values of ε (effective length factor) change slightly with CPT of different R_T of width 1m. In terms of ε the equation between resistance and length of the CPT elements can be re-written to shift the origin of the graph as shown in Figure 5.7.

$$R(l) = m(l - \varepsilon) = m l_{eff} \qquad \text{[Eq 5.2]}$$

Where;

R (l)	=	Resistance (ohms) of CPT elements of different length, l, and width W = 1m
l	=	Length of element (distance between outside edges of the rails) (mm)
m	=	Gradient of the Resistance - length linear relationship
ε	=	Effective length factor (mm)
l_{eff}	=	Effective length = (l – ε)

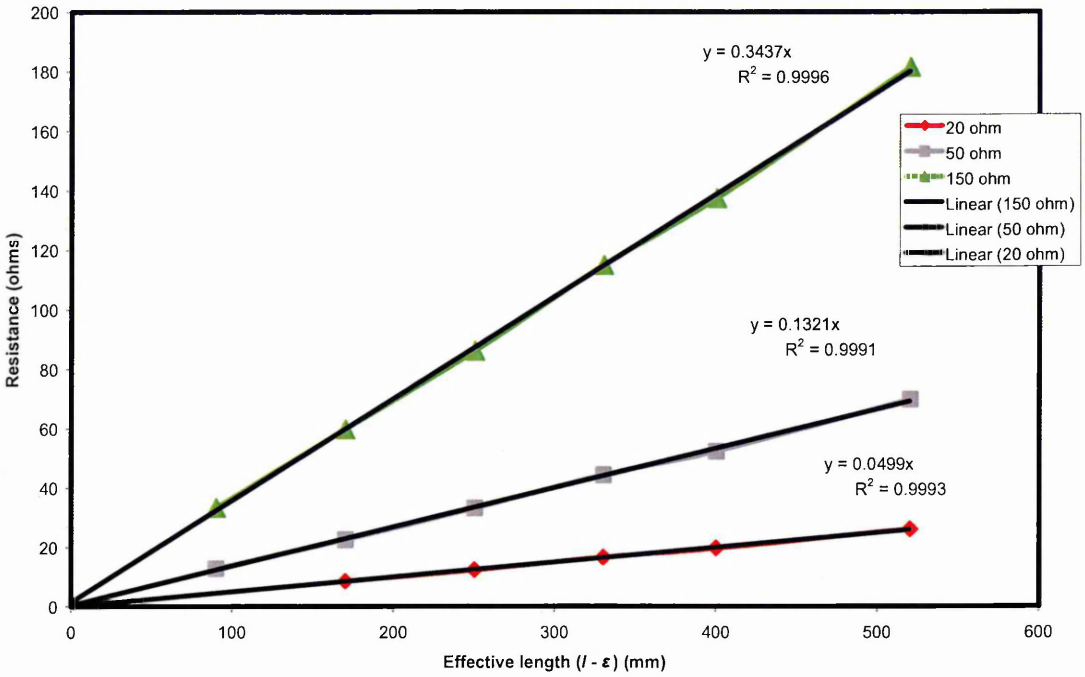

Figure 5.7. Graph of measured resistance versus effective length

Figures 5.6 and 5.7 show that for each CPT tested (R_T = 20 ohm, 50 ohm and 150 ohm) and element width W = 1m, the relationship between the element length and resistance is linear.

5.3.3. *Relationship between Element Width and Resistance*

Figure 5.8 shows the relationship between element resistance R and the element width W (length of conductive rail). The resistance was measured for elements of widths 100mm, 150mm, 200mm, 500mm, 800mm, 1500mm and 2000mm for four lengths (l) 120mm, 200mm, 280mm and 400mm. (l = distance between conductive rails).

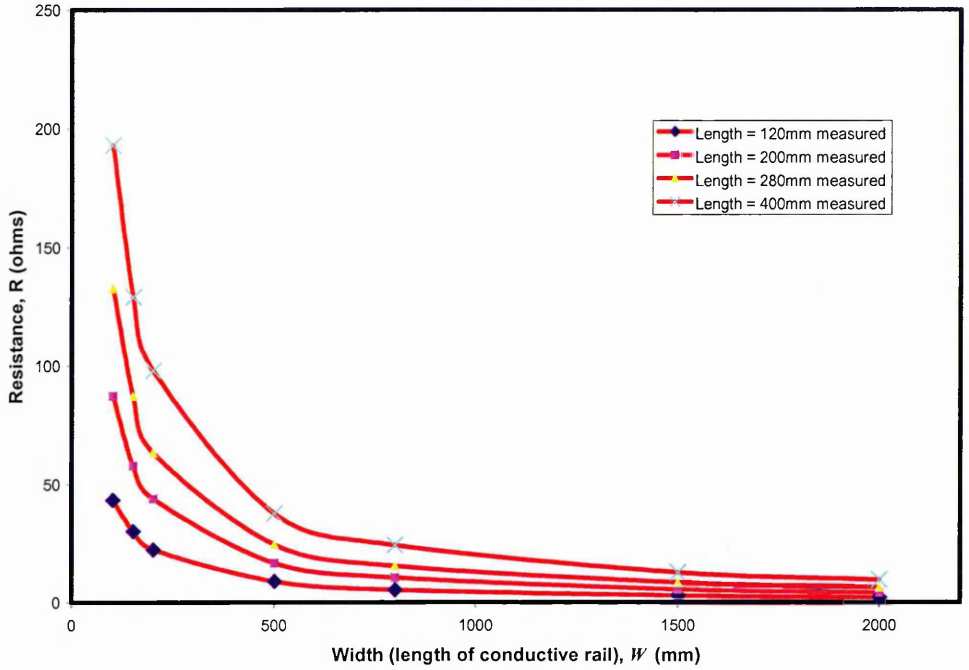

Figure 5.8. Graph of measured resistance versus element width, W, for given element lengths, l, (R_T = 20 ohm)

Figure 5.8 shows the relationships between element resistance R and the element width W (length of conductive rail) to be non-linear for the CPT of R_T = 20 ohms. This is also true for elements of various lengths for the CPT material of R_T = 150 ohms (Figure 5.9).

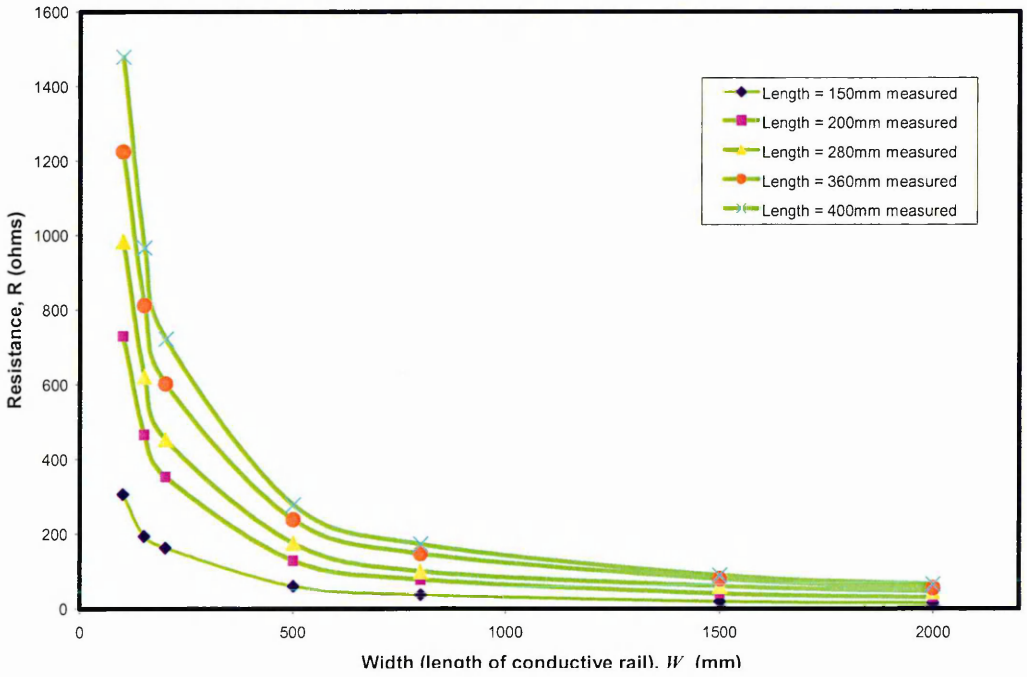

Figure 5.9. Graph of measured resistance versus element width, W, for given element lengths, l, (R_T = 150 ohm)

Figures 5.8 and 5.9 show non-linear inverse relationship between resistance and width. Figure 5.8 shows that decreasing widths below 500mm results in sharply increasing resistance (asymptotic curve), as does Figure 5.9 for the CPT R_T = 150 ohm. Above width 500mm (length of the conductive rails), the resistance for the CPT R_T = 20ohms (Red) decreases practically linearly with increasing width and the change is relatively small, i.e. resistance becomes almost constant within a small range of 4 to 30 ohms. For the Green material, R_T= 150 ohms, the resistance becomes almost constant between 25 and 100 ohms.

Considering an element of constant length, l, the general relationship between resistance, R, and width, W, can be described by either of the following exponential relationships.

$$R(W) = \beta W^{\alpha} \qquad \text{[Expression 1]} \qquad \text{[Eq 5.3]}$$

Or;

$$R(W) = \beta e^{\alpha W} \qquad \text{[Expression 2]} \qquad \text{[Eq 5.4]}$$

Where;

$R(W)$	=	Resistance (ohms) at different element width W (with (constant l)
W	=	Width of element (length of rails)
β	=	Constant that represents the rate of change with width, (CPT specific)
α	=	Correction factor (CPT specific)

5.3.4. *Relationship between Current and Voltage*

Figures 5.10, 5.11 and 5.12 show the relationship between current and length, l, (distance between rails), of the CPT element of width 1m for the three CPT materials (R_T = 20, 50 and 150 ohm). Data was obtained by applying different voltages (12, 18, 24, 30, 36 and 50 Volts) to elements with lengths (distance between conductive rails), l, of 120mm, 200mm, 280mm, 360mm, 420mm and 500mm. All elements tested had a width (length of conductive rail), W, of 1m.

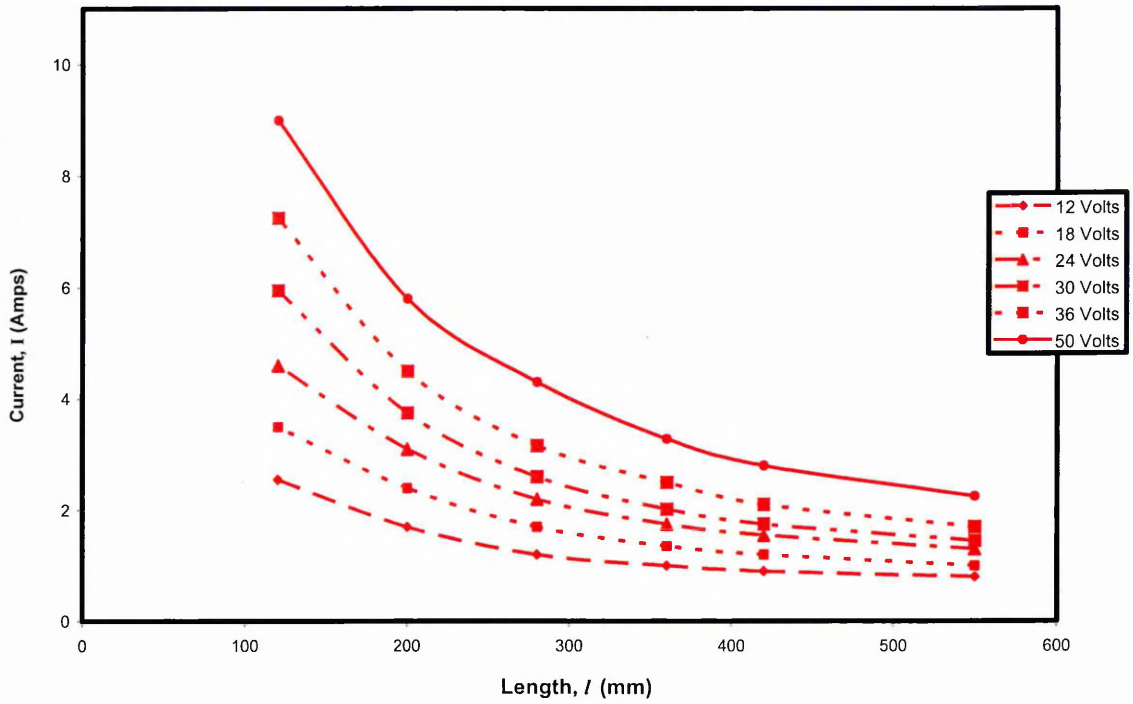

Figure 5.10. Current versus element length, l, for R_T = 20 ohm, W = 1m

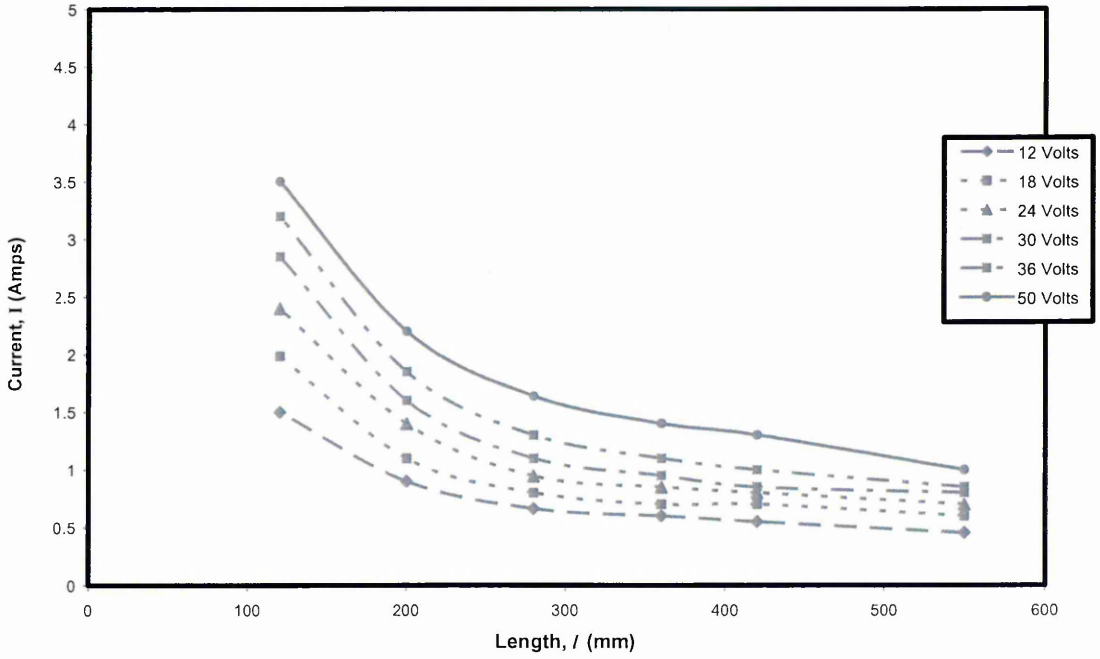

Figure 5.11. Current versus element length, l, for R_T = 50 ohm, W = 1m

In general these three relationships show that as the target resistance is decreased, the flow through similar sized elements for each CPT tested increases. For example, for the element

of length l = 280mm and W=1000mm, the flow of current for the 20 ohm material ranges between 1.1 – 4.5 Amps compared to 0.25 – 0.8 Amps for the 150 ohm CPT.

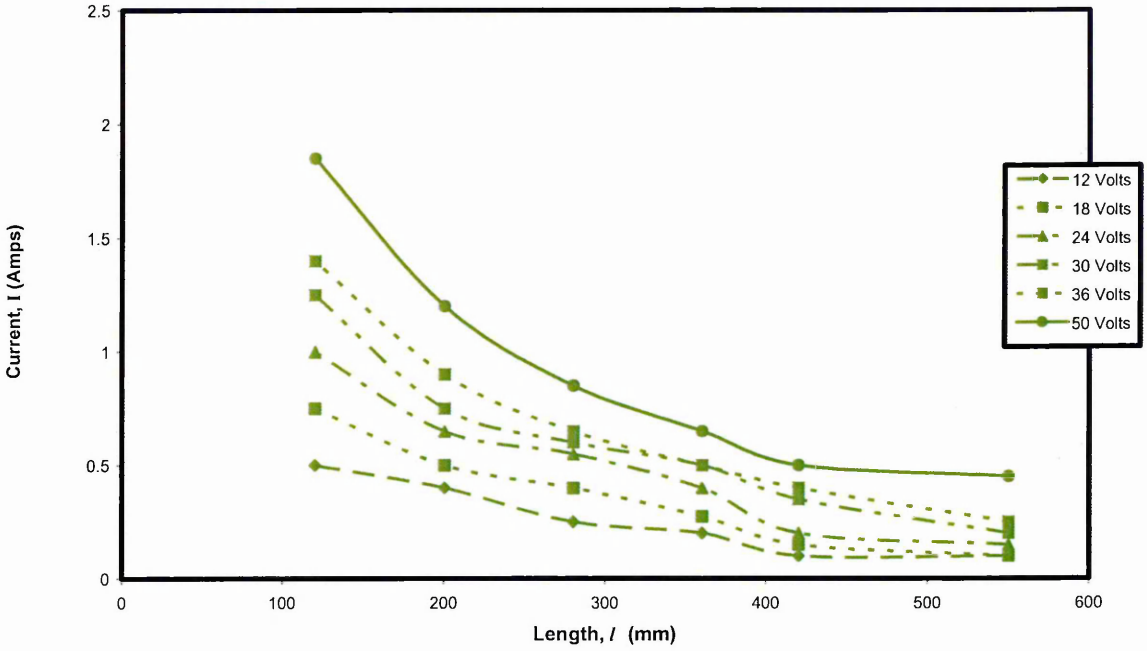

Figure 5.12. Current versus element length, l, for the R_T = 150 ohm

Figures 5.10 – 5.12 show that for a constant applied voltage, as the length of the element decreases, the current flow through it increases.

5.4. Discussion and Analysis

The resistance of any given element is a function of the length, l and width, W, a general relationship can be determined by combining the individual relationships between R and l (Equation 5.2) and R and W (Equation 5.3 or 5.4) of the element. Thereby, combining Equation 5.3 with Equation 5.2 gives:-

$$R = \beta W^{\alpha} \text{ x } m(l - \varepsilon) \qquad \text{[Eq 5.2, 5.3]}$$

$$R = M(l - \varepsilon)W^{\alpha} \qquad \text{[Eq 5.5]}$$

Combining equations 5.4 and 5.2 gives:

$$R = \beta e^{\alpha W} \text{ x } m(l - \varepsilon) \qquad \text{[Eq 5.2, 5.4]}$$

$$R = M(l - \varepsilon)e^{\alpha W} \qquad \text{[Eq 5.6]}$$

Where;

l	=	Length of test sample (element), i.e. distance between outside edges of the rails (mm)
W	=	Width of test sample (element), i.e. length of conductive rail (mm)
ε	=	Effective length factor (mm)
l_{eff}	=	Effective length = $(l - \varepsilon)$
α	=	Material constant
M	=	Material constant (m x β)
m	=	Gradient of the Resistance – Length linear relationship

Both equations Eq 5.5 and Eq 5.6 are linear and a regression analysis is undertaken to determine values for the constants M, and α. However, prior to undertaking the regression analysis for each CPT material, the value of ε for each material at varying widths is required. The value of ε has already been determined for elements of W = 1m (section 5.3.2). To determine if the value of ε varies with W, it's value will be calculated for R_T = 20 ohms and 150 ohms for elements of varying lengths, l and width, W, in the following section.

5.4.1. *Determination of Effective Length Factor*

For the CPT material of R_T = 20ohm, Figure 5.8 can be redrawn as shown in Figure 5.13. It shows the relationship between element length, l, and resistance R for elements of widths, W, equal to 100mm, 150mm, 200mm, 500mm, 800mm, 1500mm and 2000mm.

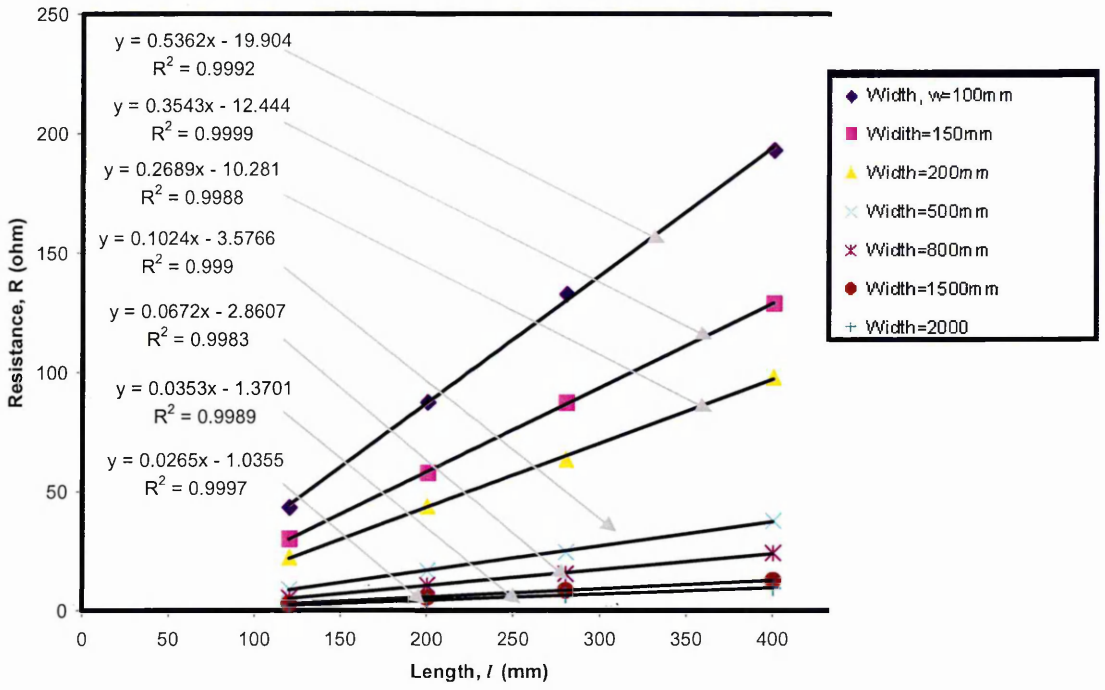

Figure 5.13. Graph of measured resistance versus element length for various element widths (R_T = 20 ohm)

Figure 5.13 shows a linear relationship between l and R with a coefficient of correlation R^2 above 0.9. All best fit lines tend towards a similar intercept on the x-axis, the effective length factor, ε. The value of ε for each width, W, of the CPT element is calculated from the linear equations and tabulate in Table 5.3. The calculation is based on the Gradient (A) of each linear equation in Figure 5.13 and their intercept on the y-axis (c).

Width W (mm)	Gradient A	Y-intercept c	ε = c/A
100	0.5362	19.904	37.12048
150	0.3543	12.444	35.12278
200	0.2689	10.281	38.23354
500	0.1024	3.5766	34.92773
800	0.0672	2.8607	42.56994
1500	0.0353	1.3701	38.81303
2000	0.0265	1.0355	39.07547
		Average =	37.98402 = 38 mm

Table 5.3. Values of effective length factor, ε (R_T = 20 ohm)

Table 5.3 shows that ε ranges between 37.12 mm and 42.57 mm for the CPT R_T = 20 ohms with an average value of 37.98 mm, say 38 mm.

Figure 5.14 and Table 5.4 show the calculation of ε for the CPT material R_T = 150 ohms.

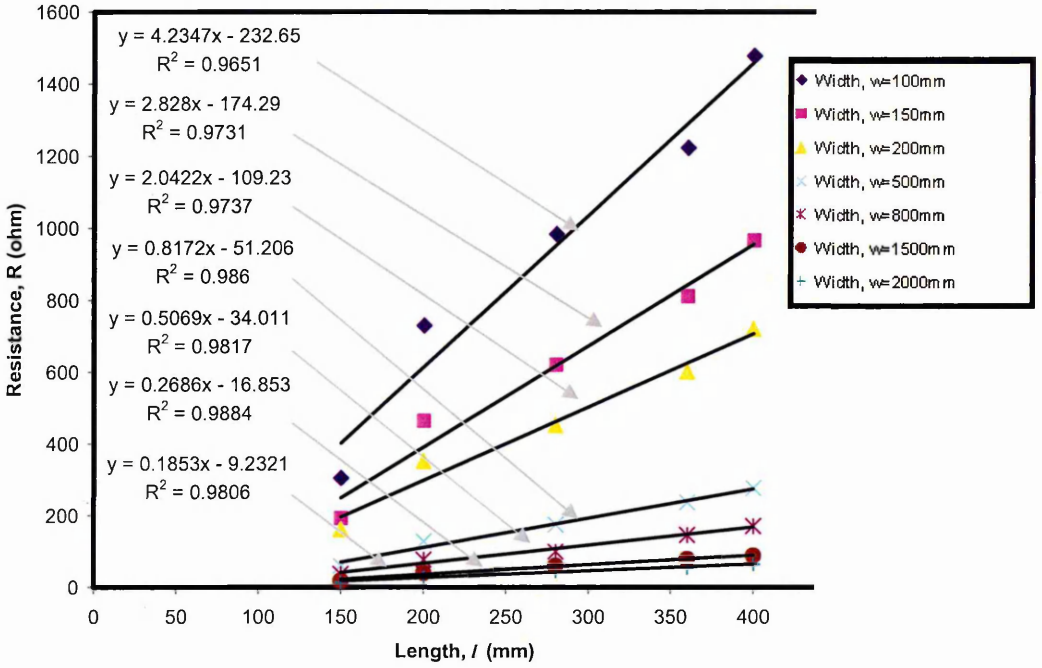

Figure 5.14. Graph of measured resistance versus element length for various element widths (R_T = 150 ohm)

The coefficients of correlation are less than those observed for the RT = 20 ohm CPT, however, at above 0.96 they are acceptable.

Width W (mm)	Gradient A	Y-intercept c	ε = c/A
100	4.2347	232.65	54.93896
150	2.828	174.29	61.63013
200	2.0422	109.23	53.48644
500	0.8172	51.206	62.6603
800	0.5069	34.011	67.09607
1500	0.2686	16.853	62.74386
2000	0.1853	9.2321	49.82245
		Average =	58.91117 = 59 mm

Table 5.4. Calculation of effective length factor, ε (R_T = 150 ohms)

Table 5.4 shows that ε ranges between 53.49 mm and 67.09 mm for the CPT R_T = 150 ohms with an average value of 58.91 mm, say 59 mm. Figure 5.15 shows ε plotted against W for the two CPTs.

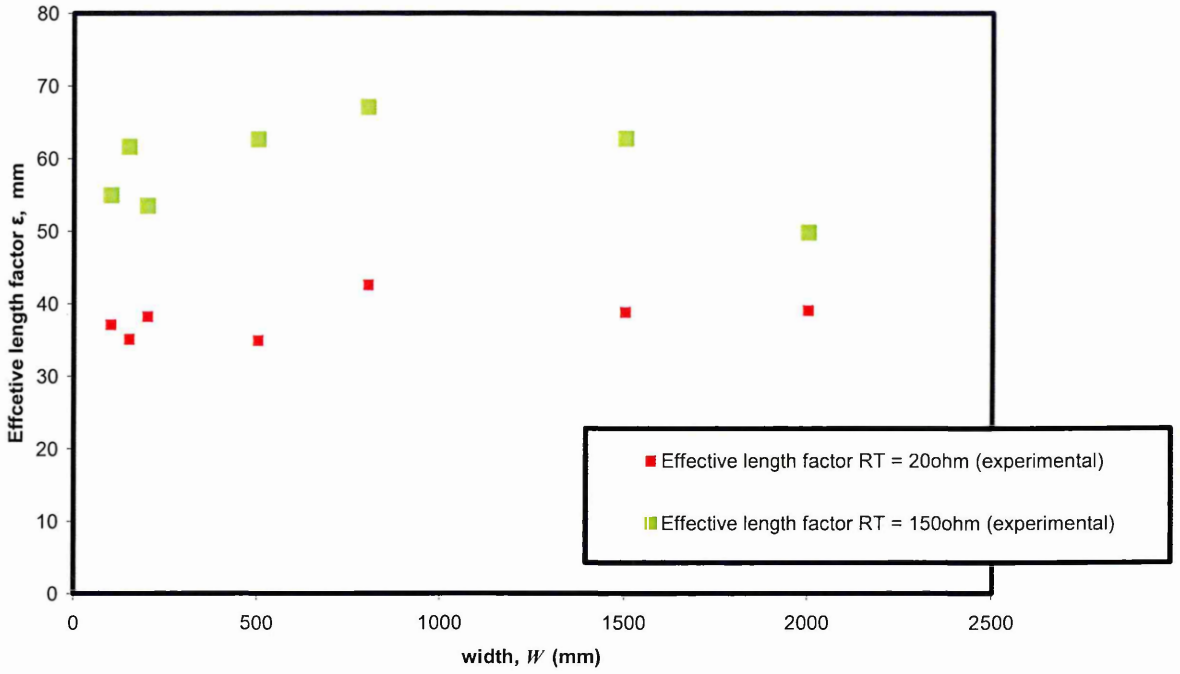

Figure 5.15. Graph of effective length factor ε versus width, W for R_T = 20 and 150 ohms

Figure 5.15 shows some variation of ε with width for the two CPT materials. This could be due to various reasons. If the application of the conductive rails was not exactly parallel, as discussed in Section 3.2.1, this would affect the value of ε. The increased range of ε values probably relates to the increased variability of the 150 ohm material compared to the R_T = 20 ohm material as shown in Table 5.1 and Figure 5.5 (Section 5.3.1). The test also assumes good bond between the CPT and the rail.

Based on these experimental variations, the value of ε will be assumed to be the average value given in Tables 5.3 and 5.4 for the CPTs R_T = 20 and R_T = 150 ohms.

5.4.2. *General Relationship between R and W*

Consider the first general relationship between R and W given in section 5.4, which is expressed in a non-linear form as follows:-

$$R = M\,(l-\varepsilon)W^{\alpha} \qquad \text{[Eq 5.5]}$$

By taking logarithms

$$\mathrm{Ln}R = \mathrm{Ln}\,M + \mathrm{Ln}\,(l-\varepsilon) + \alpha\,\mathrm{Ln}\,W \qquad \text{[Eq 5.7]}$$

Rearranging;

$$\mathrm{Ln}R = \alpha\,\mathrm{Ln}\,W + \mathrm{Ln}\,M + \mathrm{Ln}\,(l-\varepsilon) \qquad \text{[Eq 5.8]}$$

Figure 5.16 shows the plot of LnR versus LnW for the R_T = 20 ohms CPT. According to Equation 5.8, α is the gradient of each line and C is the intercept on the Y-axis, where;

$$C = \mathrm{Ln}\,M + \mathrm{Ln}\,(l-\varepsilon) \qquad \text{[Eq 5.9]}$$

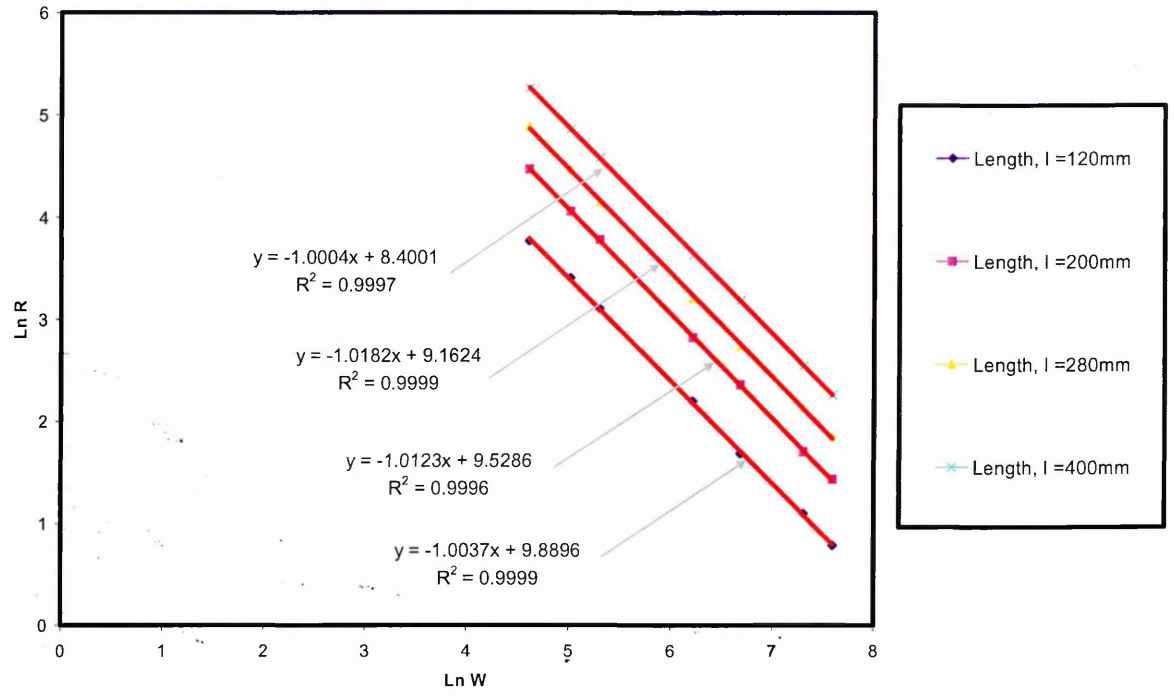

Figure 5.16. Graph of LnW versus LnR for CPT of R_T = 20 ohms

The data of the CPT elements represented in Figure 5.16 is tabulated in Table 5.5. These include the element dimensions (Length, l) and the coefficients α and C obtained from the linear graphs in Figures 5.16. The value of ε = 38 for the CPT R_T = 20 ohms (Section 5.4.1) and the values of (l – ε) are given in Table 5.5. Consequently by substituting the tabulated values in Table 5.5 into Equation 5.9 the value of M can be calculated and is also listed in Table 5.5.

l, mm	C	α	Ln (l - 38)	LnM	M
120	8.4001	-1.0004	4.4188	3.9813	53.5867
200	9.1624	-1.0182	5.0938	4.0686	58.4750
280	9.5286	-1.0123	5.4931	4.0355	56.5712
400	9.8896	-1.0037	5.8944	3.9952	54.3367
	Avergae =	-1.00865		**Average =**	55.742

Table 5.5. Calculation of the Material Constant, M, for R_T = 20 ohms

Table 5.5 shows that the values for the constants M and α are similar for the different lengths, l, of CPT represented in Table 5.5. Therefore, the average of these constants can be used to express Eq 5.5 for the CPT material of R_T = 20 ohms as follows:

$$R_{20} = 55.742(l-38)W^{-1.00865} \qquad \text{[Eq 5.10]}$$

Where, R_{20} = resistance of CPT materials of R_T = 20 ohms

The same linearisation process has been undertaken for the CPT material R_T = 150 ohms as shown in Figure 5.17 and Table 5.6.

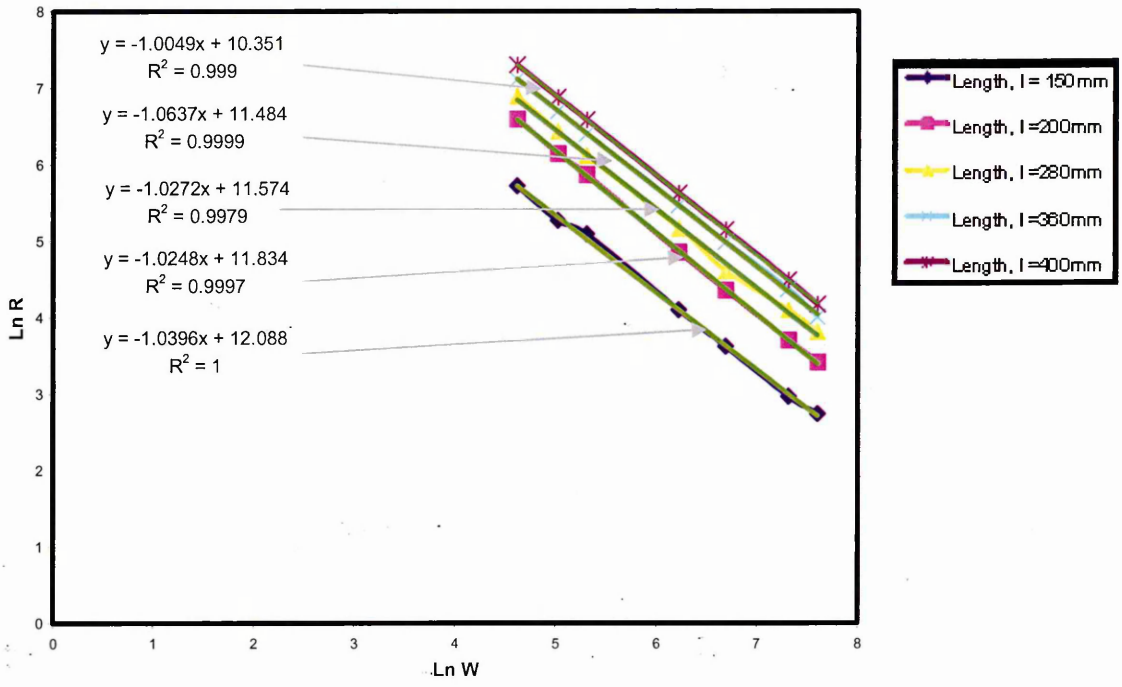

Figure 5.17. Graph of LnW versus LnR for CPT of R_T = 150ohms

Again a linear relationship between LnR and LnW is observed for the CPT elements of R_T = 150 ohms. C is the intercept on the Y-axis and α is the gradient of each line. The coefficient is calculated as before from Equation 5.9 and is given in Table 5.6.

l, mm	C	α	(l - 59)	Ln(l - 59)	LnM	M
150	10.351	-1.0049	91	4.51086	5.84014	343.8276
200	11.484	-1.0637	141	4.94876	6.53524	688.9992
280	11.574	-1.0272	221	5.398163	6.175837	480.9856
360	11.834	-1.0248	301	5.70711	6.12689	458.0094
400	12.088	-1.0396	341	5.831882	6.256118	521.1915
	Average =	-1.03204			**Average =**	498.6027

Table 5.6. Calculation of Material Constant for M for CPT R_T = 150 ohms

The average values of α and M are used to express these constants can be used to express Equation 5.5 for the CPT material R_T = 150 ohms as follows;

$$R_{150} = 498.6(l-59)W^{-1.03204} \qquad \text{[Eq 5.11]}$$

Where, R_{150} = resistance of CPT materials of R_T = 150 ohms

The calculated values of M, in Table 5.6, range between 343.8 and 689.0 which represents considerable variability. This is probably due to the variation in resistance per m^2 which occurs when CPT is manufactured and accounts for the difference in R_T and R_{ID} as discussed in Sections 5.1 There are a number of reasons for this; either the configuration of the samples of the conductive rails was not exactly parallel, as previously discussed in Chapter 3 or the bond between the CPT and the rails is not electrically consistent. The variation may be directly linked to the variation of R_{ID} as a result of manufacturing inconsistency in the proportion of carbon within the polymer or the thickness and the number of composite carbon and polymer layers applied.

Both equations (Equations 5.10 and 5.11) for the CPTs of R_T = 20 and 150 ohms show similar values of α for each CPT. The combined results of values of α for the CPTs of R_T = 20 and 150 ohms are -1.009 and – 1.032 respectively (Table 5.5 and 5.6).

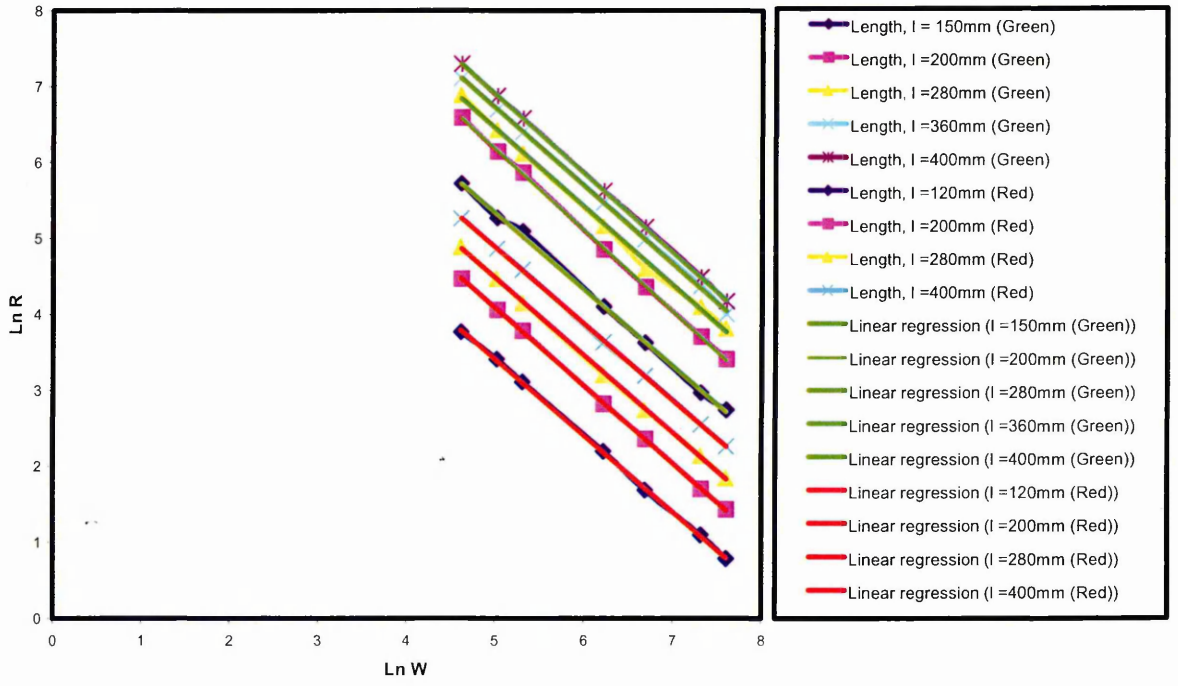

Figure 5.18. Graph of measured resistance versus element width for given element lengths

Figures 5.19 and 5.20 show the experimental results plotted alongside calculated values of R using Equations 5.10 and 5.11 for the corresponding CPT materials.

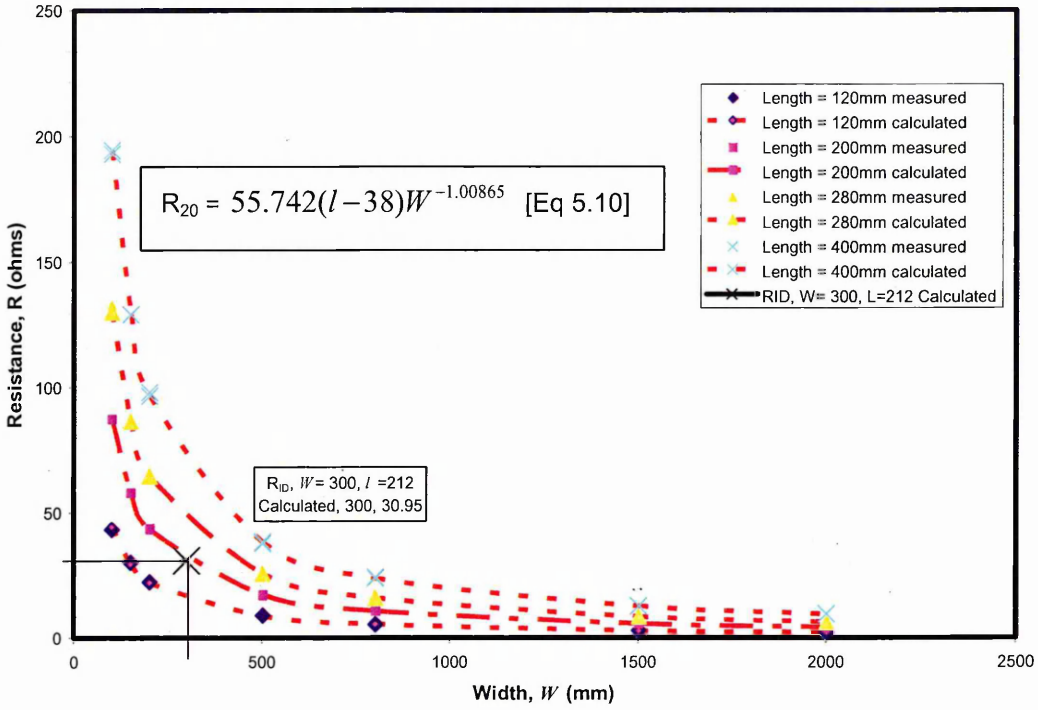

Figure 5.19. Experimental and calculated relationship between R and W, R_T = 20 ohms

Figure 5.19 shows a very close correlation between the experimental and calculated values of R for the CPT of R_T = 20 ohms. The calculated values of resistance are obtained from the R_{20} expression in Equation 5.10. The calculated resistance of CPT of W = 300mm and l = 212 mm is 30.95 ohms which is plotted in Figure 5.19. This is higher than the Characteristic Resistance R_{ID}, obtained by measuring the resistance of batch samples of W = 300 mm and l = 212mm from the CPT R_T = 20 ohms, which was 25.4 ohms as given in Table 5.1.

For the CPT R_T = 150 ohms, Figure 5.20 shows that for element widths below 500mm, the theoretical relationship calculates Resistance to be slightly higher than the experimental measured values. This is particularly noticeable for the elements of lengths l, less than 280mm. For elements of widths 360mm this is also the case, however, this is probably an experimental error due to the configuration of the test element as this is not the case for the results of the 280mm and the 400mm width elements which show good correlation between the measured and calculated values of R. Again, the reduced correlation is probably due to the materials variability, unlike the R_T = 20 ohm CPT.

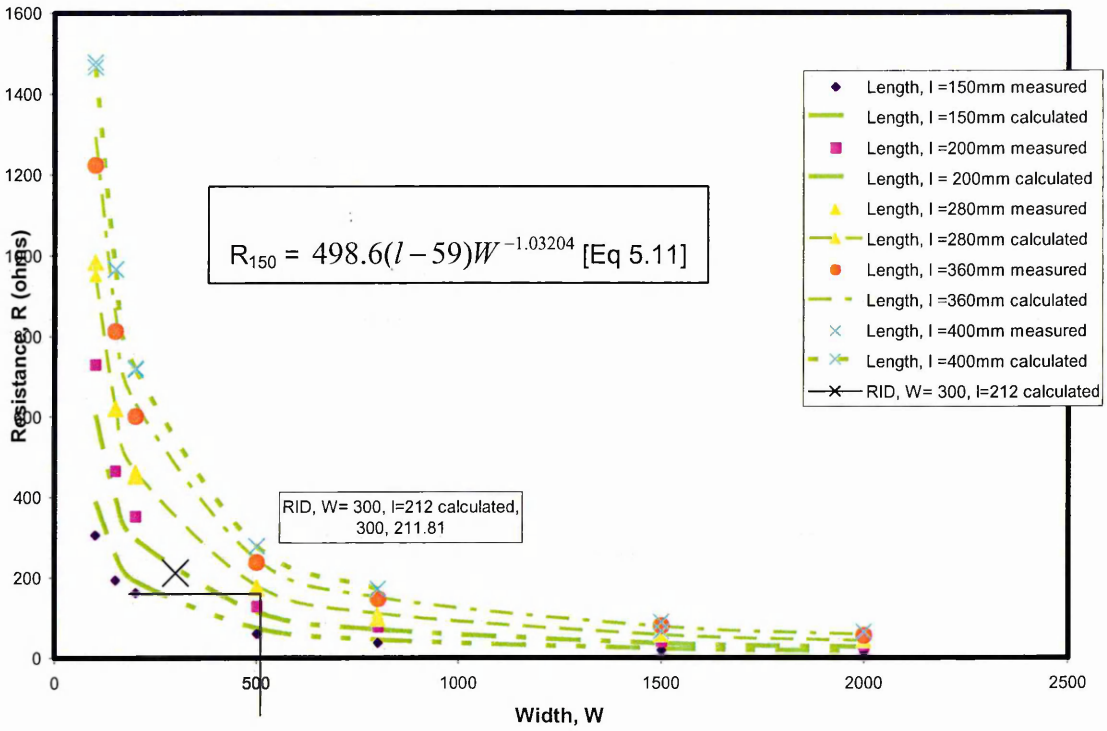

Figure 5.20. Experimental and calculated relationship between R and W, R_T = 150 ohms

The calculated resistance using the R_{150} expression and values W = 300mm and l = 212 mm is 211.81 ohms. Again, this is higher than the Characteristic Resistance R_{ID} of 167.04 ohms for the R_T = 150 ohm material characterised by measuring the resistance of batch samples of W = 300 mm and l = 212mm (see Table 5.1).

Reasons for Characteristic values for each material being lower than the calculated resistance using the general equations for R_{20} and R_{150} (Equations 5.10 and 5.11) may be the material used to derive the general expression may have had a greater resistance per m^2 compared to the average resistance of the batch samples used to calculate R_{ID} for each material. The difference may also be a function of variations in the environment in which the two tests were undertaken, particularly differences in temperature and humidity.

There is a close correlation between the measured resistance for the samples tested and the calculated values of Resistance as shown in Figures 5.19 and 5.20. Therefore, the general relationship between R, L and W for the two CPT materials R_T = 20 ohm and 50 ohm can be expressed as:

$$R = M\ (l-\varepsilon)W^{\alpha} \qquad \text{[Eq 5.5]}$$

Where;

l	=	Length of test sample (element), i.e. distance between outside edges of the rails (mm)
W	=	Width of test sample (element), i.e. length of conductive rail (mm)
ε	=	Effective length factor (mm)
l_{eff}	=	Effective length = $(l - \varepsilon)$
α	=	Material constant
M	=	Material constant m x β, see Equations 5.5 and 5.6

5.4.3. *Alternative Relationship between R and W*

Consider other relationship between R and W given in section 5.4, which is expressed as Equation 5.6:-

$$R = M(l-\varepsilon)e^{\alpha W} \qquad \text{[Eq 5.6]}$$

By taking logarithms;

$$LnR = LnM + Ln(l-\varepsilon) + W\alpha \qquad \text{[Eq 5.13]}$$

Rearranging

$$LnR = W\alpha + LnM + Ln(l-\varepsilon) \qquad \text{Where } C = LnM + Ln(l-\varepsilon) \qquad \text{[Eq 5.14]}$$

Figure 5.21 shows the plot of LnR versus W for the R_T = 20 ohm CPT where the gradient is α and the Y-intercept is C.

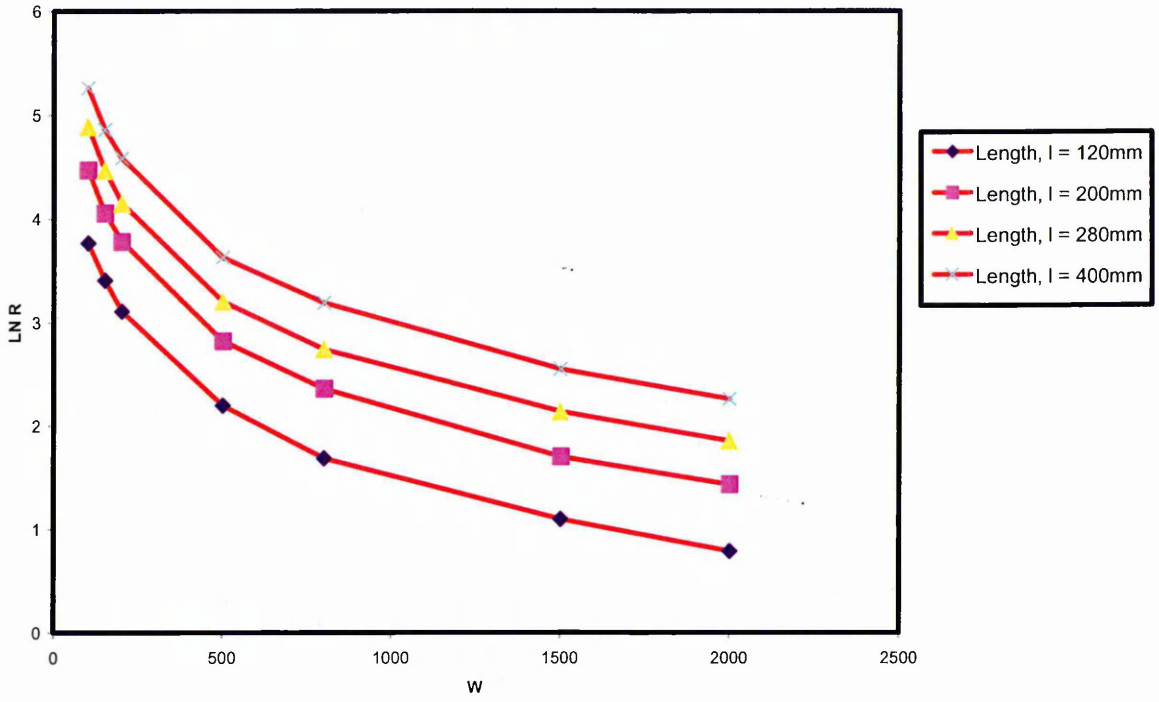

Figure 5.21. Graph of W versus Ln R for R_T = 20 ohms

Figure 5.22 shows the LnR versus W graph for the R_T = 150 ohm CPT where the gradient is α and the Y-intercept is C.

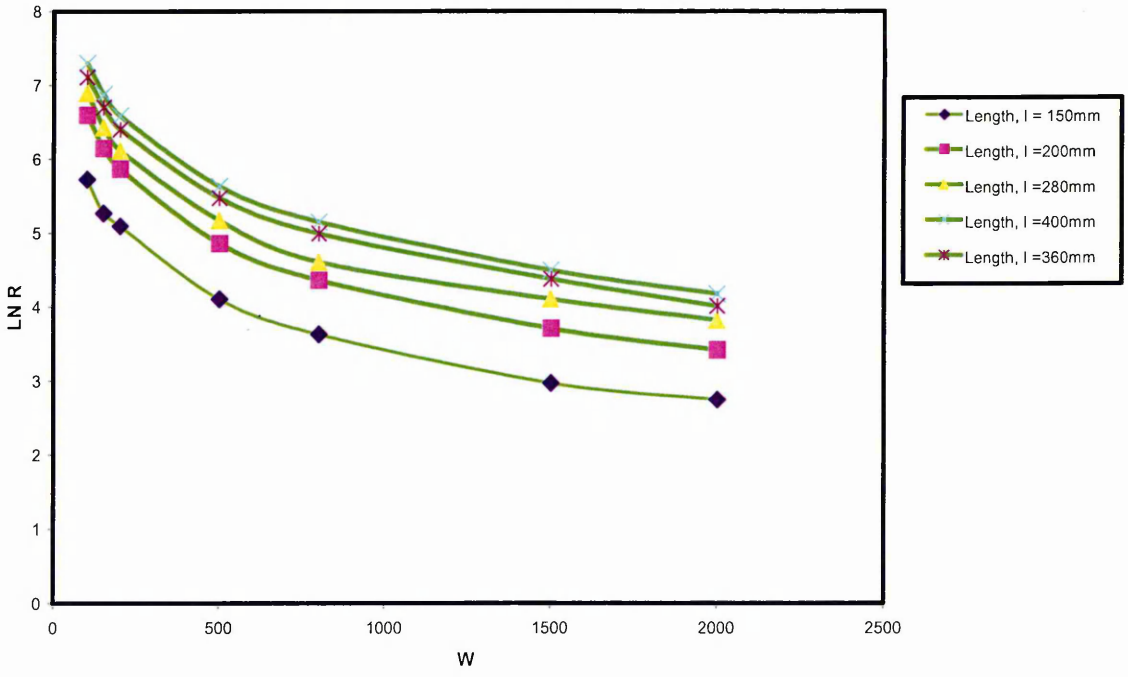

Figure 5.22. Graph of W versus Ln R for R_T = 150 ohms

Figures 5.21 and 5.22 show that the alternative relationship between R, L and W cannot be linearised. Therefore, Equation 5.6 is not recommended for use in the design of CPT elements.

5.4.4. *Voltage – Current Relationships of CPT*

In order to verify the validity of Ohms law to the CPT material, the relationship between Resistance, Current and Voltage of all data obtained for the CPTs of R_T = 20 and 150 ohms are plotted in Figures 5.23 in addition to the third CPT R_T = 50 ohms

However, for this to be true, there has to be a linaer proportionality for an element of dimensions l and W (also assuming t, the thickness of the CPT is constant). This can be shown by plotting Voltage, V versus Current, I for each CPT of various dimensions. Figure 5.24 shows the relationship between current, I and Voltage, V for three elements made using the three CPT materials of dimensions l = 280mm and W = 1m.

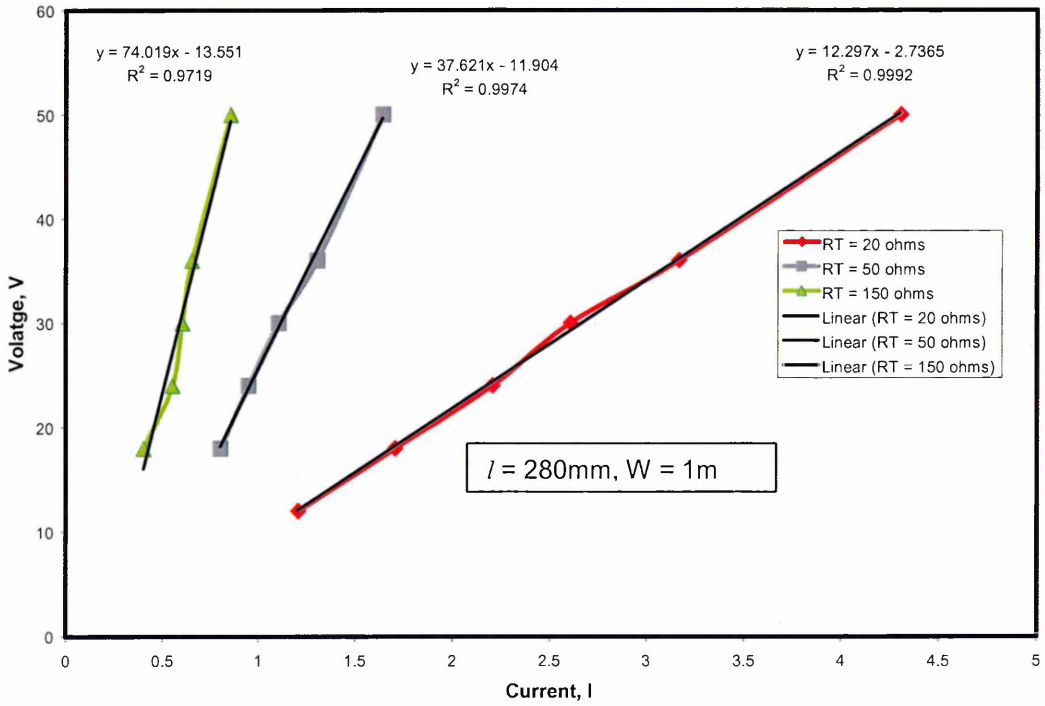

Figure 5.23. Graph of Measured and Calculated Current versus Width (R_T = 20, 50 and 150 ohms) (element l = 280mm, W = 1m)

Figure 5.23 shows that there is a linear proportionality between V and I for a given element with dimensions l and W, in this case l = 280mm and W = 1m. This is also the case for all

other elements tested. In this sense an individual element of CPT material behaves like an ohmic conductor. Full results provided in Appendices, Volume 2.

5.4.5. *Prediction of Current at given Voltages*

Having verified that the CPT material behaves as an ohmic material, Ohms law is substituted in Equation 5.12, the general equation derived for the resistance of CPT materials based on the test data obtained for CPT of R_T = 20 and 150 ohms

Substituting V = IR in Equation 5.12 gives;

$$R = \frac{V}{I} = M(l-\varepsilon)W^{\alpha} \qquad \text{[Eq 5.16]}$$

Therefore;

$$I = \frac{VW^{-\alpha}}{M(l-\varepsilon)} \qquad \text{[Eq 5.17]}$$

To determine the correlation between current and Voltage, the test data of CPT elements of various lengths l = 120mm, 200mm 280mm 360mm 420mm and 550mm, and W = 1m is considered. The measured values of I at various applied voltages V = 12Volts, 18 Volts, 24 Volts, 30 Volts, 36 Volts and 50 Volts are plotted in Figures 5.24 and 5.25 for CPT R_T = 20 ohms and R_T = 150 ohms.

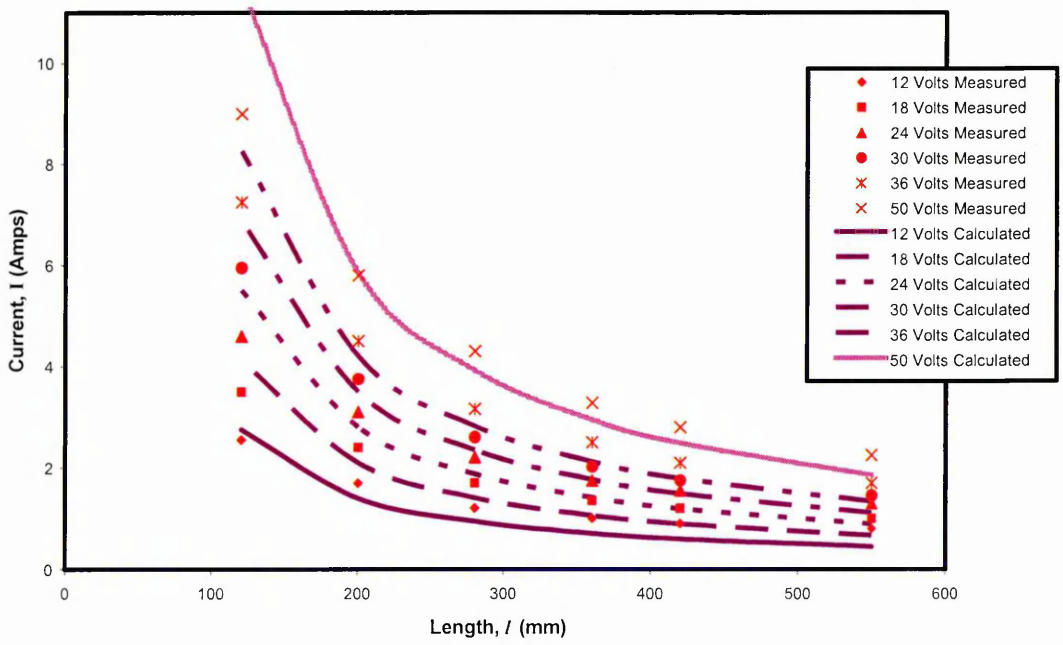

Figure 5.24. Graph of Measured and Calculated Current versus length. *l* (RT = 20 ohms)

Figure 5.24 shows a close correlation between the recorded and calculated values of Current, I (Amps) except for element lengths, l, less than 200mm when the calculated value of I becomes significantly higher than the measured at all voltages.

Figure 5.25 also shows a similar relationship for the CPT of R_T = 150 as the relationship of RT = 20 ohms in Figure 5.24. The measured and calculated values of current start deviating significantly at l under 300m.

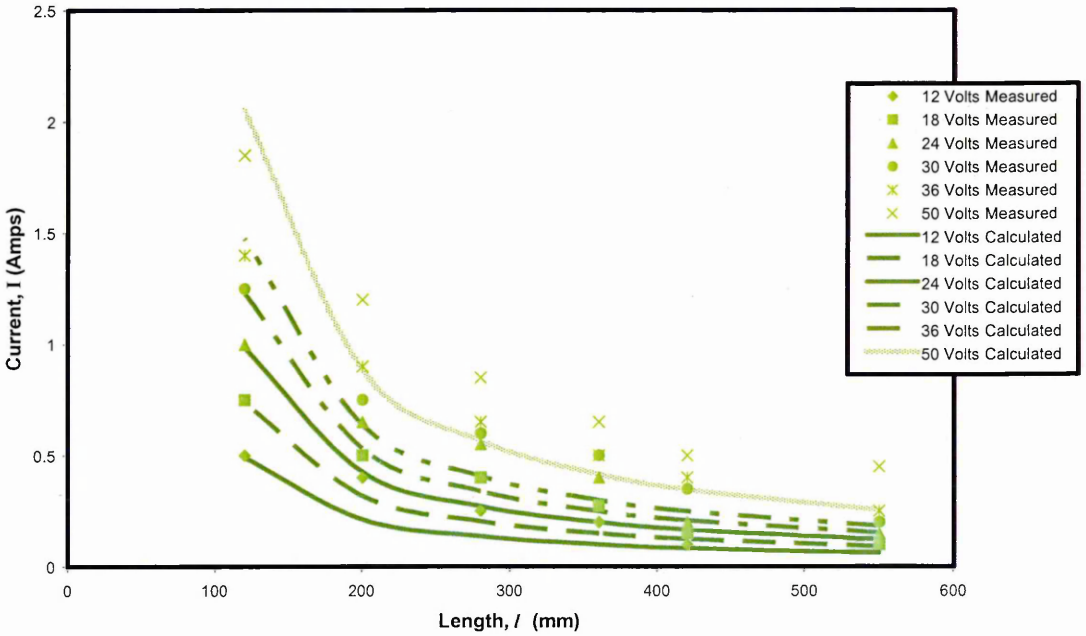

Figure 5.25. Graph of Measured and Calculated Current versus length, l (RT = 150 ohms)

Figures 5.24 – 5.25 show that the general equation for I (Equation 5.17) in terms of l and W, provides accurate predictions of current for R_T = 20 and 150 ohms. The correlation between recorded current and calculated current through the width = 1m element of for the three CPTs decreases as the Characteristic Resistance (R_{ID}) increases.

5.4.6. *Resistivity of CPT*

All materials have an electrical resistivity, also known as specific electrical resistance, which represents how strongly a material opposes the flow of electric current (I). The resistance R of the CPT elements is given by the expression derived previously as follows:-

$$R = M(l-\varepsilon)W^{\alpha} \quad \text{[Eq 5.18]}$$

The relationship between R and Resistivity ρ of the CPT material is given in by the following expression;

$$R = \frac{\rho(l-\varepsilon)}{A} \quad \text{[Eq 5.19]}$$

And A= Wt

Where;

R	=	Resistance (ohms)
l	=	Length of test sample (element), i.e. distance between outside edges of the rails (mm)
ε	=	Effective length factor (mm) which defines the length between rails through which current flows
$(l - \varepsilon)$	=	Effective length through which current flows between the rails
ρ	=	Resistivity (ohm.m)
A	=	Cross sectional area of the CPT element
W	=	Width of the CPT element (length of conductive rails)
t	=	Thickness of the CPT membrane

Substituting Equation 5.18 into 5.19 gives:-

$$M(l-\varepsilon)W^{\alpha} = \frac{\rho(l-\varepsilon)}{Wt} \quad \text{[Eq 5.20]}$$

Therefore simplifying equation 5.20 gives;

$$\rho = M\,t\,W^{(1+\alpha)} \quad \text{[Eq 5.21]}$$

It has already been discussed in the thesis that the resistivity of a materials primarily depends on temperature. For the purposes of this research programme, all measurements were taken at room temperature.

Equation 5.21 shows that the resistivity of a CPT element a function of the materials thickness, t and the materials constant of the CPT, M. It also shows that resistivity is a function of the width of the element, W, (the length of the conductive rails) but Is not a

function of the element length, l (effective length (l-e)). The thickness function, t, of the equation indicates that as the thickness of CPT increases so to does the resistivity. However is not the case as by increasing the thickness of the element will affect the value of the material constant M, hence each material has a different materials thickness, and during manufacture t, or the number of CPT layers used as method to control resistance, as well as carbon distribution within each layer, of which will also impact on M.

5.5. Conclusions

The results of this chapter have shown that the CPT behaves similar to an ohmic conductor for given element dimensions as there is a linear proportionality between Current and Voltage.

The material has a linear relationship between element length and resistance, but not between element width and resistance. Considering this the following relationship has been established.

$$R = M(l-\varepsilon)W^{\alpha} \qquad \text{[Eq 5.18]}$$

However, the linear relationship of resistance cannot be used predict current flow at a particular voltage due to the changes in the resistivity properties of the materials when a potential difference is applied a result of expected temperature increase.

The chapter has identified inaccuracies associated with the manufacture of CPT and the difficulty in producing a CPT material with a Characteristic Resistance R_{ID} equal to that of the Target Resistance RT. This is particularly the case for CPTs with high Characteristic Resistances. This was demonstrated when calculating the Characteristic resistance and the increasing variability of the standards samples.

- The manufacture of CPT elements is a highly variable process and is determined by a number of factors such and materials used, desired Target resistance and thickness of the CPT materials
- It has been shown that the Target Resistance of the material rarely matches the actual of Characteristic Resistance of the CPT manufactured.
- A CPT element has a linaer relationship between Voltage and Current at room temperature
- The CPT material has a linaer relationship between element length and resistance.

Chapter 6. Strength Development and Shrinkage of Concrete Cured with CPT

6.1 Introduction

The application of CPT Jackets for the curing of laboratory scale concrete elements is investigated. The aim of testing was to determine if CPT Jackets were capable of heating small scale laboratory samples to temperatures comparable to existing curing techniques, such as steam curing at 50 – 70 deg C, to determine the rate of strength development of 100mm cube samples cured with CPT and the shrinkage of CPT cured concrete.

The LAB100 Jacket, as described in Chapter 4, was used throughout to cure the 100mm x 100mm x 100mm cubes for testing in compression; the LAB 300 Jacket was used to cure 300mm x 75mm x 75mm concrete prisms. For all elements cast, the Mix A Concrete mix was batched using oven dry aggregates. The Pico temperature log interface with K-Type thermocouples was used throughout this phase of testing.

6.2 Initial Heating

In order to determine if the CPT was capable of heating concrete within a laboratory mould, the LAB 100 Jacket was used to heat an empty 100mm x 100mm x 100mm cast iron mould using 24 Volts ac supply. The cast iron mould shown in Figure 6.1 conformed to BS1881. A top cover to the mould was provided by using the base-plate of a second identical mould. This addition was used to serve two purposes, (i) to ensure a good contact between the heating surface of the CPT jacket and the mould at the top and bottom surface of the mould and (ii) to ensure heat was distributed evenly throughout the mould and the contained concrete. The LAB 100 Jacket was located in position at the top and bottom of the mould using the securing bolts of the base plates located through the 16mm holes manufactured within the LAB 100 Jacket, as described in Chapter 4. Unlike other jackets described in Chapter 4, the LAB 100 Jacket was designed to be an integral part of the mould rather than 'wrap' around it.

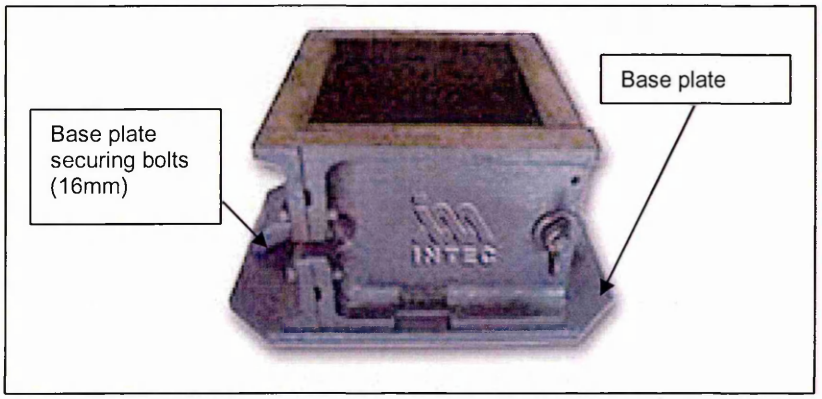

Figure 6.1. 100mm x 100mm x 100mm cast iron mould conforming to BS1881

This was done to maximise the transfer of heat to concrete when cast within the mould, given the high ratio of steel in the mould compared to the volume of concrete cast within. Figure 6.2 shows the position of the Jacket within the mould. It shows the potential for direct contact between the concrete and the heating part of the Jacket at the top and bottom face of the concrete. Figure 6.2 shows how the base plate of the mould and a similar additional plate at the top of the mould were used to secure the Jacket.

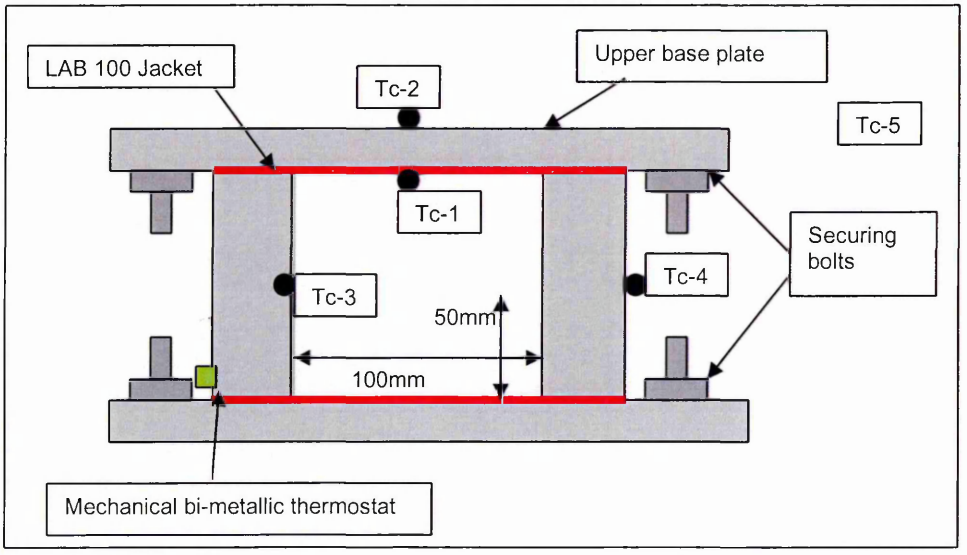

Figure 6.2. Application of LAB 100 Jacket to 100mm x 100mmx 100mm standard BS 8110 mould

Figure 6.2 shows the location of a bi-metallic thermostat set to control the maximum temperature of the mould when heated by the LAB 100 Jacket. Various thermostats were interchangeable for use with the LAB 100 Jackets. The thermostats were attached to the main

body of the mould as shown. Initially the LAB 100 CPT Jacket was controlled using a 70 +/- 5 deg C thermostat to heat an empty mould.

6.2.1 *Empty Mould*

Thermocouples were located at four positions to monitor the heating of the empty mould. The locations are shown in Figure 6.2. Thermocouple 1 (TC1) was located on the heating contact surface of the LAB 100 jacket, Thermocouple 2 on the outside face of the upper base plate, Thermocouple 3 in the middle of the inside face of the mould and Thermocouple 4 was located in the middle of the outside face of the mould. Thermocouple 5 was located to monitor ambient temperatures. The results of the empty mould heating test are shown in Figure 6.3.

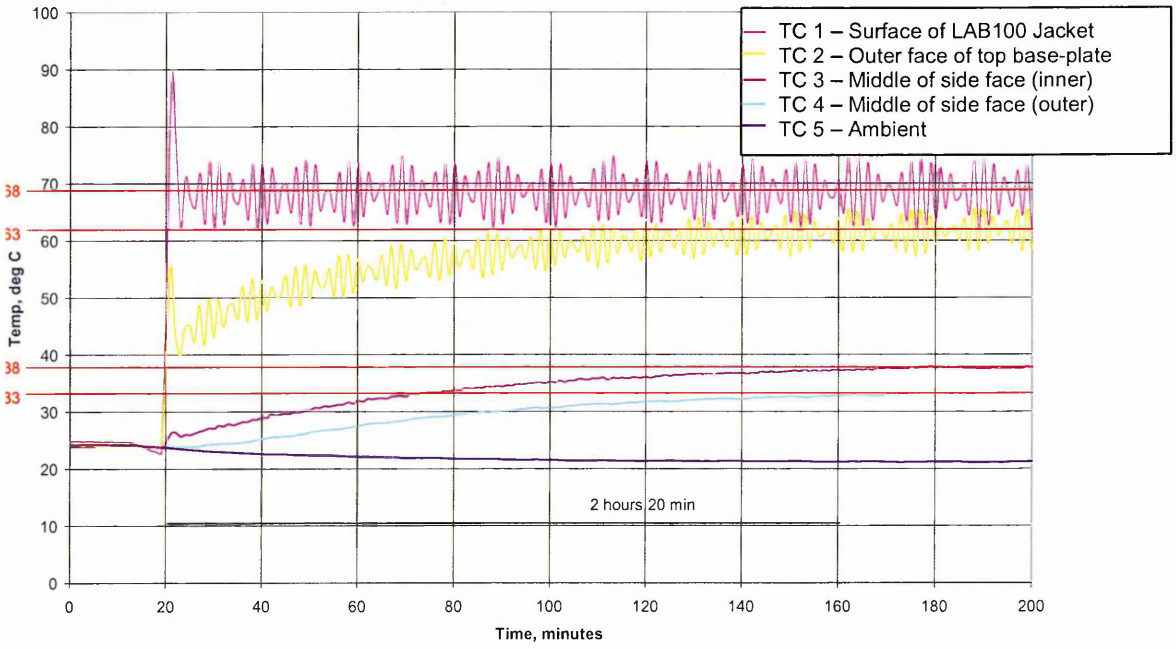

Figure 6.3. Performance of the LAB 100 CPT thermal jacket applied to the empty 100mm x 100mm x 100mm cube mould

Figure 6.3 shows that after 20 minutes of switching on the jacket, the heating surface of the CPT Jacket attained its controlled temperature of 70 deg C. The figure also shows that the bi-metallic mechanical thermostat on the surface of the jacket regularly switches 'on' and 'off' the power input to the jacket, hence controlling the temperature on the surface of the LAB 100 jacket at 70 +/- 5 deg C as expected. Figure 6.3 also displays a lag in the time the upper base-plate and the sides of the mould take to reach a steady-state temperature. The time for the outer face of the upper base-plate to reach a steady state was 80 minutes after switching on the LAB 100 Jacket, reaching a steady-state temperature of approximately 60 deg C. The steady-state temperature at the middle of the inside and outside surfaces of the side faces of

the mould was reached at 120 minutes with maximum temperatures of 38 deg C and 33 deg C respectively.

The cooling profile of the empty mould was also recorded as shown in Figure 6.4. The locations of the thermocouples remained the same as the heating profile.

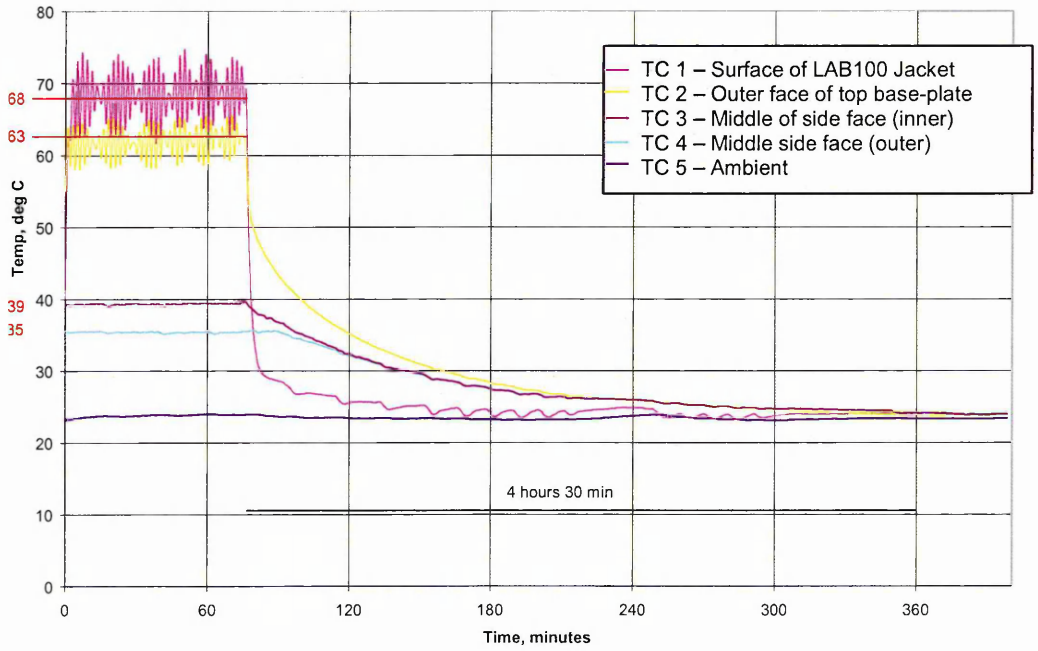

Figure 6.4. Cooling Profile of the empty 100mm cube mould following heating with the LAB 100 Jacket

Figure 6.4 shows that thermocouple 1 located on the surface of the LAB 100 Jacket cooled down most rapidly. Within 60 minutes the temperature on the surface of the jacket dropped from 58 deg C to approximately 23 deg C. In comparison the thermocouple located on the outer face of the upper base plate took approximately 240 minutes to fall to the ambient temperature. This was also the case of the thermocouples located on the inside and outside of the mould side faces. These locations fell to the ambient temperature within 270 minutes after power to the LAB 100 Jacket was switched off.

A review of the literature (Saul 1994) indicated that the optimum temperature for curing concrete is about 50 deg C, and the maximum permitted temperature is 70 deg C beyond which concrete suffers damage. The above test was, therefore, repeated using three interchangeable thermostats of 50, 60 and 70 deg C located in the same location as shown in Figure 6.2. This was done to understand how the thermostats controlled the temperature of the CPT Jackets when heating the mould.

The test was started using the 50 deg C thermostat. Upon the outer face of the top base plate (TC2) remaining at a steady-state temperature for the period from 180 - 250 minutes, the thermostat was reset to 60 deg C from 250 to 370 minutes (Figure 6.5). This process was repeated for a reset of temperature to 70 deg C and the heating profile from 370 - 580 minutes was recorded, (Figure 6.3).

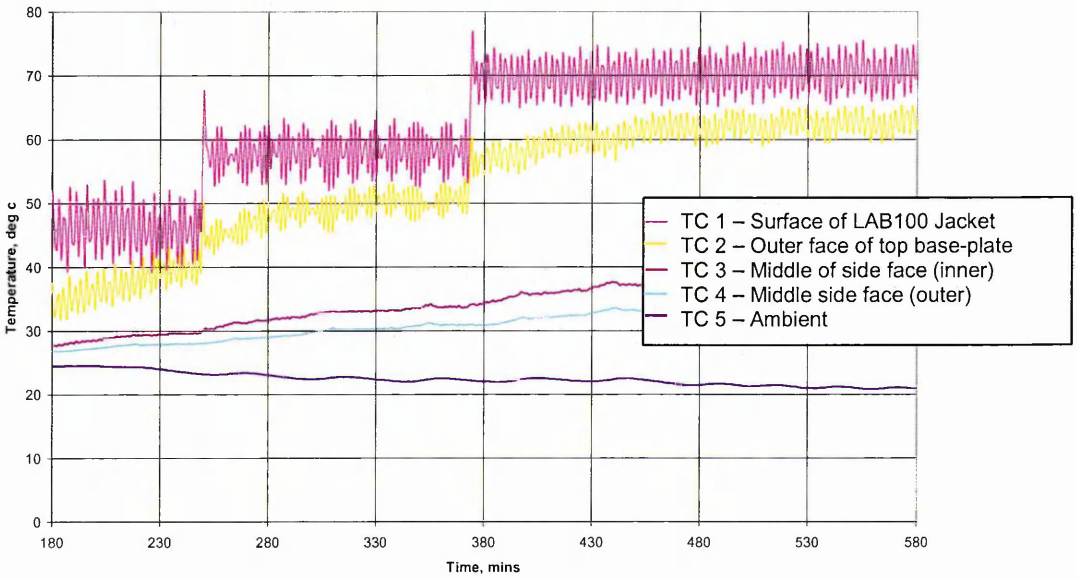

Figure 6.5. Heating profile of 100mm x 100mm x 100mm mould using 50, 60 and 70 deg thermostats in sequence

Figure 6.5 clearly shows that the CPT elements attained the new thermostat set temperature with negligible time lag. The profile, however, does display that the temperature on the other mould locations (TC2, 3 and 4) increases gradually with time as the temperature of the LAB 100 jacket is increased.

Figures 6.3 – 6.5 show that the LAB 100 CPT Jacket was capable of increasing the temperature at all the locations monitored (thermocouples 1-4). Heating the empty mould was assumed to be the worst case scenario as there was only a relatively small area of contact between the mould and the heating face of the jacket. Based on these results it was considered that the heating of the mould full of concrete would be even more efficient considering the greater contact with the heating face of the jacket.

6.2.2 Full Mould

The LAB 100 Jacket was used to heat a 100mm concrete cube cast within the mould with the bi-metallic thermostat set at 70 +/- 5 deg C. The bi-metallic thermostat was located as shown in Figure 6.2. An additional Thermocouple, Thermocouple 6, was located at the centre of the

concrete cube during casting. The results of the full mould heating test are shown in Figure 6.6.

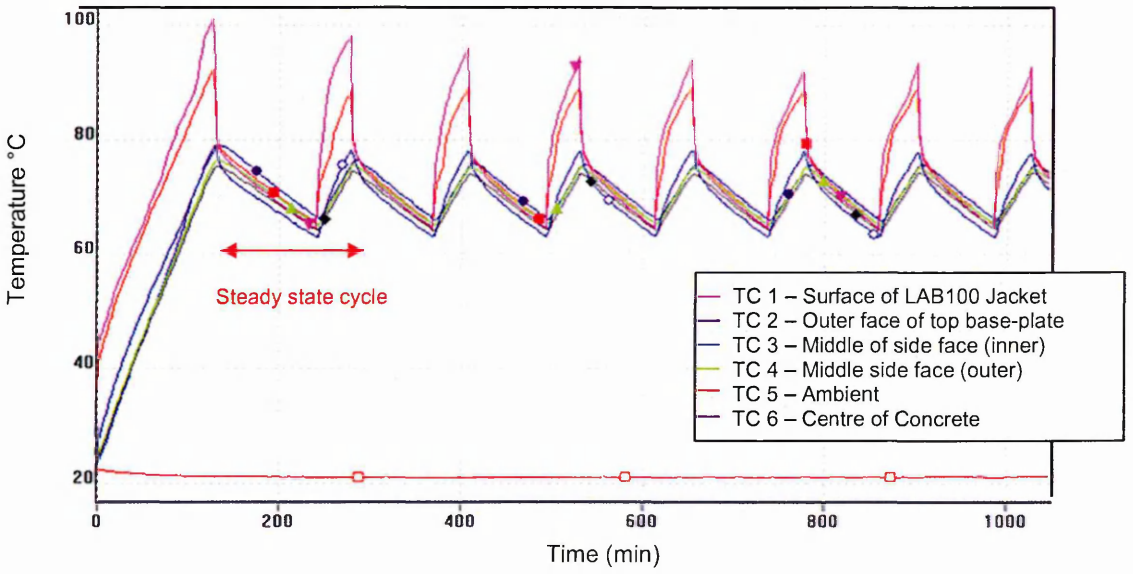

Figure 6.6. Heating profile of 100mm x 100mm x 100mm mould containing concrete, using 70 deg C thermostat

Figure 6.6 shows that the main difference in performance of the LAB 100 Jacket for heating the empty mould (Figure 6.3) and a mould containing concrete was the time taken after switching on for the mould (and concrete) reached steady state. The time taken by the empty mould to reach steady state was 80 - 100 minutes compared to 180 – 200 minutes for the mould filled with concrete. Figure 6.6 also shows that the temperature at the heating surface of the CPT LAB 100 Jacket (Thermocouple 1) traced the temperature at the centre of the concrete (Thermocouple TC6) with a difference of approximately 20 deg C. In the case of the empty mould, the Jacket achieved a temperature to the point of 'cut-out' within a very short period. Other observations are the frequency at which the temperature control thermostat cuts in and out. For the full mould, at steady state, the control cycle repeats every 200 - 250 minutes (175 minutes with no power going to the Jacket, and 75 minutes with power input raising the temperature again back to the point of cut-out). For the empty mould the control cycle is less that 2 minutes for both the 'on' and 'off' periods. The results from this section show that the LAB 100 Jackets have the ability to heat the concrete at early ages up to 70 deg C.

6.3 Effect of CPT Curing on Compressive Strength

A number of additional LAB 100 Jackets were manufactured to determine the affect of CPT curing on the compressive strength of concrete. The power capacity of each jacket was equal since the heating element dimensions within each jacket was the same. All heating elements were manufactured from CPT with the same Characteristic Resistance R_T (R_T = 20 ohms - Red). The power output of each Jacket was 35 Watts (full specification for the LAB 100 Jackets is given in section 4.5.1.).

Three temperatures were adopted, 50, 60 and 70 deg C, to cure 100mm concrete cubes. The temperature of the CPT within the blankets was controlled by using the mechanical thermostats with a tolerance of +/- 5 deg C as described in section 6.2 and the location of the thermostats and the application of the Jackets remained the same. A total of sixty cubes were cast in two batches using the Mix A (Section 4.5.1). 36 cubes were cast in the first batch, 24 in the second (Table 6.1).

Batch	Age tested	Number of cubes			
		CPT Curing Temperature (deg C)			
		50	60	70	21 (Control)
1	4 days	3	3	3	3
	7 days	3	3	3	3
	14 days	3	3	3	3
2	28 days	3	3	3	3
	90 days	3	3	3	3

Table 6.1. Test cubes cast and corresponding CPT curing temperatures

From the first batch, nine cubes were cured at each temperature of 50, 60 and 70 deg C. Nine cubes were cured in the environmentally controlled room at 21 deg C, 60% RH. From the second batch, six cubes were cast to be cured at each of the three elevated temperatures using the LAB 100 Jackets and six cured at control temperatures (21 deg C, 60 % RH). The temperature of the concrete cast within the 100mm x 100mm x 100m moulds was assumed to be the same as the mould during heating due to the small volumes of concrete being cured. It was also assumed that for such small volumes of concrete the affect of heat of hydration would not influence the performance of the CPT heating jackets.

Twenty four hours after casting, the cubes were transferred to the environment controlled room (21 deg C 60 % RH). After 3 hours the LAB 100 Jackets were applied / powered and the

cubes heat cured for a period of 21 hours. This was followed by cooling for a further period of 15 hours. The concrete samples were then removed from their moulds and returned to the environment controlled room prior to testing at different ages (Table 6.1). The average compressive strength of the three cubes tested for each curing temperature at the various ages was determined. The average results are plotted in Figure 6.7.

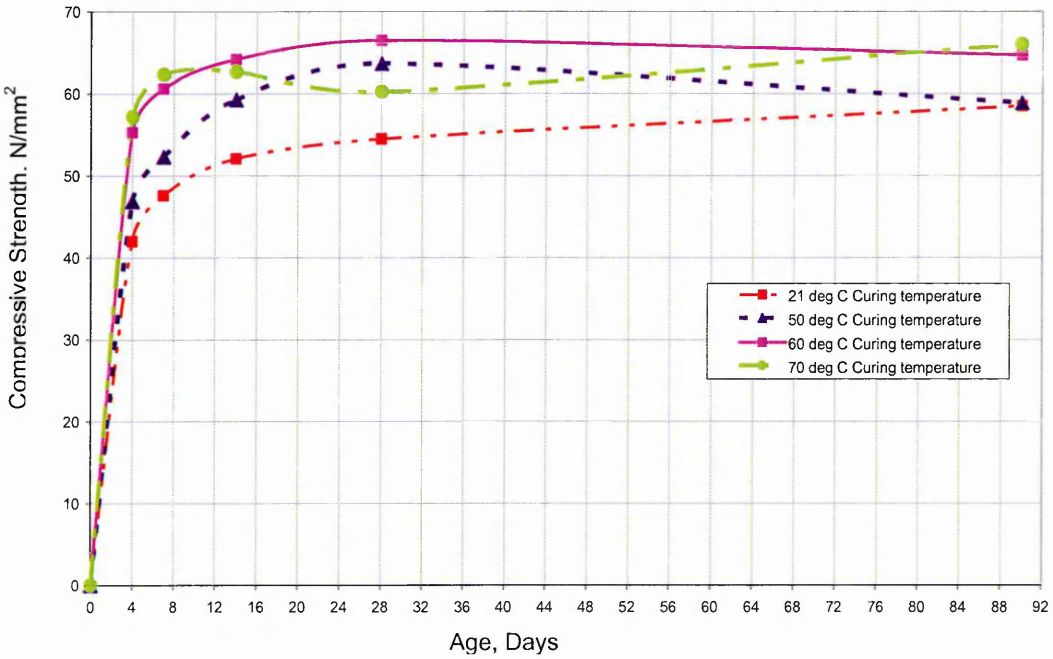

Figure 6.7. Effect of curing temperature on strength – age relationship of concrete

Figures 6.7 shows that increasing the curing temperature increases the compressive strength. At four days the optimum curing temperature was 70°C, however the strength of the 60°C cured samples was only slightly less. At 21 deg C curing, the strength continues to increase very gradually after 28 days. However, at higher curing temperatures, the strength starts to decreases very gradually after 28 days., while still remaining higher than the 21 deg C. Figure 6.7 shows that the samples cured at 70 deg C and 60 deg C achieved a maximum strength at 14 days.

6.4 Comparison of Different Heat Curing Methods

Twenty seven cubes were cast to determine the affect of different high temperature curing techniques on the strength of concrete up to 91 days age. Nine cubes were cured in an environmental chamber set at 70 deg C, 100 % relative humidity (details of the chamber is provided in Chapter 4) for 24 hours, nine were cured in an oven for 24 hours at 70 deg C and nine were cured within the thermal jackets at 70 deg C (LAB 100 Jackets) for 24 hours. The curing regime of 100% relative humidity was selected to provide the best representation of a

live steam curing environment. In contrast the oven curing provided an environment with an absence of moisture.

Prior to casting, the environmental chamber and the oven were operated to reach the selected temperature of 70 deg C and the humidity of 100 % RH within the environmental chamber. After casting, all 27 moulds remained in the laboratory environment for 3 hours (past the initial set period). Then nine cast moulds were placed in the environmental control chamber and 9 were placed in the oven. The remaining nine cast moulds were sealed by closing and securing the upper base plate (Figure 6.2), the CPT heating Jackets were connected and the power switched on. Heat curing by the three methods was applied for 24 hours. The cubes were then allowed to cool to room temperature. The cubes in the environmental chamber and the oven remained in place for 24 hours following switching them off. The cubes cured by the LAB 100 Jackets remained in the mould with the Jackets still attached but isolated.

After the 24 hour cooling period the cubes were removed from the moulds and stored in the controlled environment room at 20 deg C 60 % RH until testing at 4, 28 and 90 days age. At each age three cube samples were tested and an average compressive strength determined. The results are given in Figure 6.8.

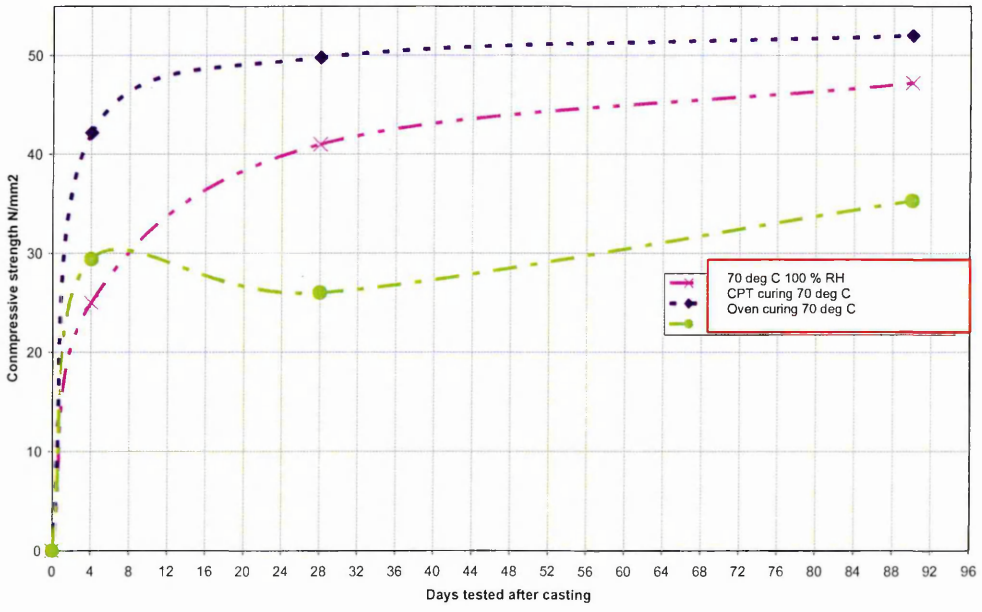

Figure 6.8. Strength development of the concrete with different high temperature curing methods

Figure 6.8 shows that the specimens cured in the CPT LAB100 Jacket performed the best. The early rate of strength development has increased with the CPT thermal curing jacket (LAB 100) compared to samples cured at 70 deg C, 100%RH. At 90 days age, there is an increase in the compressive strength of the samples cured with the CPT jackets. Compared to samples cured in an oven at 70 deg C the early age and long term strength of the CPT jacket cured samples was dramatically higher. At four days age with CPT jacket curing, the strength was 42 N/mm^2 compared to 29 N/mm^2 for the oven cured samples and 25 N/mm^2 for the 70 deg C, 100% relative humidity curing. The strength at 7 days for the CPT cured sample (42 N/mm^2) is similar to the 28 day strength of the sample cured at 70 deg C, 100% RH. (41N/mm^2).

6.5 Shrinkage

Four 75mm x 75mm x 300mm prisms were prepared to determine the shrinkage of CPT cured concrete compared to that of concrete cured under other curing regimes of 100% RH and oven cured (0% humidity).

Specimen	Curing Condition	Curing Method
Prism 1	CPT curing	LAB 300 Blanket operated at 70 deg C. (See Chapter 4 for details of Jacket)
Prism 2	High humidity curing	Environnemental chamber 70 deg C, 100% RH
Prism 3	Oven curing (low humidity)	Oven at 70 deg C
Prism 4	Control	21 deg C, 60 % RH

Table 6.2. Curing regimes for shrinkage tests

A batch of Lab Mix A (section 4.5.1) was used to cast the four prisms. The four prisms were cast in the laboratory (approximately 20 deg C). Each prism was cast with axial strain measuring points as shown in Figure 6.9. After casting, the moulds / prisms were transferred to the controlled environmental room.

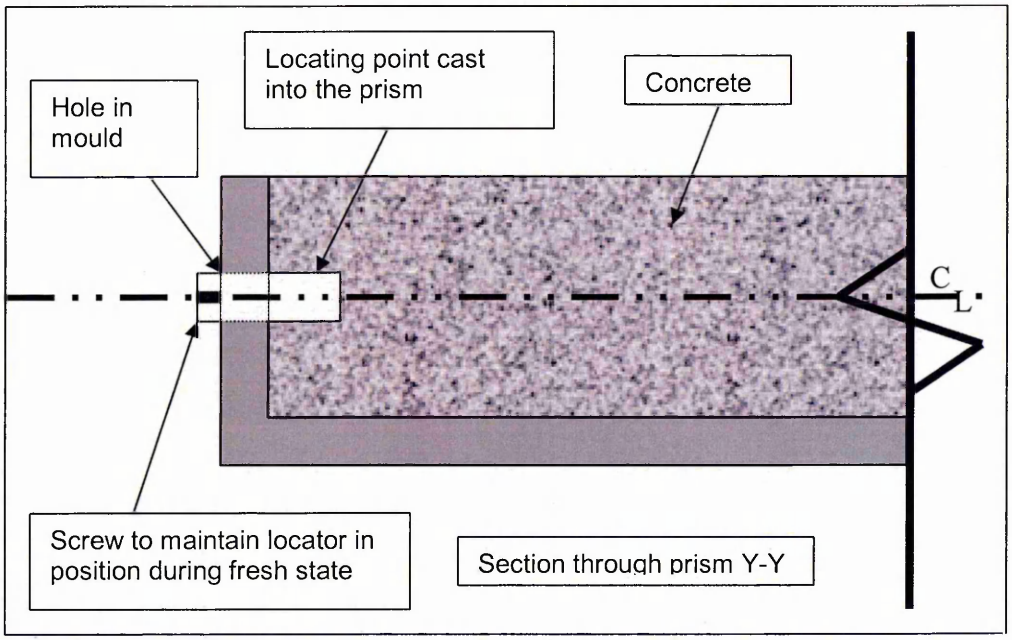

Figure 6.9. Location of axial strain measuring points

Following the initial set of the concrete (approximately 3 hours), plus 1 hour, the prisms were carefully removed from the moulds (after 4 hours the concrete had set and was significantly stiff to allow the initial reading to be taken). The initial strain measurement was taken using the apparatus as shown in Figure 6.10.

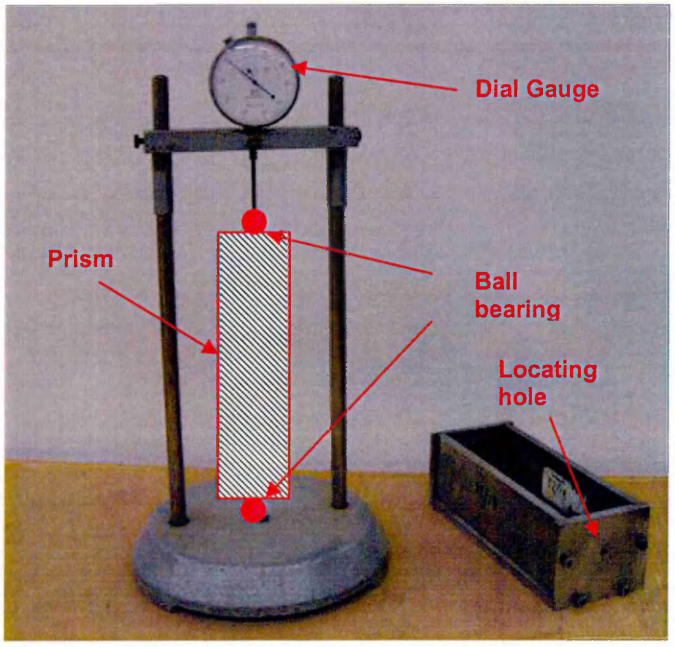

Figure 6.10. The shrinkage apparatus and the 75mm x 75mm x 300mm test sample

After recording the initial shrinkage reading, the four prisms were placed back within the moulds for curing in their respective environments. The four prisms were temperature cured,

within the moulds, for a period 24 hours in each curing environment. After 24 hours thermal curing, at elevated temperatures, the prisms were allowed to cool for a further 24 hours. The prism cured within the LAB 300 Jacket remained in the Jacket / mould during cooling. Following curing the second shrinkage reading was taken. After taking the second shrinkage reading, all the prisms were placed in the temperate controlled room, 21 deg C at 60% relative humidity. The shrinkage of the prisms was measured in micro-strain, calculated by applying the gauge factor to the readings obtained; 1 division represents a strain of 1.077 x 10^{-5}. Shrinkage measurements were taken over a 26 day period at regular intervals using the axial strain gauge. Shrinkage results are presented in Figure 6.11.

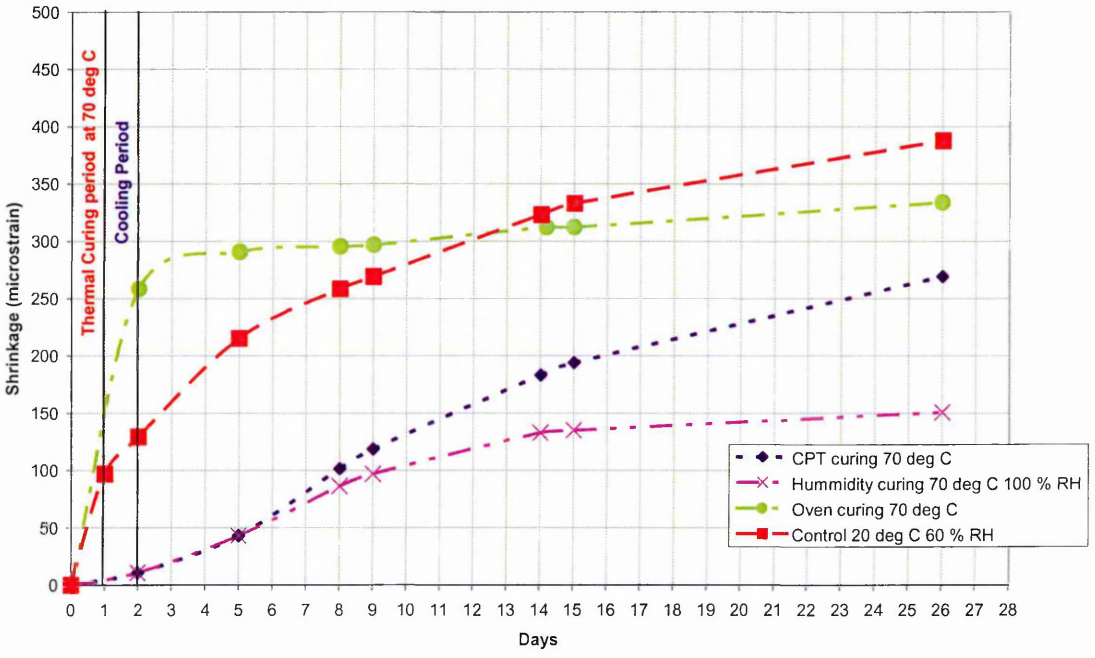

Figure 6.11. Shrinkage after 24 hours of high temperature curing, subsequent storage at 21 deg C, 60% RH

Figure 6.11 shows that the greatest 15 day shrinkage (326 microstrain) was recorded in the prism cured in the temperature control room (20 deg C, 60% RH). The high humidity (100% RH) cured sample displayed the least shrinkage, and the CPT cured prism in the LAB 300 Jacket the second least, 150 and 275 microstrain respectively of at 26 days.

6.6 Discussion of Results

6.6.1 CPT Heating

The CPT has demonstrated its ability to heat laboratory scale concrete elements within their moulds to temperatures suggested by AGA Saul and H H Patel of between 50 to 70 deg C.

The results have also shown that the LAB 100 Jacket can heat a 100mm concrete cube mould when either empty or full of concrete. The LAB 300 Jacket has also demonstrated its ability to similarly heat cure the 300mm x 75mm x 75mm prism mould. This is important as it demonstrates the ability of the CPT (at small scale) to preheat concrete moulds. Having the ability to do this has the potential for reducing temperature gradients within concrete elements cast in cold ambient environments.

Comparing the heating profile of the 100mm empty mould and the same mould when filled with concrete (Figures 6.3 and 6.6) shows a difference in the time taken until the thermostat 'cuts' out for the first time following initial operation. Inspection of the two figures also shows a difference in the 'on' – 'off' cycle due to the operation of the bi-metallic thermostat. For the empty mould, the time taken for the mould to achieve steady state temperature is 80 -100 minutes, and for the full mould 180 – 200 minutes. The different heating characteristics for the full and empty moulds are given in Table 6.3.

Insert type: LAB 100	**Time taken to reach steady state temp. 70°C**		**Min. temperature recorded**		**Max. CPT temp**	**On – off cycle time of thermostat**
	Time	Rate	Temp	Location		
Empty Mould	90 mins	33 ° C / hr	33 ° C	TC 4	85 ° C	4 mins
Full Mould	190 mins	16 ° C / hr	62 ° C	TC 6	100 ° C	250 mins

Table 6.3. Temperature characteristics of empty and full mould with CPT heating

Table 6.3 shows the LAB 100 Jacket had to operate at a higher temperature (100 deg C) to heat the full mould compared to 85 deg C for the empty mould. This demonstrates the ability of the CPT to keep increasing temperature – working harder – up until the time when the thermostat reaches the cut-out temperature.

Figures 6.3 and 6.6 show that when the full mould was heated using the LAB 100 jacket, there was a smaller differential of temperature throughout the mould, between the base-plate TC2 and the middle of the side face TC3. The difference was 5 deg C for the full mould compared to the 20 deg C for empty mould. This indicates two things:

i) There is a good transfer of heat through the concrete and the steel mould during the heating phase, and
ii) The concrete is good at retaining heat provided by the CPT.

The distribution of temperature through the air void of the empty mould where the concrete would normally be cast, is vastly inferior to the transfer of heat through the concrete cast

within the full mould. This is due to the differing thermal conductivity of hardened concrete (typically 2.34 W/m.K), fresh concrete (about 1.5 W/m.K) and the very low thermal conductivity of air (0.0257 W/m.K at 20 deg C).

Therefore, for heating purposes concrete in its fresh state has a lower thermal conductivity compared to concrete in its solid phase. This is primarily due to the higher volume of free water, as discussed in section 2.5.1. Therefore, at early age, 1- 5 hours, the transfer of heat through the concrete (plastic phase) requires a greater input of energy than say after 5 hours when the concrete has set.

This difference in thermal properties of the concrete between solid state and non-solid state is also beneficial when the concrete is at the desired curing temperature (50 - 70 deg C), or the heat soaking period of the curing profile (Figure 2.8), This is because in its solid state the specific heat capacity of a typical concrete (1.07 KJ/kg.C) is higher than in its plastic state (0.97 KJ/kg.C). This higher specific heat capacity effectively allows the concrete to maintain its own optimum curing temperature less reduced external heat input than it would if in a plastic state.

The temperature profile for the full mould shows that the CPT material and the concrete temperatures increase in parallel at the same rate, with a 20 deg C lag. For the empty mould, the CPT starts cutting 'in' and 'out' very shortly after switching on. This indicates that the CPT has a poor ability to retain heat – a consequence of having a very low mass. This could be overcome in future tests by increasing the thermal mass of the CPT by bonding it to the outside face of a mould, using the mould to retain heat, however a consequence of this would be a reduction in initial performance. The bond would also have to be good so as not to lose thermal energy at the interface. Other solutions would be to insulate the CPT Jackets better to reduce heat loss. Both of these points will be further investigated throughout the testing phase.

Table 6.3 shows that for the full mould, the rate of heating (16 deg C per hour) is below the maximum rate recommended by ACI 517.2R-87 of 22-44 deg C per hour depending on size, similar to the 13 deg C per hour recommended by H H Patel to mitigate against microcracking and slightly above the 10 – 15 deg C recommended by BS 8110, the standard adopted by UK precast concrete industry.

6.6.2 Strength

Conductive Polymer Technology increases the early age strengths of concrete at curing temperatures of 50, 60 and 70 deg C. The results show that the greater the curing temperature in the first 72 hours of curing, the greater is the strength achieved at 4 days. The

results also show that at 28 days, all the samples cured using the CPT achieved greater strengths than the samples cured under conditions of 20 deg C 60 % RH. This is not typically the case for other high temperature curing methods such as steam curing. This contradicts the finding of GJ Verbeck and RA Helmuth (1968) which are presented in Figure 2.3. Figure 2.3 showed that as curing temperatures increase from 10 deg C to 50 deg C, strengths at 1 day increased but 28 day strengths decreased from 40 N/mm^2 to less than 30 N/mm^2. In the case of CPT curing, although cubes were not tested at 1 day, Figure 6.7 shows a close predicted strength at 1 day. However, caution has to be taken when comparing these results. The elevated temperature curing undertaken by GS Verbeck and RA Helmuth was applied throughout the total curing period prior to the testing of samples at 28 days. The period of elevated temperature curing for the CPT cured samples was 72 hours, the same as adopted by DN Richardson. However the conclusion from tests undertaken by Richardson was that increasing the curing temperature for a period of three days to a maximum of 38 deg C resulted in a reduction of the 28 day strength. This has not been the case for CPT curing.

Reasons for these findings may be due to the way heat is applied to the 100mm cube samples when using the CPT. As discussed in the previous section (section 8.6.1), the CPT heats up gradually with rising temperature of the concrete element. Other thermal curing techniques, such as steam provide a source of heat with a far greater heat flux (W/m^2) at the extremes of the concrete element. This may result in thermal gradients within the elements and more sudden heating causing microcracking. The mode of heating with the CPT appears to be more 'gentle', leading to more uniform heating with less thermal shock. It is also possible that this gentle form of heating reduces the risk of ettringite formation in the hardened concrete, a known cause of long term strength reduction

6.6.3 Curing Regimes

When comparing CPT curing to the simulated regimes of live steam curing (100% RH) and dry curing in the oven, for samples cured at 70 deg C using the LAB 100 Jacket, with a heating period of 24 hours, the CPT cubes achieved grater compressive strengths at all ages (4-91 days). At 4 days the CPT cured samples had compressive strengths nearly 20 N/mm^2 greater than the high humidity (100 % RH) cured samples and 12 N/mm^2 stronger than the oven cured samples. Reasons for the results in Figure 6.8 may relate to the availability of free water for curing. In the case of oven curing the samples were not sealed on all sides during heating, allowing increased evaporation and resulting in micro cracking due to the rate of evaporation being greater than the rate of bleeding and a reduction in free water for hydration. On the contrary, the samples cured at 100 % RH were also not sealed, potentially allowing the elements not to bleed, and providing moist curing. The CPT cured samples were sealed by the LAB 100 Jacket, by the upper and lower plates. This results in water being neither

gained or evaporated maintaining the W/C ratio optimised during the mix design process. Another factor that may have been detrimental to the strengths of the samples cured under the different regimes is the rate at which the samples were heated. In the environment chamber and the oven, the ambient temperature was maintained at 70 deg C providing the freshly cast concrete to sudden exposure to 70 deg C temperature, whereas, as discussed, in the case of the CPT curing, the CPT heats with the concrete gradually, thus not inducing thermal stresses within the element.

6.6.4 Shrinkage

Figure 6.11, shows the total shrinkage following the initial set of the prisms (4 hours after casting), to 26 days age. Figure 6.11 shows the importance of moist curing conditions to reduce shrinkage. In the case of the oven cured sample (assumed humidity < 10 % RH), the sample cured at 20 deg C 60 % RH and the high humidity cured sample (100% RH) a clear relationship exists between humidity and shrinkage. High humidity curing during the initial two day curing cycle results in lower shrinkage.

Results show that the CPT curing reduces shrinkage. The LAB 300 Jacket was wrapped around the elements being cured, thus restricting the loss of moisture from the concrete, and in effect providing a micro climate of moisture ideal for reducing shrinkage within concrete. Shrinkage in the oven cured sample is greatest as free water and absorbed water is evaporated from the mix. Again this is because the sample was not sealed on all faces.

The humidity cured prisms retain the free water which continues to be available for hydration throughout the period of elevated temperature curing and beyond. Therefore, shrinkage for the two day elevated temperature curing cycle is minimal. Any excess water not used for hydration will evaporate from the element naturally as it ages.

Controlled shrinkage at early ages as demonstrated by the CPT LAB 300 curing protects the microstructure of concrete elements, particularly at elevated temperatures. Rapid thermal expansion caused by sudden temperature exposure (e.g. steam or oven curing) can break the early internal bonds within an element resulting in lower longer term strengths. It is concluded that the gentle heat provided by the CPT will help to mitigate this.

6.7 Conclusions

- CPT can be used to elevate the temperature of laboratory scale mould when empty and when filled with cast concrete.

- The application of heat from CPT can elevate curing temperatures at early ages to 50 – 7 0 deg C for laboratory scale samples
- Cubes cured with CPT display greater early age strengths than other heat curing techniques.
- CPT cured samples performed better than the oven cured samples at 4 and 28 days
- The use of CPT has no deleterious effects to long term strength
- The application of CPT can achieve ideal curing conditions in terms of temperature and humidity.
- Concrete elements cured using CPT display reduced shrinkage compared to elements cured at room temperature
- CPT curing jackets are suitable for uniform accelerated (thermal) curing of concrete of small laboratory scale elements.

Chapter 7. Interaction between Temperature and Heat of Hydration in Large Concrete Elements

7.1. Introduction

This chapter will report the results of curing a concrete element of large volume representative of those manufactured in a precast concrete plant. An element of dimensions 400mm x 400mm x 400mm will be considered which is suitably large to detect internal heat generated by hydration. This will produce interaction between the external heat applied through CPT and the heat of hydration at early ages. Of particular importance will be the understanding of the peaks of hydration of the cement as discussed in sections 2.6 and 2.7 of Chapter 2.

The LAB 400 Jacket will be used to cure the test elements. Unlike the tests undertaken in Chapter 6, the Jacket will be used in conjunction with an electronic controller (West 4000) with the ability to control the rate of heating of the CPT and concrete being cured. This is important to optimise the curing regimes identified in section 2.14 of the literature review where an 18 hour curing period is recommended with heating rates ranging from 10 to 18 deg C per hour and the curing / soaking temperature (the time at which the temperature remains constant) ranging between 50 – 70 deg C (as considered in the previous chapter). To gain a greater understanding of how the CPT heats the concrete throughout the element, thermocouples will be located throughout and cores will be taken to determine the strength.

7.2. Experimental Set up and Procedure

400mm x 400mm x 400mm steel mould was manufactured using 12mm mild steel plates: The LAB 400 Jacket was then designed and manufactured to fit around the mould as shown in Figure 7.1.

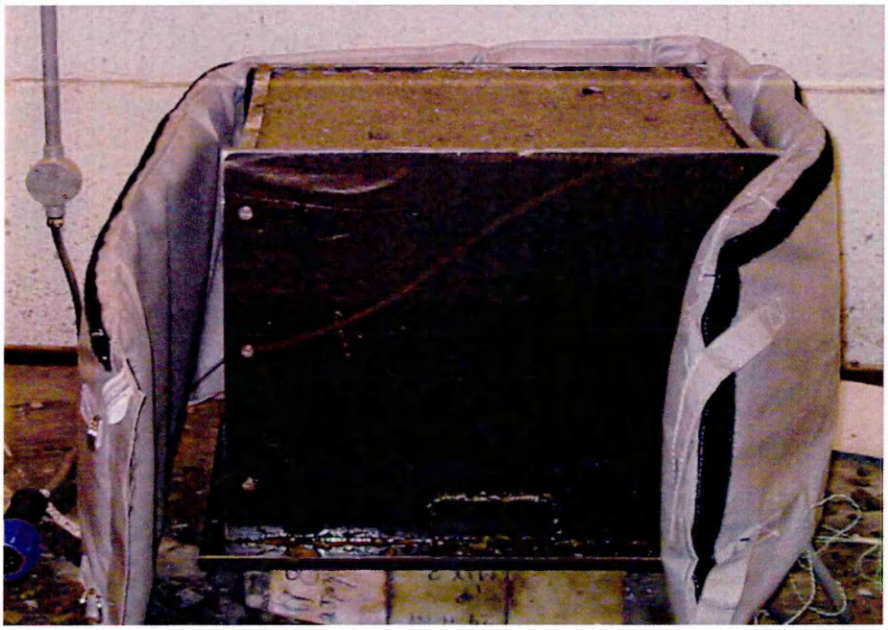

Figure 7.1. Thermal curing jacket fitted onto the 400 x 400 x 400 mm cube mould

The LAB 400 CPT jacket was configured using two CPT heating elements as described in Chapter 4. It was designed to provide a uniform temperature of up to 90 deg C over the 'internal' surface of the jacket in contact with the mould as illustrated in Figure 7.1 The rear of the CPT elements was covered with a 25mm layer of insulating mineral wool (Rock25) to minimise heat loss and maximise the transfer of heat to the concrete cast in the mould. A water resistant and high temperature resistant silicon coated glass cloth weave (SCGC) was used to protect the CPT, and provide a robust flexible finish to the jackets.

The jacket was fitted onto the mould using a combination of straps and velcro to secure its position. To minimise heat loss from the top surface of the concrete, a non-heating, insulative blanket using Rock 25 insulation was manufactured to fix to the thermal jacket. The curing jacket was designed to operate on a 24 Volt supply, controlled via a portable electronic control / transformer unit. The portable transformer unit was such that three temperature profiles could be programmed to control the rate of heating and cooling of the thermal jacket.

7.2.1. *Thermal Curing Profiles*

Three curing profiles were used throughout the testing programme to cure concrete cast within the 400 x 400 x 400 mm mould. The accelerated curing profiles are shown in Figure 7.2 Profiles 1 and 2 heat the concrete to 50 deg C at rates of 10 deg C and 15 deg C per hour respectively. Profile 3 heats the concrete to 60 deg C at a heating rate of 10 deg C per hour. In each case the heat curing cycle started from the point of casting the concrete in the mould.

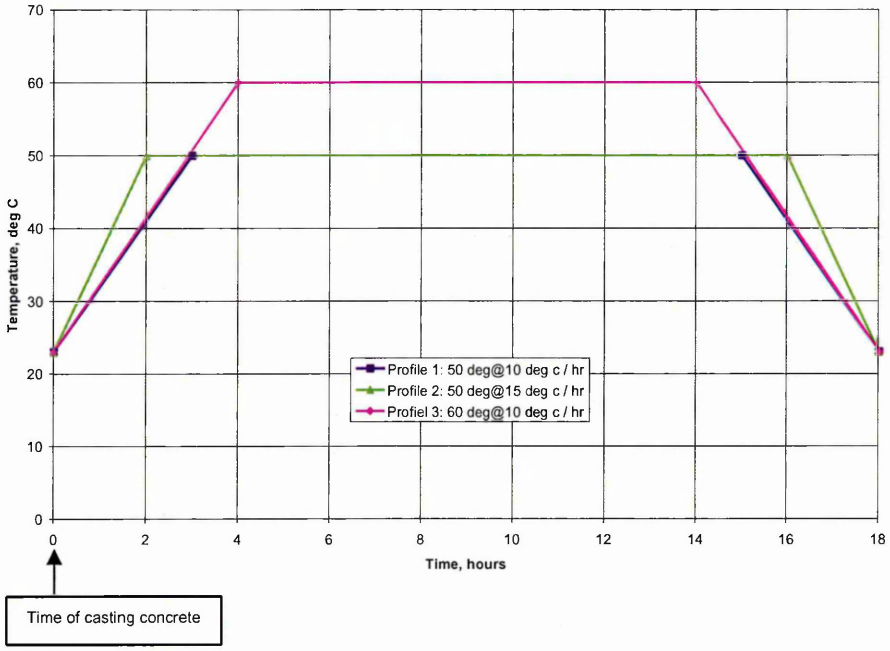

Figure 7.2. Accelerated curing profiles used throughout the test programme

The three profiles in Figure 7.2 were adopted to cure the concrete for 18 hours, including a cooling period, where the rate of cooling was the same as the rate of heating.

7.2.2. *Temperature monitoring*

A Pico temperature sensing unit (TC-08) was used to determine the operating temperatures of the heating elements and the curing jackets, and the temperature profiles throughout the concrete. Temperatures were monitored using K-type thermocouple sensors located as shown in Figure 7.3.

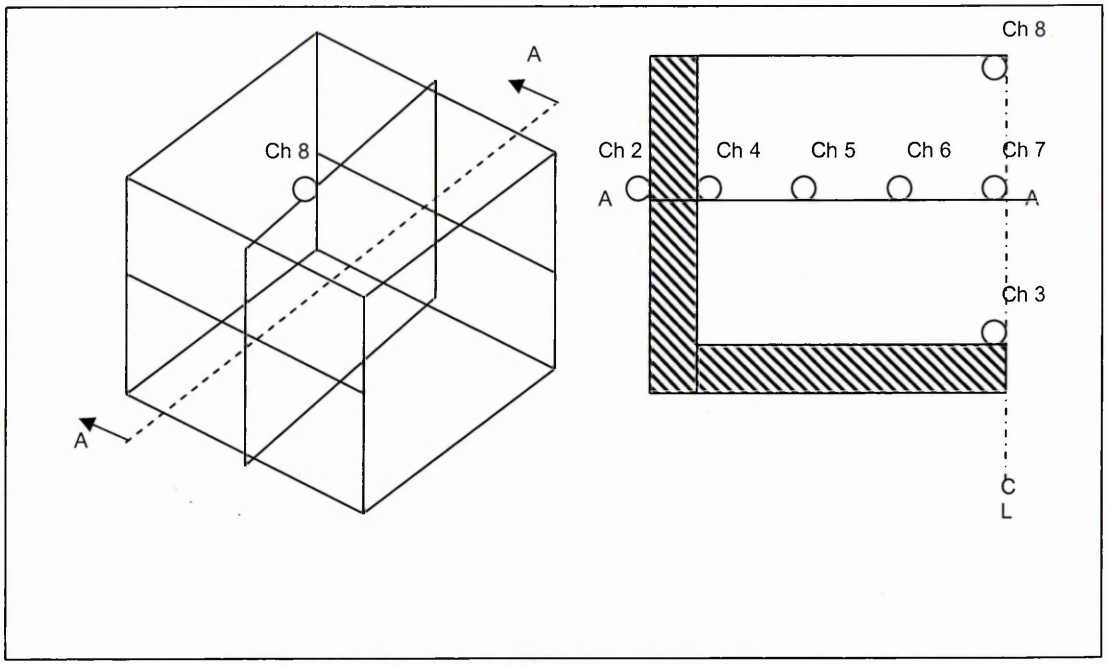

Ch1 = CPT element temperature
Ch2 = Side of the mould
Ch3 = Inside base of the mould centre
Ch4 = Internal side of the mould
Ch5 = Within the concrete (70mm)
Ch6 = Within the concrete (140mm)
Ch7 = Centre of the concrete cube (200mm)
Ch8 = Top surface of the concrete
Ch9 = Ambient

Figure 7.3. Location of temperature sensors

The thermocouples embedded within the concrete were protected from ingress of moisture by sealing with resin prior to casting of the concrete. Within the concrete cube, thermocouples Ch4, Ch5, Ch6 and Ch7 were located along the central axis of the cube. Thermocouple Ch4 was located on the inside face of the mould, and Thermocouple Ch7 was located at the centre of the cube. Thermocouples Ch5 and Ch 6 were located at intermediate points as illustrated in Figure 7.3. The same temperature monitoring equipment was also used during the calibration stages and testing of the jacket prior to thermal curing of the concrete elements.

7.2.3. *Core Sampling and Concrete Strength Testing*

In addition to monitoring the thermal profiles within the 400 x 400 x 400 mm concrete cubes, the strength of the concrete was also determined. Three days from casting (time for the 400mm cubes to fully cool) concrete cores were taken from locations as illustrated in Figure 7.4.

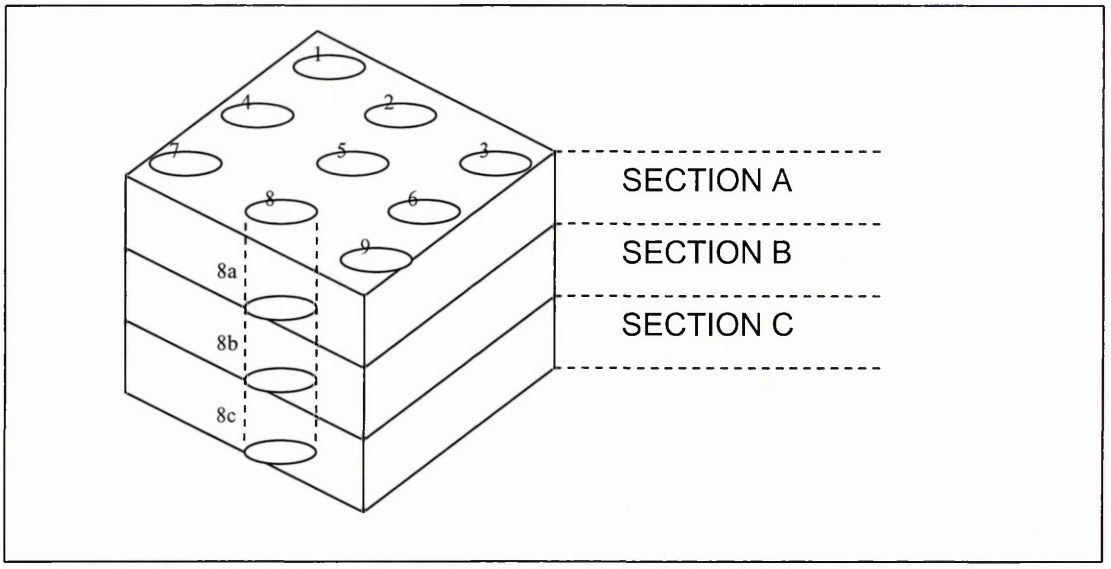

Figure 7.4. Location of core samples taken from the 400mm concrete cube

Nine 100mm diameter cores were taken from each cube, through the depth parallel to the moulded sides of the 'as cast' cube (Figure 7.4). Each core was cut into three sections A, B and C. Section A represented cores taken from the upper third of the concrete cube, section B the mid section and section C the lower section of the cube. The cores were prepared to heights of 100mm, and the surfaces squared off for compression testing to BS 1881: 1991.

7.3. Results

7.3.1. *Calibration of LAB 400 Jacket*

The performance of the CPT thermal Jacket was established using two heating profiles to calibrate prior to its application on the 400 x 400 x 400mm cube mould, as described in Figure 7.5.

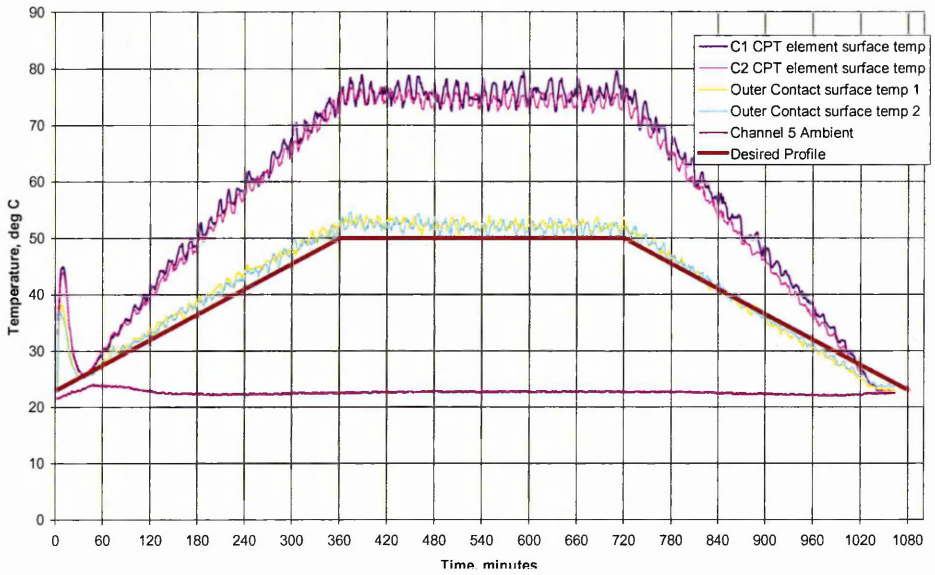

Figure 7.5. Performance of the thermal jacket when not applied to the 400mm cube mould. Operating temperature profile: 50 deg C @ 5 deg C/h

Figure 7.5 shows the operating temperature of the CPT elements and the surface temperature of the jacket designed to be in direct contact with the external face of the steel mould. Figure 7.5 shows that the control of the CPT elements allows the contact surface of the curing Jacket to be accurately maintained to close tolerances of the programmed temperature profile, 50 deg C @ 5 deg C/h. When the Jacket is free running, (not applied to the mould), a maximum average surface temperature of 75 – 80 deg C of the CPT elements corresponds to the contact surface of the Jacket operating at 50 – 53 deg C (Figure 7.5).

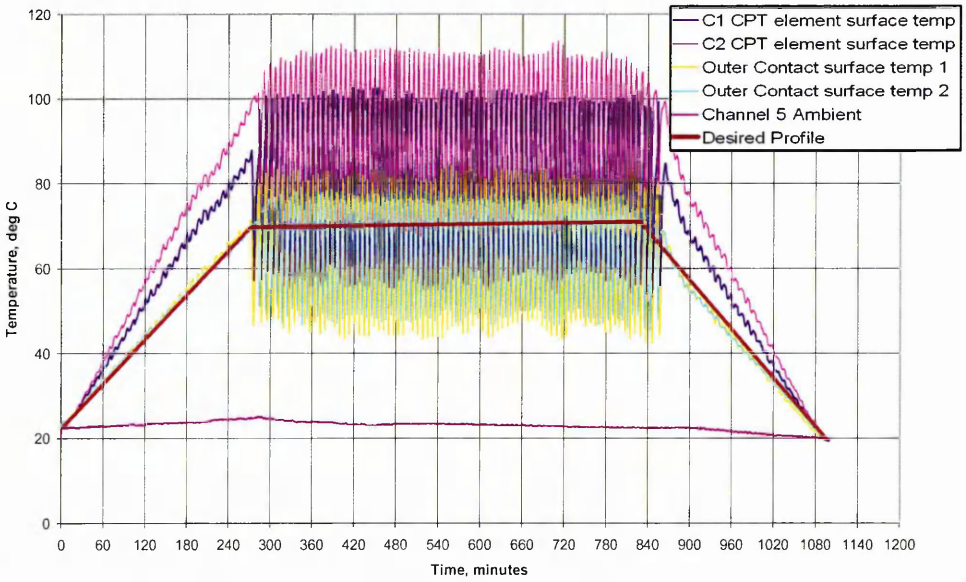

Figure 7.6. Performance of the thermal jacket when not applied to the 400mm cube mould. Operating profile 1: 70 deg C @ 15 deg C/h

Figure 7.6 shows that when the temperature and rate of temperature rise for a free running jacket is increased, 70deg C @ 15 deg C/h, the average temperature of the contact surface of the thermal jacket can be controlled to close tolerances of the programmed profile. To achieve the average surface temperature of 70 deg C on the contact surface of the Jacket, the CPT element operates at temperatures between 70 deg and 110 deg C. Figure 7.6 also shows to a greater extent than Figure 7.5 the ability of the CPT to be highly controlled. It shows very fast response times from the heating element from 70 deg C to 110 deg C, to maintain the average contact surface temperature of the jacket at 70 deg C.

7.3.2. *Curing Blanket Performance used to Heat 400mm Concrete Mould*

Having established and calibrated the performance of the Jacket, when not in contact with the concrete mould, the jacket was applied to the mould (empty) and its performance established.

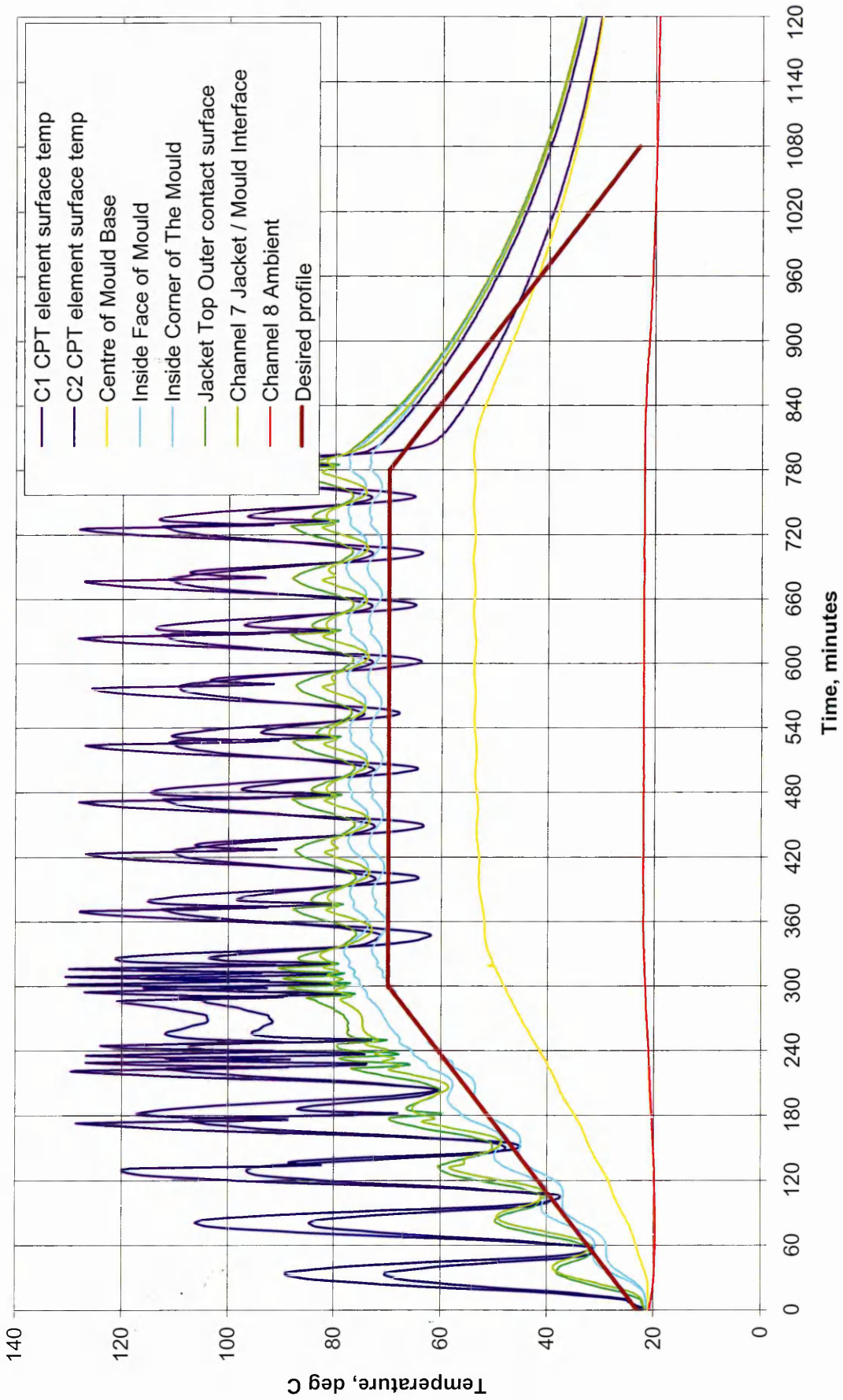

Figure 7.7. Temperature profile across the empty 400mm cube mould. Curing profile: 70 deg C @ 10 deg C/h

Figure 7.7 shows that when the Jacket was applied to the 400 x 400 x 400 mm steel mould the heat distribution through the mould followed closely the operated heating profile of the jacket 70 deg C @ 10 deg C/h. It also shows that the maximum operating temperature required to maintain the steel mould at 70 deg C was 120 deg C compared to Figure 7.6 where the free jacket operated at 100 deg C to provide the same mould contact temperature. Figure 7.7 shows that the mid point of the base of the steel mould, although not in direct contact with the thermal jacket, increased its temperature by 35 deg C compared to the ambient temperature. Figure 7.7 shows a decrease in the frequency of the heating and cutting out cycles of the CPT element surface. This is due to the increased heat storage capacity of the steel mould compared to the jacket operating freely in the air.

7.3.3. *Curing Profiles of the 400mm Concrete Cubes*

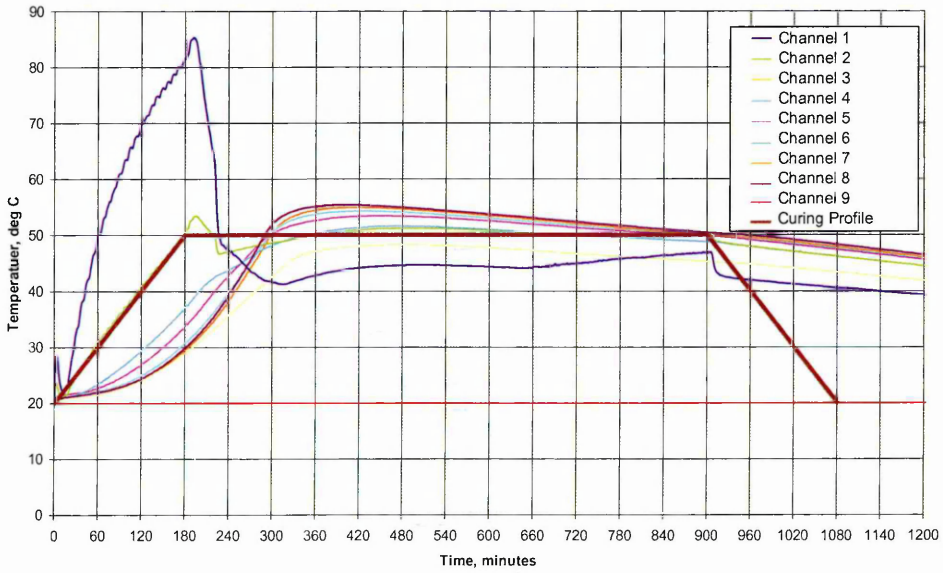

Figure 7.8. Curing profile of concrete cast in the 400mm cube mould, profile 1: 50 deg C @ 10 deg C/h

Figure 7.8 shows the temperature profiles throughout a concrete cube cast in the 400 x 400 x 400 mm steel mould. The concrete cube was cured using heating Profile 1, 50 deg C @ 10 deg C/h. Figure 7.8 also shows that the Thermal jacket maintained a very close tolerance at the interface of the thermal Jacket and the steel mould. This resulted in the cast concrete to heat up but with a heating lag of up to 3 hours for the concrete to reach the maximum curing temperature of 50 deg C. Upon reaching the constant curing temperature the concrete block was maintained at a temperature of between 50 deg C – 55 deg C. To achieve the increase in temperature the CPT operated constantly during the heating section of the profile up to a maximum temperature of 85 deg C, before cutting out. Having increased the temperature of the concrete throughout to 50 deg C, the CPT operated only to maintain the temperature. At

900 minutes the CPT cut out allowing the concrete to cool. Compared to Figure 7.7 the sensor located at the centre of the mould base (Ch 3) followed the curing profile of the thermal jacket to within 5 deg C, 27 deg C above the external ambient temperature.

Figures 7.9 and 7.10 show the temperature profiles of cubes cured using heating profiles 2 and 3.

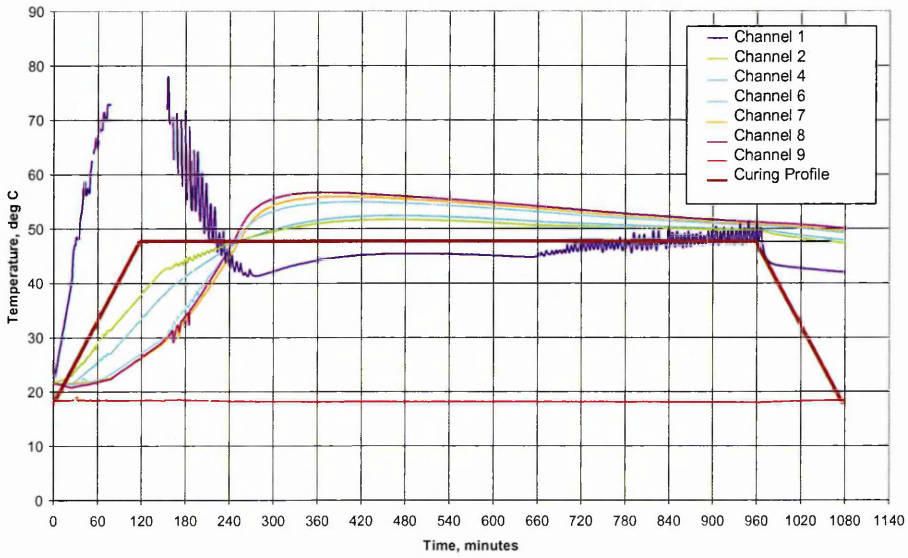

Figure 7.9. Curing profile of concrete cast in the 400mm cube mould, profile 2: 50 deg C @ 15 deg C/h

Figure 7.9 shows that the curing jacket heated the 400 x 400 x 400 mm concrete cube to 50 deg C throughout when operated to profile 2 (50 deg C @ 15 deg C/h). It shows that similar to the curing profile shown on Figure 7.8 there is a heating lag of 3 hours before 50 deg C is achieved throughout the cube. Figure 7.9 shows that initially the temperature at the centre of the block (Thermocouple Ch7, Figure 7.3) has a slower rate of temperature increase. After 2 hours this rate increases, and the temperature at Ch7 achieves 50 deg C at the same time as other locations within the cube. After achieving 50 deg C throughout, the cube temperature continues to increase in temperature to a maximum of 57 deg C at the centre of the cube (Ch7).

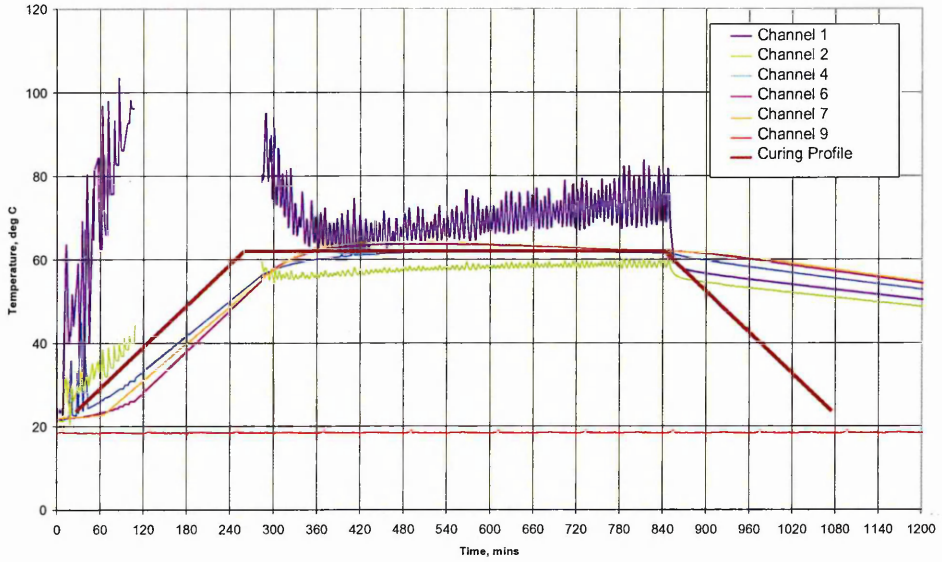

Figure 7.10. Curing profile of concrete cast in the 400mm cube mould, profile 3: 60 deg C @ 10 deg C/h

Figure 7.10 shows that at the increased temperature profile, 60 deg C @10 deg C/h, there is a reduced heating lag compared to heating profiles 1 and 2 (Figure 7.8 and Figure 7.9), and to closer tolerances throughout the concrete block at all locations (60 deg C). Figure 7.10 also shows, unlike Figure 7.8, the need for the CPT elements to continually cut in/out to maintain the temperature of 60 deg C throughout the block.

7.3.4. *Interaction of Heat of Hydration and Heat Supplied by the Thermal Jacket*

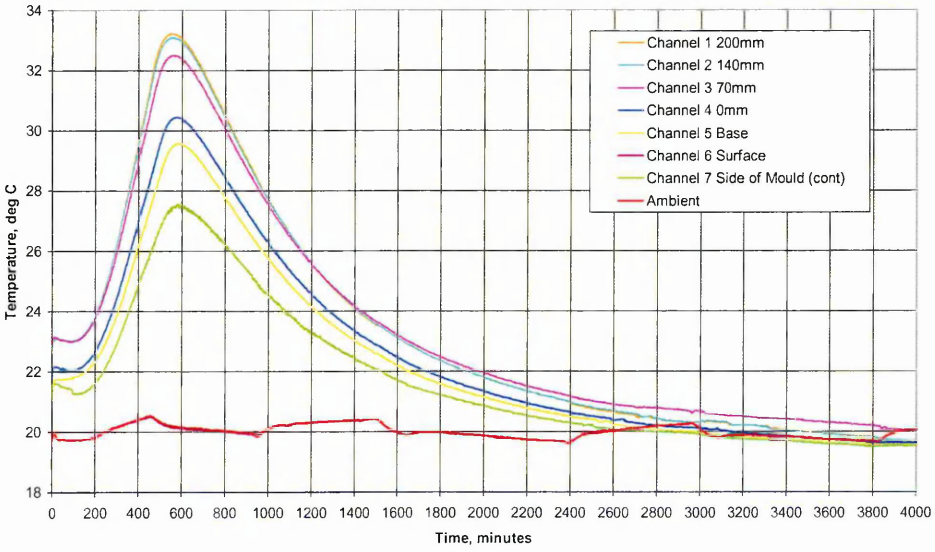

Figure 7.11. Heat of hydration generated by concrete cast in the 400mm steel mould

Figure 7.11 shows the temperature profiles generated by the heat of hydration of concrete, un-insulated within a 400 x 400 x 400 mm steel mould, at different internal locations. The concrete cube within the steel mould was kept in a controlled ambient environment of 20 deg C, 60% RH during monitoring. Figure 7.11 shows that heat is generated by the hydration of the concrete and peaks 600 minutes after casting. The data in Figure 7.11 is replotted in Figure 7.12 to show the temperature gradients step-up in the concrete cube as a result of hydration. It shows that after 600 minutes peak temperatures of 33 deg C were recorded at the centre of the cube. The corresponding temperature at the interface of the concrete and the internal face of the steel mould was 29 deg C, and the external ambient environment was 21 deg C.

7.4. Discussion of Results

7.4.1. Temperature Distribution

Figure 7.12 shows the isotherms throughout the 400mm x 400mm x 400mm concrete cube cured at 20 deg C, relative humidity 60%.

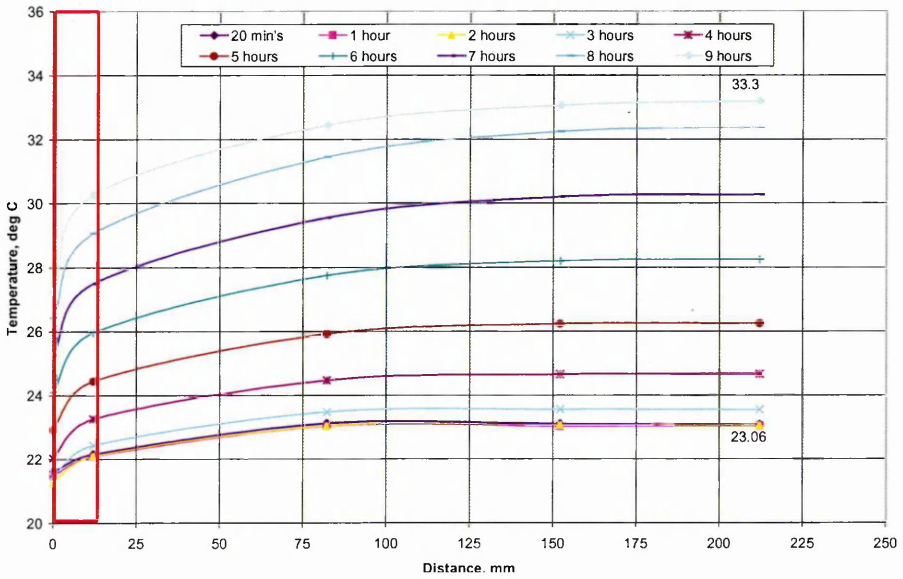

Figure 7.12. Heat of hydration temperature profiles in the 400mm concrete cube

Figure 7.12 shows that the maximum temperature is recorded at the centre of the concrete cube after 9 hours, and at that stage, the temperature differential between the centre of the cube and the external side of the mould is 10 deg C. Figure 7.13 shows the isotherms throughout the concrete cube cured with the CPT thermal Jacket using the curing profile 2, 50 deg C @ 10 deg C / h.

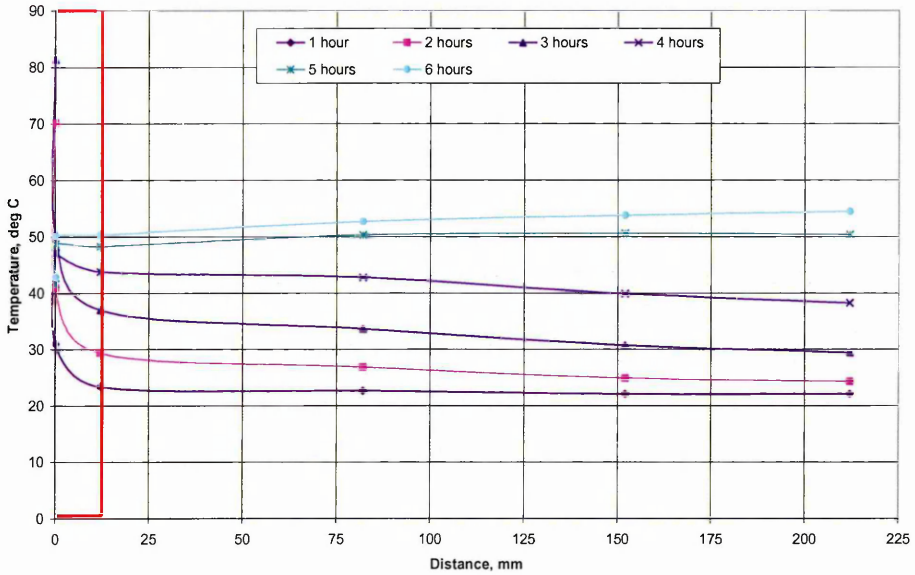

Figure 7.13. Temperature profiles through the 400mm concrete cube when cured with the thermal jacket; profile 1 50 deg C @ 10 deg C/h

Figure 7.13 shows the temperature gradients throughout the 400 x 400 x 400mm concrete block when cured using the thermal jacket set to profile 2. It shows that after 6 hours there is an even temperature distribution within the concrete block of 50 – 55 deg C, with no temperature gradients between the centre of the cube and the side of the steel mould.

The reasons for this more uniform temperature distribution throughout the concrete cube cured at an elevated temperature is due to the thermal curing jacket responding to the temperature of the side of the mould, detected by the feedback sensor located in the jacket, and the jacket's ability to respond accordingly, either by supplying or by cutting power to the jacket. The speed of the CPT materials within the blanket to raise in temperature following operation, and their ability to cool swiftly after power has been isolated make the jacket very responsive. Also because the concrete cube is of significant mass compared to the CPT material, the side of the concrete mould, and the CPT material track the temperature of one another fairly closely. Figures 7.12 and 7.13 also show that by the simultaneous insulating of the concrete mould with the Jacket and applying temperature reduces the temperature gradients within the concrete block, effectively counteracting the heat generated by hydration at the centre of the concrete cube. This has many potential advantages in reducing thermal cracking, often associated with temperature gradients within mass concrete elements. The ability of the jacket to also control the rate of cooling of the concrete cube and the insulative properties of the blanket will also minimise temperature gradients following the curing period of constant temperature of the element, again reducing the risk of thermal cracking

7.5. CPT interactions with Heat of Hydration

Figures 7.8 to 7.10 show how the CPT operates at highest temperatures during the initial heating phase of the curing profile (Figure 7.2).

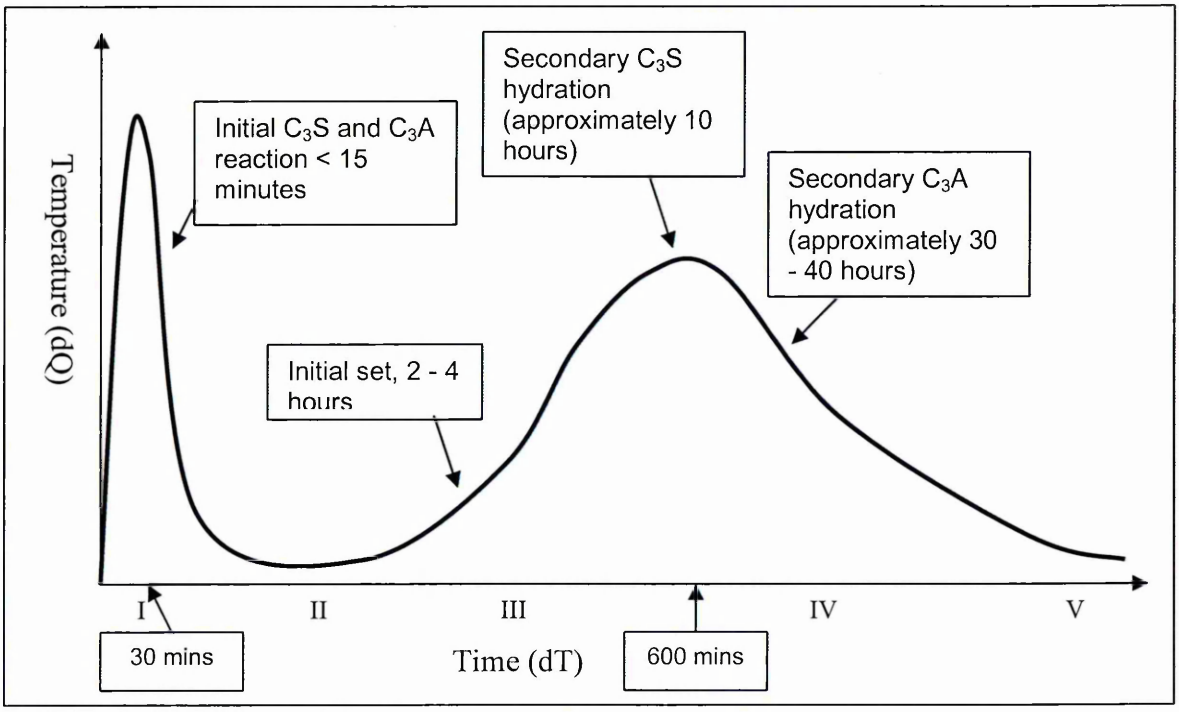

Figure 7.14. Typical Profile of heat generated by cement hydration

The hydration curves of the 400mm block given in Figure 7.11 correspond to the typical cement hydration profile in Figure 7.14. The fist peak occurs at around 30 minutes, this corresponds to the initial set of C_3S and C_3A. The main peak occurs at 600 minutes corresponding to the secondary hydration of C_3S. For the Jacket cured concrete, the peak of the secondary C_3S hydration is detectable in Figure 7.9, profile 2; 50 deg C @ 15 deg C/h at 5 hours (300 minutes) after the operation of the blanket. As a delay period was not used in this phase of testing, the time at which temperature peaks after the hydration of the C_3S compound has halved (300 minutes compared with 600 minutes for normal temperature cement hydration). This provides evidence that it is this peak of the C_3S hydration temperature which provides continuous rise in temperature even though the LAB 400 Jacket has been isolated. C_3S is largely responsible for the initial set of concrete and its early strength, therefore, accelerating this reaction provides early strengths. The application of heat by the curing has accelerated the hydration of C_3S leading to the peak hydration temperature at 300 minutes instead of 600 minutes. C_2S is not considered as it normally contributes to strength after a period of a week. C_4AF contributes little towards strength and C_3S hydrates rapidly naturally within 30 minutes and is also, therefore not affected by early age temperature.

7.6. Strength Distribution

Tables 7.1 shows the compressive strengths of core samples taken from the three concrete cubes cured using profiles 1, 2 and 3.

No.	Profile 1 50°C @ 10°C/h			Profile 2 50°C @ 15°C/h			Profile 2 60°C @ 10°C/h		
	A (Top) N/mm^2	B (Mid.) N/mm^2	C (Btm.) N/mm^2	A (Top) N/mm^2	B (Mid.) N/mm^2	C (Btm.) N/mm^2	A (Top) N/mm^2	B (Mid.) N/mm^2	C (Btm.) N/mm^2
1	-	42.4	43	28.8	36.1	45.5	38.67		46.21
2	-	-	-	35	33.1	40.6	43.45	42.65	44.98
3	29.7	47.3	37.7	30.7	33.4	40.1	38.65	36.65	39.92
4	25.3	41.8	33	31.9	31.3	43.2	34.37	34.98	55.85
5	38.1	44.9	44.1	41.3	34.6	41.1	29.12	40.58	46.86
6	40.4	-	37.9	33.5	33.3	39.1	36.38	40.66	47.83
7	34.6	45.2	35.3	-	-	-	-	41.92	-
8	40.1	44.9	39.9	-	-	-	-	-	-
9	40.9	49.9	-	-	-	-	-	-	-

Table 7.1. Compressive strengths of core samples

The location of the cores is illustrated on Figure 7.4. A Histogram of the core strengths is in Figure 7.14. Initial inspection of the results shows that the cubes cured using profile 3, 60 deg C @ 10 deg C/h, achieved the greatest compressive strength. However, these results have to be taken with a degree of caution as each cube was made with a separate batch of concrete with the possibility of slight variations in water / cement ratios, although the quality control maintained in the laboratory was very high.

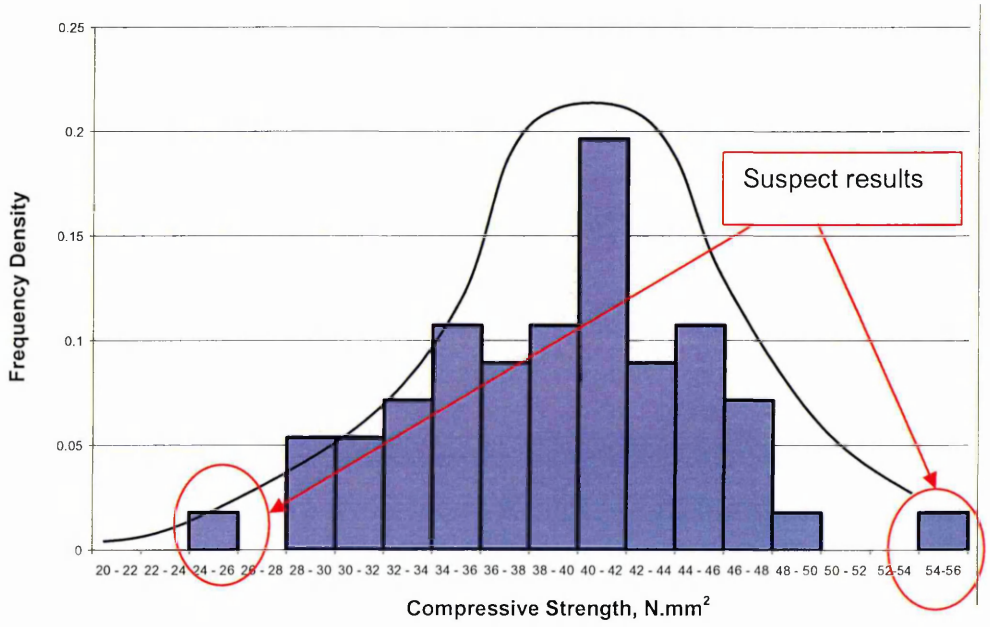

Figure 7.15. Histogram of concrete core strengths taken from 400mm cubes cured using profiles 1,2 and 3

Further inspection of Figure 7.15 appears to shows two suspect results. It also does not show a true 'bell' histogram distribution. Reasons for this could be the histogram has been plotted using limited results and it was also plotted using a culmination of results from each 400mm x 400mm x 400mm cube cured using the three different heating profiles, all three of which were manufactured independently on different occasions. Other experimental reasons for the unusual distribution could be the cores were not squared off exactly. They were cores were not capped due to time restraints. There may have been an uneven distribution of mix constituents within concrete matrix.

Although the mix proportions were the same (LAB1), each 400mm x 400mm x 400mm cube was manufactured on different occasions. it is inevitable that there will have been variations in the concrete used for each mix; different constituent temperatures, different modes of compaction and different mixing times. For this reason, the cores taken from each of the three cubes will been non-dimensionalised, i.e. the core strength relative to the central core (Core 5) for each core will be determined and given in Tables 7.2 – 7.4. Results, where, for no apparent reason, strengths were significantly higher or lower than the general strength trend within each cube will be disregarded.

No.	A (Top) N/mm^2	B (Mid.) N/mm^2	C (Btm.) N/mm^2	Average N/mm^2	Non - Dimensionalised (Core)
1	-	42.40	43.00	42.7	1.01
2	-	-	-	-	0.00
3	29.70	47.30	37.70	38.2	0.90
4	~~25.30~~	41.80	33.00	37.4	0.88
5	38.10	44.90	44.10	42.4	1.00
6	40.40	-	37.90	39.2	0.92
7	34.60	45.20	35.30	38.4	0.91
8	40.10	44.90	39.90	41.6	0.98
9	40.90	49.90	-	45.4	1.07
Average	37.3	45.2	38.7		
Non - Dimensionalised (Section)	0.88	1.07	0.91		

Table 7.2. Compressive strengths of core samples (Curing Profile 1: 50 deg C @ 10 deg C/h)

Each core has been non-dimensionalised by dividing the average compressive strength for each core (1-9) by the average of the three results taken from core 5. By taking the average of the results from the upper lower and middles sections from each core, variables such as consolidation and compaction will be eliminated. Core 5 has be used as the reference core as it is centrally located within each cube; it is the location where maximum heat of hydration would be expected as it is the maximum equal distance from each side of the mould. It is also

a unique core unlike the side and corner cores. Table 7.3 gives the non-dimensionalised results for cores taken from the 400mm x 400mm x 400mm cube cured using Profile 2.

No.	A (Top) N/mm^2	B (Mid.) N/mm^2	C (Btm.) N/mm^2	Average N/mm^2	Non - Dimensionalised (Core)
1	28.8	36.1	45.5	36.8	0.94
2	35.0	33.1	40.6	36.2	0.93
3	30.7	33.4	40.1	34.7	0.89
4	31.9	31.3	43.2	35.5	0.91
5	41.3	34.6	41.1	39	1
6	33.5	33.3	39.1	35.3	0.91
7	-	-	-	-	-
8	-	-	-	-	-
9	-	-	-	-	-
Average	33.53	33.63	41.60		
Non - Dimensionalised (Section)	0.86	0.86	1.07		

Table 7.3. Compressive strengths of core samples (Curing Profile 2: 50 deg C @ 15 deg C/h)

Table 7.4 gives the non-dimensionalised results for cores taken from the 400mm x 400mm x 400mm cube cured using Profile 3. Again, it shows which core results have been disregarded from the non-dimensional analysis.

No.	A (Top) N/mm^2	B (Mid.) N/mm^2	C (Btm.) N/mm^2	Average N/mm^2	Non - Dimensionalised (Core)
1	38.67		46.21	42.44	0.97
2	43.45	42.65	44.98	43.69333	0.99
3	38.65	36.65	39.92	38.40667	0.88
4	34.37	34.98	~~55.85~~	34.675	0.79
5	~~29.12~~	40.58	46.86	43.72	1
6	36.38	40.66	47.83	41.62333	0.95
7	-	41.92	-	41.92	0.96
8	-	-	-		
9	-	-	-		
Average	36.77	39.57	46.94		
Non-Dimensionalised (Section)	0.95	1.02	1.21		

Table 7.4. Compressive strengths of core samples (Curing Profile 3: 60 deg C @ 10 deg C/h)

The non-dimensionalised results have been plotted for each 400mm x 400mm x 400mm cube (profiles 1, 2 and 3) on Figures 7.16 to 7.18.

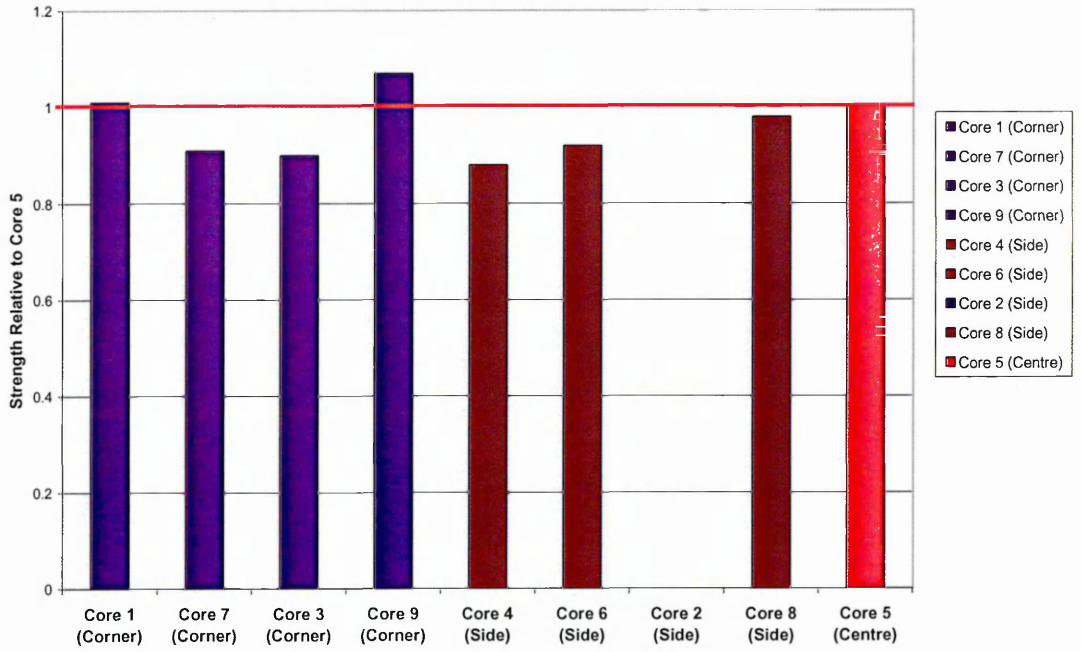

Figure 7.16. Core strength relative to core 5 (Profile 1: 50 deg C @ 10 deg C/h)

The relative core strengths for profile 1 show all cores are either very similar to, or less than the strength of core 5, except core 9.

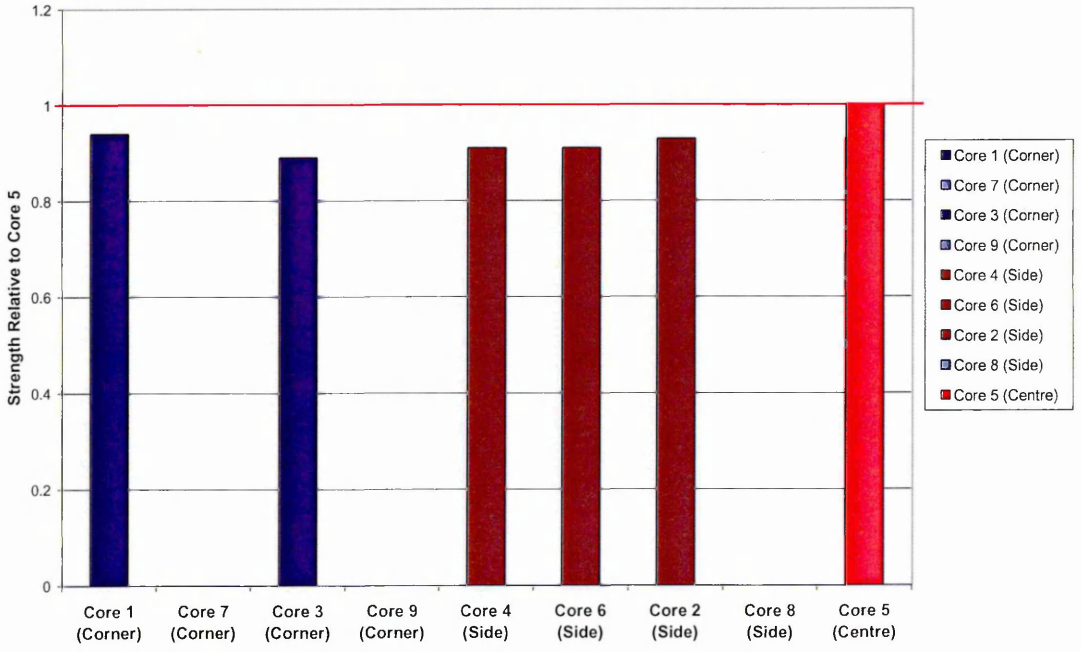

Figure 7.17. Core strength relative to core 5 (Profile 2: 50 deg C @ 15 deg C/h)

Figure 7.17 shows the relative cores strengths for Profile 2. Again, there is an even relative strength distribution. However, unlike the cores taken from the cube cured using Profile 1 all

core strengths are slightly lower than the strength of Core 5. Again there is no significant difference in strength of cores located with either at the side of the mould or at the corners.

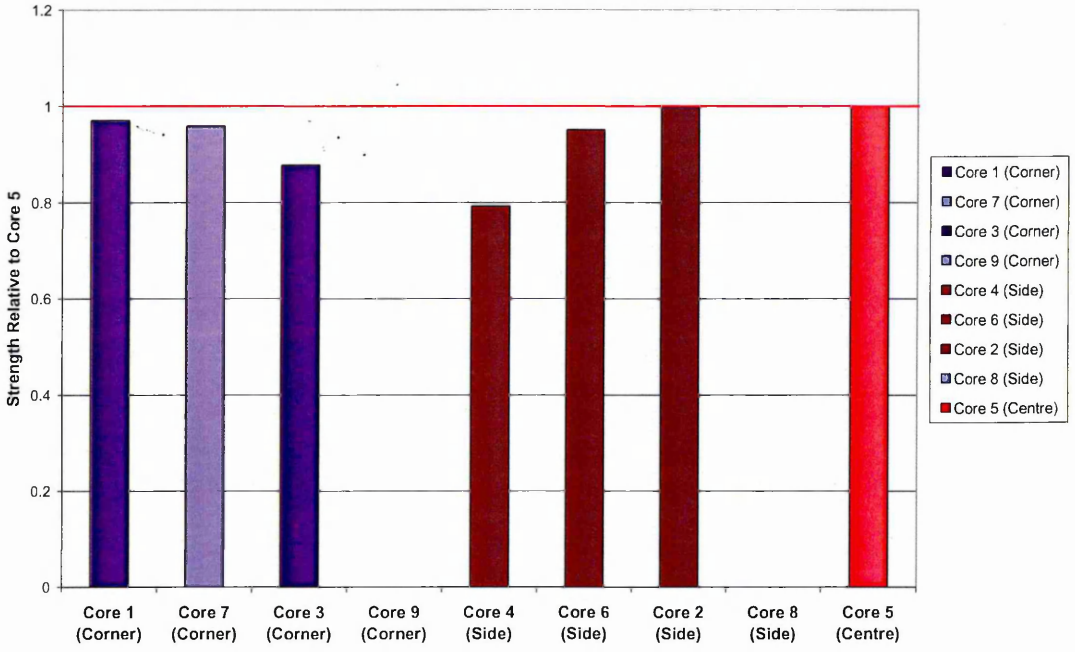

Figure 7.18. Core strength relative to core 5 (Profile 3: 60 deg C @ 10 deg C/h)

Inspection of the relative core strengths for profile 3 (Figure 7.18) shows an increased variance in relative strengths compared to profiles 1 and 2. This may be due to the increased curing temperature from 50 to 60 deg C.

The relative core strengths for each cube cured using Profiles 1 – 3 generally shows that core 5 has the highest compressive strength within each block. Reasons for this are Core 5 is located furthest from each side of the mould therefore having maximum concrete coverage around its diameter. This coverage of concrete acts as insulation. Core 5's location will always tend to be at a higher temperature due to this and also because of internal heat generated by hydration. Other reasons for the slight increased strength of core 5 are it would be expected that concrete at the centre of such a block would be better compacted. (Compaction in the vertical plane has been eliminated by the analysis – but not in the horizontal).

Slight variations in the strength of each cube, only considering, temperature, for each curing profile, could be due to the application of CPT Jacket. For each cube, the removable Jacket may have been fitted differently, i.e. the buckle may have been positioned on the side on one occasion and on the corner the next. This is an important consideration as at the conjoining area around the fixing, the heat from the CPT will be lower than at any other point on the heating surface of the Jacket. The contact between the Jacket and the mould is also an

important factor. If the Jacket was applied loose, the thermal contact between the CPT and the steel of the mould would be reduced, reducing the transfer of heat by conduction through to the concrete.

Overall there does not appear to be a trend where the strengths of concrete at the side of the mould or the corners are significantly different to each other, or the strength of the central core. Thus the results show that the CPT material / Jacket (LAB 400) can be used to cure concrete elements of a size where the heat of hydration plays a significant role in the curing of the concrete, and positively interacts with the CPT Jacket temperature input to evenly cure throughout a large concrete cube of significant mass.

7.7. Conclusions

- CPT thermal curing jackets are suitable for uniform accelerated curing of concrete.
- Thermal curing with CPT jackets accelerates the early strength development of concrete evenly
- The interaction between CPT heat and heat of hydration is mutually beneficial to both
- Thermal curing CPT jackets minimise temperature gradients throughout concrete elements caused by heat of cement hydration
- CPT thermal jackets provide highly controlled uniform and gently increasing temperatures (without thermal shock) for the accelerated curing of concrete.

Chapter 8. Applications

8.1. Introduction

Concrete elements can be constructed either insitu, on site, or within precast concrete plants. This chapter will consider the application of CPT curing systems within both of these environments. The construction of building elements off site is becoming increasingly common. Primary advantages of doing this are construction times, site layouts and labour workforce can be reduced. Key advantages of precast concrete are an increased quality of product, whether in terms of strength and performance, or the tighter tolerances and degrees of accuracy that can be achieved. However, for applications where concrete is used as foundations and for earth-works (mass concrete applications), insitu concrete is needed due to uncertainty of soil parameters. This is the case for individual foundations used to support stanchions for electrification lines along railway lines whose construction method will be considered in this chapter.

To maximise production and productivity in a precast concrete plant, a balance between the production time and production costs has to be made. As discussed in Chapter 2, most precast concrete manufacturers use a thermal curing method. Typically this is steam but it is very costly, inefficient and provides poor performance within large precast concrete plants. It can accelerate strength and production but can be very costly in terms of fuel. This is similar when erecting stanchion foundations for overhead line equipment. It is essential that construction time is minimised to reduce shutdown periods of the rail line. The construction of such foundations is usually undertaken during mild periods. The use of CPT will allow construction during winter periods.

This chapter will report the results of curing full scale concrete elements within two precast concrete plants using CPT and also on-site for the construction of a rail stanchion foundation adjacent to a rail line.

8.2. Experimental Set-up

The on-site trial was conducted at a track maintenance training centre in Selby North Yorkshire. The first precast trial was undertaken at Tarmac Precast Concrete at Tallington and the second location was CR Longley Precast Plant in Dewsbury, West Yorkshire. The first precast trial was undertaken at the Tarmac Plant using a mould for casting terrace sections for new stadia. The second precast trial at CR Longley used CPT to cure T-shaped floor beams. All the trials were conducted in exposed conditions. Although the trials within the precast plants were conducted undercover, the large sheds in which the moulds were located were unheated and had open sides.

To determine the maximum potential of the CPT systems within the precast plants, the trials were conducted during winter months, the time where thermal systems, such as steam, are most relied on. For the construction of the foundation on site, a day was selected where the conditions were defined as 'cold weather' in ACI 306R – 6, which states that a cold weather period is a '"period when, for more than 3 consecutive days, the following conditions exist: 1) the average daily air temperature is less than 5 deg C (40 deg F) and 2) the air temperature is not greater than 10 deg C (50 deg F) for more than one-half of any 24 hour period." Prior to casting on site the temperature and weather forecast was monitored to ensure such conditions were met when casting the foundations on site. Details of tests undertaken to determine the effectiveness of CPT both in a precast concrete plant and on-site are given in this Chapter.

8.2.1. *Stanchion Foundation*

Steel stanchions are required along railway lines to support overhead electric lines. Concrete foundations are constructed to support the steel stanchions as detailed in Figure 8.1. These foundations are cast adjacent to the rails in restricted time due to limited rail closure and the foundation is required in service promptly. The INSITU 1500 CPT Jacket was designed and manufactured to line a typical foundation excavation.

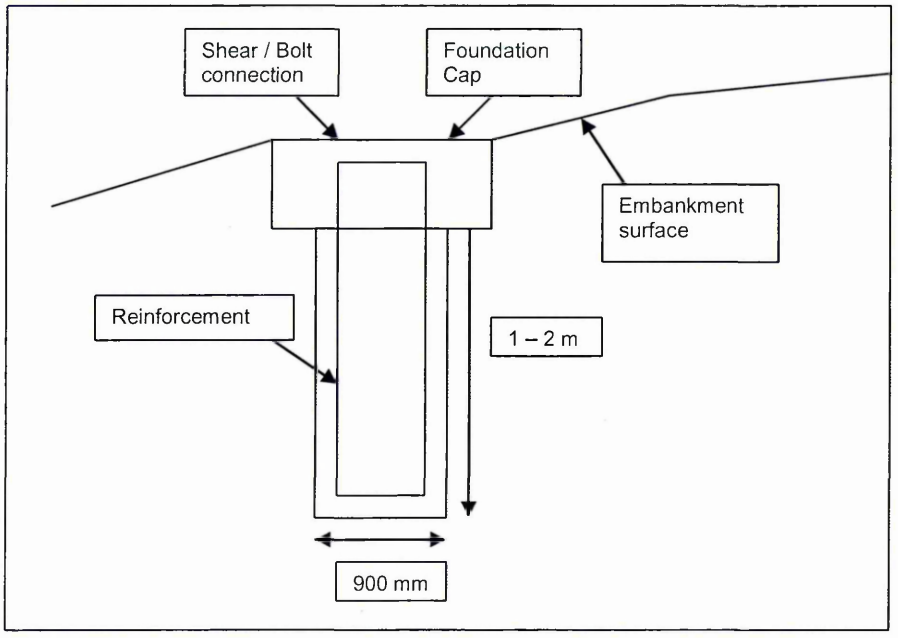

Figure 8.1. Cross-section of a typical stanchion foundation

Two excavations were made with approximate dimensions 2.0m deep and 0.9m x 0.9m in cross-section. One of the excavations, A, was lined with the INSITU 1500 heat curing CPT linaer. The four liner sections, as described, were attached to the sides of the excavation

using 'pegs' to secure in position and to maintain their location during the pouring of the concrete. Figure 8.2 shows the location of the lined excavation A in relation to the un-lined Foundation B.

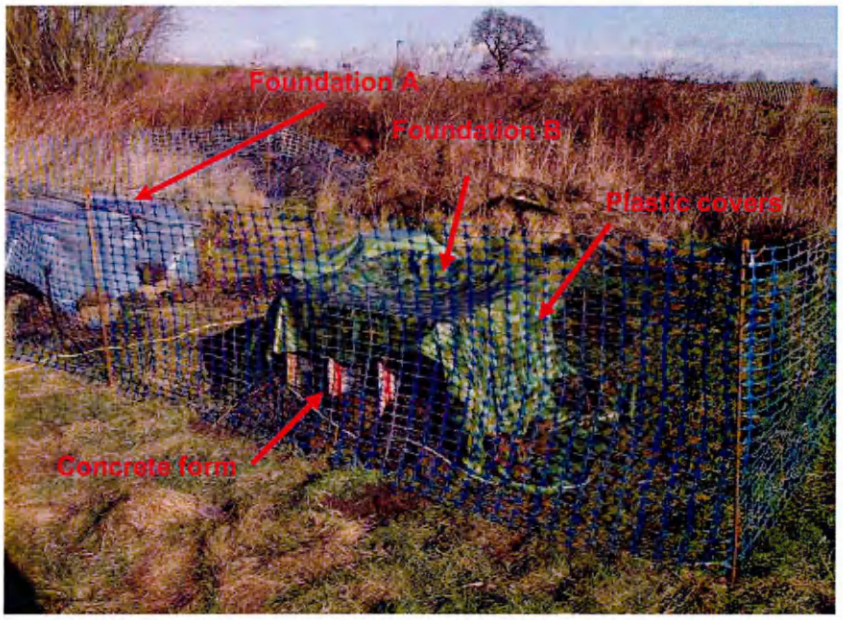

Figure 8.2. Location of foundations in relation to each other

Foundation A was the first to be poured. Approximately 300 – 500mm layer of concrete was poured into the base of the foundation. A reinforcement cage with thermocouple probes located on it was lowered and maintained in position while the remaining concrete was poured. Care was taken to ensure no concrete was poured behind the liners. Foundation B was cast using the same procedure.

After casting, Foundation A was covered with the thermal curing blanket and Foundation B was covered with a Hessian material and then a plastic sheet to protect them both from rain, as shown in Figure 8.2. For each foundation, thermocouple sensors were located throughout to monitor the temperature variations through each block. Details of the senor locations within the blocks is given in section 8.5.1.

During the casting of each foundation, two cubes 150 x 150 x 150mm of the concrete mix were prepared. The cubes of Foundation A concrete were labelled A1 and A2, and B1 and B2 for Foundation B. The 150 x 150 x 150mm cube concrete samples of each foundation were tested at 7 and 28 days in accordance to BS 1881. The samples were cured in a moist condition at an ambient temperature of about 20 deg C.

8.2.2. *Precast Concrete*

Figure 8.3 shows a precast concrete mould used to manufacture concrete elements for the casting of reinforced concrete terrace elements for stadia. Traditionally the precast concrete mould would have been heated to accelerate the strength development of the cast concrete by running steam pipes adjacent to it to heat the concrete by convection. PRECAST 6500 Jackets were manufactured and installed on the precast concrete mould. The mould was used to manufacture terrace sections for a new stadium in London. The PRECAST 6500 system was fitted to an existing mould retrospectively, (i.e. after the mould had already been manufactured). The PREACST 6500 Jacket was used as a alternative mode of heating instead of captured steam pipes. The Jackets were wedged between the ribs of the steel mould to maintain them in position.

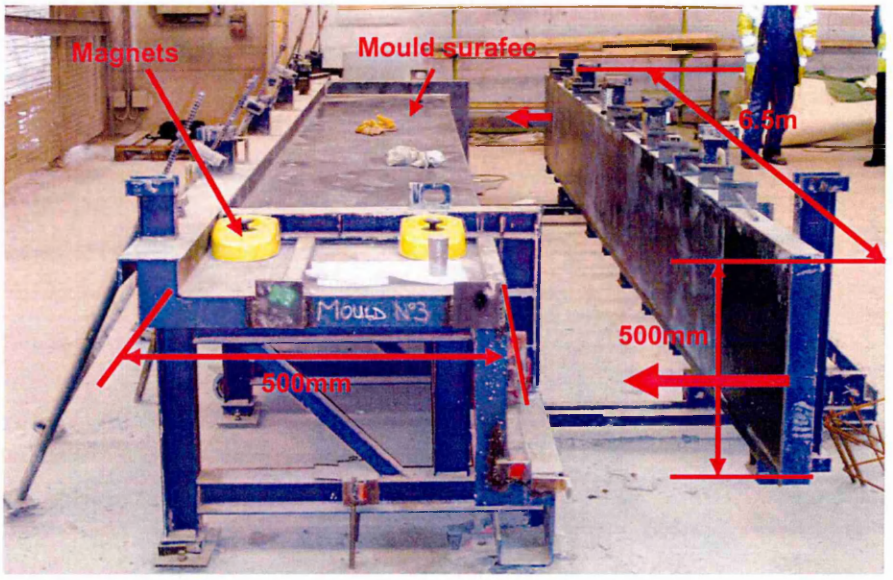

Figure 8.3. Positioning of CPT Jackets on the terrace mould

Dimensions of the mould were 6500m in length by 500mm x 500mm. The thickness of the finished cast section was 150mm. The concrete was cast at the start of a shift following mould preparation which included the removal of any concrete particles and oiling the mould prior to casting. The concrete was supplied using concrete from the batching plant (Mix C) at the precast concrete factory. In parallel to casting the CPT trial mould, an identical mould was cast using no thermal curing systems

For both trials a delay period of two hours was allowed prior to the operation of the CPT liners and Blankets, as recommended in the literature review (Section 2.14). This delay period was to eliminate the impact of initial internal stresses within the concrete elements at early ages as a result of heating. This is standard practice recommended for the high temperature accelerated curing of concrete.

8.3. CPT Jackets

To minimise heat loss from the heating liners, an insulative closed cell foam (FOAM) was used at the rear of the CPT elements for both the PREACST and INSITU Jackets. The CPT elements were bonded to the foam. The CPT and foam composite was then sandwiched in a PVC outer material (front and back) to protect the elements from chemical attack and damage during the pouring of the concrete. To reduce ingress the PVC material was RF welded at the seams.

8.3.1. *INSITU 1500 Jacket*

For the INSITU 1500 Jacket four CPT elements were used within each section to line the four vertical sides of the foundation as shown in Figures 8.1 and 8.4 and described in Chapter 4. Two CPT elements 0.3m wide (W) were used in the surface blanket,. The four vertical liners were wired in parallel to operate simultaneously, all at the same voltage of 50 Volts. The Grey CPT material, R_T= 50 ohms, was used to manufacture the elements in each section of the liner. The surface blanket was operated separately form the vertical lines, and connected to the 50 Volt step down transformer. Each of the elements within the main sections of the liner were 0.7m (l) in length; this was also the case for the elements within the surface Jacket.

It was thought that the use of the CPT liners INSITU 1500 would provide protection to the concrete to stop freezing at early ages, and potentially accelerate the hydration reaction of the concrete allowing construction times to be reduced and to be undertaken throughout the year. For such an application it was essential that the CPT could be used very easily and quickly.

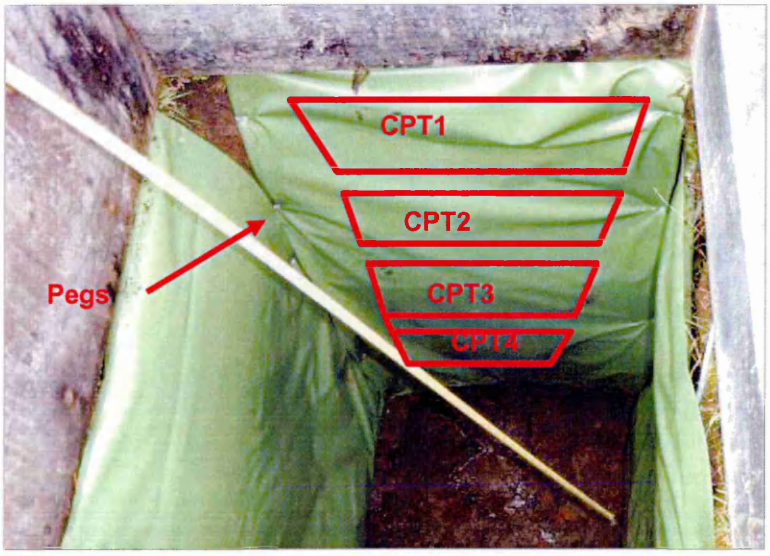

Figure 8.4. Curing liner in position prior to casting of Foundation A

The Liner was designed with this in mind, making it light, flexible and easy to connect and left insitu after casting the foundation. The liners had to be particularly flexible to follow the contours of the excavation and not allow any weakness at the interface affecting the ultimate performance of the foundation. Following construction of the foundation the liners remain in place as a consumable item.

8.3.2. *PRECAST 6500 Jacket*

For the PREACST 6500 Jacket two CPT Jackets 3250mm each were manufactured using the R_T= 50 ohms CPT material. The element length l was 120mm and the element width, W, for each was 3220mm. The two separate Jackets were connected in parallel to form the 6500mm length of the mould. Five pairs of Jackets were used. Each pair of Jackets were connected individually to the control unit and controlled independently using a Carrel electronic controller.

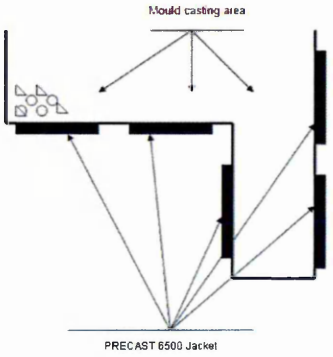

Figure 8.5. Precast mould and CPT jacket positioning

Figure 8.5 shows the positioning of the PRECAST 6500 Jackets on the terrace mould. The Jackets were positioned by feeding them under the upright cross members of the mould. The Jackets remained in place through friction instead of bonding them with any adhesive. The dimensions of the Jacket were such that they could be 'wedged' into position.

Unlike the INSITU 1500 Jacket, the PREACST 6500 Jacket was a non-consumable system installed to be a permanent integrated heating element within the mould for repeated re-use.

8.4. Control and Transformer unit

For the foundation trial, the INSITU 1500 CPT blankets were operated using a standard on site yellow-GRP housed step-down transformer to 50 Volts a.c (Appendices, Volume 2), typical for on site application for the operation of hand power tools and general equipment. Alternatively the blankets could have been operated using a portable 50 volt secondary output

(Figure 8.6) (alternating or direct current) generator. Specification for the transformer / control unit is given in Appendices Volume 2.

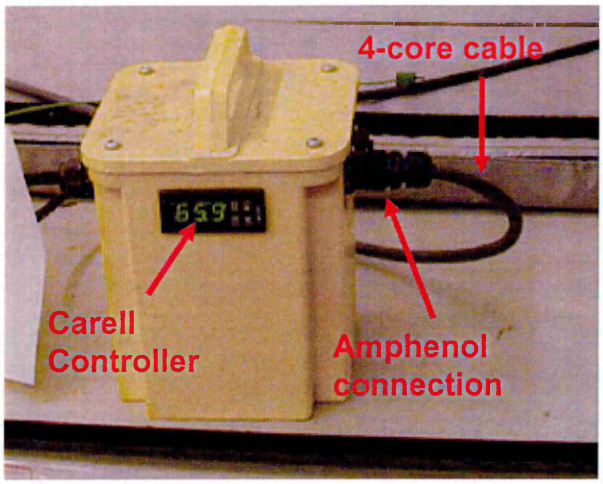

Figure 8.6. Control unit for the INSITU 1500 Jacket

For the precast trial the PREACST 6500 was operated using the control units shown in Figure 8.7. The unit had five independently controlled out-puts with PID (proportional integral differential) temperature feedback probes to monitor the temperature of each pair of Jackets.

Figure 8.7. Control unit for the INSITU 1500 Jacket

In addition, the control panel unit had the option of supplying either 24 Volts or 36 Volts to the PREACST 6500 Jackets, in case a boost of power to the Jackets was required. The panel had a lockable front door to protect the control panel. The panel was operated by a 3-phase 400 Volt supply from the factory's main switchboard. Full specification for the panel is given in Appendices, Volume 2.

8.5. Concrete

The insitu rail stanchion foundation was cast using the concrete Mix B, details of which are given in Table 8.1. The mix was supplied by the local ready mix supplier Tarmac Ready mix.

Constituent	Value
Minimum cement content	325 kg/m^3
Maximum free w/c ratio	0.55
Nominal maximum aggregate size	20mm
Workability (slump)	75mm

Table 8.1. Foundation concrete specification (Mix B)

The precast concrete element was cast using the Mix C described in Chapter 4 Details of the mix is given in Table 8.2.

Constituent	Quantities kg/m^3
Cement CEM I 52.5	312
GGBS	133
0-4mm limestone dust	776
4-10mm granite	1018
Admixture	3.2
Water	180

Table 8.2. Precast concrete specification (Mix C)

The light colouring of the section, as can be seen in Figure 8.8, was achieved by using GGBS. Implications of using a high proportion of GGBS were the delay in early age strength development and also a reduced heat of hydration at early ages, therefore, making the need for a reliable thermal curing system more important.

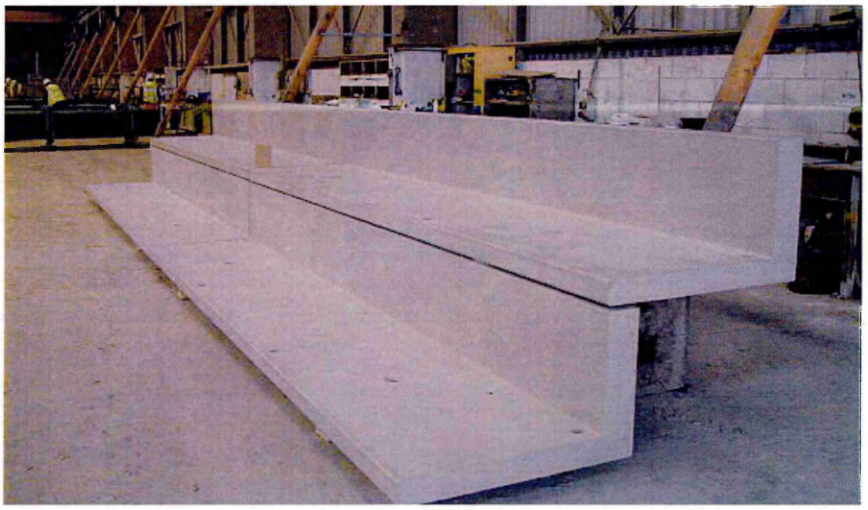

Figure 8.8. Typical precast terrace section cast within the mould

8.6. Temperature Monitoring and Data Acquisition

Both applications were operated with a PID feedback probe using the Carrel controller set to 70 deg C. The temperature within the element being cured was recorded by *Datataker equipment*. To ensure that the thermocouples were not damaged by the fresh concrete during casting they were sealed at the end by using heat shrink tubing as described in Section 4.6. The thermocouple location and positioning within each application is as follows.

8.6.1. *Foundation thermocouple positioning*

The foundations were reinforced using a steel cage as detailed in Figure 8.9. The cage was fabricated using 12mm diameter reinforcement steel. The reinforcement cages were 2.0m long and 700mm x 700mm. In order to monitor the curing temperatures in the concrete foundations provided by the CPT liner, T-type thermocouple probes were attached at different locations of the reinforcement cage. The positions of the thermocouples are shown in Figures 8.9 and 8.10.

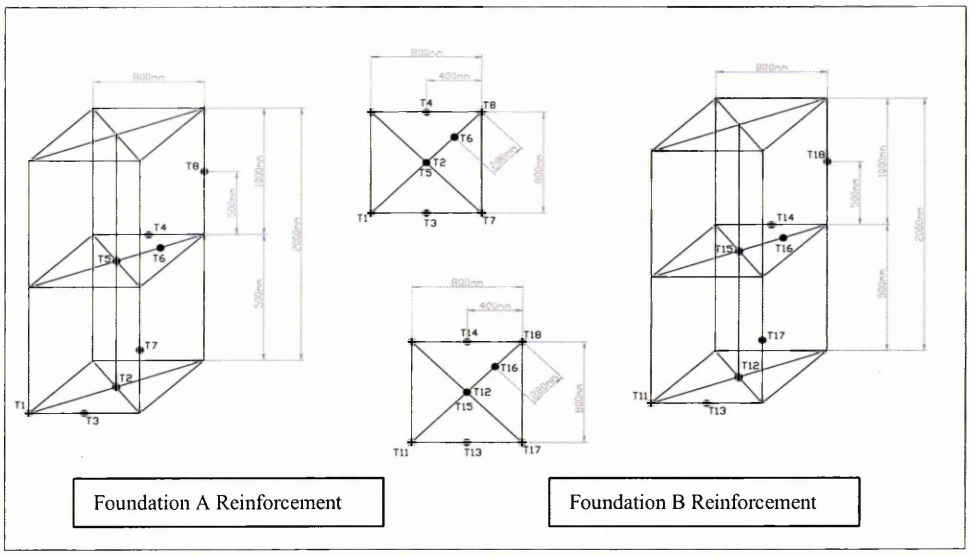

Figure 8.9. Reinforcement cage arrangement showing position of thermocouple sensors

Thermocouples T1-T8 were attached to the reinforcement cage of foundation A which was heated with CPT liners Foundation A. Thermocouples T11 – T18 were attached to the reinforcement cage of the control foundation, Foundation B. Thermocouple T9 was located at the surface of Foundation A and T10 monitored the temperature the ambient air adjacent to the foundation. Thermocouples T19 and T20 logged the surface temperature of the control foundation and its adjacent ambient air temperature.

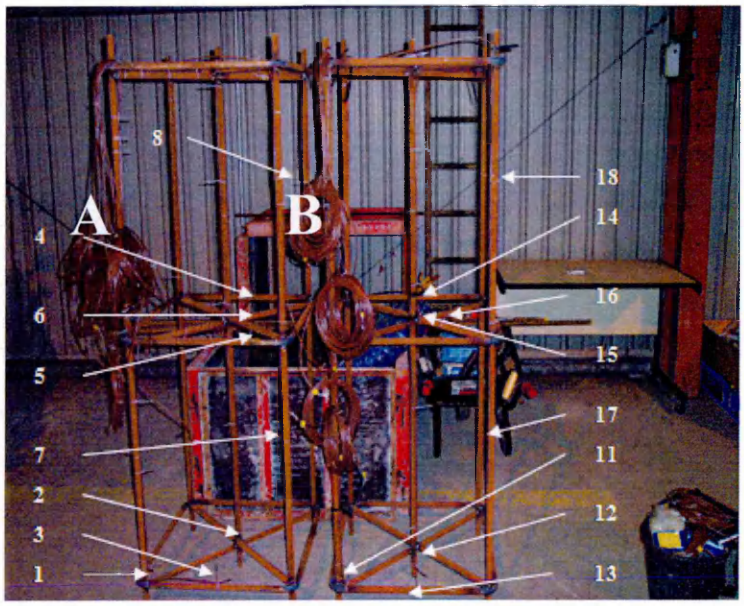

Figure 8.10. Thermocouple sensor location on cages of Foundations A and B

The T-type thermocouples were attached to the reinforcement using cable ties to secure them in place prior to casting the concrete.

8.6.2. *Precast concrete thermocouple positioning*

Three thermocouples were used to monitor the temperatures, TC 1 to monitor the temperature within the concrete element 75mm from the side face of the mould, TC2 to monitor the temperature on the side of the mould adjacent to the PREACST 6500 Jacket and a third TC 3 to monitor the ambient temperature, as shown in Figure 8.11.

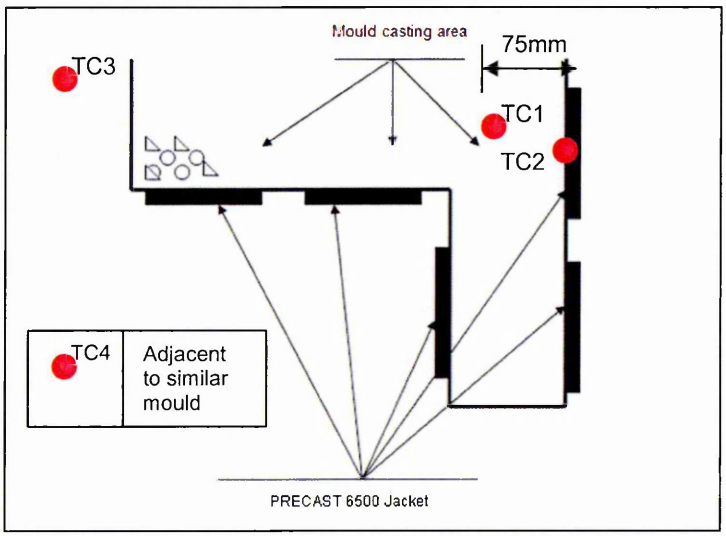

Figure 8.11. Precast concrete mould thermocouple locations

8.6.3. *Thermocouple Calibration*

Prior to using the T-type thermocouples within the trial applications, all thermocouples were calibrated. To do this they were they were placed in a container of ice and water for a period of three minutes then into a glass of water at 70 deg C.

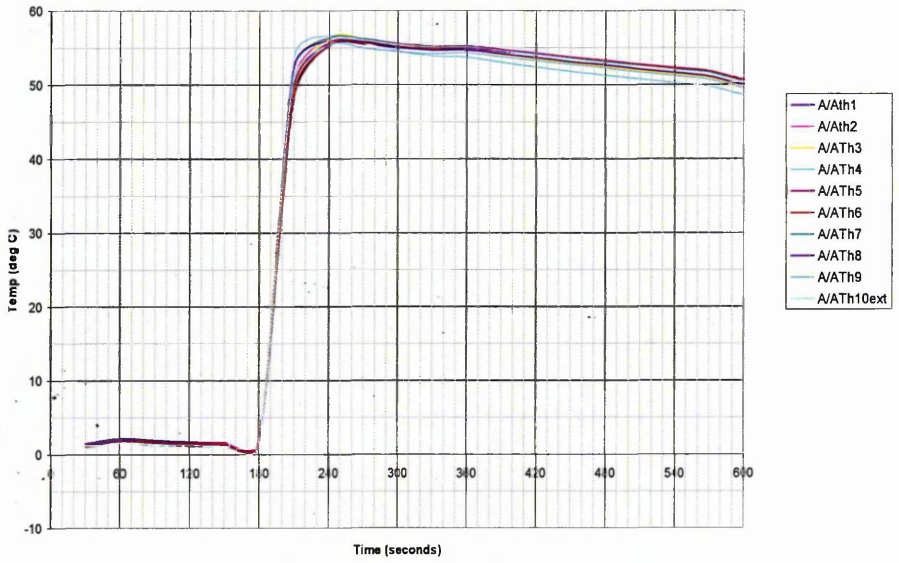

Figure 8.12. Calibration graph thermocouple Sensors T1-T10 (Foundation A)

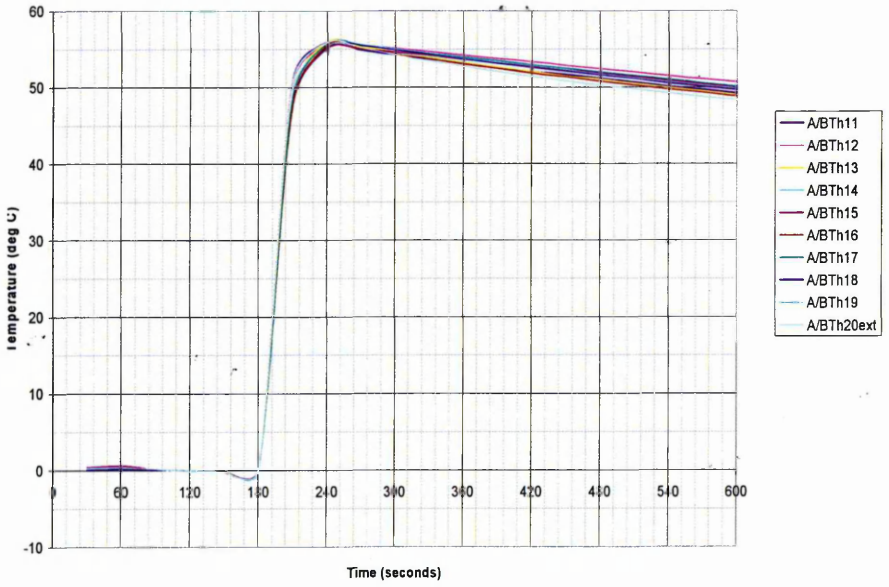

Figure 8.13. Calibration graph thermocouple sensors T10-T20 (Foundation B)

The calibration curves in Figures 8.12 and 8.13 show that both sets of thermocouples attached to the reinforcement cages for each foundation have close tolerances. These were

Type T thermocouples as described in Chapter 4.0 sealed using resin and butt-crimps. The same calibration procedure was repeated for the thermocouples used for the precast trial.

8.7. Results

8.7.1. *Stanchion Foundation*

Figure 8.14 and Figure 8.15 show the temperature profiles of the thermocouples located in Foundation A and Foundation B respectively.

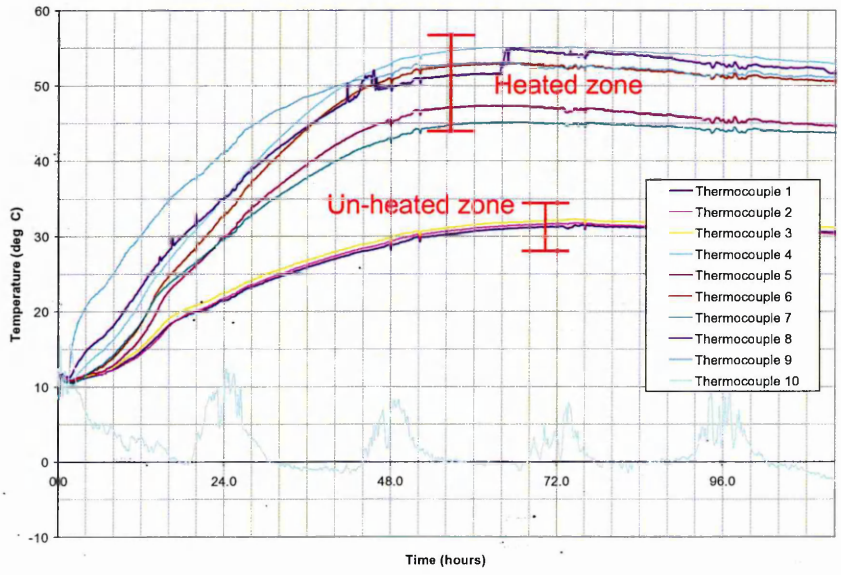

Figure 8.14. Temperature curing profile of Foundation A. (Cured with CPT liner)

Figure 8.14 shows that the (CPT) liner heated the concrete to a maximum temperature of 55 deg C at thermocouple T4 located in the middle of the rear face of the reinforcement cage as shown in Figure 8.9. Other locations to achieve temperatures within 5 deg C of thermocouple T4, were thermocouples T6, T8 and T9. Thermocouple T6 is located along the centre plane of the reinforcement, thermocouple T8 is at the corner of the top half of the foundation, and thermocouple T9 is located just below the surface. Thermocouple T9 at the surface of the foundation recorded a higher rate of temperature increase than all other locations up to 40 hours, at which point thermocouples T6 and T8 recorded higher temperatures. Thermocouples T5 and T7 at the centre of the reinforcement cage, and at the midpoint of the lower half of the cage respectively achieved a maximum constant temperature of 40 – 45 deg C. The locations that achieved the lowest constant temperature (30 deg C at 50 hours) within the cast foundation were thermocouples T1, T2, and T3, which were all located at the base of the reinforcement cage.

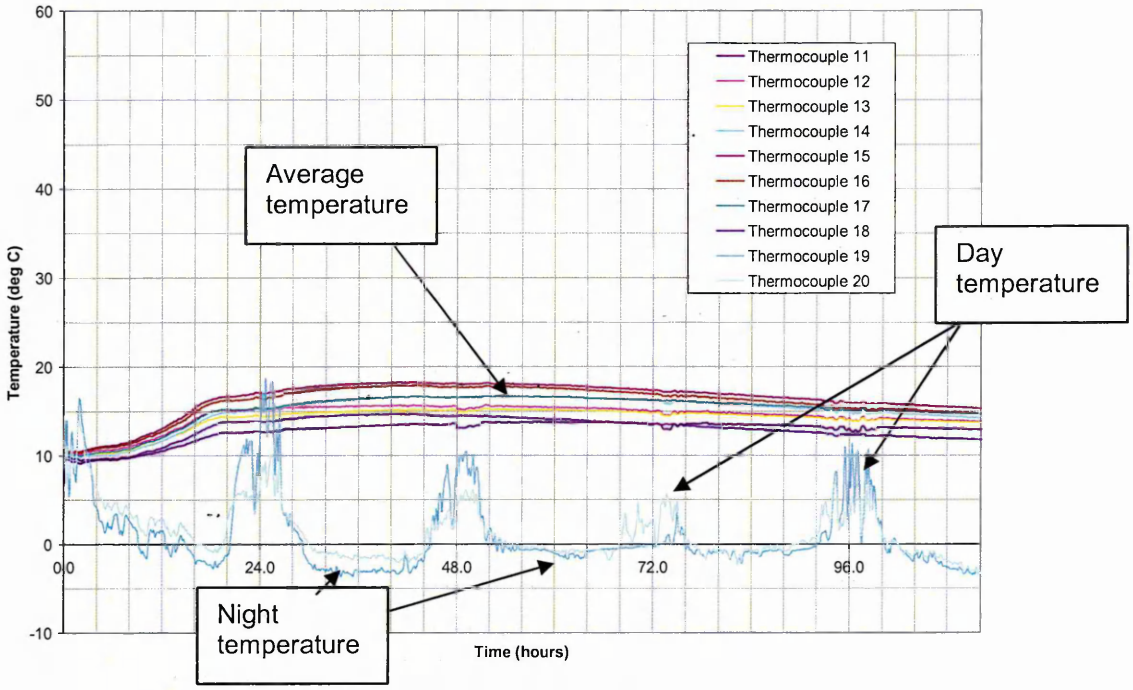

Figure 8.15. Temperature curing profile of Foundation B.(No CPT liner)

Figure 8.15 shows the temperature distribution within the un-heated control Foundation B. It shows that the maximum temperature recorded within the foundation was 17 deg C at thermocouple T15 located at the centre of the reinforcement cage, along the central plane as shown in Figure 8.9 and Figure 8.10. The areas where the minimum temperatures were recorded within the foundation were at thermocouples T11, T12 and T13 at the base of the reinforcement cage, at the parallel locations to T1, T2 and T3 in Foundation A. At location T18, corresponding to location T8 in Foundation A at the corner of the foundation, the temperatures recorded were similar to those recorded at thermocouples T11, T12, and T13. The maximum temperature (17 deg C) within the foundation was recorded at approximately 40 hours. Thermocouple T19 located at the surface of the foundation, in the equivalent location to thermocouple T9 in Foundation A, recorded similar temperatures to the ambient temperature recorded by thermocouple T20.

Figure 8.14 shows that there are two distinct 'zones' of temperature profiles as a result of the CPT liner heating. Thermocouples T1, T2 and T3 achieved a lower maximum recorded temperature of 33 deg C, and a reduced rate of temperature increase compared to other thermocouple locations within Foundation A. This difference can be accounted by the fact that the depth of the foundation and reinforcement cage was 2.5m and the depth of the CPT liners was only 2.0m. The location of thermocouples T1, T2, and T3 at the base of the foundations was in the zone not directly heated by the CPT liner. All other sensors were in the zone enclosed by the CPT liners and hence recorded a rapid temperature rise and a higher temperature of up to 55 deg C.

Comparing the two temperature profiles for each foundation, it can be seen that for the unheated foundation, Foundation B, there is small increase in temperature throughout the test with maximum temperatures of 18 deg C recorded between 24 and 48 hours. This is due to internal heat generated by hydration of the concrete. In comparison, Foundation A shows an approximate increase of 25 deg C within the same time period. The curve shows no sharp increases in temperature demonstrating a positive interaction with the heat generated by hydration in Foundation A. Further comparison shows that the temperature of the unheated section of Foundation A was 27 deg C rather than 17 deg C for Foundation B indicating that heat was distributed throughout Foundation A from heated zone to the unheated zone. Also, where the temperature in the unheated foundation peaked between 24 and 48 hours and then decreased, once the maximum temperature within the heated foundation, Foundation A, was achieved, the temperature remained constant for the remaining duration of the test.

Table 8.3 shows the results of 150mm x 150mm x 150mm cubes tested at 7 and 28 days taken from the concrete delivered to site by ready mix.

Cube ref No	Dimensions (mm)	Area (mm^2)	Age (Days)	Mass (gms)	Density ($Kg.m^3$)	Failure load (kN)	Compressive strength (N/mm^2)
21B(1)	150 x 146	21900	7	7714	2360	478.1	22
22B(2)	150 x 148	22200	28	7841	2390	1098	49.5
23A(1)	144 x 150	21600	7	7747	2370	450.2	21
24A(2)	150 x 146	21900	28	7833	2400	783.3	48.5

Table 8.3. Compressive strength results of 150mm cubes tested at 7 and 28 days

8.7.2. *LAB 6500 Jacket performance*

The results of the initial PRECAST 6500 trial are given in Figure 8.16. The initial trial was conducted at 24 Volts following a delay period of 2 hours after casting. The temperature profiles at the three locations can be seen in Figure 8.16.

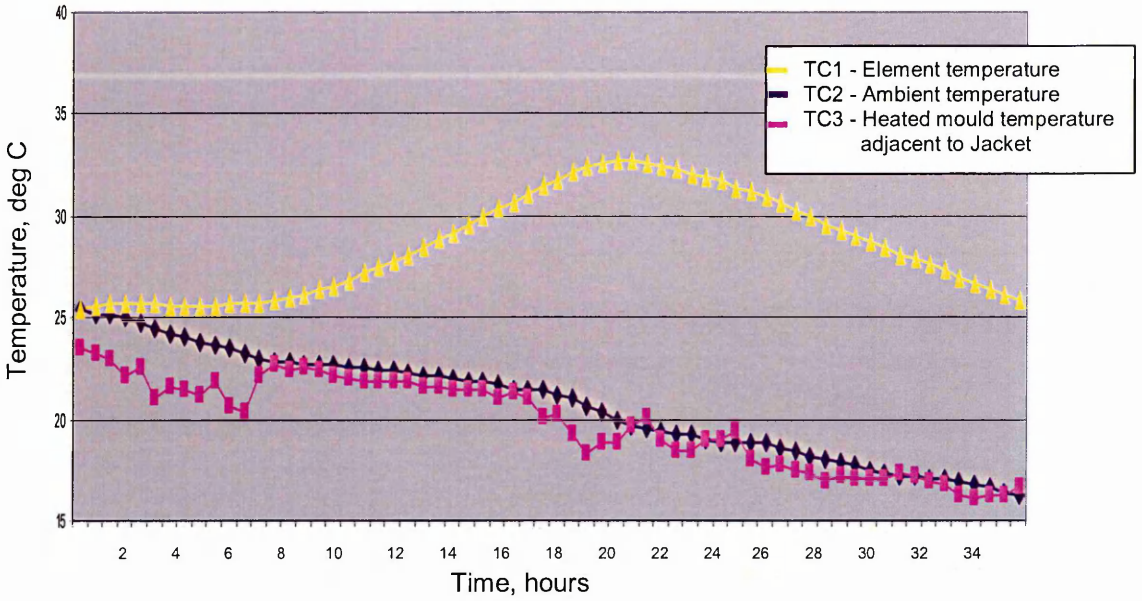

Figure 8.16. Terrace section cured at 24 Volts using the PRECAST 6500 Jacket on the mould (24 Volts)

Figure 8.16 shows that although the system was powered and operating, there was little heat being transferred to the concrete element; there is a gradual increase in the temperature reaching about 33 deg C which is considered to be mainly due to the heat of hydration of the concrete rather than due to the influence of the PRECAST 6500 Jacket. This is further confirmed by inspection of the graph for the temperature on the side of the mould adjacent to the Jacket which did not increase and tracked the ambient air temperature. There were two possible reasons for this, either the Jacket was not operating correctly or the transfer of heat to the side of the mould was being hindered. Operation failure of the system was ruled out as inspection of the control unit confirmed that current was passing to the system. It was concluded that the failure of the system to heat the element was due to a poor thermal contact between the PRECAST 6500 Jacket and the side of the mould.

To confirm if the poor transfer of heat to the concrete was due to poor thermal contact between the system and the mould, the Jackets were removed, tested electronically and their width reduced (width of foam, not the width of the element, *l*). This ensured that the jackets were not folding when in position resulting in a void between them and the mould. After re-positioning the Jackets, wedges and boards were inserted to push the jacket tight up against the mould. The results from this test are given in Figure 8.17. In addition a fourth thermocouple was used to monitor the side of an unheated mould cured naturally with no heating (TC4).

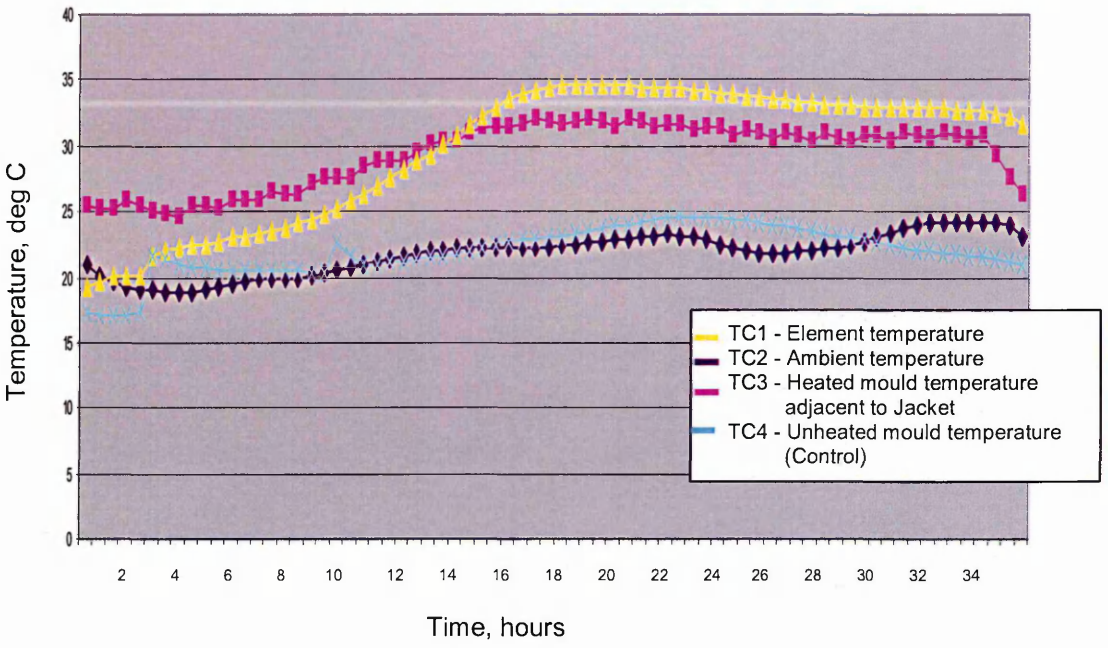

Figure 8.17. Terrace section cured at 24 Volts using the PREACST 6500 Jacket (24 Volts, modified)

Figure 8.17 shows the results following the operation of the PRECAST 6500 system after modifications to its design to ensure a better thermal contact with the mould. The key difference between Figures 8.16 and 8.17 is the plot for Thermocouple TC 1 - Yellow. The maximum temperature within the mould, in Figure 8.17, reached approximately 35 deg C, relative to the ambient temperature of 20 – 25 deg C. However unlike the trial with the poor thermal contact (Figure 8.16), the temperature was maintained without significant decrease for the remainder of the curing period. The graph also shows that the thermocouple on the side of the mould tracked the temperature within the concrete. Although there was an improvement in performance, it was not at the desired or permissible rates as described in the literature review. To overcome this, it was decided that the operating voltage of the PRECAST 6500 system should be increased from 24 Volts to 36 Volts. This effectively double the heat output from the system (Power = V^2/R) knowing that the resistance of the system remained constant. Again a fourth thermocouple was used to monitor the side of an unheated mould cured naturally with no heating (TC4).

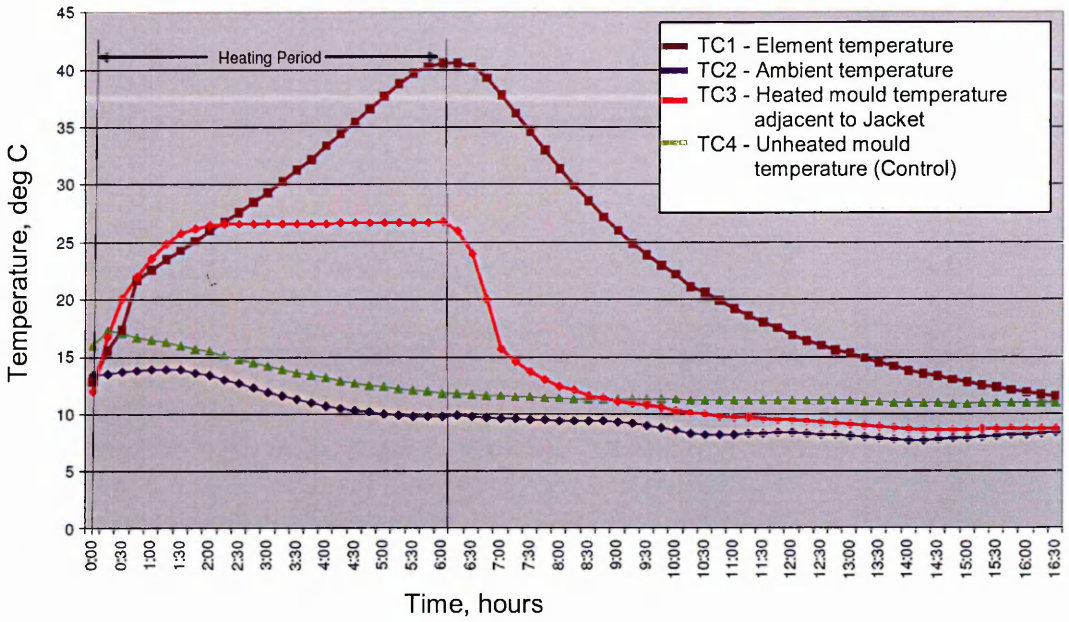

Figure 8.18. Comparison of naturally cured terrace sections cured using INSITU 6500 Jacket (36 Volts)

Figure 8.18 shows the heating profile of the concrete element cast within the similar concrete mould in the same mould as the initial tests with the PREACST 6500 Jacket operated a 36 Volts. It shows a clear increase in the temperature of the concrete being cured (TC1). It shows that during the first few hours that the temperature of the concrete (TC1) tracked the temperature of the heated mould side (TC3), with only a slight time lag. After three hours it can be seen that the heat input from the CPT through the mould (TC3) remained constant, whilst the temperature of the concrete continued to increase significantly and peaked at 41 deg C at 6 hours. For this tests the heating period was removed after 6 hours, after which the Heated / CPT (TC3) cooled rapidly down to ambient (approximately 3 hours). Comparing the mould side temperatures of the heated mould (TC3) and the unheated mould (TC4) it can be seen that there is a very significant influence on the mould temperature by the LAB 6500 Jacket operated at 36 Volts, compared to when operated at 24 Volts. The element was removed from the mould after 16 hours as by this time the strength had been achieved as the mould was required again for production.

Comparing the results of the terrace section cured using the LAB 6500 Jacket operated at 24 Volts with it operated at 36 Volts it can be seem that the 36 Volt test had a far greater influence on the temperature of the concrete being cured. Where for mould operated at 24 Volts (both initial and second test) the concrete temperature peaked at 35 deg C after 18 hours whereas the 36 Volt test peaked at 41 deg C after 6 hours.

The findings from the trial undertaken with Tarmac were considered when developing systems for curing precast, prestressed T-beams used in floor construction at C R Longley's.

For this application the blankets were designed and manufactured to have a direct contact with the concrete being cured. The CPT system for Longley's comprised of six 60m lengths of blankets 1.5m wide used to cure T-beams of concrete at a maximum of 40 deg C, allowing de-moulding to be undertaken within 16hours. The use of the blankets allowed the company to use of self-compacting concrete with reduced cement content from 400kg/m^3 to 350kg/m^3 by replacing with fly-ash conforming to EN450 part 1. Details of the system can be seen in Figure 8.19.

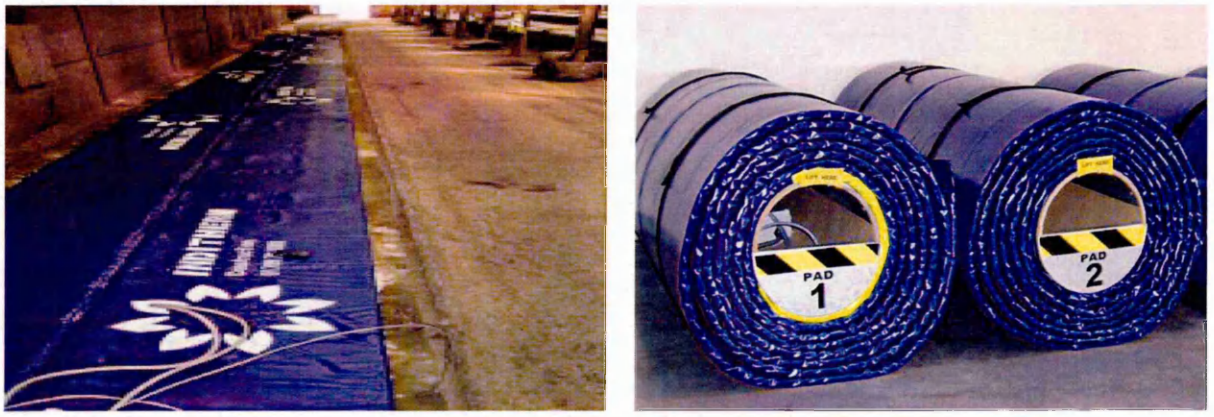

Figure 8.19. T-beam curing blankets used at CR Longley's

8.8. Discussion of Results

The CPT liners INSITU 1500 were used to provide protection to the concrete against freezing at early ages, and potentially accelerate the hydration reaction to reduce construction times and enable construction throughout the year (including winter). For such an application it was essential that the CPT could be used very easily and quickly. Therefore, the INSITU 1500 Liner was designed to be a consumable product which is particularly flexible to follow the contours of the excavation and not allow a weakness at the interface affecting the ultimate performance of the foundation.

At early ages, 1-24 hours, following the casting of the foundations, an increase in temperature throughout both foundations A and B was recorded. Figure 8.14 shows that the temperature within Foundation A continues to increase up to 48 hours after casting, whereas Figure 8.15 shows that the temperature increase within the unlined foundation, B, peaks between 20 – 28 hours. At 24 hours the average temperature throughout Foundation A was 35 deg C (neglecting temperature profiles recorded at T1, T2 and T3). In the control Foundation B, the average temperature throughout was 15 deg C. The increase in temperature within Foundation B is due to heat generated by hydration (hydration of C_3S) of the cement and the thermal mass of the foundation which results in a fairly constant temperature of the concrete while the ambient temperature significantly fluctuates.

Figure 8.15 shows that the gradient of the heating curves of Foundation B increases as the rate of the hydration reaction of the cement increases to peak at 18 hours. In comparison, Foundation A (Figure 8.14), heated by the CPT liner, maintains a steady rate of heating throughout the 24 hours after casting and shows no sharp peak caused by maximum heat of hydration. This is due to a positive combination of the hydration heat and the CPT input heat generating a uniform temperature rise throughout the foundation. This gentle heating protects the concrete at early ages up to 24 hours when it is most vulnerable to damage from freezing. It also prevents any deleterious impact on the long term strength of the concrete by minimising temperature gradients setting up in the mass concrete foundation and also by avoiding thermal shock which occurs with sudden exposure to high temperature curing such as steam curing.

The profiles for both foundations show a fluctuation in the ambient temperature of between -2 and 10 deg C. However, Figures 8.12 8.13 show no parallel fluctuation of temperature within the mass of the foundations. At the surface, however, the temperature of Foundation A increased steadily to 50 deg C (Figure 8.12) whereas the surface temperature of Foundation B resembled the ambient temperature. Colder ambient conditions in winter would result in the temperature profile of Foundation B being further reduced.

For the precast concrete trial, the impact of the CPT liner was not as great as expected, however, modification to the system and the increased operating voltage of the system did improve performance. Table 8.4 gives details of the average curing temperature from figures 8.14 - 8.18 for the trials, the corresponding ambient temperatures and the temperature differences between the heated and unheated elements for the precast trial (Tarmac) and the foundation trial.

	Ambient (°C)	Average Curing Temp					
		0 - 24 Hours			Beyond 24 hours		
		Ave. T (°C)	Diff. in curing temp (°C)	Temp. above ambient (°C)	Ave. T (°C)	Diff. in curing temp (°C)	Temp. above ambient (°C)
Foundation A	5	25	13	20	45	30	40
Foundation B		12		7	15		10
Precast 24	20	30	8	10			
Precast 36		22		2			

Table 8.4. Element curing temperatures

Table 8.4 shows the difference in the average curing temperature of the heated and the control foundation was 13 deg C (see Figure 8.15). The difference between the average temperature throughout the unheated foundation (Foundation B) and the ambient was 7 deg

C. The corresponding value for Foundation A was 20 deg C. Beyond 24 hours this was 10 deg C for the unheated foundation and 40 deg C for the heated foundation (Foundation A). For the precast elements, the first 24 hours is critical due to the requirement to free the mould for the next cast. The difference between the average temperature throughout the unheated precast element (Precast 36) and the ambient was 2 deg C; for the heated precast element, it was 10 deg C. The difference in the curing temperature between the two was 8 deg C. This data will be used to determine the periods for protection after casting as recommended by BS8110 and the minimum striking periods discussed in Chapter 2 using Table 2.10 and 2.11. The concept of maturity and volume / surface ratio will be discussed in Chapter 10.

8.8.1. *Protection Period*

The ACI standard for cold weather, ACI 306 – R recommends a period of protection to a concrete element. It recommends permitted exposure temperature of concrete, advice on temperature records and the duration of protection. It recommends insulative covers, such as plastic sheeting with Hessian which was used for the un-heated foundation. It also recommends foam which was used for the INSITU 1500 Jackets. Primarily, the period of protection is to maintain the concrete above its 'critical saturation point,' above this point, the concrete will have developed compressive strengths above 3.5 N/mm^2 (CSA Standard A23.1 and ACI 306 (1997 Cold weather concreting) to withstand the risk of frost attack.

The results of the two foundations have shown that the temperature within the foundation lined with the CPT is, at all ages, above 10 deg C throughout the concrete. 10 deg C is the minimum air temperature that concrete should be cast in, and that of all surfaces the concrete will have contact with, as recommended by the British Rail Specification EHQ/SP/0/105. After casting the temperature within the CPT lined foundation continues to increase. At a minimum temperature of 10 deg C the minimum strength of 3.5 N/mm^2 as recommended by ACI 306 will be achieved with ease (Section 2.15) within 24 hours. The top surface liner also protects the foundations from exposure to solar radiation and wind, whose affect is greatly increased at low ambient temperatures.

Table 8.5 uses equations extracted from Table 2.11 from BS8110 used to estimate the minimum protection period for concrete elements. The protection period is the period after casting for which the element should be protected from cold weather and exposure (not just temperature but also wind and solar exposure). For the foundation element was cast using OPC PC 42.5. it was cast in ambient conditions after casting assumed to be poor - from table 2.11. The protection period is calculated using the equation given in Table 2.11, given in table 8.5 for any temperature between 10 deg C and 25 deg C. The same criteria applied to the Precast concrete elements. For the Foundation only the average temperature throughout the foundations within the first 24 hours will be used (This is the same as the CPT surface

temperature). For the unheated elements for both the precast and the foundation the temperature is assumed to be ambient. This has only been conducted for the foundation as within a precast plant, elements are typically removed from their moulds with 18 hours.

		Days protection after casting			
		0 - 24 Hours		Beyond 24 hours	
		Ave. curing temp. (°C)	Protection (days)	Ave. curing temp. (°C)	Protection (days)
Foundation A	$\frac{80}{t+10}$	25	2.28 Days	45	1.45 Days
Foundation B		5	5.33 Days	5	3.2 Days

Table 8.5. Protection period (BS8110) required to prevent frost attack

For the foundation, the protection period is reduced from 5.33 days to 2.28 days assuming the temperature surrounding the heated foundation remains at 22 deg C compared to 5 deg C the ambient temperature. The standard recommends a protection period of between 4 and 6 days. Using the CPT Jackets, this can be reduced by up 3.5 days.

8.8.2. *Period before striking*

Table 8.6 is extracted from Table 2.11, BS8110 used to estimate the minimum period for striking formwork which can be achieved when using a thermal curing method, such as CPT. It is assumed that the most vulnerable zone, from the BS8110 table and corresponding to the equation in 8.6 is the surface zone which records the lowest temperature.

		Protection before striking (hrs)	
		Temperature	Hours
Foundation A	$\frac{300}{t+10}$ h	25	8.57
Foundation B		5	20
Precast A	$\frac{100}{t+10}$ days	30 (Ave)	2.5
Precast B		20	10

Table 8.6. Period before striking of formwork is permitted (BS8110)

For the two trials, Insitu and Precast, a comparison between the CPT cured and the non CPT cured elements can be made. For the foundation, increasing the curing temperature results in formwork striking period to be reduced by over 11 hours, and for the elements a striking period reduction of 7.7 hours

8.8.3. *Maturity Factor*

The results of these tests show the potential for the application of Maturity method as discussed in section 2.17. The maturity of the foundations could be established from the temperature – time history of the foundation by using maturity in terms of deg C – hours. This will be discussed in the discussion Chapter 10, comparing test data from all tests

8.9. Conclusions

- CPT thermal liners can be used to elevate the curing temperature of concrete foundations during cold weather construction.
- The CPT liners eliminate the risk of frost damage to the concrete, particularly within 24 hours after casting.
- The CPT liners can be used to heat cure the concrete uniformly throughout to a pre-selected optimum temperature.
- The CPT liner is required to extend to be extended to the entire depth of the foundation to provide uniform heat distribution.
- CPT thermal curing reduces the striking time of formwork. This allows rapid commissioning and loading of the foundations.
- The CPT liners provide a gentle gradient of heating to the mass concrete with no thermal shock.
- CPT can be used for precast concrete curing. However, if used to heat concrete through a mould, good contact is required.
- It is essential that a good contact between the CPT Jacket and outside face of the mould is to enable the transfer of heat for the CPT
- CPT within Jackets does not convect or radiate heat to the concrete through the mould
- CPT heats full size concrete elements better when the CPT jackets are in direct contact with concrete

Chapter 9. Durability of CPT and Cover Materials

9.1. Introduction

Environments where concrete practices are undertaken are extremely harsh. The use of heavy machinery, formwork bolts, reinforcement and power tools, coupled with the need to undertake work within short time periods presents risks in terms of damage or penetration to elements of CPT. Construction sites are also exposed with little shelter resulting in the likelihood that CPT systems may be exposed to extremely wet or freezing conditions. In addition, there is the potential for exposure to chemicals such as mould oils and high pH materials including concrete.

For all the above reasons the durability of CPT materials used to manufacture CPT jackets has been investigated within this chapter. Tests have been designed to represent the above scenarios. Tests include freeze thaw cycles, wetting & drying cycles and direct exposure to concrete. In addition tests simulating damage to the CPT materials through penetration and the formation of holes has also been undertaken. For all the tests, standard CPT samples with dimensions 212mm x 300mm were used. The effect of the exposure conditions was established by measuring the resistance of the CPT samples after exposure by bonding conductive rails to the samples and comparing the measured resistance to control samples maintained in control conditions of 20 deg C 60% RH. The durability tests were based upon BS EN 12226:2000 for the testing and conditioning of geotextiles.

9.2. Experimental Set-up and Procedure

For each test, samples were cut from the Red CPT (R_{ID} = 25.4 ohms). The sample dimensions were 212mm x 300mm. For the freeze / thaw, wet/dry and heating/cooling samples, conductive rails were bonded to the samples after exposure when completely dry and free from foreign matter. For the tests investigating the effect of penetration, the rails were bonded prior to holes being punched. The resistance of the samples, following the durability exposures, was measured at the three points, shown in Figure 9.1 and an average taken. This was then compared to the resistance of a control sample maintained at 20 deg C 60% RH. The samples were cut from three areas from the same roll of CPT. One sample was taken from each end of the roll and one from the middle. For each sample, resistance was measured at opposite locations along the conducting rails using the Fluke True-rms Clamp Meter (type 600 A AC/DC). The resistance was measured following a conditioning period of 24 hours after each test. The samples remained in the temperature and humidity controlled room (20 deg C 60% RH) during this period in accordance to BS EN 12226:2000, British Standards Institution, 2000, which applies to conditioning and testing of geotextiles.

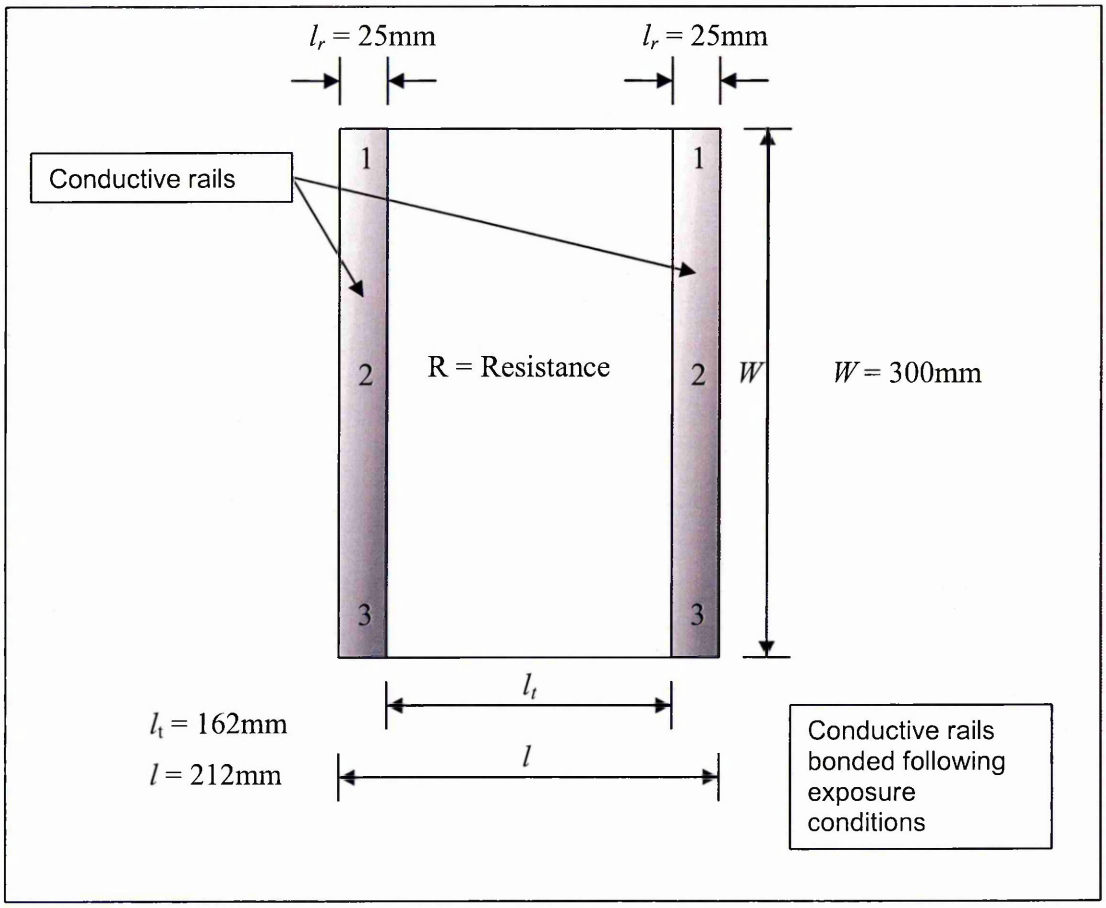

L	=	Element length (mm)
l_t	=	Distance between conductive rails (mm)
l_r		Width of conductive rails (mm)
L	=	Distance between outer edges of rails (mm)
W	=	Width of element (length of conductive rail) (mm)

Figure 9.1. Locations of resistance measuring points

9.2.1. *Freeze Thaw Cycles*

To determine the affect of freeze thaw cycles on the resistance of the CPT, newly cut 212mm x 300mm samples (Figure 9.1) were exposed to cyclic temperatures between - 10 and 115 deg C within the Sanyo Atmos Chamber Type MTH – 4400/4400 PR (details of which are given in Chapter 4). The specimens were soaked in plastic containers filled with distilled water at 20 deg C for a period of 24 hours before the start of the freezing-thawing process. Details of this can be seen in Figure 9.2.

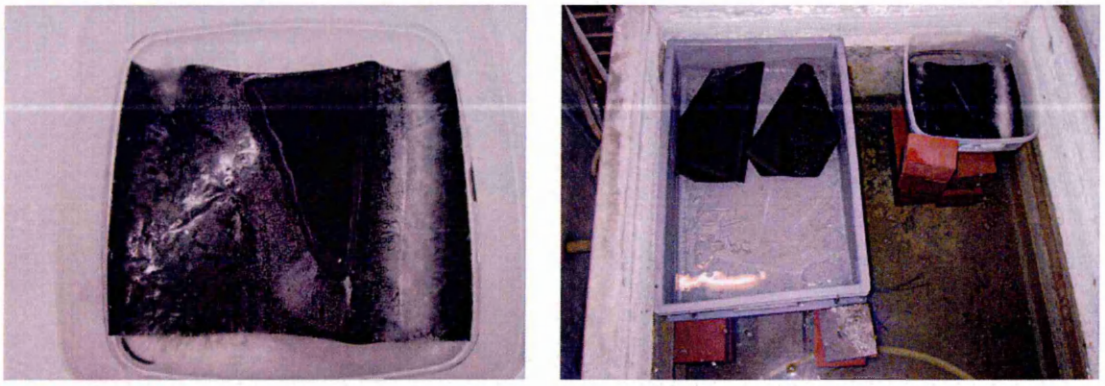

Figure 9.2. Samples during freeze / thaw durability testing

The containers were then placed in the freeze thaw chamber separated by 60 mm from each other and the side walls. The samples were subjected to 10 freeze-thaw cycles as follows, in accordance with EN 1367-1, 1999 (British Standards Institution, 1999):-

- The temperature was reduced from 30 deg C to 0 deg C in 180 minutes
- It was held at 0 deg C for 220 minutes
- The temperature was reduced from 0 deg C to -10 deg C in 210 minutes
- It was held at -10 deg C for 600 minutes
- After each freeze cycle the containers were immersed in a tank filled with water that had a constant temperature of 20 ± 2 deg C (Figure 10.2)
- After a period of 24 hours in the water tank the test was repeated for 10 cycles

After 10 cycles and the 24 hour conditioning period, conductive rails were applied and the average resistance measured.

9.2.2. *Wetting and Drying*

New CPT samples 212mm x 300mm, as described in Figure 9.1 were prepared and subjected to a 10 day wet and dry cycle test. This test was undertaken in the temperature and humidity controlled room at conditions of 20 deg C +/- 1 deg C and a RH of 60 %. The weight of the samples prior to the initial saturation was taken. The CPT samples were then subjected to a period of soaking in water for 24 hours in a plastic container filled with distilled water. The samples were then hung to dry in the environment control room (20 deg C 60% RH) for a period of 24 hours. The weight of the sample following drying was compared to the initial weight of the sample. This was done to check that the samples were fully dried. This process was repeated for 10 wetting and 10 drying cycles. Following 10 cycles conductive rails were applied and the resistance measured after a 24 hour conditioning period.

9.2.3. *Heating and Cooling*

Newly prepared 212mm x 300mm specimens were soaked in plastic containers filled with distilled water as described in section 10.2, at 20 deg C for 24 hours. The containers were placed in the chamber separated by 60 mm from each other and the side walls. The samples were subjected to 10 heating-cooling cycles as follows:

- The temperature was kept at 20 deg C for 30 minutes
- It was increased to 30 deg C in 30 minutes and kept at 30 deg C for 90 minutes
- It was increased to 40 deg C in 30 minutes and kept at 40 deg C for 90 minutes
- It was increased to 50 deg C in 30 minutes and kept at 50 deg C for 90 minutes
- It was increased to 60 deg C in 30 minutes and kept at 60 deg C for 90 minutes
- It was increased to 70 deg C in 30 minutes and kept at 70 deg C for 90 minutes
- It was increased to 80 deg C in 30 minutes and kept at 80 deg C for 90 minutes
- It was increased to 90 deg C in 30 minutes and kept at 90 deg C for 180 minutes

The above heating cycle is displayed on Figure 9.3.

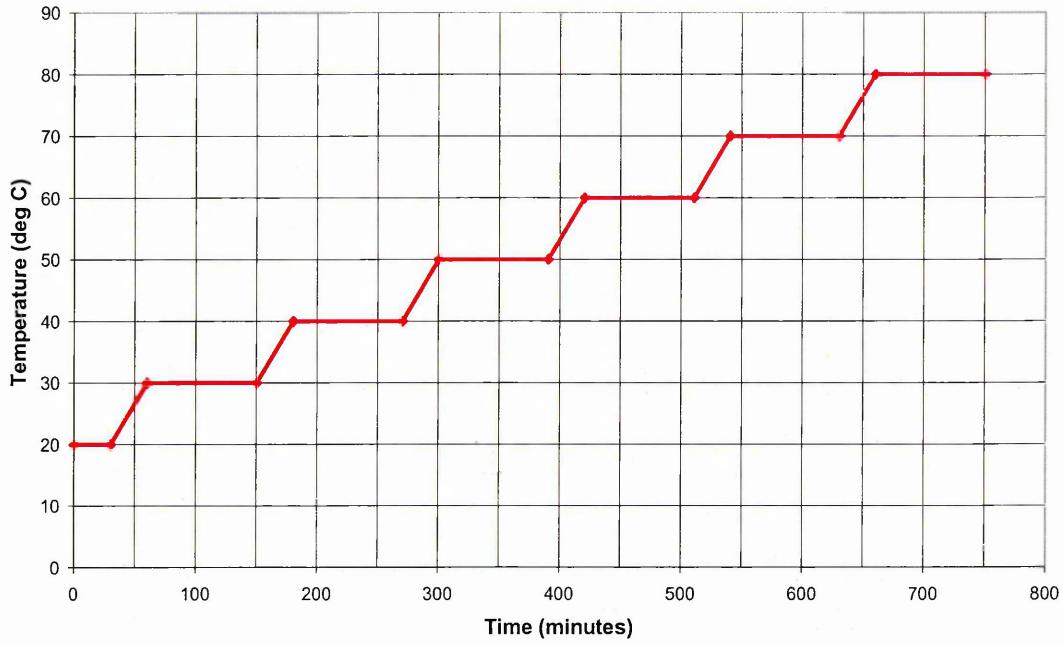

Figure 9.3. Heating and cooling cycle

After the completion of the heating cycle, the water-filled containers were immersed in a tank filled with water (without coming into contact with the water in the tank) at a constant temperature of 20 ± 2 deg C for 24 hours. Following 10 cycles and a 24 hour drying / conditioning period, conductive rails were applied and the resistance measured.

9.2.4. *Exposure to Cement Alkalinity*

Tests were carried out to determine the effect of direct contact with cement paste of CPT samples, 212mm x 300mm. Three standard samples as described in Figure 9.1 were cut and cast in a specially manufactured moulds of dimensions 212mm x 300mm x 50mm as shown in Figure 9.5. These were designed to exactly fit the sample of CPT 212mm x 300mm. Mix A concrete, as described in Chapter 4, with a 28 day strength of 50 - 60 N/mm^2 and a cement content of $400kg/m^3$ and w/c ratio of 0.45 was then cast into the moulds with the CPT elements cotton backing side down. Concrete was placed directly onto the CPT heating surface. Figure 9.5 shows the CPT positioned within the mould prior to and following casting.

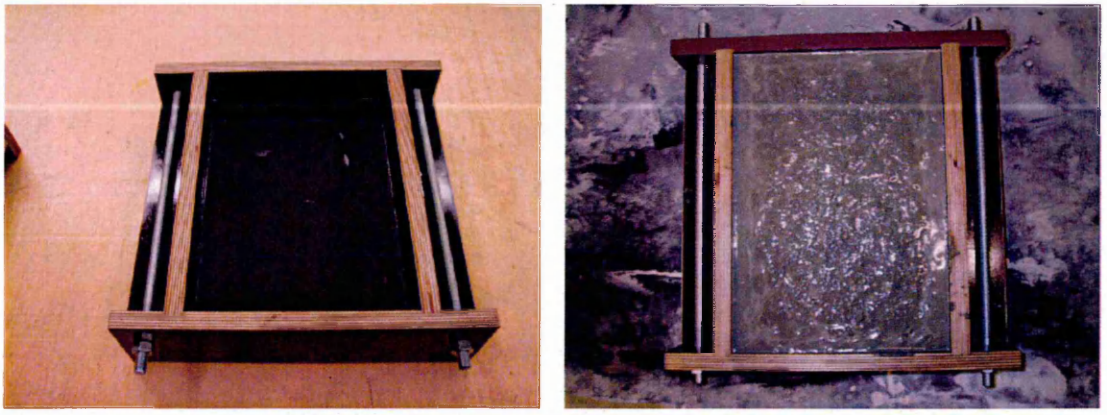

Figure 9.4. Concrete mould containing CPT sample, before and after casting

After placing concrete on the CPT sample, the moulds were left to cure in the controlled conditions of 20 deg C, 60% RH within the control environment room for 7 days, after which the concrete elements were removed from the moulds and CPT samples removed from the underside of concrete blocks.

In addition 70mm x 70mm samples of PVC, Aluminium coated Glass Cloth, Silicon Coated Glass Cloth and Glass Cloth Weave were cast within 100mm x 100mm x 100mm concrete cubes for one month to determine what impact fresh concrete had on the materials used to manufactured the outer layers of the CPT Jackets. A 70mm x 70mm of CPT with a rail bonded on was also cast to determine what affect the cement paste had on the bonded conductive rail.

9.2.5. *The Effect of Holes in CPT Elements*

Six samples of dimensions 212mm x 300mm were configured as described in Figure 9.1. Conductive strips of 25 mm wide were attached along the edges. Three samples were punched with 5mm diameter holes. Three sets of 5mm holes were located perpendicular to the conductive rails at the middle and each edge of the element, 10mm from the edge as shown in Figure 9.5. The first sample had one hole punched between the three points on the rails, the second 3, and the third 5, all equally spaced. Figure 9.5 shows the axis along which the holes were punched for the 5 hole sample and the testing points on the element.

A fourth sample was punched with two larger 25mm holes between the three locations, a fifth with 2 larger 35mm holes

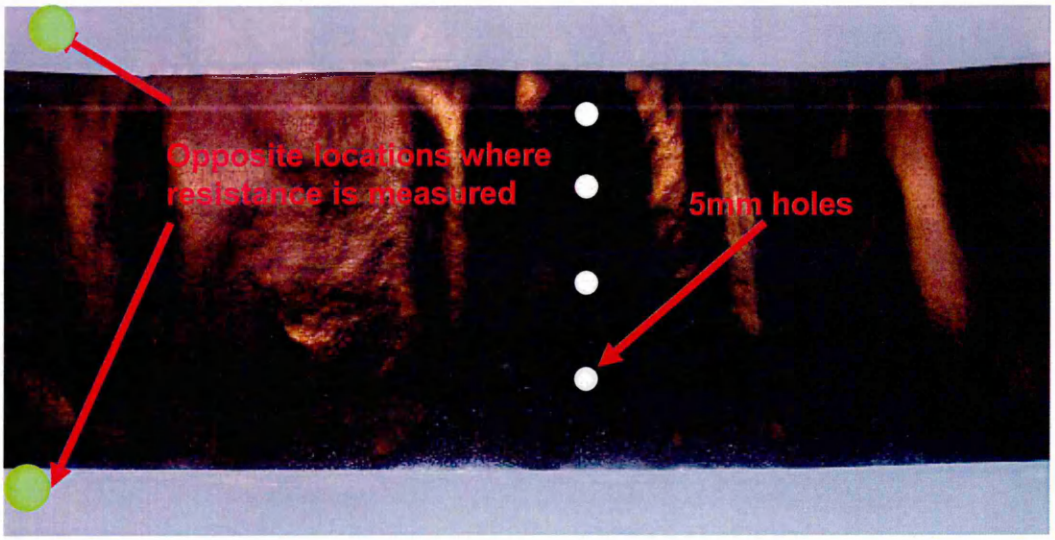

Figure 9.5. Location of holes and resistance testing points

Table 10.1 summarises the location, diameter and number of holes located in each sample.

Sample	Number of holes			Dia, of holes (mm)	Spacing of holes (mm)	Area removed (mm^2)
	Edges	Centre	Total			
1	1	1	3	3mm	-	58.89
2	3	3	9	3mm	50mm	176.68
3	5	5	15	3mm	30mm	294.47
4	2	2	6	25mm	50mm	235.47
5	2	2	6	35mm	50mm	329.70
6 Control	0	0	0	-	-	-

Table 9.1. Summary of holes and locations

After making the holes in the samples, they were maintained in the control conditions of 20 deg C at 60% RH for 24 prior to the resistance of the samples being measured.

9.2.6. *The Effect of constant and cyclic operation*

Two samples of dimensions 212mm x 300mm were configured as described in Figure 9.1. Conductive strips of 25 mm wide were attached along the edges. The samples were been connected to a 48 V power supply and have been left to run for 24 h a day one providing constant power, the other providing cyclic power. The first CPT sample was electrically connected via the conductive rails to a constant 48 Volt ac supply (constant) and the other was connected to a intermittent 48 Volt supply switching on and off every 6 hours.

The temperature of each CPT samples was recorded at the same time everyday 1pm, just prior to the cyclic sample being isolates for a period of 6 hours, following 6 hours of operation. Both elements were maintained at a constant temperature within the environment controlled room and not moved throughout the duration of the test (10 months). The temperature of each was monitored daily using a K-Type thermocouple attached to the surface of each element throughout.

In addition to testing just the CPT materials described, a composite CPT heating element (1.8 m long and 380 mm wide) similar to the Jacket designed for the heating of the Large concrete block as described in Chapter 7 was monitored, It comprised of CPT material (R = 20 ohms), glass wool Rockwool insulation (ROCK) and a PVc outer cover. It was tested for its long term performance. The Jacket was connected to a 48 V supply and the heat produced by the material was measured at two points, 0.5 m from the edges of the blanket.

9.3. Results and discussion

9.3.1. *Durability of CPT*

The average resistance of each test sample, measured using the Fluke True-rms Clamp Meter (type 600 A AC/DC), is given in Table 9.2 below.

Durability test	Nominal Resistance (ohms)	% Change
Control	90.7	-
Freeze and thaw	99.0	9.1
Wet and dry	101.3	11.7
Heating and cooling	93.8	3.4
Concrete contact	99.1	9.3
Holes, 1 holes, 5mm dia.	93.1	2.6
Holes, 3 holes, 5mm dia.	94.2	3.9
Holes, 5 holes, 5mm dia.	94.1	3.7
Holes, 2 holes, 25mm dia.	97.1	7.0
Holes, 2 holes, 35mm dia.	98.3	9.4

Table 9.2. Average resistance of CPT samples after different durability test regimes

Table 9.2 lists the average resistance of each sample after durability testing, including the control samples which were kept in the laboratory control environment, 20 deg C, 60% RH throughout. Table 9.2 shows that the resistance of all samples exposed to the various

durability processes increased compared to the control samples. However, for most cases the increase in resistance was less than 10% and, therefore, acceptable.

Any resistance increase effectively reduces the power output of each sample – in terms of the equation for power output $P = V^2/R$. Effectively increasing the resistance of the materials reduces the power output of the sample, assuming operation at the same voltage. The durability test regime that had the greatest effect on the resistance of the standard samples was the wet and dry regime. Excluding the punching of holes into the samples, the regime that had the minimal affect on the resistance of the sample was the heating and cooling regime. This indicates that the CPT material is stable during heating and cooling and, therefore, the long term operation of CPT materials with repeated heating and cooling the will have no detrimental affect to its performance.

Considering the resistances of the samples punched with holes, the greatest increases came when the larger holes, with the greatest areas removed. However, for the 5mm diameter holes, the difference in resistance recoded when 1, 3 and 5 holes were removed was very small. A possible explanation of this is that at the location of the holes perpendicular to the to the conductive rails, the number of holes is not important, it is effectively the width reduction (δ) that causes a change in resistance. For each case 1, 3 or 5 respectively 5mm diameter holes, this is 5mm as shown in Figure 9.6 This is demonstrated in Figure 9.6 below. The width reduction δ/W for the 5mm diameter holes is 5/300 x 100% which is insignificant.

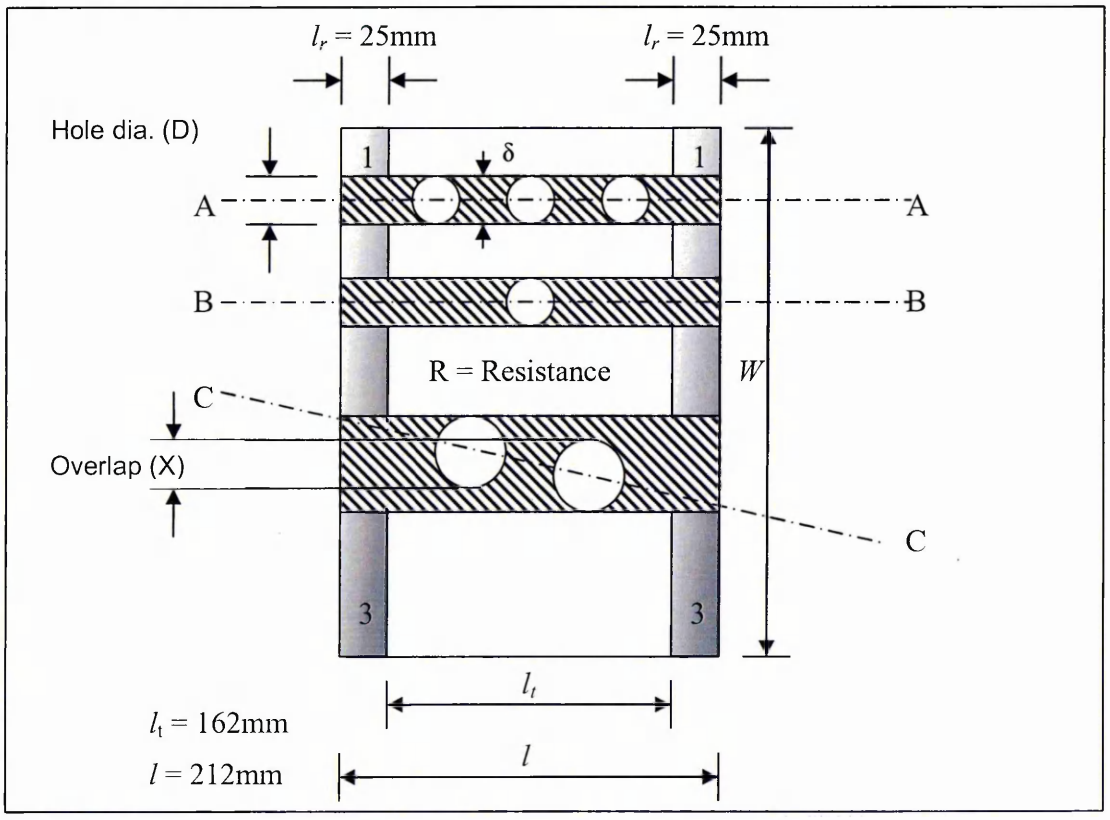

Figure 9.6. Effective CPT width

If 5mm holes were punctured in the CPT along axis A-A perpendicular to the conductive rails, the increase in resistance would be the same as if one hole was punched in the CPT (axis B-B). I.e the resistance increase will be proportional to the diameter of the holes. If holes are punched non-perpendicular to the conductive rail as shown along axis C-C, the effective loss of CPT has to be calculated geometrically. In general terms, the effective width of a CPT element with holes or section removed can be calculated using Eq. 10.1.

$$W_{Eff} = W - \left[\left(\sum D_1, D_2 D_3 ..... D_n\right) - X\right] \qquad \text{[Eq 10.1]}$$

Where;

W	=	Width of element (length of Conductive rail)(mm)
W_{Eff}	=	Effective Width (mm)
D_n	=	Diameter of hole (mm)
X		Overlap of adjacent holes (mm)

This hypothesis could have easily been verified by punching holes along different axis as shown in Figure 9.6.

This agrees with the prediction in theory of CPT (Chapter 3) which assumed that CPT can be likened to a number of parallel resistors connected by the two 'common' conductive rails (conductive silver tape) (Section 3.3). Therefore, heating (temperature performance) within the area where holes have not been removed will remain constant. However, the overall resistance of the element will increase due to the effective reduction in CPT surface area and conductive path, and hence power consumption for the element will reduce, as will the element heat flux (W/m^2)

9.3.2. *Durability of Cover Materials*

The results of all durability tests have all resulted in an increase of up to 11% of resistances compared to the control sample. The CPT should be protected in concrete manufacturing applications. The appropriateness of the various outer protecting materials will be discussed in the following section.

Figure 9.7 shows the various cover material samples which were cast within 100mm x 100mm x 100mm concrete cubes, cured in water for 28 days then crushed

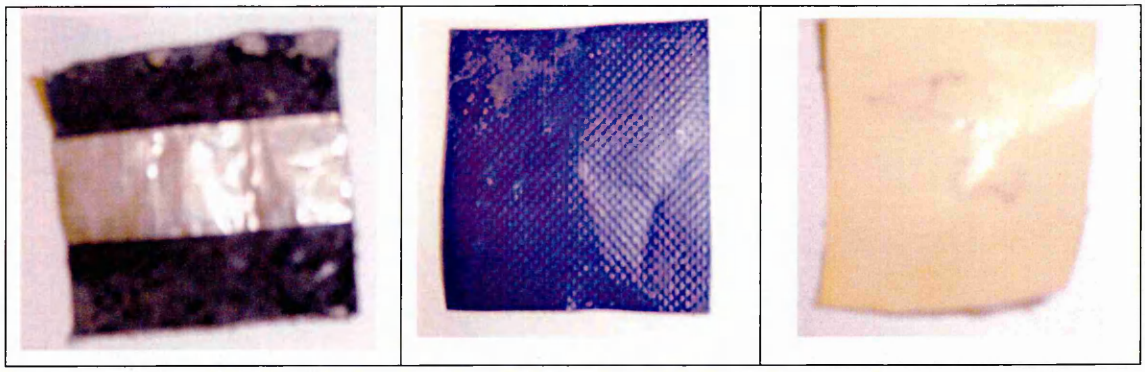

(a) CPT material (b) Blue PVC (c) Aluminium glass cloth

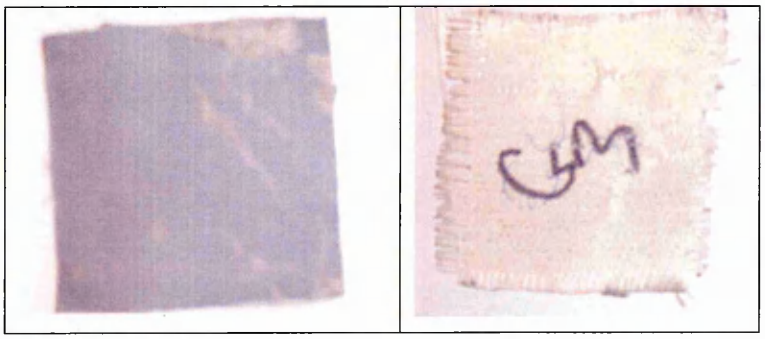

(d) Silicon coated glass cloth (e) Glass cloth weave

Figure 9.7. Visual inspection of CPT and outer materials

The following observations were identified when inspecting the materials.

- **CPT material** a good bond was formed with the concrete on the cotton side of the material. A limited bond between the concrete and the CPT material heating face was formed. The smooth lacquered finish of the CPT material, appeared to be pitted, possibly a reaction between the concrete and the silicon in the lacquer.
- **Blue PVC:** there was no visual effect on the PVC material.
- **Aluminium Coated Glass Cloth**: limited bond to the rear / underside of the Aluminium coated glass cloth. No evidence of the aluminium coating remained on the upper surface of the glass cloth.
- **Silicon Coated Glass Cloth**: little / no bond was formed on the rear glass cloth surface of the material. A limited bond was formed between the Silicon coating of the material and the concrete. An unusual smell not associated with or the material was present.

- **Glass Cloth Weave:** the glass cloth material appeared to not be effected by being cast within the concrete cube. There was no / little bond between the glass cloth and the concrete. A clear indentation of the materials weave was formed at the Interface of the concrete and the material.

Visual inspection of the materials has provided evidence that some of the materials used to manufacture CPT jackets are not to be used when direct contact with concrete is expected. These are the Aluminium coated glass cloth the silicon coated glass cloth and the glass cloth weave.

Although there is much literature advising of the incompatibility of both glass (silica) and aluminium with concrete, the above materials were tested as their contact with fresh concrete when used as part of a composite jacket is for a relatively short period of time (during curing only) compared to the life of a concrete element. The materials are also primarily designed to be in contact with the mould to heat the concrete rather than having direct contact, or cast within the concrete. As demonstrated through the results the impact of concrete (or calcium hydroxide) on aluminium is far greater than that on the glass based cloths. Concrete interaction with silica tends to relate to long term consequences such as alkali silica reaction, whereas aluminium (in powder form, Section 2.9) is used in as a foaming agent for foamed concrete and also for cellular blocks and is known to react far more freely and immediate with concrete. Direct contact with CPT and the rails was not recommended in the literature review (Section 2.11) due to the risk of electrolysis of the cement paste.

9.3.3. *CPT long-term Temperature performance under constant and cyclic operation*

Figure 9.8 gives the results of the long term temperature testing of the CPT element operated constantly over for a period of 10 months at 48 Volts AC.

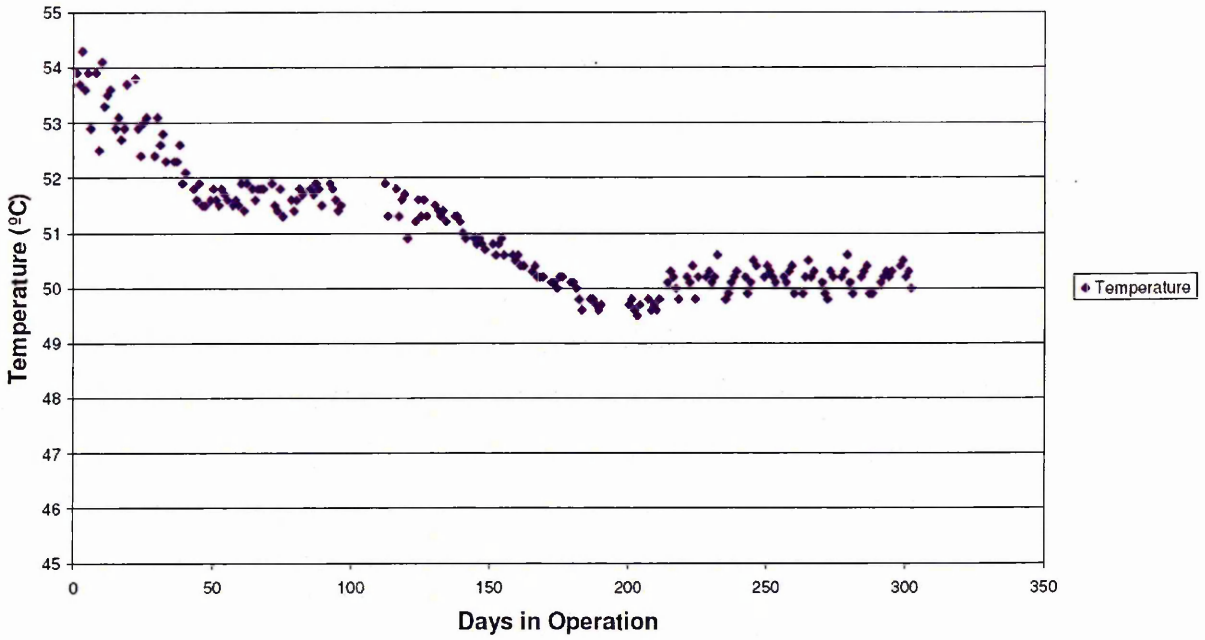

Figure 9.8. Temperature output under constant operation (48 Volts)

Figure 9.8 shows that the initial temperature on the surface of the CPT element constantly operated falls constantly in the first forty days. It then stabilises for a period and remains at between 51 and 52 ºC between 80 and 120 days. The temperature again drops to an average of just below 50 ºC between 120 days and 190 days, before then maintaining a constant temperature for the remaining duration of the test of between 50 and 51ºC

Figure 9.9 gives the results of the long term temperature testing of the CPT element operated cyclically over for a period of 10 months at 48 Volts AC.

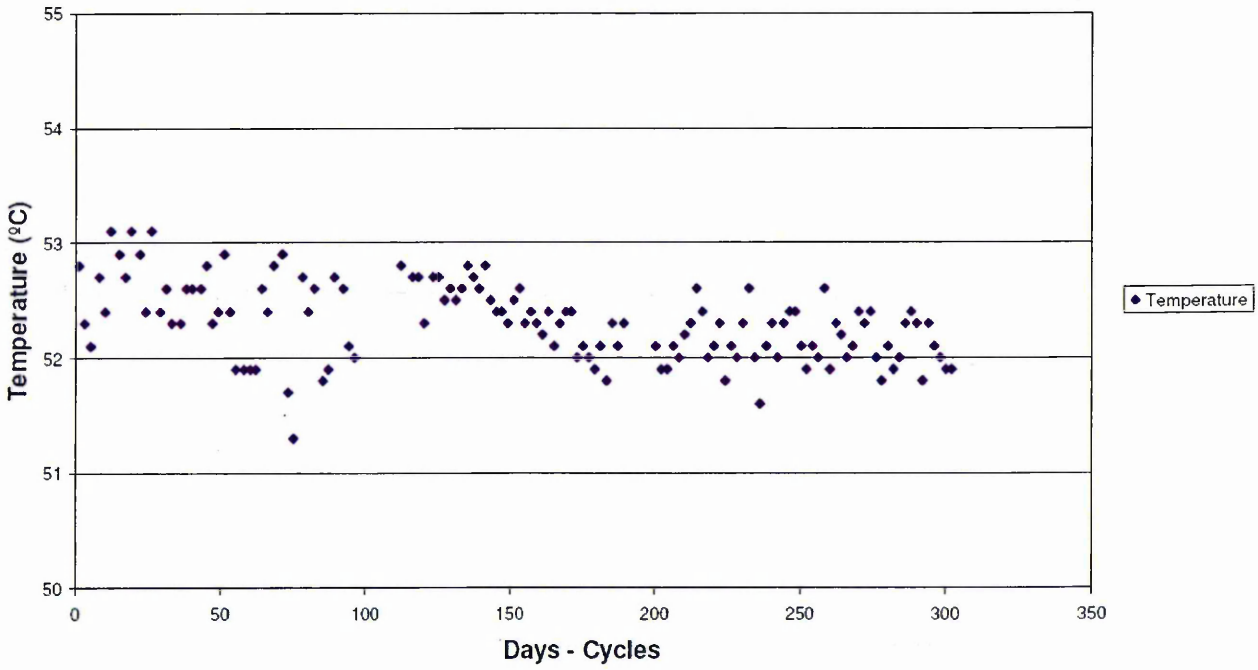

Figure 9.9. Temperature output under cyclic operation (48 Volts)

Unlike the element operated constantly there does not appear to be a fall in temperature performance over time. Over the 300 day period the temperature of the CPT is between 51 and 53 °C. The nominal resistance the two CPT samples is presented in table 6.

	Resistance, R (ohms)	
Months from start of the test	**Constant Operation**	**Cyclic Operation**
2	95.8	98.3
4	97.3	98.7
6	97.5	98.8
8	97.5	98.7
10	97.7	98.6

Table 9.3. The resistance of the CPT elements throughout constant and cyclic operation

Table 9.3 shows that there is an increase of the resistance of the element electrically operated constantly from 95.8 to 97.7 ohms. The resistance of the CPT element cyclically operated remains constant. These results correspond to the temperatures recorded and shown on Figures 9.8 and 9.9.

Figure 9.10 presents the average temperature (from the two recording points) recorded for a period of about 4 months. It shows that the composite element has performed consistently through this period (with almost all the reading between 64 and 65 °C) and the constant use has not affected its performance.

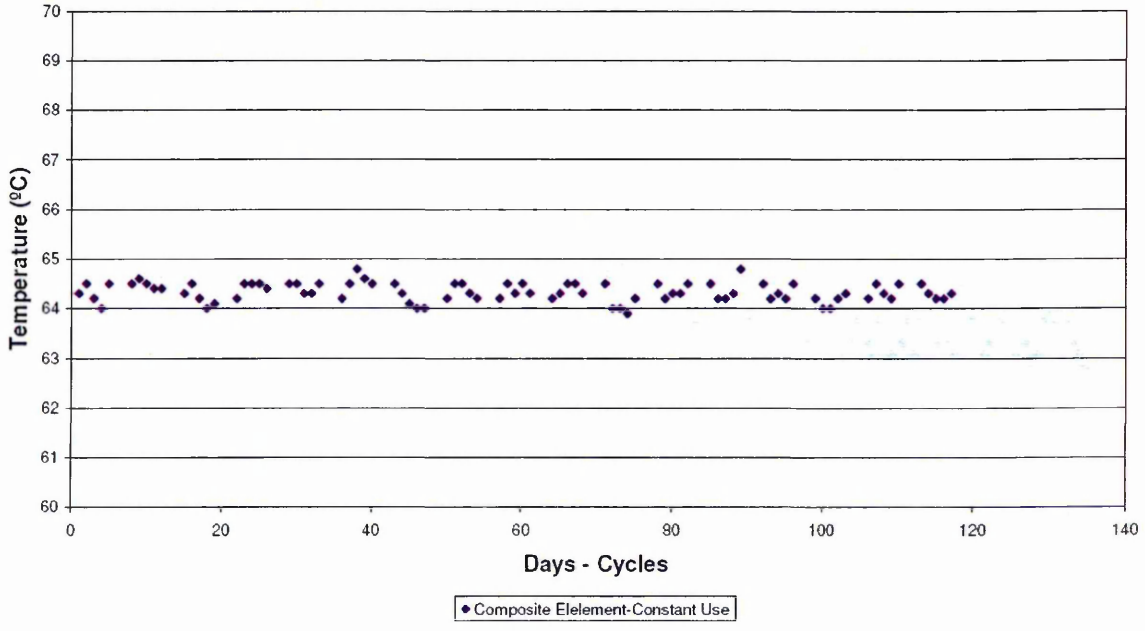

Figure 9.10. Temperature output of composite element under constant operation

The results indicate that the temperatures produced by the cycle operation remain more stable that the ones from the constant operation. Even though the initial temperatures are lower, after long duration of the tests they appear to be of one degree centigrade more than the constant operation temperatures since the large majority of the temperatures falls within the range of 52 to 53 °C In addition the composite CPT heating element (1.8 m long and 380 mm wide), also maintained a constant temperature over a period of 120 days.

9.4. Conclusions

- The resistance of CPT increases by up to 11% when exposed to different durability processes.
- The heating and drying durability cycle had the least affect on resistance change, indicating good long term stability of CPT.
- Direct concrete of CPT with cement paste should be avoided.
- Glass cloth based materials are not suitable for CPT Jackets which have direct contact with concrete.
- When holes are made within CPT, the resistance is reduced by up to 9.4%.
- CPT maintains a more uniform heating performance over time when operated cyclically rather than constantly.

Chapter 10. General Discussion and Analysis

10.1. Introduction

This Chapter analyses and discusses the results of the tests reported in Chapters 6-8 of this thesis. It considers what affect different geometric properties of concrete elements have on the performance of the CPT Jackets used to cure concrete. This chapter uses the concept of concrete maturity as previously discussed in Chapter 2. Maturity is used to determine what influence the Volume / Surface ratio has on the performance of CPT curing systems. The affect of CPT systems on the compressive strength of concrete, the interaction with heat of hydration and the relationship with cement content of various concrete is also considered. This chapter will discuss other state-of-the-art work undertaken to establish the performance of CPT Jackets for curing concrete in adiabatic conditions, with varying Volume / Surface ratio, and the properties of resulting concrete.

10.2. Performance of CPT Jackets

Two main properties of the Jackets will be considered, the total contact area of the Jacket, and the area of CPT elements within the Jackets. The power / heat output of each CPT Jacket will be considered by calculating heat flux (W/m^2). This is the power out-put per unit area. The heat flux will be considered and calculated using i) the surface area of the CPT elements within each Jacket (element heat flux) and ii) for the whole Jacket contact surface area with the concrete or the mould (Jacket flux).This is shown in Figure 10.1.

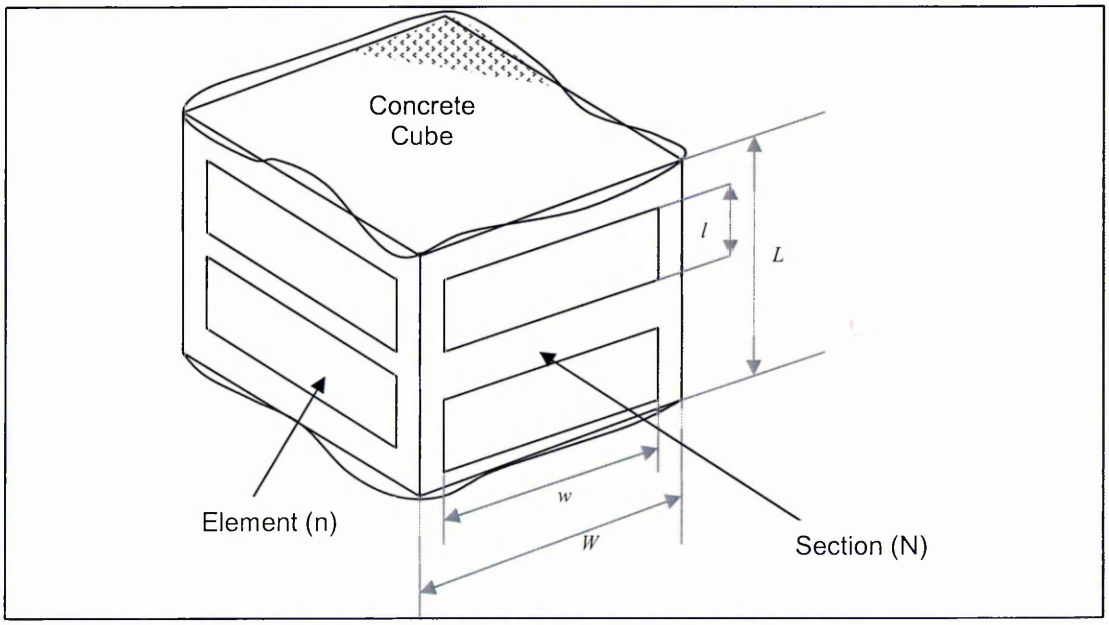

Figure 10.1. Element configuration, Jacket and Heat flux

Where;

$$\text{Jacket Heat Flux, } Q_{Jacket} = \lfloor P_{N(Max)} / (W \times L) \rfloor N \qquad \text{[Eq 10.1]}$$

$$\text{Element Heat Flux, } Q_{CPT} = \lfloor P_{N(Max)} / (n(w \times l)) \rfloor N \qquad \text{[Eq 10.2]}$$

Q_{Jacket}		Jacket Heat Flux (W/m^2)
Q_{CPT}		Element Heat Flux (W/m^2)
l	=	Element length (mm)
w	=	Element width (mm)
L	=	Jacket dimension (length) (mm)
W	=	Jacket dimension (Width) (mm)
$P_{N(Max)}$	=	Maximum power output per section (Watts)
n	=	Number of elements per section
N	=	Number of Jacket sections

10.2.1. *Heat Flux*

Table 10.1 gives the Jacket dimensions and the area each jacket covers for each mould / application used throughout the thesis, e.g. the PRECAST 6500 system was made up of 5 pairs of CPT Jackets which equals 10 No. Sections (N) (Chapter 4, Section 4.3.6). The total Jacket area, therefore equals the area of a single Jacket multiplied by 10 (the number of sections). The Concrete Heating Area is the concrete area in contact with the inside face of the mould or the area of concrete in contact with the Jacket when direct contact between the Jacket and the concrete occurs, I.e. for the INSITU 1500 application 4 sides (1.5 x 0.9) x 4 + 1 Lid (0.8 x 0.8), and for the Lab 400 mould this is 0.4m x 0.4 x 4 = $0.64m^2$ (See Chapter 4, Section 4.3.4 and 4.3.5).

Jacket ID	Total Jacket heating Area [m^2]		Concrete Heating Area [m^2]	
LAB 100	0.275 x 0.510 x 1	= 0.140	0.100 x 0.100 x 2	= 0.020
LAB 300	0.300 x 0.435 x 1	= 0.130	0.300 x 0.075 x 4	= 0.080
LAB 400	1.800 x 0.450 x 1	= 0.810	0.400 x 0.400 x 4	= 0.640
INSITU 1500*	(1.500 x 0.9 x 4) + (0.800 x 0.800 x 1)	= 6.040	(1.500 x 0.9 x 4) + (0.800 x 0.800 x 1)	= 6.040
PRECAST 6500	2.700 x 2.800 x 10	= 7.600	2.700 x 2.800 x 10	= 7.600

* The INSITU 1500 Jacked has a heated lid in addition to the heated sides

Table 10.1. Jacket heating area

Table 10.2 summarises the overall surface area of each of the Jackets used from Table 10.1. For each application the surface area of each Jacket will be calculated and then multiplied by the number of sections used to complete the system as described in Figure 10.1. All measurements for the Jacket dimension were taken when the Jackets were laid out flat on the laboratory bench rather than when they were on the mould / application they were to heat. This is important when considering the LAB 400 Jacket. Although the Jacket had to wrap round a mould of perimeter of 1600mm (4 x 400mm), the Jacket was manufactured 1800mm long to enable the Jacket to be fitted around corners and to compensate for the thickness and flexible nature of the Jacket.

Jacket ID	**LAB 100**	**LAB 300**	**LAB 400**	**INSITU 1500***	**PREACST 6500**
Jacket / section heating Area [m^2]	0.14	0.13	0.81	1.35 (0.64)	0.76
Number of Sections [N]	1	1	1	4 + 1	10 (2 x 5)
Total Jacket heating Area [m^2]	0.14	0.13	0.81	6.04	7.60
Concrete Heating Area [m^2]	0.02	0.08	0.64	6.04	7.60

Table 10.2. Jacket heating area summary

Table 10.3 shows the element heating area. This is the actual area of the CPT elements within each Jacket rather than the Jacket heating / contact area given in Table 10.1 and 10.2. Within each Jacket section there can be more than one CPT element (n). Therefore the CPT heating element area is calculated as (the area of each element) x (the number of elements) (n) within each section multiplied by the number of sections (N) for the application as described in Eq 10.2. Again the area of the mould heated by the blankets is given in Table 10.3.

Jacket ID	LAB 100	LAB 300	LAB 400	INSITU 1500	PRECAST 6500
CPT element dimension [mm]	110 x 335	406 x 300	1800 x 180	400 x 600	2500 x 250
No. of CPT elements within each section [n]	1	1	2	3 + 2	1
Number of Sections [N]	1	1	1	4 + 1	10 (2 x 5)
Total CPT element heating Area [m^2]	0.04	0.12	0.58	3.3	6.30
Concrete Heating Area [m^2]	0.02	0.08	0.64	6.04	7.60

Table 10.3. CPT element heating area

Table 10.4 compares the total heat out-put of each of the CPT systems; the property which defines the CPT - Characteristic Resistance, R_{ID}, and the operating Voltage of the Jacket system for each application. The power ($P_{N(Max)}$) for each Jacket is the power demand for each system when the jackets are initially powered. It is the value when all elements within each system are operating and are not being controlled by the mechanical or electrical thermostats. Essentially it is the maximum power out-put of each system. The power, $P_{N(Max)}$, for each system was recorded throughout the tests described in Chapters 6-8.

Jacket ID	LAB 100	LAB 300	LAB 400	INSITU 1500	PRECAST 6500 [24 V]	PRECAST 6500 [36V]
R_{ID} [Ohms]	25.4 (RED)	57.9 (GREY)	57.9 (GREY)	57.9 (GREY)	25.4 (RED)	25.4 (RED)
Power [$P_{N(Max)}$][Watts]	35 Watts	63 Watts	440 Watts	162 Watts	384 Watts	864
Operating Voltage [Volts]	24 Volts	24 Volts	24 Volts	50 Volts	24 Volts	36 Volts

Table 10.4. CPT Jacket Electrical Properties

Tables 10.5 and 10.6 give the Jacket Heat Flux (Q_{Jacket}) and Element Heat Flux (Q_{CPT}) for each CPT Jacket / system respectively. Heat flux (W/m^2) rather than temperature is used

since heat output is a combined function of temperature and time. The Heat flux is the power out-put of the Jacket (CPT system) divided by the Jacket heating contact area, as calculated in Table 10.2, Row 4.

Jacket ID	LAB 100	LAB 300	LAB 400	INSITU 1500	PRECAST 6500 [24V]	PRECAST 6500 [36V]
Power [Watts]	35 Watts	63 Watts	440 Watts	810 Watts	1920 Watts	4320 Watts
Total Jacket heating Area [m^2]	0.14	0.13	0.81	6.04	7.6	7.6
Jacket Heat Flux [Q_{Jacket}] [W/m^2]	250.00	484.00	543.21	134.11	252.63	568.42

Table 10.5. Jacket Heat Flux

Table 10.6 gives the element heat flux. This is the power out-put of each CPT system divided by the area of the CPT elements within the Jackets / system given in Table 10.3, Row 5.

Jacket ID	LAB 100	LAB 300	LAB 400	INSITU 1500	PRECAST 6500 [24V]	PRECAST 6500 [36V]
Power [Watts]	35 Watts	63 Watts	440 Watts	810 Watts	1,920 Watts	4320 Watts
Total Jacket heating Area [m^2]	0.04	0.12	0.58	3.36	6.3	6.3
Element Heat Flux [Q_{CPT}] [W/m^2]	875.00	525.00	758.62	241.07	304.76	685.7

Table 10.6. Element Heat Flux

Tables 10.5 and 10.6 show the heat flux for all the different element configurations used throughout testing. The heat out-put of these elements ranges from 250 W/m^2 for the INSITU 1500 Jacket to 543 W/m^2 for the LAB 400 Jacket when considering the heating area of the Jacket (Q_{JACKET}). When considering the element solely the area of the CPT elements (Table 10.6)(Q_{CPT}), the CPT heat flux ranges from 241 W/m^2 INSITU 1500 Jacket to 875 W/m^2 for the LAB 100 Jacket. The increase in element heat flux from 304.76 W/m^2 for the PRECAST 6500 (24 Volts) to 685.7 W/m^2 is more than double the heat flux for a voltage increase of 50%.

The difference between the Jacket heat flux and the CPT heat flux is directly proportional to the difference between the surface areas of the Jackets and the area of CPT within. For the LAB 300 Jacket, the difference between the two flux is small as the area of the CPT element within the LAB 300 Jacket was approximately the same as the final external dimensions of the Jacket – the Jacket contact area. This was not the case for the INSITU 1500 Jacket, where multiple independent CPT elements within each Jacket section were used, with a relatively large spacing between the elements within the Jacket, or the LAB 100 Jacket where Q_{JACKET} = 250 W/m^2 to Q_{CPT} = 875 W/m^2, again due to the design of the Jacket (Section 4.3.1)

10.2.2. *Volume of Concrete*

A key factor of the performance of the CPT Jackets is the volume of concrete the Jackets are required to heat. For each application, chapters 6-8, the volume of concrete was different. Table 10.7 shows the volume of concrete heated in each application.

Jacket ID	**Volume of Concrete (m^3)**	
LAB 100 CUBE	0.1 x 0.1 x 0.1	0.001
LAB 300 PRISM	0.075 x 0.075 x 0.3	0.00168
LAB 400 CUBE	0.4 x 0.4 x 0.4	0.064
INSITU 1500 BLOCK	2.0 x 0.9 x 0.9	1.62
PRECAST 6500 TERRACE	(0.15 x 0.5 x 6.5) x 2	0.975

Table 10.7. Volume of concrete

Table 10.8 gives the equivalent heat input per 1m^3 of concrete for each application. This has been calculated by dividing the maximum power out put for each Jacket $P_{(NMax)}$ by the volume of concrete.

Jacket ID	**LAB 100**	**LAB 300**	**LAB 400**	**INSITU 1500**	**PREACST 6500 [24V]**	**PREACST 6500 [36V]**
Power $P_{(NMax)}$ [Watts]	35 Watts	63 Watts	440 Watts	810 Watts	1,920 Watts	4320 Watts
Volume of Concrete [m^3]	0.001	0.00168	0.064	1.62	0.975	0.975
Power in-put per m3 of Concrete [W/m^3]	35,000 W/m^3	37,500 W/m^3	6,875 W/m^3	500 W/m^3	1,969.23 W/m^3	4430.77 W/m^3

Table 10.8. CPT power in-put comparisons

Table 10.8 shows that the heat input of the LAB 100 and LAB 300 Jacket is significantly higher than the heat input per m^3 for the other three Jackets. However, this simple scaling up of the power out-puts from each Jacket per m^3 of concrete does not consider the different ways the Jackets were applied, the geometry of the elements being heated and internal heat generated by hydration of cement.

Table 10.8 shows that the INSITU 1500 Jacket provided the least input of heat per m^3 of concrete. However, when used to heat the foundation, in Chapter 8, the Jacket raised the temperature of the concrete by 30 deg C, when steady state was achieved. This is comparable to the other Jackets required to raise the temperature of the concrete in their respective applications from approximately 20 deg C to 50 – 70 deg C, an increase of temperatures of 30-40 deg C. The INSITU 1500 Jacket heated the concrete directly – the concrete was cast directly adjacent to the Jacket, whereas the LAB100 jacket (for example) heated the concrete indirectly through the cast iron mould. As a result the power input of LAB100 and INSITU1500 is 35,000 and 500 W/m^3 respectively. This clearly indicates that the way in which CPT is used and applied is as important as the power output of the CPT Jacket. Table 10.2 does not consider how the different Jackets were applied and the shape of the elements being heated nor the heat generated by the concrete due to hydration.

Figure 10.2 shows the relationship between the volume of concrete heated in each application and the power out-put from each jacket used to heat that volume of concrete in each of the 5 investigations conducted.

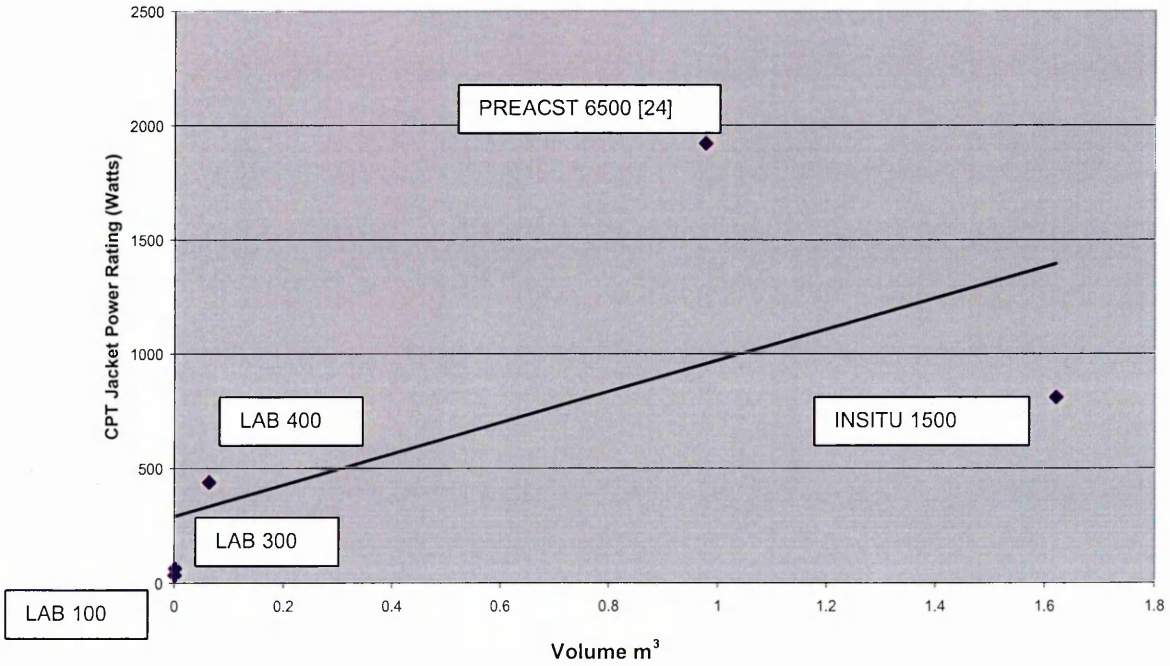

Figure 10.2. Graph of Power vs Volume of Concrete

Figure 10.2 does not show any correlation between the power input and volume of concrete being heated for each application. There are a number of reasons for this; some of the Jackets may have been underpowered for the application; the contact of the CPT Jackets may have been poor. Figure 10.2 assumes the maximum CPT Jacket power rating for each jacket rather than the average. This is an important consideration when considering Jackets that use electronic and mechanical thermostat controls (Chapter 4) that repeatedly isolate and power-up CPT Jackets to maintain average operating temperature.

Figure 10.2 indicates that per m^3 of concrete cured, the rating of CPT used to cure the PREACST 6500 application was far greater than that of the INSITU 1500 Jacket. However, from the performance and results of each Jacket, the INSITU 1500 Jacket out performed the PREACST 6500 (24 Volts) Jacket considerably, this is also shown in Table 10.9.

Figure 10.3 considers the Volume of concrete against Heat Flux (area over which heat is applied) for each application. Again, there is a lack of correlation between heat flux and volume of concrete.

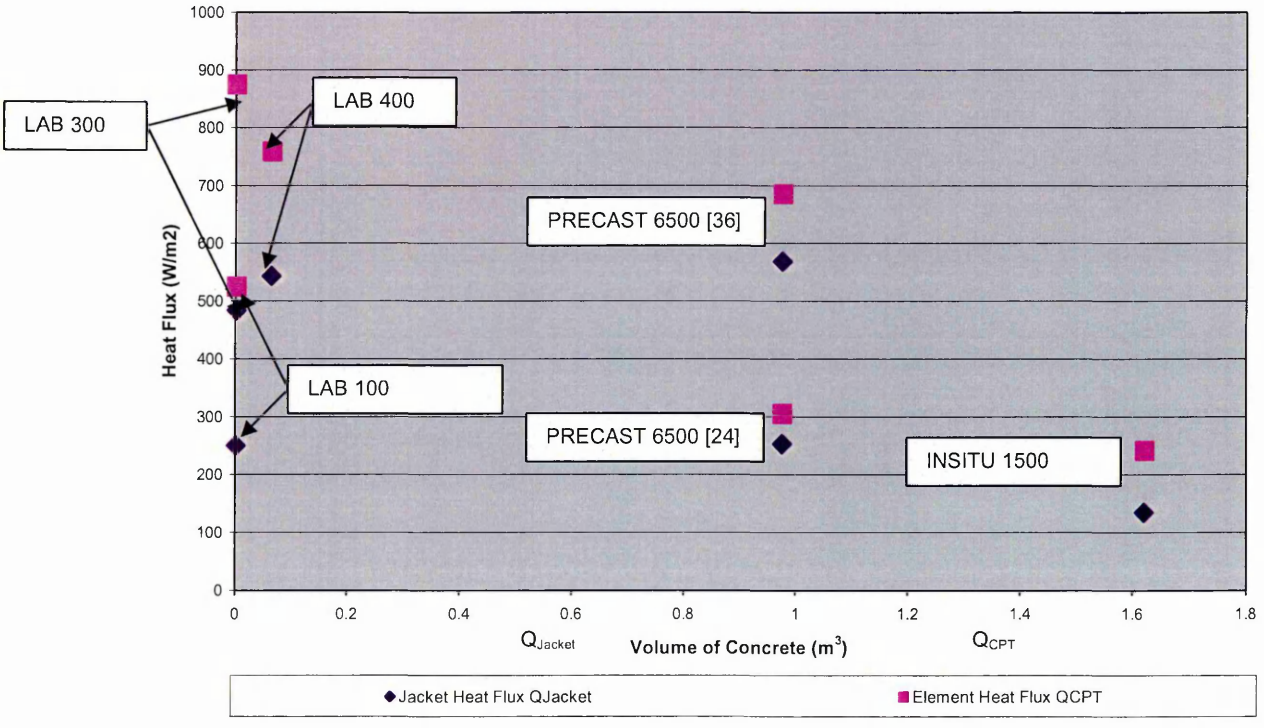

Figure 10.3. Graph of Concrete Volume vs Heat Flux of Jackets

Figures 10.2 and 10.3 consider only the volume of the concrete being cured. The lack of correlation is due to the different ways the CPT in each application (Chapters 5-8) is applied

and over what area of the concrete elements the CPT is applied. Figure 10.3 does not consider the proportional volume of the mould which the CPT also has to heat: For the laboratory scale samples, LAB 100 and LAB 300, this is very large. Figure 10.3 has been re-plotted (Figure 10.4) by excluding the results of LAB 100 and LAB 300, in Figure 10.5. These have been eliminated since for such small trials the volume of concrete being cured was comparable to the volume mass of mould and, therefore, comparisons of heat input with larger volumes are more meaningful.

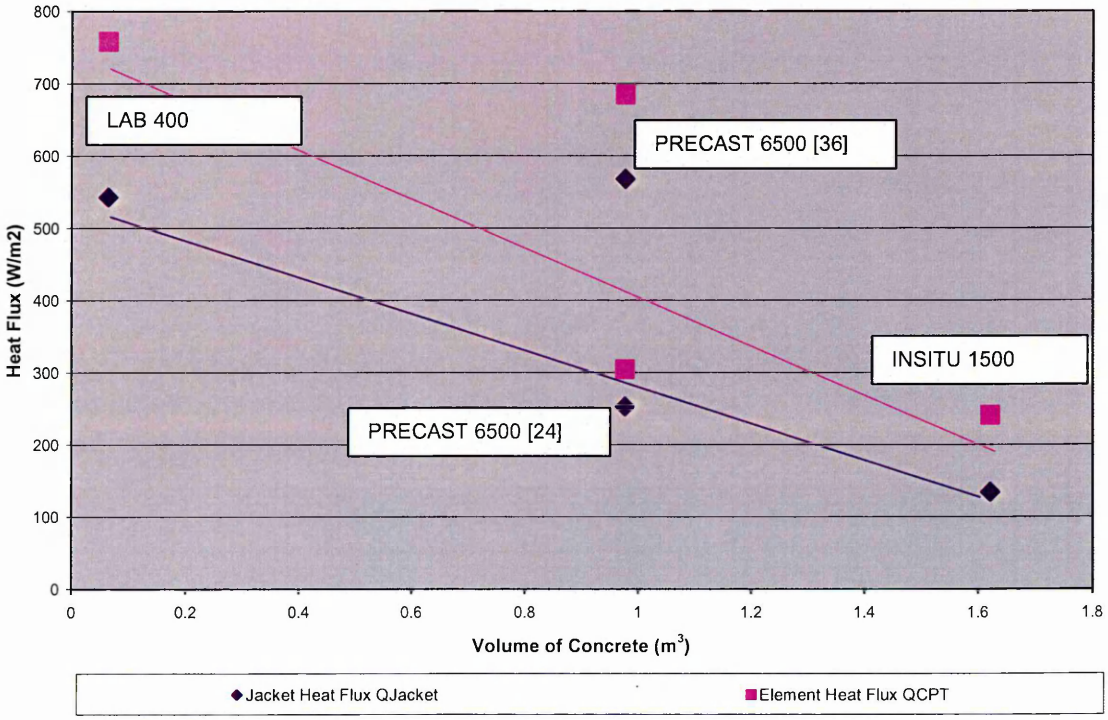

Figure 10.4. Graph of Volume vs Heat Flux (Large elements)

Considering only the larger elements, Figure 10.4 indicates that as the volume of concrete increases the Heat flux (Density of heat applied per m^2) decreases for the elements powered at 24 Volts. This is assuming that all CPT Jackets performed significantly. The PRECAST 6500 results fall below the best fit line. An explanation for this linear relationship could be that as volume of concrete increases so does the internal heat generated by hydration. However, in order to make a direct comparison, the geometry of each element needs to be considered. This will be done by considering the Volume / Surface ratio. (Section 10.4.2)

Table 10.9 considers the change in temperature of the concrete elements cured rather than the heat flux as shown in Figure 10.4. For this comparison, the different curing profiles of the LAB 400 Jacket used to heat the 400mm x 400mm x 400mm mould will be considered.

Jacket ID	Jacket Power Rating per [m3]	Initial Concrete Temperature, deg C	Maximum Concrete Temperature, deg C	Change in Temperature, deg C [dT]	Time, hours [dt]
LAB 100	35,000	21	79	58	2 (120mins)
LAB 300	37,500	-	-	-	-
LAB 400 - 1	6,875	20	53	33	7 (420 mins)
LAB 400 - 2	6,875	20	57	37	6 (360 mins)
LAB 400 - 3	6,875	20	64	44	7 (420 mins)
INSITU 1500	500	0	23	23	24 (1440 mins)
PREACST 6500 [24]	1,969	18	33	15	15 (900 mins)
PREACST 6500 [36]	4320	18	41	23	3 (180 mins)

Table 10.9. Increase in temperature per application

For the LAB 400 Jacket, time vs temperature curves for each of the three curing profiles used to heat the 400 x 400 x 400 mm volume of concrete have been plotted (Chapter 7). These profiles were;

- Profile 1 – 50 deg C @ heating / cooling rate of 10 deg C / hour
- Profile 2 – 60 deg C @ heating / cooling rate of 15 deg C / hour
- Profile 1 – 60 deg C @ heating / cooling rate of 10 deg C / hour

Figure 10.5 shows the plot of Power Output of each CPT Jacket used and the maximum change in temperature achieved within the concrete, due to CPT heating.

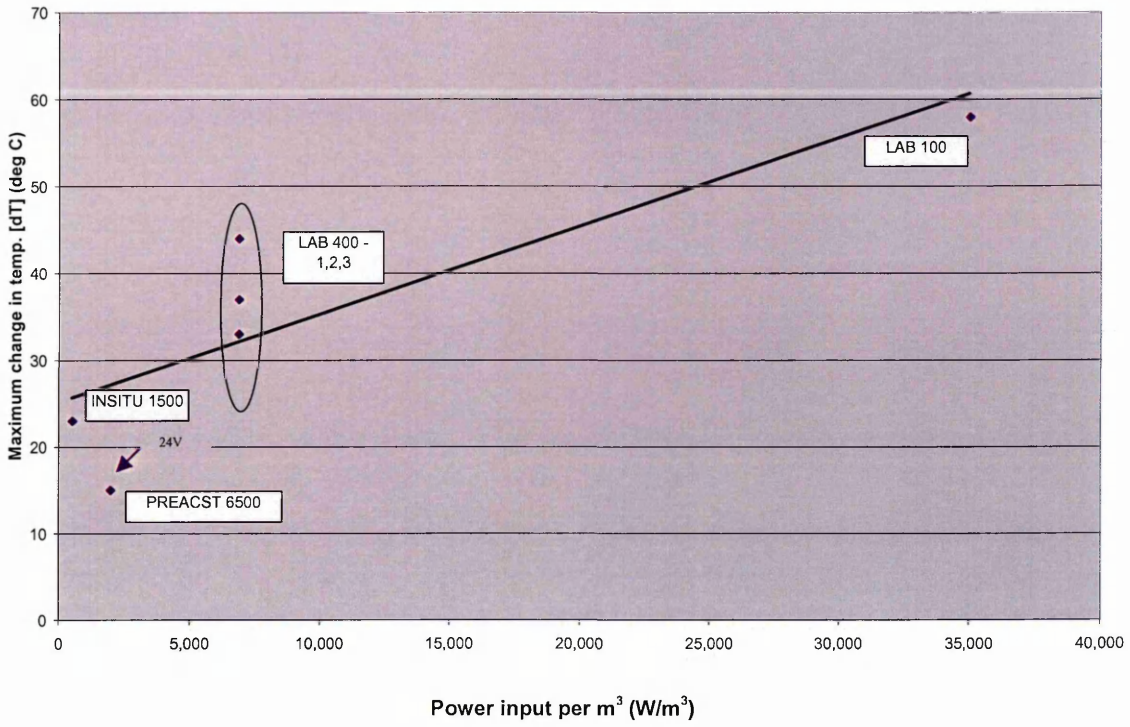

Figure 10.5. Maximum change in Temperature versus Power Input per m^3 of concrete

Figure 10.5 shows no correlation between the maximum change in temperature of the concrete elements being heated and the equivalent heat input per m^3 of concrete. The points for each of the LAB 400 Jacket heating profile have been highlighted – in this case - the rate of heating was controlled with preset thermostats, as well as the maximum operating temperature of the Jacket. The affect of this would be that the actual power output per m^3 of concrete would be different for each of the three profiles, whereas on the graph it is represented as equal. This will be considered in greater detail in the next sections.

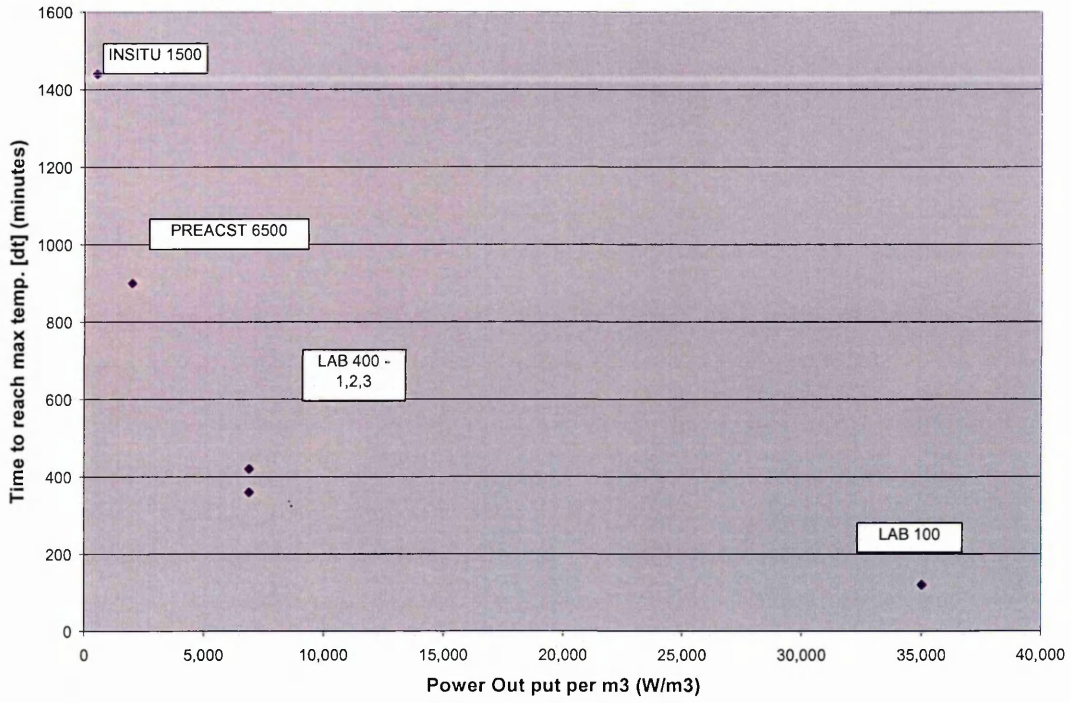

Figure 10.6. Time to reach maximum temperature versus Power per m3

Figure 10.6 from Table 10.9 show the plot of Power Output of each CPT Jacket used and the time taken for the maximum temperature within the concrete to be achieved. It shows that for the CPT Jackets and application used in Chapters 6-8 there is a correlation between the power out-put of each of the CPT jackets and the time taken for the jacket to increase the temperature of concrete to a maximum.

However, again, when comparing the elements directly, consideration has to be given to the Volume / Surface ratio and to the heat generated by hydration – directly related to thickness of a concrete section (and volume) and also to the cement content within a concrete mix. For the three large blocks considered, LAB 400, INSITU 1500 and PRECAST 6500, cement content / mix design for each was different. The affect of cement content will be considered in greater detail later (Section 10.5).

10.3. Maturity

When comparing the data collected in this thesis, as discussed in the previous section, parameters relating to the curing of concrete using CPT have become apparent. These are;

- Volume / surface ratio of the concrete elements
- Heat delivered by CPT to concrete elements
- The resulting increases in temperature,
- Period of heating time

Throughout all investigations using CPT, the following test parameters have been recorded;

- maximum (internal) temperatures within the cured concrete elements, T_{MAX}
- time needed to achieve the maximum temperature, t_{MAX}
- the period of time when the heating system was working t_h (i.e not cut of by the thermostat)
- the energy output from the CPT Jackets, Q.

As all elements were cured at different temperature within different ambient curing temperatures the maturity concept is adopted rather than a direct relationship of temperature to compressive strength. The concept of maturity was introduced in Chapter 2 where is stated that.

$$M(t) = \sum (T_a - T_0)\Delta t \qquad \text{[Eq 10.3]}$$

or in the limit

$$M(t) = \int_0^t (T_a - T_0)dt \qquad \text{[Eq 10.4]}$$

Where;

Δt = time interval

T_a = Average temperature during the time interval

T_0 = datum temperature*

* datum temperature is considered as a temperature below which the hydration is will not take place and there is no gain in strength. ASTM C 1074 recommends 0°C as a datum temperature; in this report 0°C will be used as a datum temperature;

As discussed in Chapter 2, the Maturity index relies on the temperature history of the concrete to estimate strength development during the curing. The temperature history, monitored at strategic locations, is used to calculate the *Maturity Index*. The *maturity index, also* known as the temperature-time factor (Carino, N.J. and Lew H.S. 2001), is based on the maturity rule that states "*Concrete of the same mix at the same maturity (reckoned in temperature-time) has approximately the same strength whatever combination of temperature and time go to make up that maturity*". The maturity method can be adopted to determine the in-situ strength of concrete if specimens are cured at multiple, constant temperatures and the compressive strength is determined at multiple intervals (Carino, N.J. and Lew H.S. 2001). The maturity index can be recorded or calculated from temperature history of a concrete element and then compared to the pre-determined data in graphical form to obtain the approximate strength of the in-situ concrete.

Although the method is used in concrete science and technology, and some researchers report good correlation between compressive strength and maturity there are also limitations of the method. The temperature and time are not the only factors influencing the properties of hardened concrete. The maturity concept does not take into the consideration the humidity, which plays an important role in concrete hardening.

For the results obtained throughout this study, maturity will be used to quantify the amount of heat delivered and evolved in the system rather than the temperature history with time used to determine maturity. In addition to this work the results form parallel, state-of-the-art work conducted under the LOVACS project (LOVACS, 2007) used to further strengthen the analysis. This additional work considers the influence of volume/surface ratio of concrete elements and their thermal behaviour during adiabatic curing and non adiabatic curing. The findings of this work will also be used along with the results and data reported on in Chapters 6-8. A brief overview of each experimental set-up will be given.

10.3.1. *Non-adiabatic Beam Curing*

The work involved the curing of beams with various volume-to-surface ratios, between 40mm and 100mm. Beams were cast in steel moulds. The length and the height of the mould was kept constant. The different volume-to-surface ratios were achieved by varying the element width. Three mould sizs were used referred to as 'small', 'medium' and 'large', The beam sizes and volume / surface ratios for each is given in Table 10.10.

	Dimensions (mm)			Volume (m^3)	Volume/Surface ratio
Beam Sample	**Length**	**Depth**	**Width**		
Small	1500	380	150	0.0855	50
Medium	1500	380	260	0.1482	70
Large	1500	380	380	0.2166	84

Table 10.10. Details of beam elements

Three different arrangements of the heating blankets for curing the concrete beams were used:

- A heating element on the top face of the beam
- Two heating elements each positioned along the longest face (together with an insulation blanket (unheated) on top of the mould
- Three heating elements each positioned on the longest sides and top of the mould. These positions were chosen as being representative of the procedures followed by the precast industry.

An additional three different concrete mixes were investigated in order to determine the influence of cement content on the temperatures produced by the mix during thermal curing. Three variations to the MIX A concrete mix (Section 4.5.1) with varying cement contents of 300 400 and 500 kg/m^3 respectively were used. A constant water / cement ration of 0.45 was used.

After casting, the beams were cured with external heating applied through CPT Jackets. Temperatures were monitored at different locations within the concrete, at the surface and at the core of the beams.

10.3.2. *Adiabatic Slab testing*

Similar to the beam testing, described above, work conducted as part of the LOVACS project (LOVACS 2007) investigated the affect of CPT curing of slabs of different volume / surface ratios. The dimensions of elements were 750mm x 750mm with three thicknesses: 100mm, 150m and 250mm. The volume / surface ratios for those samples are 40mm, 54mm and 75mm respectively. Three tests for each slab were conducted, heating one side of the slab, two sides and no heating. The cement content of the mix was 370 kg / m^3 with water / cement ratio of 0.45.

The key difference between the slab and beam investigation were that beam tests were conducted within the lab where the ambient was maintained at approximately 20 deg C, and the beam was un insulated apart from to the sides where the CPT Jackets were applied as shown in Figure 10.1. However the investigations conducted using the slab were done in adiabatic conditions, ie the slab was 100% insulated on all sides. CPT heating was applied to the beam elements immediately after casting and maintained over 24 hours. CPT heating to the slab elements was applied at immediately after casting and maintained for 24 hours.

10.4. The Influence of Surface Volume Ratio on Temperature Profile

Time (t) vs Temperature (T) curves for the LAB 400, INSITU 1500 and PRECAST 6500 curing regimes, as described in Chapters 7 and 8 have been plotted on Figure 10.7. The time vs temperature curves for the LAB 100 and LAB 300 applications have not been plotted due to the small volume of concrete cured in each application compared to a comparatively high volume of mould (steel). For the LAB 400 Jacket, time vs temperature curves for each of the three curing profiles used to heat the 400 x 400 x 400 mm volume of concrete have been plotted. These profiles were;

- Profile 1 – 50 deg C @ heating / cooling rate of 10 deg C / hour
- Profile 2 – 60 deg C @ heating / cooling rate of 15 deg C / hour
- Profile 1 – 60 deg C @ heating / cooling rate of 10 deg C / hour

Each profile has been plotted over a period of 24 hours. Within the first 24 hours of curing, after casting, concrete elements are at their most vulnerable (as discussed in Chapter 2) to freeze / thaw. Also in precast concrete plants, curing periods beyond 24 hours become un economical for concrete producers.

For each profile, the average temperature of the thermocouples located within each concrete element was taken. These were thermocouples;-

- LAB 400 Average – Channels 5, Ch 6 and Ch 7
- INSITU 1500 Average – Thermocouple 5, TC 6 and TC 7
  (TC's 15, 16 and 17 for the unheated foundation)
- PREACST 6500 Average (Embedded thermocouple)

The time vs temperature profiles for each can be seen on Figure 10.7. Figure 10.8 shows the time vs temperature profiles for elements cured at a constant ambient (naturally cured, 20 deg C 60% RH) both of these graphs only consider each Jacket when operated at 24 Volts.

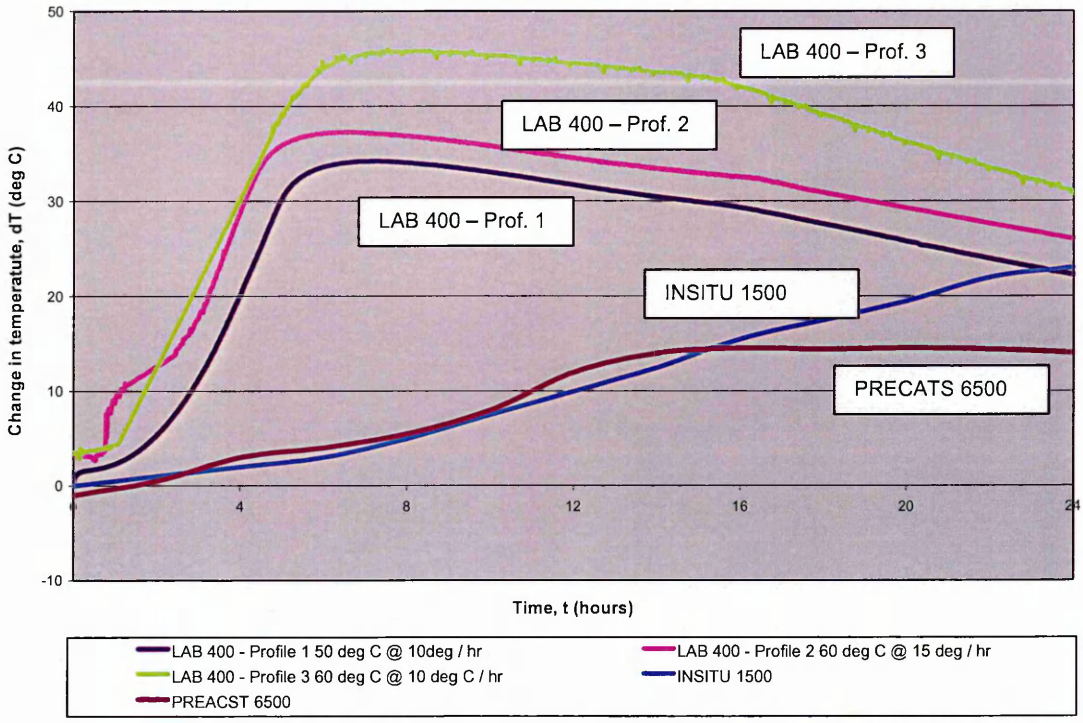

Figure 10.7. Temperature vs time for heated applications (Non – adiabatic)

In addition to plotting the time vs temperature curves for the concrete elements when heated using CPT. Curves for each element when not heated have also been plotted on Figure 10.8

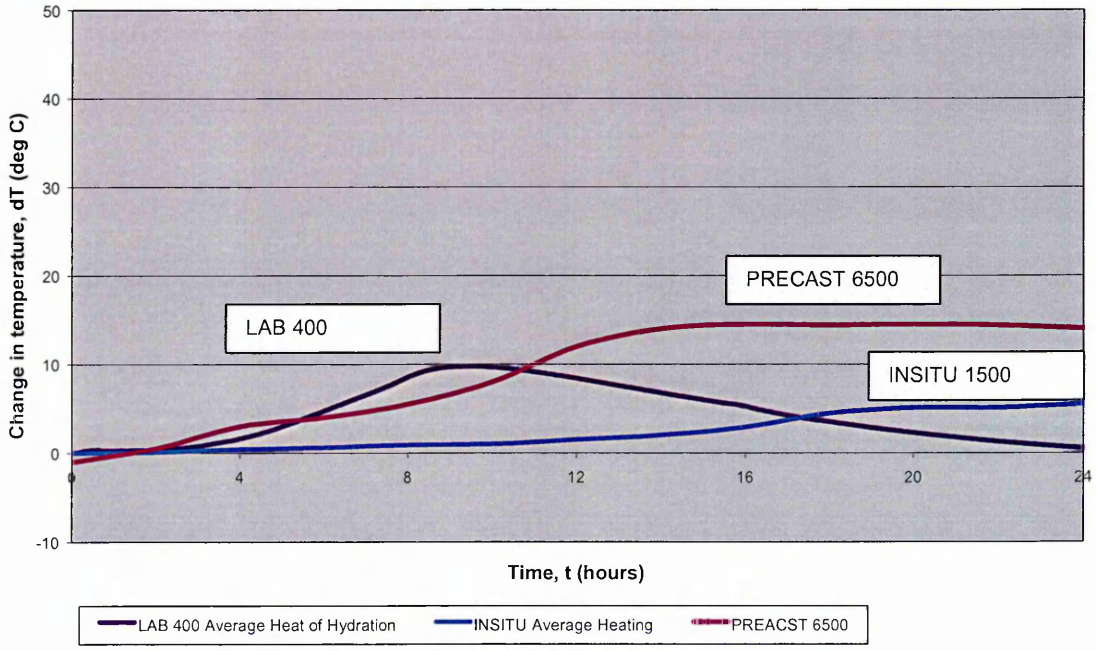

Figure 10.8. Temperature vs time for un heated curing (Non – adiabatic)

For each curve, the maturity of the concrete cured using the CPT Jackets can be established by calculating the area under each curve. For each application this has been done between the limits 0 and 24 hours

$$M(t) = \int_0^{24} (T_{24} - T_0)dt \qquad \text{[Eq 10.5]}$$

Using a spreadsheet;

$$M = [(0.5\ (T_{n+1} + T_n)\ x\ (t_{(n+1)} - t_{(n)})) + (0.5\ (T_{(n+2)} + T_{(n+1)})\ x\ (t_{(n+2)} - t_{(n+1)})) \ldots\ldots] \qquad \text{[Eq 10.6]}$$

The maturity for each concrete element cured, including the elements cured naturally (without CPT) is given in Table 10.11. Also in Table 10.11 is an estimate of the energy delivered by each of the CPT Jackets. This is calculated by multiplying the power by the duration of curing, in this case 24 hours. For the case of the LAB 400 Jacket, an operating factor was also applied - for Profile 1, the Jacket was assumed to be operational (due to the electronic control cutting 'in' and 'out') 50% of the time (defined as diversity), for Profile 2, it has been assumed the Jacket was operational for 60% of the time, and 70% of the time for profile 3. This has been summarised in Table 10.11.

Jacket ID	Power rating [Watts]	Operating time [hours]	Diversity [%]	Energy Delivered [Wh]	Energy Delivered [KWh]
LAB 400 – Profile 1	440	24	0.5	5280	5.28
LAB 400 – Profile 2	440	24	0.6	6336	6.336
LAB 400 – Profile 3	440	24	0.7	7392	7.392
INSITU 1500	162	24	1	19440	19.44
PRECATS 6500	384	24	1	46080	46.08

Table 10.11. Energy applied by CPT Jackets

Table 10.12 summarises the Maturity and energy delivered for the CPT systems described in Chapters 7 and 8 conducted in non – adiabatic conditions, i.e on site or within precast concrete plants

Jacket ID	Maturity [°C · h]	Energy Delivered [kWh]
LAB 400 – Profile 1	615	5.28
LAB 400 – Profile 2	709	6.336
LAB 400 – Profile 3	868	7.392
LAB 400 - Unheated	105	0
INSITU 1500	265	19.44
INSITU – Unheated	53.6	00
PRECATS 6500	130	46.08
PRECATS 6500- Unheated	97.5	0

Table 10.12. Maturity for non adiabatic applications (24 hours)

Table 10.13 summarises the maturity and energy input by CPT elements for the test on adiabatically cured slab elements. For the adiabatic testing, slabs of dimension 750mm x750mm x 100mm and 250mm thick were heated with two CPT Jackets. For each thickness, a slab was cured by heating the top only face (H) and the top and bottom faces (DH) of the slab. All other faces / surfaces of the slab – including behind the heating elements were fully insulated to create adiabatic conditions.

sample	Volume / Surface	maturity [°C · h]	Energy delivered [kWh]
10	40	897	0
10H	40	1167	0.64
10DH	40	1406	1.25
25	75	863	0
25H	75	1080	0.89
25DH	75	1355	1.44

Table 10.13. Maturity of adiabatically cured slab elements (24 hours)

For each of these applications and temperature time curves described above, the tests were conducted in varying ambient temperatures with CPT only applied to some of the sides of the concrete elements.

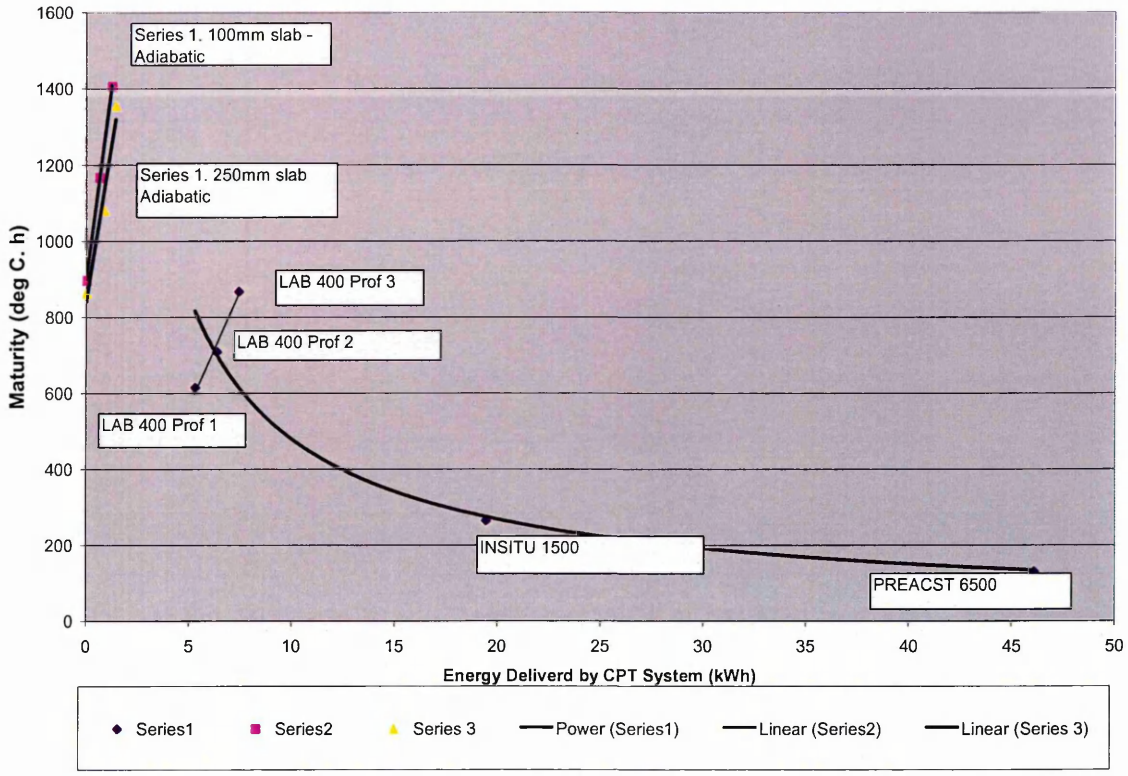

Figure 10.9. Graph of Maturity vs Energy delivered by each system

Figure 10.9 shows that for the LAB 400 element and the two different thicknesses of beams cured adiabatically, there is a linear relationship between the energy delivered to the element and the maturity in each case. For the elements cured adiabatically, the gradient of the line decrease as the Volume of the slab increases (100mm tick slab to 250mm thick slab). When considering the LAB 400 block there is also a linear relationship. However, what is not taken account for is heat of hydration and the shape, or Volume / Surface ratio for the elements being cured as previously noted.

The results of the non adiabatically cured beams could not be included in Figure 10.9 as there was no record of the Power rating / Energy delivered by the CPT curing systems used in the work undertaken.

10.4.1. *Element Volume*

Table 10.14 and 10.15 give the energy delivered per m^3 of concrete for the elements cured in Chapters 6-8 and also for the elements cured adiabatically.

Jacket ID	maturity [oC · h]	Volume	Energy delivered [kWh]	Energy Delivered per m3
LAB 400 – Profile 1	615	0.064	5.28	82.5
LAB 400 – Profile 2	709	0.064	6.336	99
LAB 400 – Profile 3	868	0.064	7.392	115.5
LAB 400 - Unheated	105	0.064		0
INSITU 1500	265	1.62	19.44	12
INSITU – Unheated	53.6	1.62		0
PRECATS 6500 [24]	130	0.975	46.08	47.26153846
PRECATS 6500 - Unheated	97.5	0.975		0

Table 10.14. Energy delivered per m^3 of concrete

Sample	maturity [oC · h]	Volume	Energy delivered [kWh]	Energy Delivered per m3
10	897	0.0563	0	0
10 H	1167	0.0563	0.89	15.8081705
10 DH	1406	0.0563	1.25	22.2024867
25	863	0.1406	0	0
25 H	1080	0.1406	0.64	4.55192034
25 DH	1355	0.1406	1.44	10.2418208

Table 10.15. Energy delivered per m^3 for non adiabatic curing

Figure 10.10 shows the relationship between the energy delivered per m3 of concrete for the LAB 400, INSITU 1500 and PRECAST 6500 elements and also the 75mm x 75mm slabs cured adiabatically. For all elements the maturity is with a 24 hour period.

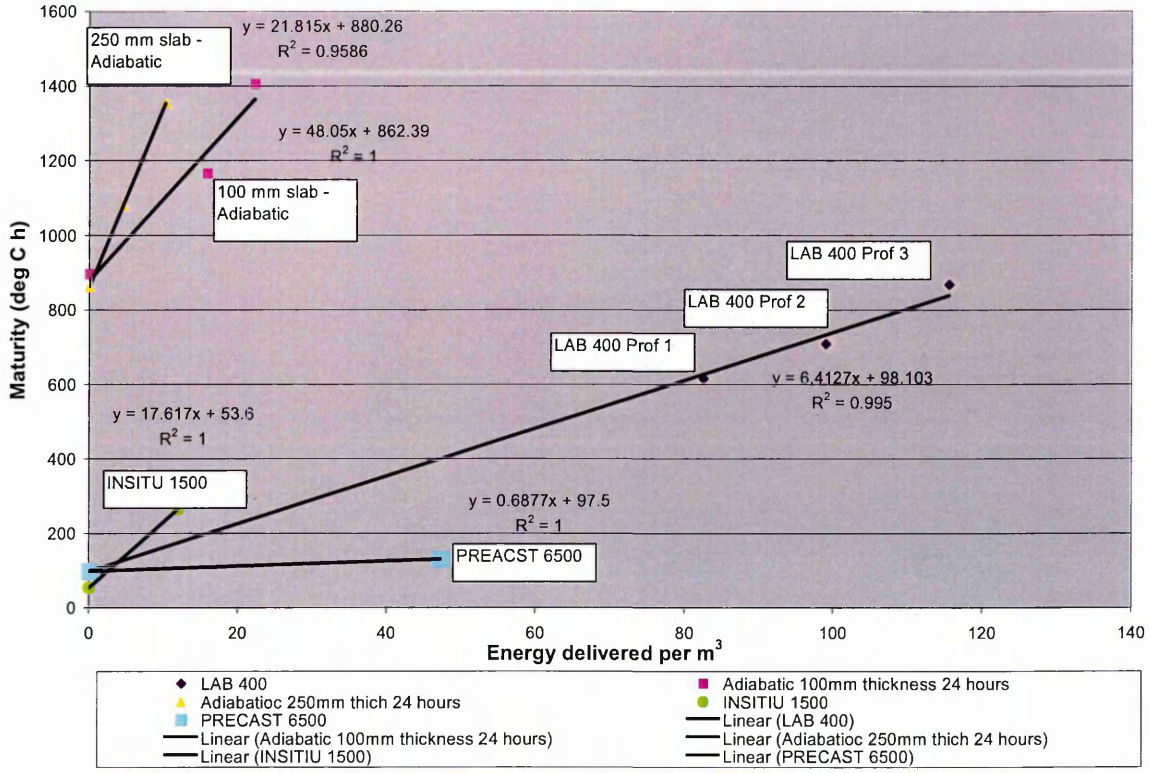

Figure 10.10. Graph of Maturity vs Energy delivered by each system per m3

Figure 10.10 shows the relationship between energy delivered per m^3 of concrete cured and the maturity of the various elements cured over a period of 24 hours. In addition results from the adiabatic testing of 750mm x 750mm slabs of thicknesses 100m and 250mm have been plotted. Figure 10.10 shows that for the LAB 400 and the 100mm and 250mm slabs cured adiabatically, there is a separate linear relationship between the energy delivered per m^3 of each element being cured and the maturity of each element over 24 hours. The figure shows that there is a linear relationship between maturity and element volume for the adiabatic curing; and maturity and power input for the LAB 400 element. From inspection of the graph it may concluded that for shapes with greater surface are, like the PREACAST 6500 element, the gradient of the power per m^3 versus maturity relationship decrease. This could also be the case for the adiabatic curing – as the thickness of the slab reduces to 100mm from 250mm, the relative surface area (to volume) decreases, as does the gradient of the best fit line for that element. The graph also shows a clear difference between the maturity of concrete after 24 hours in non adiabatic conditions compared to the elements cured adiabatically. What this shows is that when cured adiabatically, heat that would have been lost, had contributed to maturity at 24 hours of between 750 – 800 deg C hours. This clearly highlights the importance of insulating concrete elements during curing. Figure 10.10 considers only the volume of the concrete being cured. It does not take into account the shape of the element, i.e the Volume / Surface are a ratio.

10.4.2. *Volume / Surface Ratio*

A variety of different sizes and shapes of concrete elements have been cured in Chapters 6-8. Chapter 6 considered small cubes and prisms, Chapters 8 considered larger cubes and a large foundation blocks and a slender more complicated terrace section. There are two considerations of element shape, these are, the surface area of the element being heated, and the volume of each element. The relationship of the these two values is used to calculate the Volume / Surface ratio of each element. This is sometimes refereed to as the slenderness of an element. Table 10.16 calculates the total surface area of each element heat cured throughout the thesis.

Jacket ID	Shape	Concrete Element Surface Area (m^2)		
LAB 100	Cube	0.1 x 0.1 x 6		0.06
LAB 300	Prism	0.075 x 0.075 x 2 0.3 x 0.075 x 4	= 0.01125 = 0.09	0.10125
LAB 400	Cube	0.04 x 0.4 x 6		0.96
INSITU 1500	Block	2.0 x 0.9 x 4 0.9 x 0.9 x 2 *	= 7.2 = 1.62	8.82
PRECAST 6500	Terrace section	0.5 x 0.015 x 4 6.5 x 0.015 x2 6.5 x 0.5 x 2 6.5 x 0.485 x 2	= 0.03 = 0.195 = 6.2 = 6.305	12.73

Table 10.16. Concrete element surface area

Table 10.17 calculates the mould internal surface area. This is the total surface area of the element minus areas exposed. For the cube elements, the exposed area is the upper surface area which is open. For the PRECAST 6500 element this is the upper surface of the terrace section which is exposed.

Jacket ID	Shape	Mould (Internal) Surface Area (m^2)		
LAB 100	Cube	0.1 x 0.1 x 5		0.05
LAB 300	Prism	0.075 x 0.075 x 2 0.3 x 0.075 x 3	= 0.01125 = 0.0675	0.07875
LAB 400	Cube	0.04 x 0.4 x 5		0.8
INSITU 1500	Block	N / A		N / A
PRECAST 6500	Terrace section	0.5 x 0.015 x 4 6.5 x 0.015 x2 6.5 x 0.5 x 2 6.5 x 0.485 x 1	= 0.03 = 0.195 = 6.2 = 3.1525	9.5775

Table 10.17. Mould internal surface area (excludes the open faces)

These different area values, along with the area of heated mould / Jacket in contact with the concrete as calculated in Table 10.17 are summarised in Table 10.18 below.

ID	Shape	Volume of Concrete	Total concrete surface area	Mould Surface area	Jacket heating area	CPT heating area
LAB 100	Cube	0.001	0.06	0.05	0.14	0.04
LAB 300	Prism	0.00168	0.10125	0.07875	0.13	0.120
LAB 400	Cube	0.064	0.96	0.8	0.81	0.580
INSITU 1500	Block	1.62	8.82	N / A	6.04	3.360
PRECAST 6500	Terrace section	0.975	12.73	9.5775	7.6	6.3

Table 10.18. Volume surface ratio

Section 10.2 identified that the Jacket that performed best in terms of the least power input required to heat the concrete was the INSITU 1500 Jacket. The concrete element cured using the INSITU 1500 Jacket had the highest Volume / Surface ratio and the least power input (W/m^2), indicating that there is a link between the two parameters. This can be further explored by comparing the Volume / Surface ratio with the % of surface heated for each element (Table 10.21)

Figure 10.11 below shows the relationship between maturity and energy delivered per m^2 of concrete.

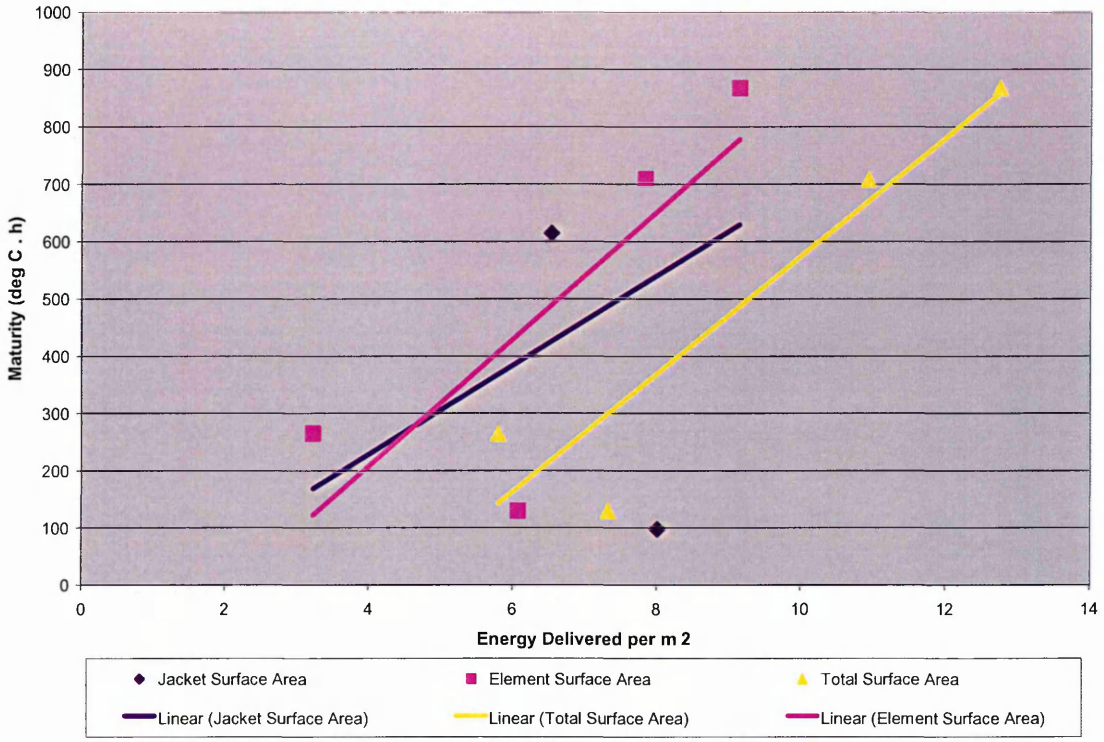

Figure 10.11. Graph of Maturity vs Energy Delivered per Area

This is also summarised in Table 10.19. It shows the percentage of surface area of each concrete element heated when using the CPT Jackets in each application. It can be assumed that the greater the heating area, the better the overall performance of a Jacket. This is particularly the case for the INSITU 1500 Jacket which has low heat in-put, high heating area, and overall good performance. This argument is further strengthened by comparing the analysis for the LAB 100 Jacket and the LAB 300 Jacket. Both heated the small scale lab samples to the required temperatures of 50 - 70 deg C, in Chapter 6, with similar performance in terms of temperature. However the heat in-put per m^3 of concrete was lower for the LAB300, but this was compensated by the heating area being nearly three times greater.

ID	Volume / Surface	Surface Area (m^2)	Surface Area heated (m^2)	% surface area heated
LAB 100 CUBE	0.016	0.06	0.02	33%
LAB 300 PRISM	0.015	0.1012	0.09	88%
LAB 400 CUBE	0.06	0.96	0.64	66%
INSITU 1500 BLOCK	0.23	7.02	6.21	88%
PRECAST 6500 TERRACE	0.075	13.03	6.5	0.49

Table 10.19. CPT power output comparisons

	Maturity	Volume of Concrete	Volume / Surface Ratio	Volume / Jacket Heating Surface Area Ratio	Volume / Element Heating Surface Area Ratio
LAB 400 – Profile 1	615	0.064	0.066666667	0.079012346	0.110344828
LAB 400 – Profile 2	709	0.064	0.066666667	0.079012346	0.110344828
LAB 400 – Profile 3	868	0.064	0.066666667	0.079012346	0.110344828
LAB 400 - Unheated	105	0.064	0.066666667		
INSITU 1500	265	1.62	0.183673469	0.268211921	0.482142857
INSITU – Unheated	53.6	1.62	0.183673469		
PRECATS 6500	130	0.975	0.076590731	0.128289474	0.154761905
PRECATS 6500 - Unheated	97.5	0.975	0.076590731		

Table 10.20. CPT power output comparisons

Figure 10.12 below shows the relationship between maturity and the Volume / Surface Area ratio for the large elements thermally cured in Chapters 6-8.

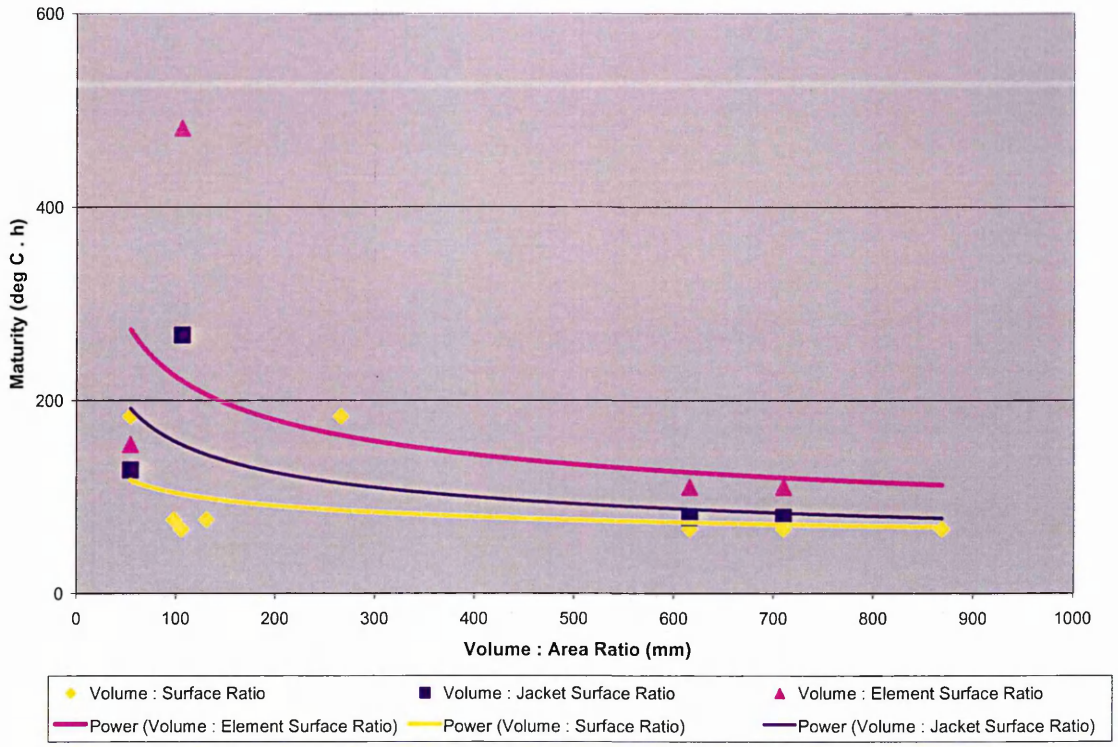

Figure 10.12. Graph of Maturity vs Volume / Surface area ratio

	Maturity		
	Location of Heating Elements		
Volume to Surface Ratio	Top	Sides	All
50.2	258	584	790
70	122	496	600
84.3	70	404	573

Table 10.21. Maturity values for central points for different locations of heating elements (Non-adiabatic)

The maturity results for the adiabatic beam tests conducted through the LOVAVS study (LOVACS 2007 Final Report) have been plotted with results from the test programme for maturity versus Volume / surface area ratio on Figure 10.13 below.

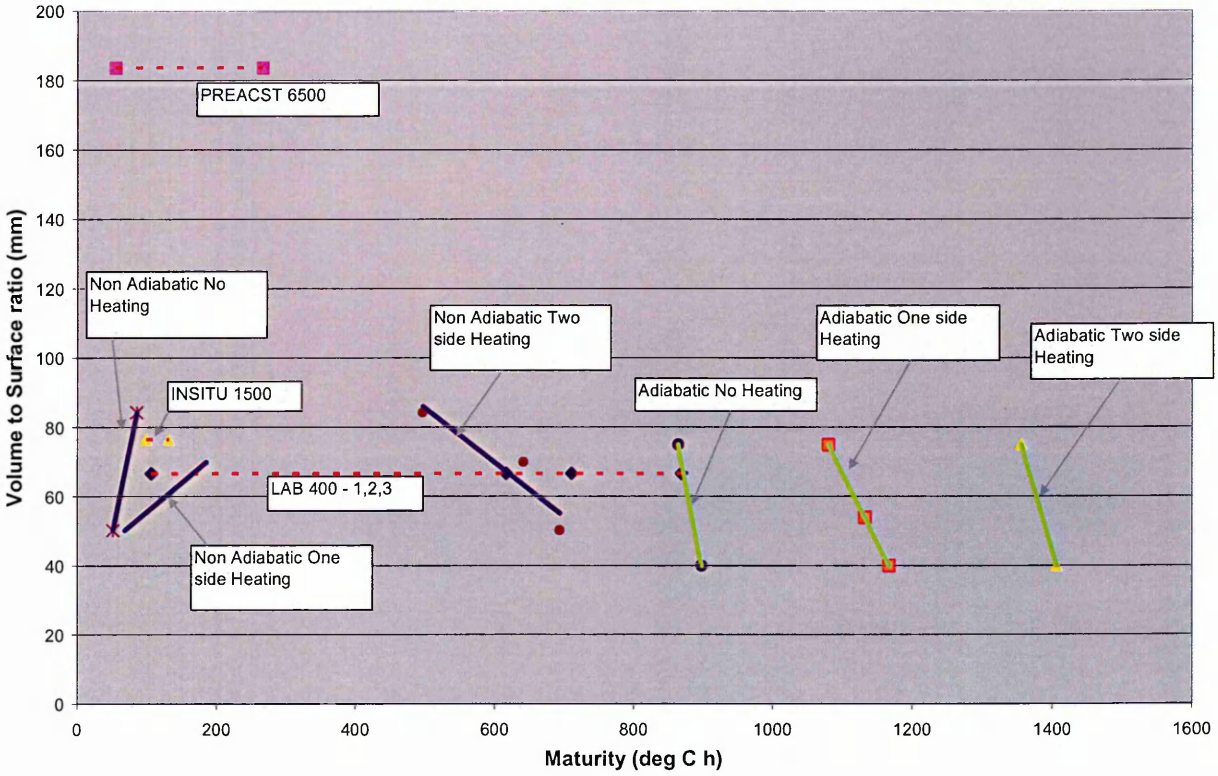

Figure 10.13. Maturity against volume to surface ratio

Figure 10.14 below shows the relationship between Volume / Surface Area ratio and the power input per m^3 for the large elements thermally cured in Chapters 6-8.

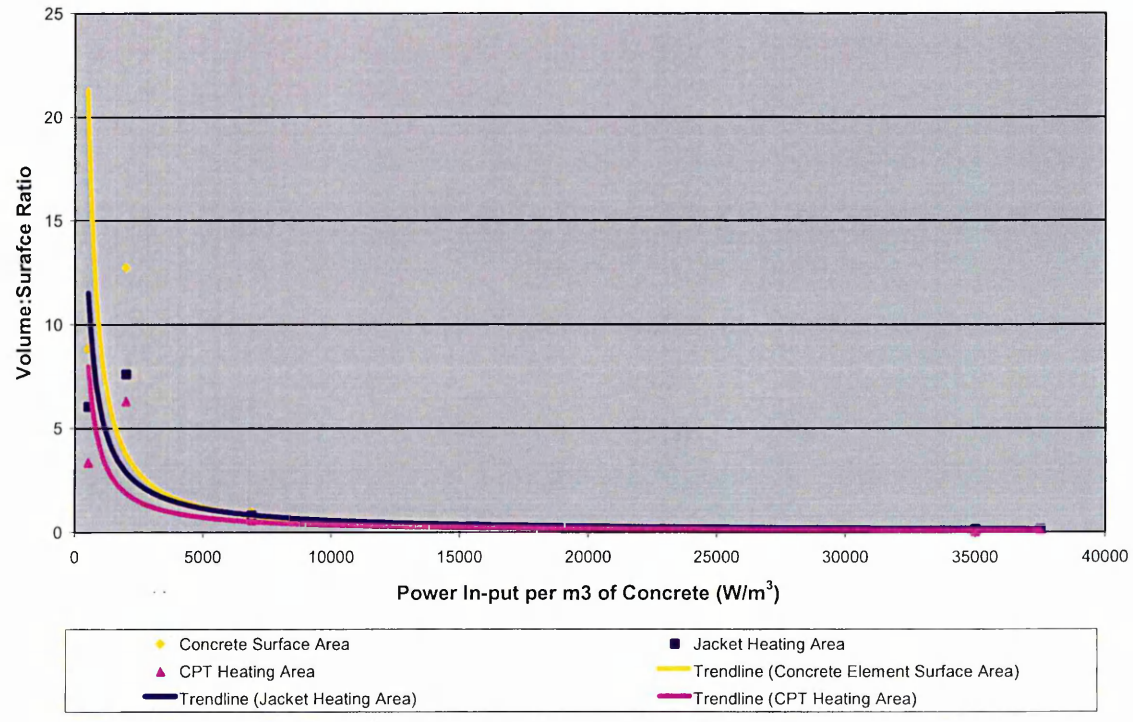

Figure 10.14. Graph of Power In-put vs Volume / Surface Ratio

The parameters show that the surface/volume ratio is an important factor influencing temperature evolution of the samples. When the concrete is cured in adiabatic conditions without external heating the maximum and final temperatures are higher for samples of higher volume/surface ratio. In opposite to this, in case of samples cured with the novel thermal curing system, the final temperatures are higher for samples of smaller volume/surface ratio. The dynamic of temperature development is higher for smaller samples both in case of unheated and heated ones. The difference is that in unheated samples the curves crossover is present. The volume/surface ratio – power output relationship seems to be important also for the phenomenon of interaction of heat of hydration and heat delivered by the thermal curing system. Comparing values of t_{60} for different samples it can be noticed, that for samples with two sides heating the difference in T_{60} between 10 and 25 cm thick samples is significantly smaller (21%) comparing to the one for one side heated samples (84%). It suggests that in case of two sides heated samples the interaction of heat delivered on heat of hydration is greater.

Analyzing maximum temperatures and also the temperature development rate for each samples, it can be seen that for two sides heated samples the maximum temperature exceeded 60°C which was the temperature set on the controller. The reason for it is that for DH samples there were two curing blankets used, but only one sensor. It was attached to the smaller, bottom blanket. Although the sample was very well insulated, there were some differences between the top and the bottom of the sample. When the bottom blanket reached 60°C (which was set as a final temperature) and turned off, the temperature of upper blanket was higher, what caused the overheat of concrete, over established temperature of 60°C. The conclusion is that for precise temperature controlling it is better to have sensors on all heating elements.

10.5. Conclusions

- The maturity increases with reducing volume to surface ratio
- The maturity of concrete increases with cement content but with different ratios for each of the locations of the heating elements

Chapter 11. Conclusions and Recommendations

11.1. Conclusions

This study has investigated the application of CPT for curing of concrete elements from first initial trials to full scale production units. What has become apparent through the study is that it is not only the performance and design of CPT that is critical to the CPT curing concrete as required, but also the way in which CPT is applied. From discussion, the following conclusions can be made:-

- CPT is suitable in terms of heating performance to cure concrete at elevated temperatures.
- CPT is suitable in terms of heating performance to protect concrete at early ages during low ambient conditions.
- CPT performs better when there is direct contact between CPT and the concrete being cured.

Other conclusions made throughout the thesis include;

- The manufacture of CPT elements is a highly variable process and determined by a number of factors such and the materials used for manufacture and the thickness of the CPT materials.
- Sampling showed that the initial Target Resistance R_T of the three CTPs, the resistance aimed for during manufacture, did not correspond with actual, or Characteristic Resistance R_{ID} of the CPT.
- The material does have a liner relationship in terms of an elements Length resistance; and a non-liner relationship in terms of element Width and Resistance
- The use of resistive properties cannot be used to predict current flow at a particular voltage do the changes in resistive properties of the materials when a potential difference is applied.

- CPT can be used to elevate the temperature of laboratory scale mould when empty and when used to cast concrete.
- The application of heat from CPT can elevate curing temperatures at early ages to 50 – 7 0 deg C for laboratory scale samples.
- Cubes cured using CPT display greater early age strengths compared to cubes cured at elevated temperatures an oven an in the environmental control chamber.

- CPT cured samples performed better than the oven cured samples at 4 and 28 days.
- The use of CPT has no deleterious effects to long term strength.
- The application of CPT can allow ideal curing conditions in terms of temperature and humidity to be achieved.
- Concrete elements cured using CPT displayed reduced shrinkage compared to elements cured at room temperature.
- CPT thermal curing jackets are suitable for uniform accelerated (thermal) curing of concrete of small laboratory scale samples.

- CPT thermal curing jackets were suitable for uniform accelerated (thermal) curing of concrete of large concrete elements.
- Thermal curing with CPT jackets accelerates the early strength development of concrete elements evenly throughout.
- The interaction between CTP heat and heat of hydration is mutually beneficial.
- Thermal curing CPT jackets minimise temperature gradients throughout concrete elements caused by heat generated by cement hydration, thus reducing internal stresses.
- CPT thermal jackets provide highly controlled uniform and gently increasing temperatures (without thermal shock) for the accelerated curing of concrete.

- CPT thermal liners can be used to elevate the curing temperature of concrete foundations during cold weather construction.
- The CPT liners eliminate the risk of frost damage to the concrete, particularly within 24 hours after casting.
- The CPT liners heated the concrete uniformly throughout to a pre-selected optimum temperature.

- For all exposure conditions, the resistance of CPT increased.
- The exposure of CPT to free thaw cycles, wetting and drying cycles and direct contact with concrete should be avoided.
- The heating & drying durability cycle had the least affecting terms of durability to CPT samples indicating good long term stability of CPT.
- Direct concrete of CPT with cement paste should be avoided.
- Glass cloth based materials are not suitable for CPT Jackets which have direct contact with concrete.

- When holes are made within CPT, the resistance is reduced. The width of the CPT element is effectively reduced by the sum of the hole diameters less any overlap.

11.2. Recommendations

This thesis has been the first time the application of CPT for curing concrete has been investigated. The investigation within this project has produced some interesting results and demonstrated that CPT materials can be used for the curing of concrete. However, the subject area is large and not all areas for related to the application have been covered by this thesis. Aspects that require further study are as follows:-

1. The relationships between operating voltage, Characteristic Resistance R_{ID} and material size need to be further investigated to predict operating temperature of the CPT when used for curing concrete.

2. Performance relationships for various CPTs used to cure concrete with various properties such as self compacting concrete.

3. The manufacturing process of CPT and control of R_{ID} compared R_T requires further investigation. This will enable design relationships to be greater understood and greater design accuracies.

4. The heating mechanism of CPT. By understanding how heat is generated on the surface of CPT a greater understanding of how it heats concrete can be achieved

5. Operation of CPT at other voltages, currently all CPT used throughout this investigation has been operated by using low voltage <50 Volts. Further investigation is required to determine if CPT can be operated using mains voltages. This will make the application of CPT in precast plants more effective

6. Thermal analysis of internal and external heat by using finite element techniques relating heat of hydration with external curing temperature; using this information for models to improve CPT design.

7. Fully understanding how heat is transferred away from the surface of CPT i.e Conduction or convection or a combination, and how the transfer of heat can be optimised by using materials to enhance the performance of CPT.

8. Investigating whether the curing profiles used in practice are the most suited to CPT curing. Can these be optimised now a thermal heating technology with close control is available

9. Investigation to determine if the electrical and thermal properties which CPT can be use with the Maturity method.

10. Investigate whether CPT can be cast within concrete to cure it during construction and then be used as a means for infrastructure during its service life (Heated ramps, wall, bridge decks)

11. Long term performance and stability; the technology is new, can CPT products perform thermally the same after a number of years.

References

A M Neville (1995) Properties of Concrete, 4th Edition, Longman London

"Concrete Conductor", Construction Materials, Chemistry & Industry News, 17 March 1997, http://biotech.mond.org/9706/970611.html

"Conductive Concrete Seeks Licensing Agreements", Construction Innovation, Vol. 1, No. 1, NRC-IRC, July 1995, http://www.nrc.ca/irc/newsletter/v1no1/v1no1p8.html

"Conductive Concrete Wins Popular Science Prize", Construction Innovation, Vol. 2, No. 3, NRC-IRC, Winter 1997, http://wolf.cisti.nrc.ca/irc/newsletter/v2no3/popular_e.html

CRAFTPROJECT (LOVACS): 016374, Sixth framework Programme Horizontal Research Activities involving SME's Co-operative Research. Final Report,2007

"L1 Conservation of fuel and power in dwellings" DTLR April 2002

"L1 Conservation of fuel and power in Industrial Buildings" DTLR April 2002.

A G Louden and E F Stacey, The Thermal Acoustic Properties of Lightweight concretes, Structural Concrete, 3, No. 2, pp. 58-95 (London 1966)

ACI 306R-88, 1989. "Cold Weather Concreting" American Concrete Institute, Practitioners Guide to Cold Weather Concreting. Pp 9-31.

ACI 517.2R-87, Revised 1992. "Accelerated curing of concrete at atmospheric pressure – state of the Art", ACI Manual of Concrete Practice Part 5-1992: Masonry, Precast Concrete, Special Processes, 17pp. Detroit, 1994.

B. Mather, A discussion of the paper "Theories of expansion in sulphoaluminate-type expansive cements: schools of thought," by M. D. Cohen, *Cement and Conceret Research,* 14, pp. 603-9 (1984)

British Rail, 1992. Specification for Concrete for Overhead Line Equipment Structure Foundations. EHQ/SP/0/105

British Standards Institution, 1993, "Guide to methods for assessing the durability of geotextiles-An interim document", British Standard Published Document PD 6533, United Kingdom

BS 5449:1990. "Specification for forced circulation hot water central heating systems for domestic premises"

BS 8110-1:1997 Structural use of concrete. Code of practice for design and construction.

BS EN ISO 6946:1997 Building components and building elements- Thermal resistance and thermal transmittance – calculation method

Carino, N.J. and Lew H.S. 2001. The maturity Method: From theory to application. Building and Fire Research Laboratory National Institute of Standards and technology. Gaithersberg, MD 20899-8611 USA

D N Richardson (1991), Review of variables that influence measured compressive strength, Journal of Materials in Civil Egineering, 3, No. 2, pp. 95-112

D.C. Teychenne, R.E. Franklin, H.C. Erntroy, (1997). "Design of normal concrete mixes". Building Research Establishment Ltd 2nd ed. / amended by b K Marsh

Catley (2002), Design and Testing of Inditherm Inserts in Conjunction with CV Buchan, Project Development I 2441, Knowledge Transfer Partneship, DTi 2005.

Department of Transport, UK, Highways Work Series1700.

Egan Report, Report of the Construction Task Force on the Scope for Improving Quality and Efficiency in the UK Construction Industry.

Euroconstruct. The European Construction Market. European Construction Trends 2001-2003

European Committee for Standardisation, 2000, "Geotextiles and geotextile-related products - General tests for evaluation following durability testing", European Standard EN 122261, Brussels

Frank P. Incropera, David P. DeWitt. Fundamentals of heat and mass transfer. 4th Edition John Wiley & Sons

G S Hasanain, T A Khallat & K Mahood (1988), Water Evaporation from freshl placed concrete surfaces in hot weather, *Cement and Concrete Researh,* Vol . 19 pp. 465-475

G.J. Verbeck and R.A. Helmuth, Structures and Physical properties of cement paste, Proc. 5th Int. Symp. On Chemistry of Cement, Tokyo, Vol. 3, pp. 1-32 (1986)

Gaynor, R.D,: Meininger, R. C.: and Khan, T.S. Effcets of Temperature and delivery time on concrete proportion" Temperature effects on concrete, STP-858, ASTM, West Conshohocken Pa., 1985, pp 68-87

H Al-Khaiat and M. N Haque. (1999) Effect of curing on concrete in hot exposure conditions. Magazine of Concrete Research. 51, No. 4 pp 269-274

H H Patel C H Bland and A B Poole (1995) The Microstructure of Steam-cured Precast Concrete, Advances in Cement Research, 8, No. 29, Jan., 11-19

H. F. W. Taylor, The Chemistry of Cements, Academic press, London 1964

H. L. Malhotra, Effect of temperature on the compressive strength of concrete, Mag. Concr. Res. 8(23) (1956) 85-94

I Heritage, Fouad M Khalaf and John G Wilson (2000), Thermal Acceleration of Portland Cement Concretes Using Direct Electronic Curing, *ACI Materials Journal,* V.97, No 1, pp 37-40.

J Sousa Coutinho (2001), Effect of Controlled Permeability Formwork (CPF) on White Concrete, *ACI Materials Journal* Vol. 98, No.2, pp. 148-156

K C Mahboub ad Q A Cutshaw (2001). Effects of Fresh Concrete Temperature and Mixing Time on Compressive Strength of concrete, V. 98, No.1 pp.59-62

K. W.Nasser, Properties of mass concrete when using fly ash at high temperatures, AM. Conc. Inst., J. 76 (pp 537-550)

Kirkbride T., Review of accelerated curing procedures#. Precast concrete, V. 2, No.2, 1971, pp93-106

Latham Report, 1994, 'Constructing the Team' by Sir Michael Latham, Final Report of the Government/Industry Review of Procurement and Contractual Arrangements in the UK Construction Industry, HMSO Department of the Environment (1994).

Lui Baoju Xie Youjun Zhou Shiqiong Li Jian (2001) Some factors affecting early compressive strength of steam-curing concrete with ultrafine fly ash. *Cement and Concrete Research* Vol. 31 pp 1444-1458.

Luke K. and Glasser F. P. Effect of temperature on the hydration chemistry and durability of cement concrete. Proc. 4th Conf. On durability of building ,materials and components, Singapore, 1987, pp. 188-195

Michel Plante, Georg Cameron and Arezki Tagnit-Hamou (2000) Influence of Curing Conditions on Concrete Specimens at Construction Site. *ACI materials Journal.* V.97, No.2 pp.120-126.

National Ready Mix Concrete Association, Cold weather ready mixed concrete, *Publ. No 34* (Washington DC, Sept. 1960)

NHS Estate Health Guidance Note "Safe Hot Water and Surface Temperature" 1998 Editions

Odler I. Et al. Effect of Hydration temperature on cement paste structure. Mater. Res. Soc. Symp. Proc., 1987, 85 139-144

P. K. Mehta, Sulphate attack on concrete – a critical review, *Materials Science of Concrete III,* Ed. J. Skalny, American Ceramic Society, pp. 105-30 (1993).

Patel H. H. et al. Concrete cured at elevated temperatures: its microstructure and properties. Departmental working paper GR/J149361/1, Geomaterials unit, Queen Mary and Westfield College, London, 1993.

Patel H. H. et al. The microstructure of concrete cured at elevated temperatures. Cem Conc. Res. 1995. 25 485-498

Pfeifer D. W., and landgreen, J. R., Energy efficient Accelerated Curing of Concrete," Prestressed concrete institute, 1981

Pfeifer, D. W, and Marusin S., "Technical report No. 1- Energy efficient Accelerated Curing of Concrete" Prestressed concrete institute, 1981.

Pico Technology TM. Pico Technology – Temperature & Humidity monitoring solutions www.picotech.com.

Ping Xie, Ping Gu and J.J. Beaudoin, "Electrical Percolation Phenomena in Cement composites Containing Conductive Fibres", Journal of Materials Science 31, 4093-4097 (1996).

W. Kurdowski "Chemia cementu" PWN Warszawa 1991 (in polish)

Powers, T. C. , Mar. 1962, "Prevention of Frost Damage to Green Concrete," RILEM Bulletin (Paris), No. 14, pp. 120-124. Also, Reasearch Dept. Bulletin No. 148, Portland Cement Association.

S. Erdogdu, S. Kurbetci, Optimum heat treatment cycle for cements of different type and composition, Cem. Concr. Res. 28 (11) (1998) 1595-1604

S. Ghosh. K.W. Nasser, Effects of high temperature and

Sakir Erdogdu and Siren Kurbetci. (1998) Optimum treatment cycle for cements of different type and composition. Cement and Concrete research . Vol. 28, No. 11, pp. 1595-1604.

Saul, A . G. A., 1951, "Principles Underlying the Steam Curing of Concrete at Atmospheric Pressure" Magazine of Concrete Research, Vol. 2, No.6, March pp. 127-140.

Scrivener K. L. The effect of heat treatment on inner product C-S-H. Cem. Conc. Res., 1992, 22 1224-1226

Thermocrete http://www.tarmacprecastconcrete.co.uk/p-therm.htm

Tuan, C., "Conductive Concrete Overlay for Bridge Deck De-icing," http://www.engext.unl.edu/CE/Profiles/tuan/deck.html

UK Concrete and Concrete Products Market Research Report. Market and Business Development. 2003

W Lerch and C L Ford. (1948) Long-time study of cement performance in concrete, Chapter 3: Chemical and Physical Tests of the Cements, J Amer. Concr. Inst., 44 pp. 743-95

W. Czernin (1962), Cement Chemistry and Physic for Civil Engineers, Crosby Lockwood, London.

West Controllers™. West temperature control solutions

www.west-inst.co.uk/

Y Xu, Y L Wong, C S Poon, M Anson (2000). Impact of High Temperature on PFA concretre, *Cement and Concrete Research* Vol. 31 pp.1065-1073.

Y. Maltais, J. Marchand, Influence of curing temperature on cemnt hydration and mechanical strength development of fly ash mortars, Cem. Concr. Res. 27 (7) (1997) 1009-1020.

S P Shah and G Winter, Inelastic behaviour and fracture of concrete, Symp. On causes, mechanisms, and control of cracking in concrete, ACI SP-20, PP. 5-28 (Detroit, Michigan 1968.

Portland Cement Association, *Ettringite Formation and the Performance of Concrete,* IS417, Portland Cement Association, 2001.

Day, Robert L., *The Effect of Secondary Ettringite Formation on the Durability of Concrete: A Literature Analysis*, RD108, Portland Cement Association, 1992.

Yildiz Bayazitoglu, M Necati Ozisik 1988, Elements of Heat Transfer. McGraw-Hill International Editions

Research Awards

As a result of the work undertaken by this research programme, the following research grants were awarded to continue and further develop the concepts researched and discussed in this research:-

i. **CRAFT FP6** "Low Voltage Accelerated Curing Systems" European Development Programme. Tarmac Precast Concrete Ltd (UK); ERBA Holland BV (Holland); Angio S.A. (Spain); Bikani S L (Spain); Kalab Building Ltd (Czech Republic); Prefa IP j.s.c. (Czech Republic); WPS SA (Poland); Prefabet - Kolbuszowa SA (Poland); Academia Gorniczo - Hutnicza(UMM); Fundacion Labein (Spain); and RIBM Brno Ltd (Czech Republic).

ii. **Yorkshire Forward – Large Company Grant** "Development of CPT materials for continuous rail de-stressing", Corus Rail Infrastructure, GrantRail, Sheffield Hallam University and Inditherm plc

Awards and Acknowledgements

The following awards were presented during the research programme in recognition of the research work undertaken between the partnership of Sheffield Hallam University and Inditherm plc.

i. **KTP Award Winning Research Programme – David Catley, Prof. P.S. Mangat**, "Development of Conductive Polymer Technology for Construction Applications". Inditherm plc and Sheffield Hallam University. DTi Knowledge Transfer Partnership Awards 2006.

ii. **KTP Business Leader of Tomorrow – David Catley**, "Development of Conductive Polymer Technology for Construction Applications". Inditherm plc and Sheffield Hallam University. DTi Knowledge Transfer Partnership Awards 2004.

Publications

P.S. Mangat and D.G. Catley. "Low Voltage Accelerated Curing System for Future Precast Concrete", International Precast Concrete Conference Proceedings, BIBM (May 2005), Amsterdam, pp. 111-112.

P.S. Mangat and D.G. Catley. "Low Voltage Heating Systems for the Curing and Protection of Early Age Concrete". Concrete Plant International, Issue #4, August 2005. p106-112, ISSN 1439-7706.

P.S. Mangat and D.G. Catley. "Energy Efficient Integrated Heating Systems for Bridge Deck De-icing", Proceedings of the 7th International Conference on Short & Medium Span Bridges, Montreal (August 2006), pp ##.

P.S. Mangat and D.G. Catley. "Low Voltage Curing Liners for Railway Electrification Concrete Foundations" Jarvis Rail in conjunction with August 2005.

P.S. Mangat and D.G. Catley. Introduction to CPT Technology for Cold Weather Concreting, Presentation to ACI306 committee, ACI winter conference, Las Vegas Autumn 2005.

D.G. Catley. "A Thin, Tough, Flexible 'Electric Blanket' That Provides Uniform Heat on Low Voltage Power". New Civil Engineer – New Concrete Engineering, September 2004, London.

D.G. Catley. H. Russell. "Low Voltage Heating Material Promises an End to De-icing Salts", Bridge Design and Engineering, 2nd Quarter September 2004. London, pp10

D.G. Catley. "Art Warming". New Civil Engineer – New Concrete Engineering, September 2005, London, pp9

D.G Catley P.S. Mangat. "Electric Blanket for Concrete". Concrete Magazine, September 2005, London pp34-35.

P.S Mangat D.G Catley, International Patent Application "Heating Surfaces" Patent Application No. PCT/GB2004/004243, Publication Number. WO/2005/036930. Publication Date. 21.04.2005. International Filing Date. 07.10.2004

Thermal Curing of Concrete with Conductive Polymer Technology

David Gerald Catley

A thesis submitted in partial fulfilment of the requirements of
Sheffield Hallam University
for the degree of Doctor of Philosophy

Appendices, Volume 2

March 2009

Contents

Appendix 1. CPT Batch Resistances

Resistance (ohms)	20 ohm (RED)			50 ohm (GREY)			150ohm (GREEN
Sample No.	A	B	C	A	B	C	A
1	27.2	26.6	27	59	60	58	132
2	27.5	28	28.3	54.9	55.3	55.5	176
3	25.1	25.3	26.1	54.5	54.3	56.6	190
4	24.1	24.2	24.7	57.1	55.6	55.7	180
5	26.2	25.4	26.4	62.4	58.3	59.4	138
6	24.5	24.1	24.7	55.2	55.1	54.9	129
7	26.3	25.8	26.8	63.3	60.6	60.2	171
8	26	26.1	26.5	59	57	56.8	162
9	26.1	25.6	26.7	57.2	55.5	55.1	157
10	26.3	25.7	27.4	56.4	55.1	53.1	128
11	27	26.4	27.1	61.6	60.4	60.3	200
12	26.2	25.3	26.3	58.2	57.3	56.8	156
13	25.4	25.7	25.9	57.8	57.6	56.7	181
14	27	26.1	26	58	56.7	56.3	203
15	27.2	26.1	25.9	60.1	57.7	58.2	193
16	25.1	24.9	24.9	59.9	56.9	56.4	193
17	26.1	25.7	25.6	63.9	61.1	58.7	150
18	25.3	24.7	24.2	61.1	57.8	58	180
19	26.7	26.4	25.9	66.3	59.4	60.1	162
20	25.6	25.6	24.7	57.7	55.3	57.6	161
21	26.1	25.7	26.3	57.5	56.9	56.2	166
22	27.1	25.8	25.7	61.5	58.3	57.3	
23				58.8	57	57.3	

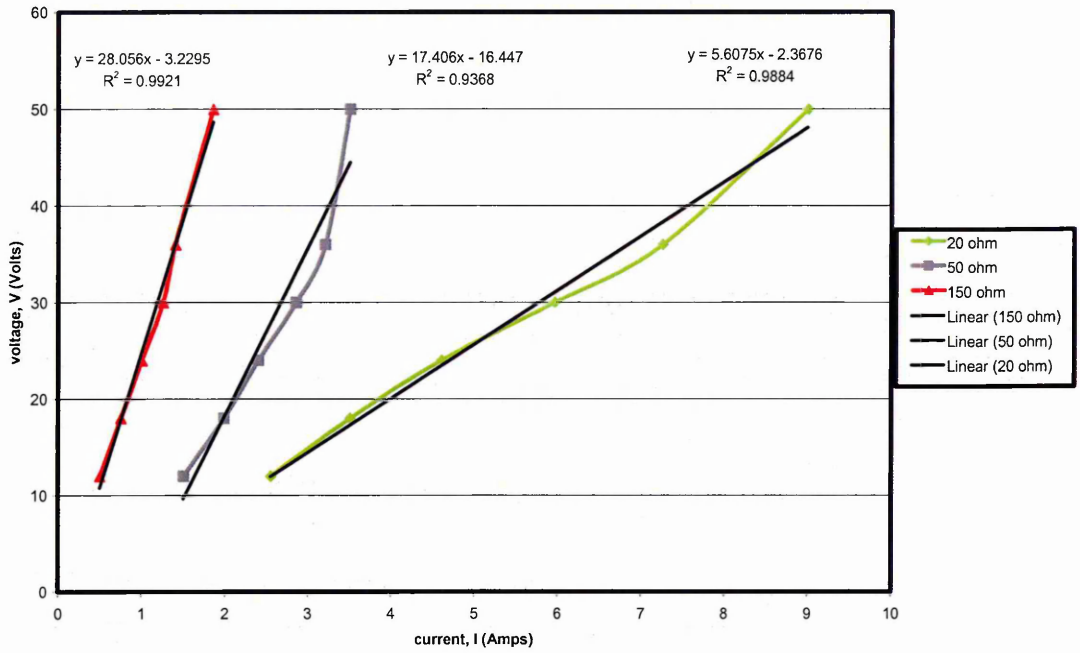

Current vs Voltage for CPT, length *l* = 120mm (R_T = 20, 50 and 150 ohms)

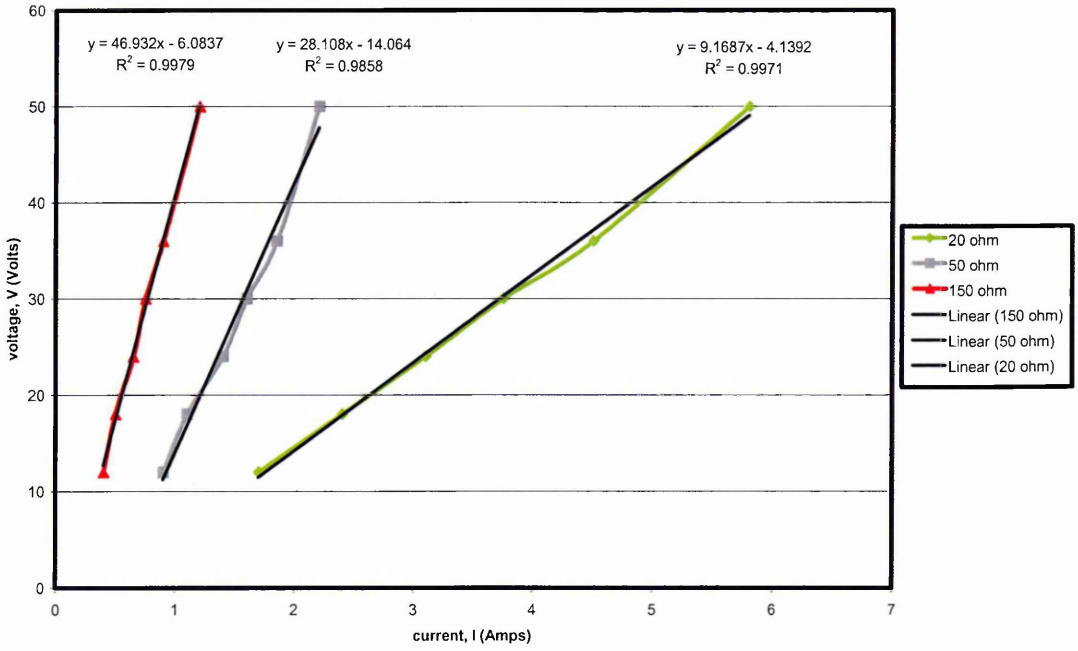

Current vs Voltage for CPT, length *l* = 200mm (R_T = 20, 50 and 150 ohms)

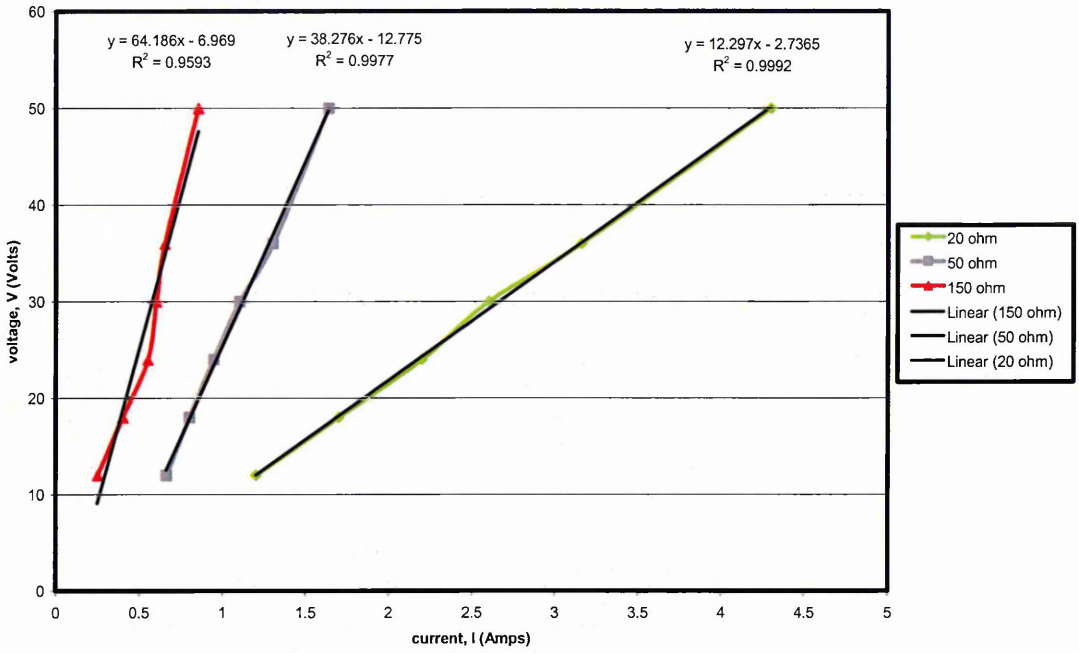

Current vs Voltage for CPT, length *l* = 280mm (R_T = 20, 50 and 150 ohms)

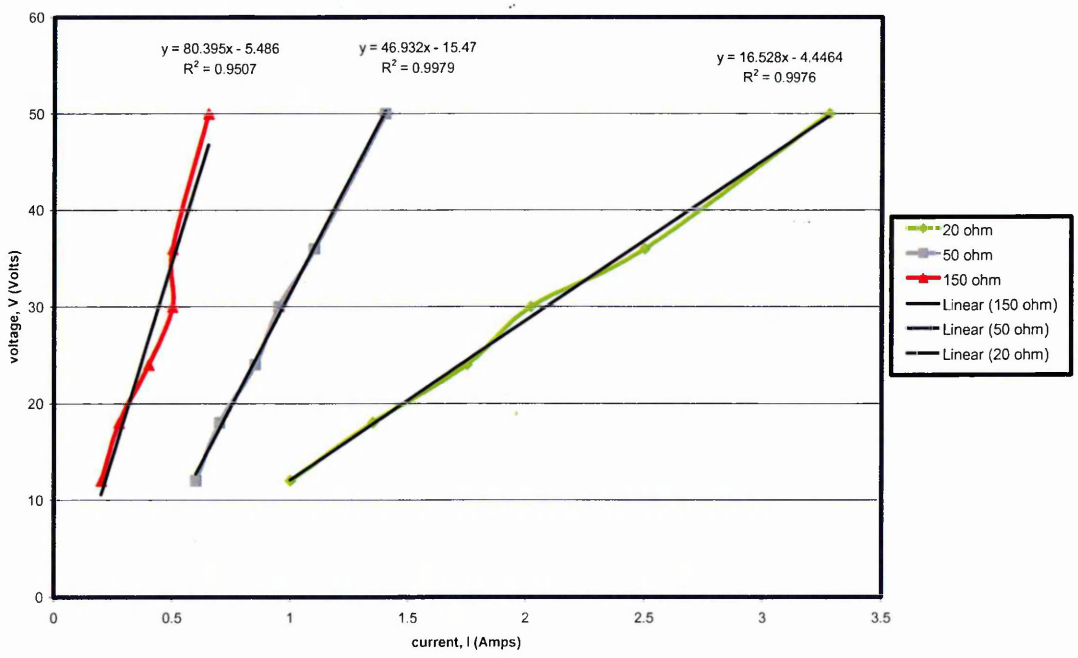

Current vs Voltage for CPT, length *l* = 360mm (R_T = 20, 50 and 150 ohms)

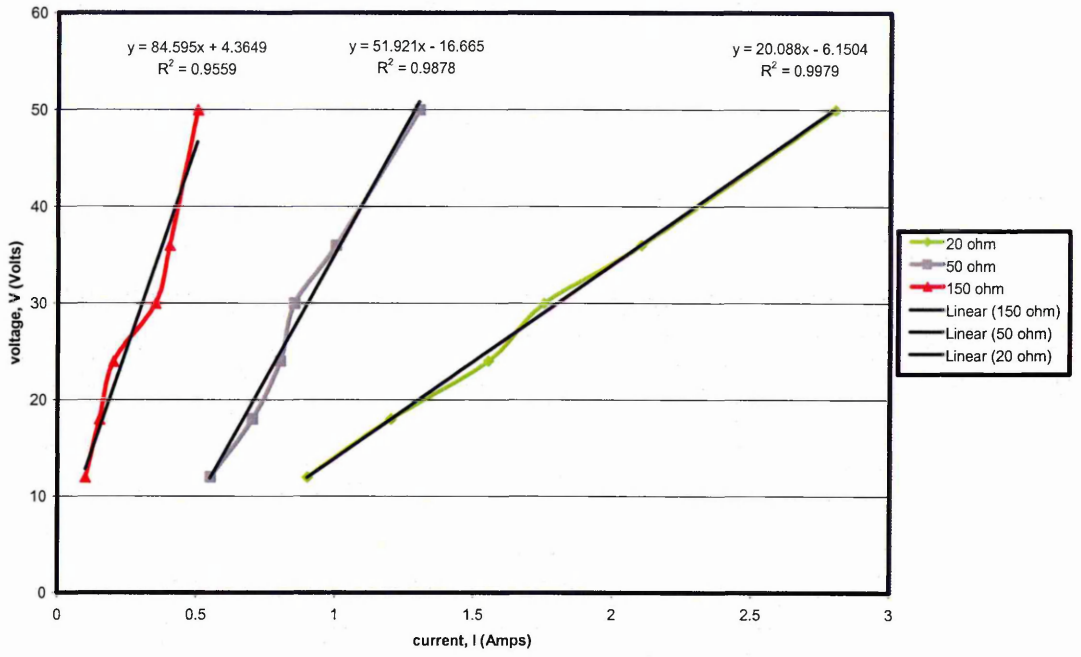

Current vs Voltage for CPT, length *l* = 420mm (R_T = 20, 50 and 150 ohms)

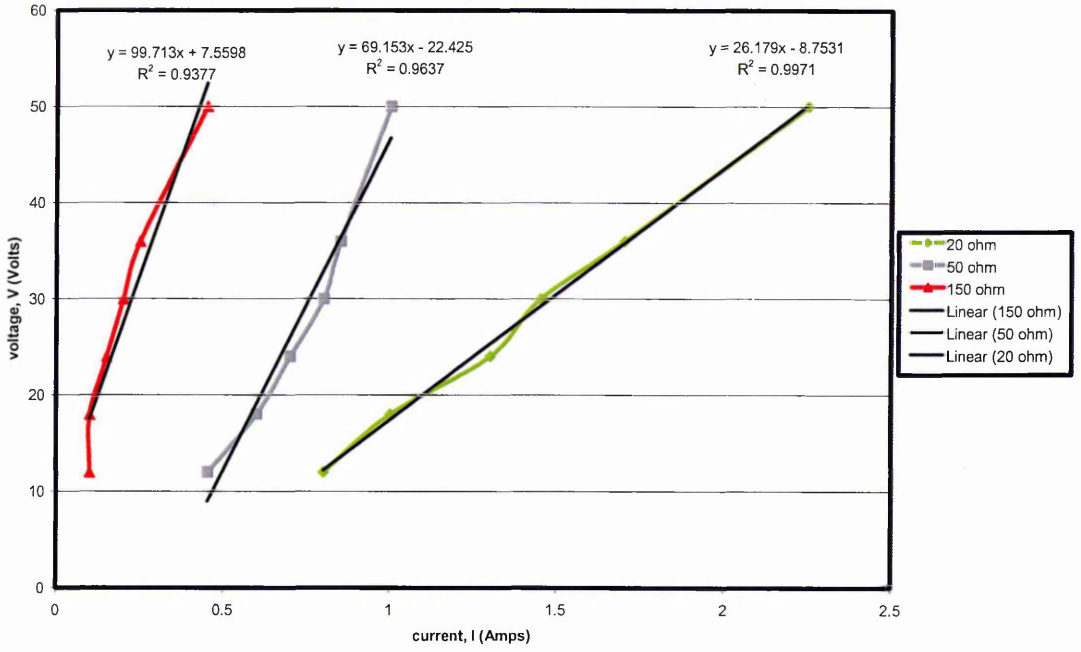

Current vs Voltage for CPT, length *l* = 550mm (R_T = 20, 50 and 150 ohms)

Appendix 2. Results from Core Sampling

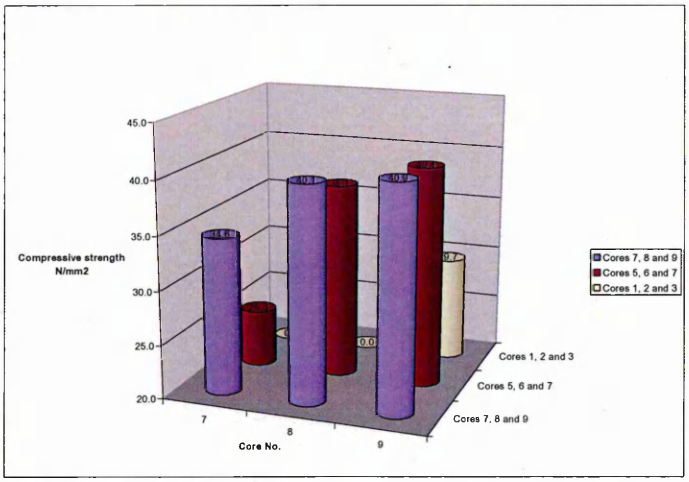

Compressive strength results from the cores taken from section A of the 400mm^3 concrete block cured using profile 2

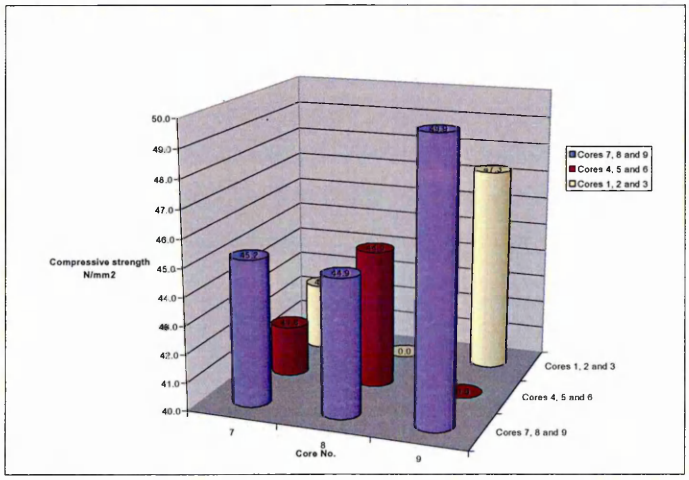

Compressive strength results from the cores taken from section B of the 400mm^3 concrete block cured using profile 2

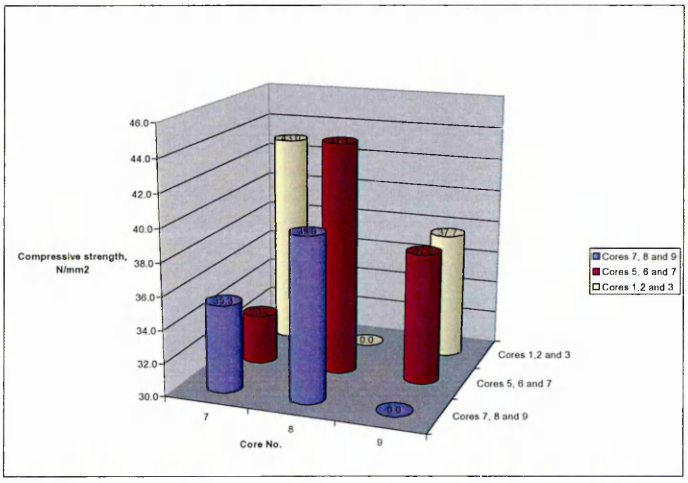

Compressive strength results from the cores taken from section C of the 400mm^3 concrete block cured using profile 2

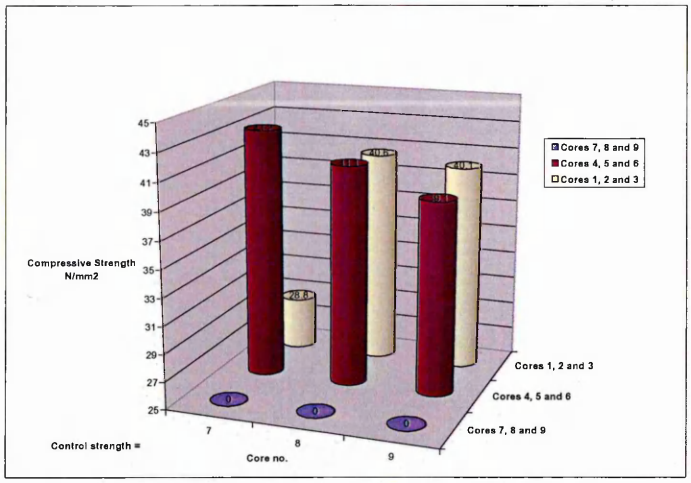

Compressive strength results from the cores taken from section A of the 400mm^3 concrete block cured using profile 3

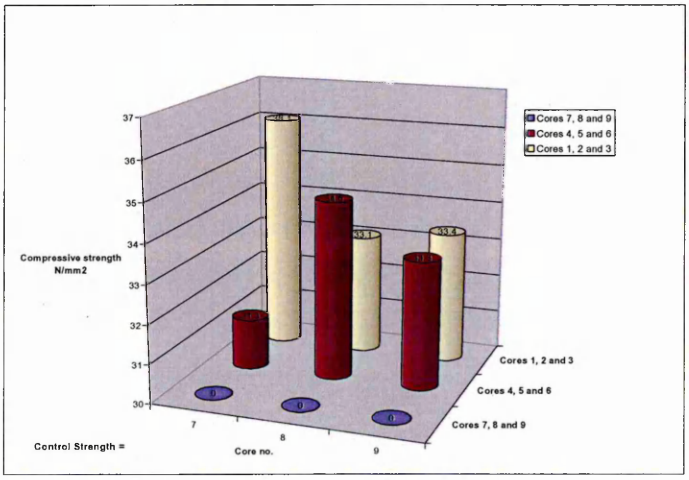

Compressive strength results from the cores taken from section B of the 400mm^3 concrete block cured using profile 3

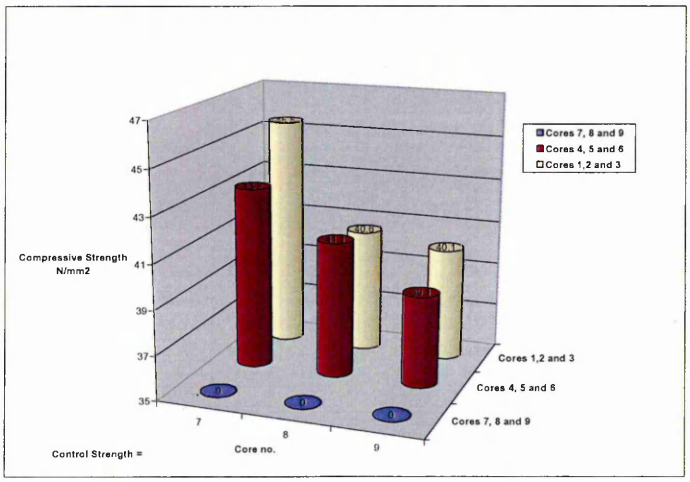

Compressive strength results from the cores taken from section C of the 400mm^3 concrete block cured using profile 3

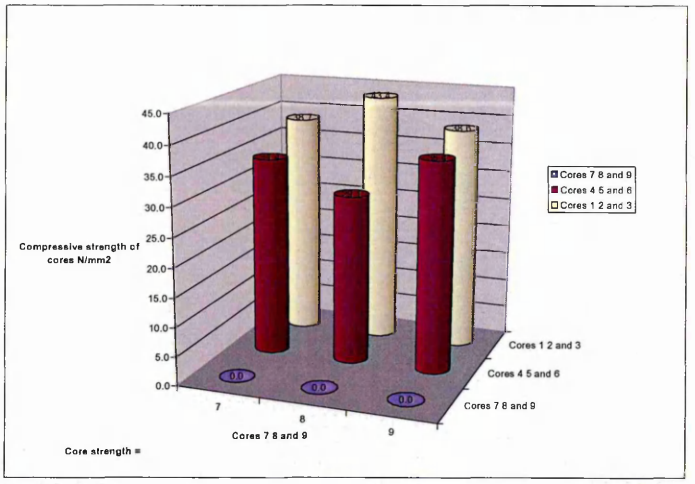

Compressive strength results from the cores taken from section C of the 400mm^3 concrete block cured using profile 3

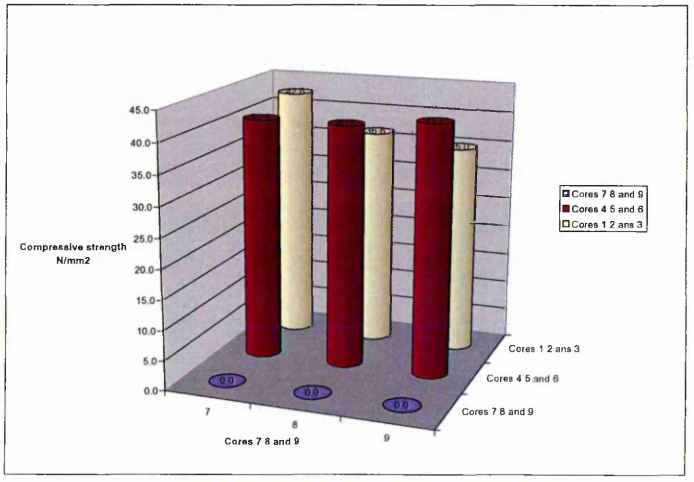

Compressive strength results from the cores taken from section C of the 400mm^3 concrete block cured using profile 3

Appendix 3. Steam versus. CPD Curing in a Precast Concrete Factory

Tarmac Precast concrete is part of the Tarmac Ltd group, the leading supplier of building materials in the UK. Tarmac's precast factory at Tallington is one of two in the country. The Tallington factory products include, railway sleepers, bridge beams, double T beams, car parks, stairs and wall panels. Steam curing of precast concrete elements is used throughout the factory at Tallington and the following calculations are a break down of the costs incurred, and the potential savings that could be made if Inditherm solutions were adopted. The following cost and energy estimates are based on data obtained from Tarmac Precast concrete has been applied to the UK precast concrete market and the European Precast Concrete Market.

Steam Curing

Fuel consumption:

4,000-5,000 litres per day

Energy consumption per week

Winter	=	5000 * 5.5 x 23	= 632,500	litres
Summer	=	4000 x 5.5 x 22	= 484,000	litres
Total	=		1,116,500	litres per annum

Total Energy Consumed $= 4 \times 10^7 \times 1{,}116{,}500$

$= 4.466 \times 10^{13}$ Joules per annum

Total concrete produced $= 48{,}817\ m^3$ per annum

Energy Consumed per m^3 of concrete $= 4.466 \times 10^{13} / 48{,}817$

$= 9.1 \times 10^8$ Joules / m^3

CPT Curing

The operating outputs of the Inditherm material can vary between 150 W/m^2 and 800 W/m^2, Operating costs;

150 W/m^2 =	0.75 pence per hour
800 W/m^2 =	4 pence per hour

Appendix 4. Materials data sheets

CI/SfB | | | m1 | (M2) | Feb 2007

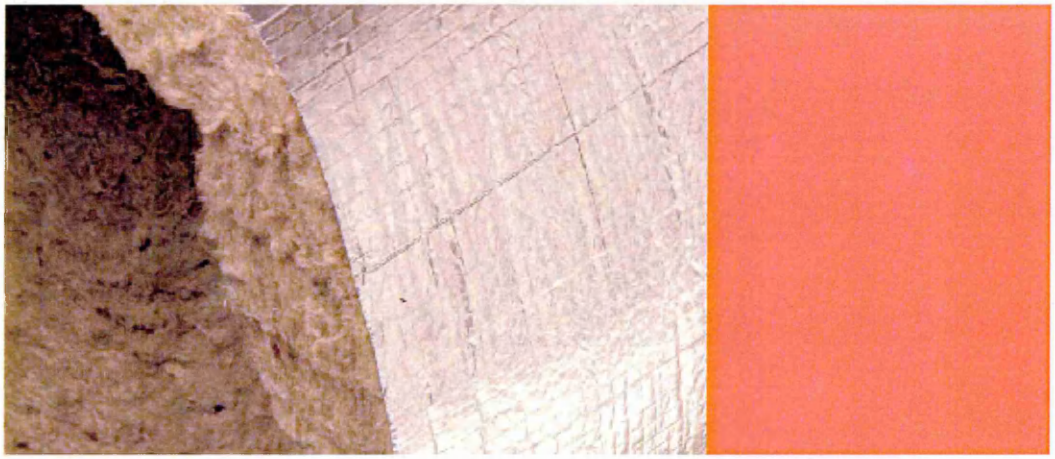

Icerock Ductwrap

Description

Icerock Ductwrap is a strong, flexible roll of non-combustible rock mineral wool with a Bright Class 'O' reinforced aluminium foil facing on one side.

Application

Icerock Ductwrap is for the thermal insulation of round, oval and square internal ductwork operating at temperatures up to 200°C.

Icerock Ductwrap can also used be used for the thermal insulation of cold water storage, feed and expansion tanks.

Standards

Icerock Ductwrap is made from non-combustible, inorganic rock wool, defined as mineral wool in BS 3533:1981. It complies with BS 3958: Part 5 and with the requirements of BS 5422 and BS 5970. It is manufactured to a Quality Assurance system which complies with BS EN ISO 9001:2000.

Product Data

Thickness	Thermal conductivity	Thermal resistance	Length	Width	Area per
(mm)	(W/mK)	(m²K/W)	(m)	(mm)	pack (m²)
50	0.033	1.50	7.50	900	6.75
40	0.033	1.20	8.50	900	7.65
25	0.033	0.75	10.00	900	9.00

Performance

Thermal

The thermal conductivity of Icerock Ductwrap is 0.033W/mK at 10°C.

Fire

The rock mineral wool of Icerock Ductwrap is classified as non-combustible to BS 476: Part 4: 1970 (1984), Class 1 Surface Spread of Flame to BS 476: Part 7: 1997. The base rock mineral wool and the foil facing comply with the Class 'O' requirements of the Building Regulations when tested to BS 476: Part 6: 1989 and Part 7: 1997.

Benefits

- Non-combustible
- Acoustically absorbent
- Easy to handle and install
- Superior foil finish

Customer Service (Sales) Tel: 0844 800 0135
Technical Advisory Centre Tel: 01744 766666
Literature Tel: 08700 668660
www.knaufinsulation.co.uk

KNAUF INSULATION

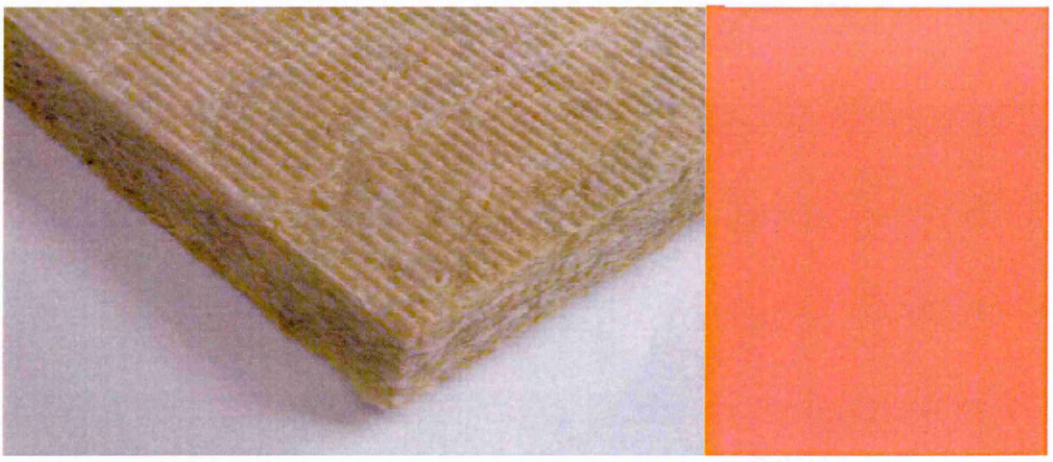

Rocksilk Universal Slab

Description
Rocksilk Universal Slabs are unfaced, rock mineral wool slabs, available in a range of densities from 33 to 200 kg/m³. The standard product is supplied unfaced, but slabs can also be manufactured with a factory applied foil or tissue facing and are also available with a water repellent additive.

Application
Rocksilk Universal Slabs are used for a wide range of thermal and acoustic insulation applications in buildings, building services and industry.

Standards
Rocksilk Universal Slabs are made from non-combustible inorganic rock wool, defined as mineral wool in BS 3533: 1981 and are manufactured to a Quality Assurance system which complies with BS EN ISO 9001:2000.

Durability
Rocksilk Universal Slabs are odourless, non-hygroscopic, rot proof, do not sustain vermin and will not encourage the growth of fungi, mould or bacteria.

Environmental
Rocksilk Universal Slabs are free from CFCs, HCFCs and any other material with ozone depletion potential in their manufacture and content and represent no known threat to the environment.

Rocksilk Universal Slab's manufacture has a low impact on the environment and is classified as Zero ODP and Zero GWP.

Performance

Thermal
The thermal conductivity of Rocksilk Universal Slabs varies with density from 0.035 to 0.037 W/mK – see table overleaf.

Fire
Rocksilk Universal Slab is classified as Euroclass A1 to BS EN ISO 13501-1.

Benefits

- Wide range of densities
- Non-combustible
- Excellent thermal and acoustic properties

Customer Service (Sales) Tel: 0844 800 0135
Technical Advisory Centre Tel: 01744 766666
Literature Tel: 08700 668660
www.knaufinsulation.co.uk

Plastazote® LD24MC

Low Density Polyethylene Foam Property Data Sheet

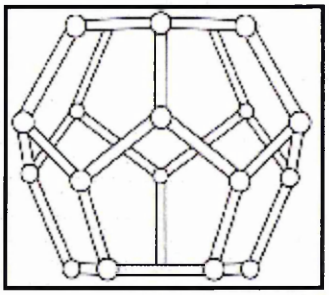

Plastazote® is a closed cell, cross-linked polyethylene foam manufactured using Zotefoams unique production process. This data sheet characterises Plastazote foam LD24MC which is available in sheet form and is fabricated by modern techniques and can be thermoformed into shapes.

Property	Test Procedure	Units	LD24MC
Nominal Density - Skin/Skin	BS ISO 7214 1998	kg/m³	24
Cell Size – Typical Diameter	Internal	mm	0.5
Compression Stress-Strain	BS ISO 7214 1998		
10% compression		kPa	33
25% compression		kPa	52
40% compression		kPa	84
50% compression		kPa	116
Compression Set	BS ISO 7214 1998		
25% comp., 22hr, 23°C	25 mm cell-cell		
½ hr recovery		% set	13
24hr recovery		% set	4.5
50% comp., 22hr, 23°C			
½ hr recovery		% set	28
24hr recovery		% set	18
Tensile Strength	ISO 7214 1998	kPa	325
Tensile Elongation		%	120
Tear Strength	BS EN ISO 8067 1995	N/m	480
Shore Hardness OO Scale	ISO 868 1985		
10mm cell/cell thickness		OO	49
Recommended operating temperature range*	Internal	°C	+100 max -70 min
Flammability			
Automotive	FMVSS 302 – Burn rate	<100mm/min.	Pass: 12 mm and thicker
Horizontal Burn Rate	ISO 7214 1998		
5mm thick		mm/sec	2.1
13mm thick		mm/sec	1.5

ZOTEFOAMS

January 2004

Appendix 5. Transformer drawings and photographs

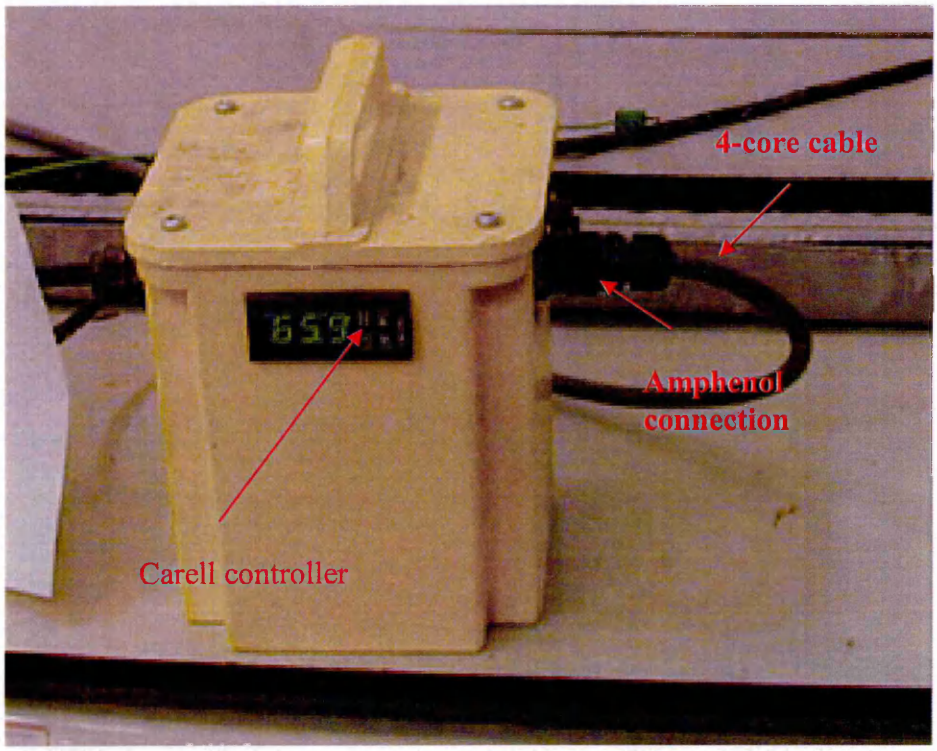

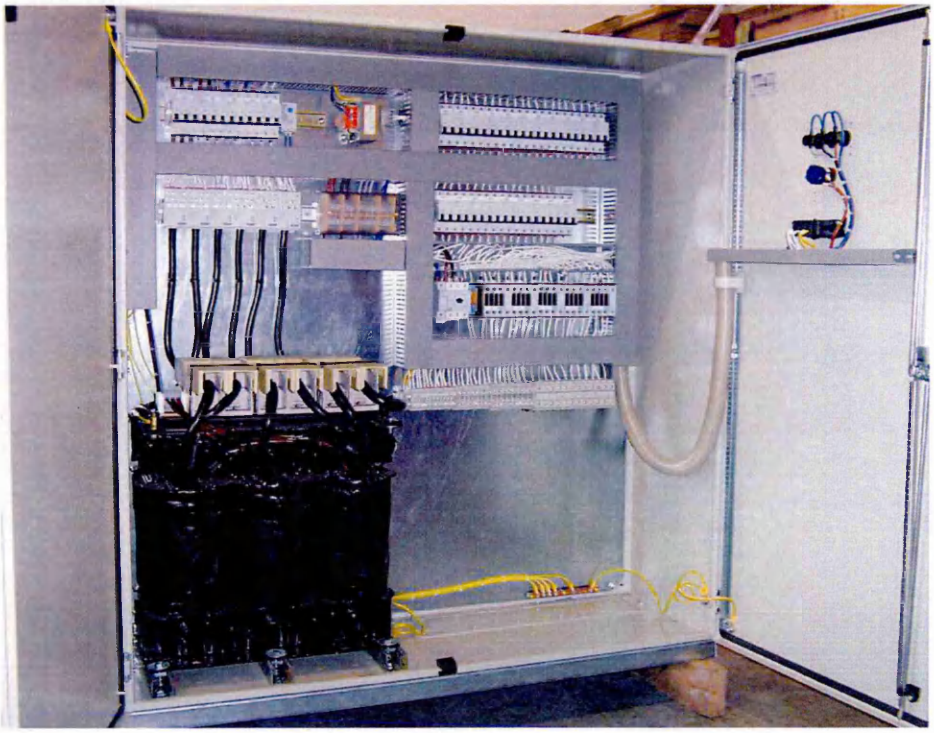

Appendix 6. Multi meter specification

		Fluke 321	Fluke 322	Fluke 323	Fluke 324	Fluke 325	Fluke 326	Fluke 327
~A	Range	0 - 400.0 A	0 - 40.00 A 40.0 - 400.0 A	0 - 400.0 A	0 - 600.0 A	0 - 600.0 A	0 - 600.0 A	0 - 999.9 A
	Accuracy	1.9% ± 5 counts (50 - 60 Hz) 3.0% ± 5 counts (60 Hz - 400 Hz)	1.9% ± 5 counts (50 - 60 Hz) 3.0% ± 5 counts (60 Hz - 400 Hz)	2% ± 5 counts (50 - 60 Hz)	2% ± 5 counts (50 - 60 Hz)	2% ± 5 counts (50 - 60 Hz)	2% ± 5 counts (10 - 100 Hz) 6% ± 5 counts (100 - 400 Hz)	2% ± 5 counts (10 - 100 Hz) 6% ± 5 counts (100 - 400 Hz)
	Crest Factor (50/60 Hz)	–	–	–	–	2.4 @ 500 A 2.0 @ 600 A add 2% for C.F.>2	3 @ 500 A 2.5 @ 600 A add 2% for C.F.>2	3 @ 500 A 2.5 @ 600 A 1.42 @ 1000 A add 2% for C.F.>2
	AC Response	Averaging	Averaging	Averaging	Averaging	True-rms	True-rms	True-rms
Inrush	Integration Time	–	–	–	100 mS	100 mS	100 mS	100 mS
⎓A	Range	–	–	–	–	–	0 - 600.0 A	0 - 999.9 A
	Accuracy	–	–	–	–	–	2% + 3 counts	2% + 3 counts
~V	Range	0 - 400.0 V 0 - 600 V	0 - 400.0 V 0 - 600 V	0 - 600.0 V	0 - 600.0 V	0 - 600.0 V	0 - 600.0 V	0 - 600.0 V
	Accuracy	1.2% + 5 counts (50 - 400 Hz)	1.2% + 5 counts (50 - 400 Hz)	1% + 5 counts (50/60 Hz)	1% + 5 counts (50/60 Hz)	1% + 5 counts (50/60 Hz)	1% + 5 counts (20 - 100 Hz) 6% + 5 counts (100 - 400 Hz)	1% + 5 counts (20 - 100 Hz) 6% + 5 counts (100 - 400 Hz)
	AC Response	Averaging	Averaging	Averaging	Averaging	True-rms	True-rms	True-rms
⎓V	Range	–	0 - 400.0 V 0 - 600 V	0 - 600.0 V	0 - 600.0 V	0 - 600.0 V	0 - 600.0 V	0 - 600.0 V
	Accuracy	–	1% + 5 counts	1% + 5 counts	1% + 5 counts	1% + 5 counts	1% + 5 counts	1% + 5 counts
Ω	Range	0 - 400.0 Ω	0 - 400.0 Ω	0 - 600.0 Ω	0 - 600.0 Ω 601 - 6000 Ω	0 - 600.0 Ω 601 - 6000 Ω	0 - 600.0 Ω 601 - 6000 Ω	0 - 600.0 Ω 601 - 6000 Ω
	Accuracy	1% ± 5 counts	1% ± 5 counts	1.5% ± 5 counts	1.5% ± 5 counts	1.5% ± 5 counts	1.5% ± 5 counts	1.5% ± 5 counts
Continuity		≤ 30 Ω	≤ 30 Ω	≤ 30 Ω	≤ 30 Ω	≤ 30 Ω	≤ 30 Ω	≤ 30 Ω
Hz	Range	–	–	–	–	–	–	5.0 - 400.0 Hz
	Accuracy	–	–	–	–	–	–	0.5% ± 5 counts
	Trigger Level	–	–	–	–	–	–	10 - 100 Hz ≥ 5 A 5 - 10 Hz, 100 - 400 Hz ≥ 10 A
MIN/MAX		No	No	No	No	No	No	Yes
Backlight		No	No	No	No	Yes	Yes	Yes
Display Hold		Yes	Yes	Yes	Yes	Yes	Yes	Yes
Size	Height	7.5"	7.5"	9.375"	9.375"	9.375"	9.875"	9.875"
	Width	2.5"	2.5"	3.125"	3.125"	3.125"	3.125"	3.125"
	Depth	1.4"	1.4"	1.625"	1.625"	1.625"	1.625"	1.625"
	Jaw Opening	1" (25.4 mm)	1" (25.4 mm)	1.2" (30.5 mm)	1.2" (30.5 mm)	1.2" (30.5 mm)	1.2" (30.5 mm)	1.2" (30.5 mm)
Max. Wire Size		500 MCM	500 MCM	750 MCM	750 MCM	750 MCM	750 MCM or two 500 MCM	750 MCM or two 500 MCM
Weight		9 oz.	9 oz.	11 oz.	11 oz.	11 oz.	11 oz.	11 oz.

Appendix 7. Case Studies

Subsequent installations of the systems following the development work undertaken as part of this post graduate degree:-

Terminal 5 – Heathrow

The findings and analysis of this post graduated degree were used to develop blankets that were supplied to heat 150mm thick concrete decks to a maximum temperature of 40 deg C. In heating the concrete decks at early ages, the hydration reaction of the cement within the concrete is accelerated, increasing the rate at which the compressive strength of the concrete develops. This transfers the stresses and loadings to the concrete sooner, saving the main contractor money through faster completion and minimising the risk of penalties associated with project delays. In addition, the heated blankets help to protect the early age concrete from damage during cold weather.

CPT Blankets used to protect and accelerate the strength development of post tensioned prestressed concrete deck

The principle contractor for the car park is Laing O'Rourke, a leading international contractor, and the project client was BAA. The 24 CPT blankets, each measuring 17m by 2m, covered a total of over 800m2 when unrolled over the concrete. After curing for about 2-3 days, they are simply rolled up for use again on the next concrete pour. The blankets incorporate the Company's unique, patented conductive polymer technology, and are encased in a rugged PVC cover, allowing the blankets to be re-used for numerous concrete pours. The contract also included the associated power supply units.